Executive Committee on
RESEARCH
Fostering Innovation at MGH

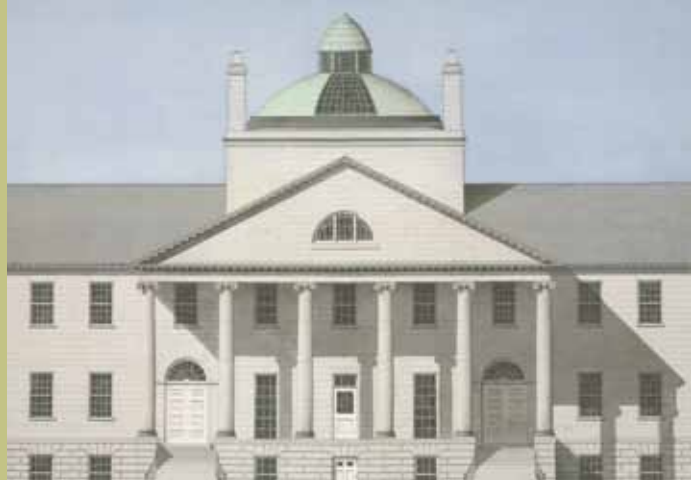

66th Annual Meeting of the
MGH Scientific Advisory Committee

SAC 2013

Poster Session Abstracts

March 20, 2013
Holiday Inn at Beacon Hill
5 Blossom Street, 15th Floor

MGH 1811
RESEARCH Management
Mainstay of MGH Innovation

66th Annual Meeting of the
MGH Scientific Advisory Committee

SAC 2013

Contents

SAC 2013 Annual Celebration of Science at MGH

Agenda: Day One, Wednesday, March 20, 2013

11:00 am–1:45 pm, ***Holiday Inn, 15th Floor***

SAC 2013 Poster Session (light lunch available)

2:00 pm–5:00 pm, ***Simches 3.110***

Scientific Presentations

WELCOME
Peter L. Slavin, MD, President, Massachusetts General Hospital

OPENING COMMENTS AND INTRODUCTIONS
Robert E. Kingston, PhD, Chair, Executive Committee on Research (ECOR)

2:15 pm

2013 Martin Prize for Basic Research

Reach and grasp by people with tetraplegia using a neurally controlled robotic arm

Leigh R. Hochberg, MD, PhD

2:45 pm

2013 Martin Prize for Clinical Research

Sequencing chromosomal abnormalities reveals neurodevelopmental loci that confer risk across diagnostic boundaries

Michael E. Talkowski, PhD

3:15 pm

Goodman Award

Fishing for therapies to treat T-cell acute lymphoblastic leukemia

David M. Langenau, PhD

3:45–4:00 pm BREAK

4:00 pm

Keynote

INTRODUCTION
Peter L. Slavin, MD

DISSECTING THE NATURE OF PROTECTIVE HUMORAL IMMUNITY
Galit Alter, PhD

2012 MGH Research Scholar, Ragon Institute

HOW THE IMMUNE SYSTEM SEES DNA: DEGRADATION AND DETECTION
Nir Hacohen, PhD

2012 MGH Research Scholar, Rheumatology

Agenda: Day Two, Thursday, March 21, 2013

8:00–8:20 am, *Simches 3.110*

WELCOME AND OPENING COMMENTS
Peter L. Slavin, MD, President, Massachusetts General Hospital

8:20–8:45 am

ECOR REPORT 2012
Robert E. Kingston, PhD, Chair, Executive Committee on Research (ECOR)

8:45 am–12:00 pm

DEPARTMENT REPORTS
8:45 am ***Pathology,*** **David N. Louis, MD**
9:30 am ***Psychiatry,*** **Jerrold F. Rosenbaum, MD**

10:15–10:30 am

BREAK

10:30 am ***Rheumatology, Allergy and Immunology,*** **Andrew D. Luster, MD, PhD**
11:15 am ***Martinos Center,*** **Bruce R. Rosen, MD, PhD**

1:30 pm–4:00 pm, *Simches 3.110*

Next Generation Science at MGH

1:30–1:40 pm

MGH/MGPO 2012–2013 STRATEGIC PLANNING PROCESS: OVERVIEW
Harry W. Orf, Senior Vice President for Research

1:40–2:40 pm

RESEARCH STRATEGIC PLANNING WORKGROUP
- Overview
- Research Institute

***Panel Moderator*:** **Harry W. Orf, PhD, Senior Vice President for Research**
Panelists: **Randy L. Gollub, MD, PhD**
Robert E. Kingston, PhD
Joren C. Madsen, MD, DPhil
Ramnik J. Xavier, MD, PhD

2:40–3:00 pm

BREAK

3:00–4:00 pm

RESEARCH ↔ CLINICAL INTEGRATION WORKGROUP
- Overview
- Translational Medicine Program

Panel Moderator: **Andrea B. Paciello, MHSA**
Panelists: **R. Rox Anderson, MD**
Maurizio Fava, MD
Mason W. Freeman, MD
Frances Toneguzzo, PhD

Session Floor Plan

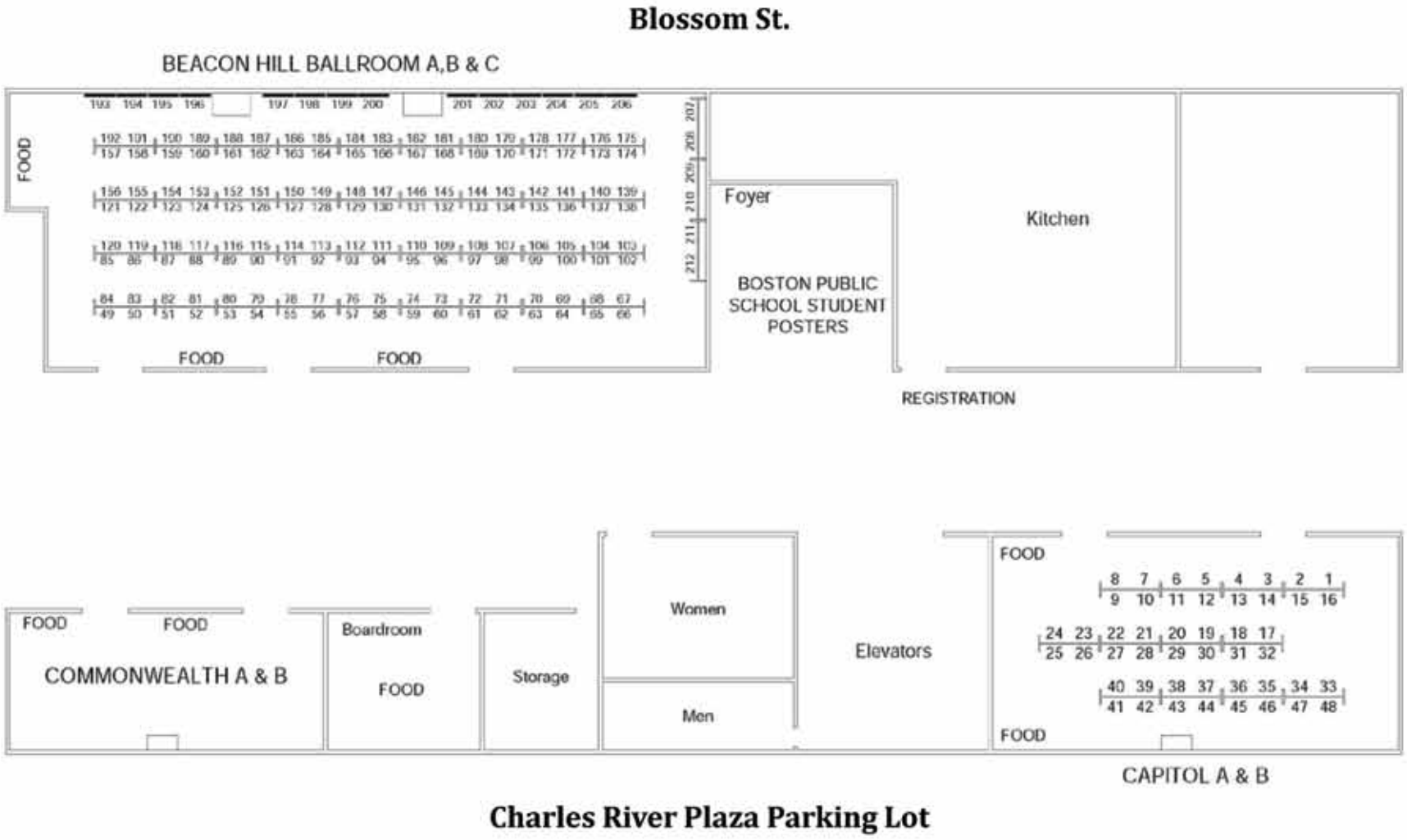

Boston Public School Students

We would like to acknowledge the hard work of the students whose work is on display today. The schools' participation is coordinated by the MGH Youth Programs Team in the MGH Center for Community Health Improvement (CCHI). Below is a list of the schools and the participating students from each school; their MGH mentors are shown in parenthesis.

The James P. Timilty Middle School

- **Marta Castillo,** Grade 8—What is the effect of different amounts of salt on water density and on the buoyancy of different objects?
  (Sara Chung, Clinical Research Coordinator, Psychiatry)
- **Clarence Joseph,** Grade 8—What is the effect of the size of a plane on light reflection?
  (Thomas Battey, Clinical Research Coordinator, Neurology)
- **Jocelyn Reyes,** Grade 8—Which fruit produces the greatest electric voltage as a battery?
  (Shonda Sumpter, Administrative Manager, Medicine)
- **Kira Tejeda,** Grade 8—How does disrupting perception affect one's ability to learn and improve at three different tasks over time?
  (Maritza Ebling, Research Technician, Radiology)
- **Loren Ferguson,** Grade 7—Green Is the Way to Clean!
  (Julie Berkley, Research Assistant, Neurology)
- **Ivonne Ramos,** Grade 7—How fast does a paper clip rust in different solutions?
  (Cathy Zhang, Intern, Neurology)
- **Tyeray Williams,** Grade 7—What are the combined effects of fatigue and eyesight on balance?
  (Richard Erali, Graduate Student, Orthopedics)
- **Jamir Sobers,** Grade 7—How does light affect perception of distance?
  (Nicholas Ramirez, Molecular Biology)

MGH Youth Scholars from the following high schools were selected by their schools as having the most outstanding projects from each school. They do not have MGH mentors.

East Boston High School

- **Claudia Cabrera,** MGH Youth Scholar, East Boston High School

Edward M. Kennedy Academy for Health Careers

- **Audrey Lang,** MGH Youth Scholar, Edward M. Kennedy Academy for Health Careers

Posters of Distinction / BASIC

POSTER #12

Engineered Skeletal Muscle for Craniomaxillofacial Reconstruction

Olive Mwizerwa, BA
Research Technician, Center for Regenerative Medicine

POSTER #19

In-vivo single cell RNA-Seq analysis of osteolineage cells within the HSPC niche identifies interleukin-18 as a novel hematopoieitic regulator

Lev Silberstein, MD, PhD
Instructor, Center for Regenerative Medicine

POSTER #29

Chemical genetic dissection of an autophagic defect in a neuronal cell model of JNCL

Uma Chandrachud, PhD
Research Fellow, Center for Human Genetic Research

POSTER #96

Microscopic Imaging of Neuro-Capillary Coupling in Brain Cortex

Jonghwan Lee, PhD
Research Fellow, Radiology

POSTER #109

A single mutant HTT allele is sufficient to elicit neuronal phenotypes in a knock-in mouse model of Huntington's disease

Vanessa Wheeler, PhD
Associate Professor, Center for Human Genetic Research

POSTER #116

Single cell evolution of AKT pathway activation drives T-cell acute lymphoblastic leukemia relapse

Jessica Blackburn, PhD
Research Fellow, Cancer Center

Posters of Distinction / CLINICAL

POSTER #151

Increased hypothalamic-pituitary-adrenal drive is associated with decreased appetite and hypoactivation of food motivation neurocircuitry in anorexia nervosa

Elizabeth Lawson, MD
Assistant Professor, Medicine

POSTER #176

A New Risk Scheme to Predict Ischemic Stroke and Other Thromboembolic Events in AtrialFibrillation: The ATRIA Study Risk Score

Daniel Singer, MD
Professor, Medicine

POSTER #185

The Cost-effectiveness of Treatment as Prevention: Analysis of the HPTN 052 Trial

Rochelle Walensky, MD, MPH
Professor, Medicine, Infectious Diseases

POSTER #191

Human inhibitory single neurons switch off before dramatic increases in seizure intensity

Omar Ahmed, PhD
Research Fellow, Neurology

POSTER #206

2-aminoadipic acid is a novel biomarker of diabetes risk and modulates glucose homeostasis

Nikolaos Psychogios, PhD
Research Fellow, Heart Center

POSTER #207

Combinatorial Mutations in Two Genes Link Disordered Ubiquitination with a Syndrome of Ataxia, Dementia, and Hypogonadotropic Hypogonadism

Stephanie Seminara, MD
Associate Professor, Medicine

Index

Index

Index

Index

Index

Index

Index

Index

Index

Index

Index

Index

BASIC–OTHER

Poster Number 1

Buikema, Jan MD
Research Fellow, Heart Center
jbuikema@partners.org

Wnt/β-catenin Signaling Promotes the Expansion of early Ventricular Cardiomyocytes

Investigators: Jan Willem Buikema, MD; Ahmed S. Mady, MD; Nikhil V. Mittal, PhD; Ayhan Atmanli, BA; Leslie Caron, PhD; Joost P.G. Sluijter, PhD; Pieter A. Doevendans, MD, PhD; Ibrahim J. Domian, MD, PhD

Background and aim: Heart failure is a major cause of mortality and morbidity in the developed world. The clinical syndrome results from the loss of functional CMs and an inability of the heart to meet the metabolic demands of affected individuals. Generating a sufficient number of functional CMs to restore normal cardiac function remains a major therapeutic goal of regenerative cardiovascular medicine. Untangling the molecular pathways that control early CM proliferation during differentiation will not only lead to a better understanding of normal cardiac development, but will also allow advances in stem cell biology to be adapted for clinical endpoints. Recent work has allowed for the in vitro isolation of functional mouse ventricular muscle from embryonic stem cell (ESC) derived cardiac progenitors. The expansion of these committed Isl1+/Nkx2.5+ early ventricular CMs remains limited, however. We hypothesize that Wnt signaling plays an important role in regulating the proliferation and maturation of early ventricular CMs.

Methods and results: We have thus generated double transgenic mouse ESC cell lines with the anterior-heart-field (AHF) enhancer of the Mef2C gene driving the expression of the red fluorescent protein and the Nkx cardiac enhancer driving the expression of enhanced green fluorescent protein. We were thereby able isolate early ventricular CMs from a renewable cell source. These double transgenic ESCs were differentiated in vitro in cardiogenic culture conditions. At day 6 of in vitro differentiation, CMs were FACS isolated and plated in 384-well plates. Cells were then cultured in the presence or absence of small molecules known to influence Wnt/β-catenin signaling pathway for an additional 3, 5 and 7 days (+3, +5, +7). At day 6+5, at least 90% of the cells stained positive for Troponin T. Cells cultured in presence of 6-bromoindirubin-3′-oxime (BIO), a GSK-3α/β inhibitor, increased exponentially in number. At day 6+5 we found an 8-fold ($P<0.001$) increase in Troponin T positive cells in the presence of BIO. Next we validated the role of Wnt/β-catenin signaling on proliferation of early CMs in vivo and human ESC-derived CMs

Conclusions: This work shows that proliferation of early ventricular CMs is mediated through Wnt/β-catenin signaling. The ability to control CM proliferation is an important step forwards in order to generate the amount of CMs lost after an adverse cardiac event. Future experiments will focus on unraveling the cardiac specific Wnt/β-catenin transcriptional targets.

Poster Number 2

Cervantes, Thomas BS
Research Engineer, Center for Regenerative Medicine
tcervantes@partners.org

3D Image Analysis of Composite Scaffolds for Tissue Engineered Ear Reconstruction

Investigators: Thomas M. Cervantes, BS; Erik K. Basssett, MS; Alan Tseng, BS; Anya Kimura, BS; Nicholas Roscioli, BS; Rajiv Gupta, MD, PhD; Mark A. Randolph, MAS; Joseph P. Vacanti, MD; Irina Pomerantseva, MD, PhD; Cathryn A. Sundback, ScD

The tissue engineered ear has been an iconic symbol of the field since 1991, when an engineered ear grown in a mouse model was first published. Since then, there have been many efforts to adapt the technology for clinical use. Ear reconstruction can benefit patients with congenital and acquired ear defects. The principle requirements for a replacement ear are to recreate the complex geometry of the outer ear and the unique flexibility of auricular cartilage. These goals are difficult to achieve using current surgical options. Tissue engineering technology can match both requirements through the use of a composite scaffold, comprised of a porous collagen matrix with an embedded titanium wire framework. The shape of the ear is defined by the wire framework, which maintains dimensions during cartilage growth, yet does not impede the flexibility of the cartilage. The composite scaffold concept was previously shown to be successful in a small animal study. The shape of the scaffold has been improved to more closely match the size and contours of an adult human ear. High-resolution image analysis was performed to understand the three-dimensional behavior of the wire framework during the formation of new cartilage in the collagen matrix.

Composite scaffolds with the embedded wire framework maintained overall size and shape during a large animal study, and demonstrated flexibility commensurate to the range of the native ear. Image analysis revealed specific areas of the framework that are at increased risk for dimensional changes during in vivo growth. The magnitude of bending forces experienced by the ear during implantation were also calculated from the image studies. Knowledge of these forces will aid in scaffold design and guide the selection of new candidate materials and manufacturing approaches. Based on these results, 3D printing technologies have been targeted as a method to further reduce dimensional changes during implantation.wThese rapid prototyping processes are capable of increased precision and accuracy, and could lead to the development of patient-specific shapes for the ear scaffold.

Poster Number 3

Cha, Thomas MD
Assistant Professor, Orthopaedics
tcha@partners.org

Cortical Thickness and Endplate Shape of Cervical Spine—Implication for Cervical Arthroplasty

Investigators: Thomas Cha, MD; Shaobai Wang, PhD; Qi Yao, MD; Kirkham Wood, MD; Guoan Li, PhD

Endplate preparation and drilling is necessary during cervical disc arthroplasty (CDA). Inappropriate removal of the endplate may damage the structural integrity of the cortical bone and cause strength related problems such as implant subsidence. The objective of this study was to quantify the cortical thickness and endplate shape to provide 3D guidelines regarding the amount of endplate removal during CDA.

CT scans of the subaxial cervical spines of 40 normal asymptomatic cervical spine subjects (20 men and 20 women, mean age 38.2 years) were analyzed. Bony endplates from C3 to C7 (a total of 400 endplates) were digitized and 3D reconstructed. Local cortical thickness and local height were measured along the endplate normal direction using custom Matlab codes (Fig 1). To keep cortical integrity, safe region was assumed to be the region that the bony endplate can be grind to flat without exposing trabecular bone (Fig 1). Safety index was defined as the percentile of safety region with respect to the whole endplate region, and calculated in both mid-sagittal and mid-coronal planes.

The cortical structures were typically thinner in the middle and thicker at the outer rim, ranging from 0.8 to 1.6 mm (Fig 1). The bony endplates in general formed concave shapes, lower in the center and higher at anterior and posterior (minimum-maximum difference of about 2 mm). In the sagittal direction, it was safer to remove the superior disc endplates than the inferior endplates (safety indices 84%-94% vs. 74%-78%, respectively). However in the coronal direction, it was less safe to remove the superior disc endplates than the inferior endplates (safety indices 66%-80% vs. 83%-95%).

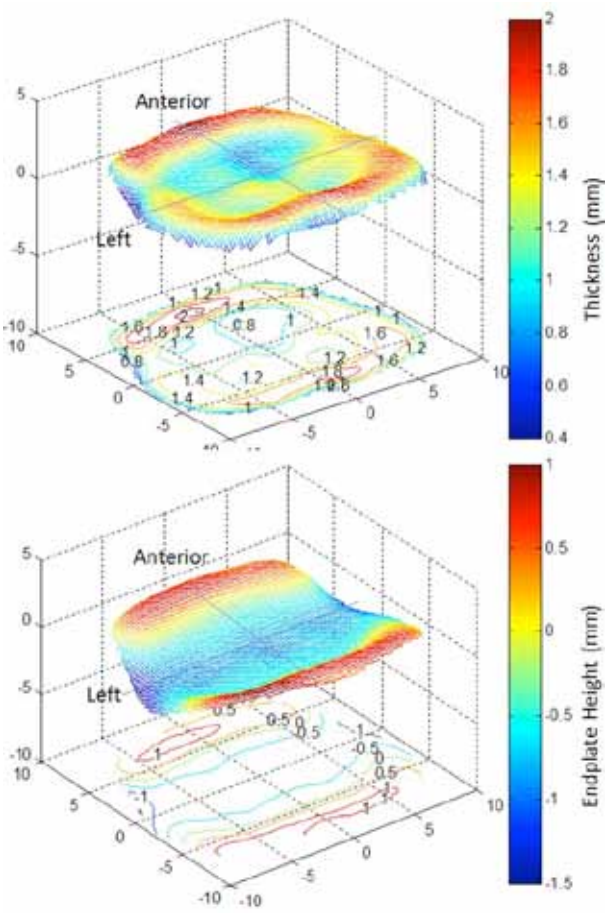

It is important to know how much endplate can be safely removed for cortical structure integrity to withstand implant subsidence. From our results, endplate removal is safer for the superior disc endplates in the sagittal direction and the inferior endplates in the coronal direction. The difference can be related to the complicated yet different 3D curvatures of superior and inferior endplates in sagittal and coronal planes. Future investigations can calculated the safety index in other directions relevant to CDA implantation. These findings may guide surgical technique of endplate preparation during CDA and help implant design.

Poster Number 4

Chenelle, Christopher BA
Research Technician, Anesthesia, Critical Care and Pain Medicine
cchenelle@partners.org

A comparison of leak compensation in adult acute care ventilators during pediatric non-invasive ventilation; a lung model study

Investigators: Christopher T. Chenelle, BA; Jun Oto, MD, PhD; Andrew D. Marchese, BS; Robert M. Kacmarek, PhD, RRT, FAARC

Introduction: Ventilators used for non-invasive ventilation (NIV) must be able to synchronize in the presence of system leaks. We compared the ability of 9 ventilators to compensate for leaks during pediatric NIV.

Hypothesis: Some ventilators are not suitable for pediatric use due to ineffective leak compensation.

Methods: Using an ASL5000 lung simulator, the Maquet Servo-i, Drager V500, Drager Carina, Covidien PB840, Respironics V60, Respironics Vision, General Electric Carestation, CareFusion Avea, and Hamilton C3 were compared during increasing (n=6) and decreasing leaks (n=6). Leak levels used were: BL (baseline of 2–3 L/min), L1 (5–6 L/min), L2 (9–10 L/min) and L3 (19–20 L/min). Three patient sizes (10, 20, and 30 kg) with three different lung mechanics (normal, obstructive, and restrictive) were simulated by the ASL5000. Ventilator settings included non-invasive ventilation mode, pressure support ventilation at 10 cmH2O, and PEEP 5 cmH2O. The percentage of properly triggered breaths delivered by the ventilator in response to inspiratory demand of the lung simulator, or the rate of synchronization, was recorded for each scenario.

Results: The median rate of synchronization across all ventilators was 65% (range: 0%–99%). Significant differences in the rate of synchronization were observed between the 10 kg (synchronization rate: 24%; range: 0%–97%), 20 kg (56%; 0%–99%), and 30 kg models (72%; 19%–99%) ($p < 0.0001$). The synchronization rate in the obstructive model (31%; 0%–98%) was significantly lower than the normal (68%; 0%–98%) and restrictive (71%; 0%–99%) models ($p < 0.0001$). Significant differences existed between the ventilators (0%–98%, $p < 0.0001$). The PB840 and the Carina were the only ventilators with synchronization rates greater than 90%.

Conclusions: In this study we show that leak compensation in NIV for pediatric use can partially compensate for leaks, but varies significantly across ventilators, patient weights, and lung mechanics. The ability of ventilators to synchronize diminishes with smaller patients and obstructive lung conditions. Significant differences exist between the performances of commercially available ventilators for NIV in pediatric patients.

BASIC–OTHER

Poster Number 5

Giedt, Randy J. PhD
Research Fellow, Center for Systems Biology
giedt.randy@mgh.harvard.edu

Single cell analysis of drug distribution by intravital imaging

Investigators: Randy J. Giedt, PhD; Peter D. Koch, BS; Ralph Weissleder, MD, PhD

Recent advances in the field of intravital imaging have for the first time allowed us to conduct pharmacokinetic and pharmacodynamic studies at the single cell level in live animal models. Due to these advances, there is now a critical need for automated analysis of pharmacokinetic data in intravital imaging. To address this, we have developed a novel algorithm specifically designed for analysis of intravital images. We began by surveying common thresholding methods on a representative set of intravital images to determine which would be most appropriate for identifying fluorescently labeled drugs. We utilized this analysis to develop a segmentation algorithm that allows semi-automated analysis of pharmacokinetic data at the single cell level. Specifically, data such as single cell variability of drug concentration over time, single cell drug concentration over time, the number of cells receiving a therapeutic dose of drug, and the cytosolic versus nuclear fraction of drug localization were designed as outputs in the algorithm. This segmentation algorithm was verified on intravital imaging videos of a fluorescently labeled PARP inhibitor, a system where pharmacokinetics is of particular interest. Ultimately, we were able to show that drug concentrations can indeed be extracted from serial intravital imaging in an automated fashion. We believe that the application of this algorithm will be of value to the analysis of intravital microscopy imaging particularly when imaging drug action at the single cell level.

Poster Number 6

Golberg, Alexander PhD
Research Fellow, Surgery
agolberg@partners.org

Regeneration and Control of Human Fibroblast Cell density by Intermittently Delivered Pulsed Electric Fields

Investigators: Alexander Golberg, PhD; Marianna Bei, DMD, PhD; Robert L. Sheridan, MD; Martin L. Yarmush, MD, PhD

Proliferative scarring is a human disease with neither available effective treatment nor relevant animal model. One of the hypotheses for scar formation involves deregulation of fibroblast signaling and delayed apoptosis. Here we introduce a new chemical-free method for fibroblast density control in culture by intermittently delivered pulsed electric fields (IDPEF), which cause irreversible damage to cell membranes. Using 5-100 pulses with electric field strength of 150 V mm-1, pulse duration 70 μs, and frequency of 1Hz, we investigated the effects of pulsed electric field application on growth, death, and regeneration of normal human dermal fibroblasts in culture. We found that the fraction of fibroblasts that survive depends on the number of pulses applied and follows a Weibull distribution. We have successfully developed an IDPEF protocol that controls fibroblasts density in culture within predicted limits. Specifically, through application of IDPEF every 72 hours for 12 days, we maintain a normal human dermal fibroblast density of 43±4–100% confluence. Our results suggest that IDPEFs may prove useful as a non-chemical method for fibroblast density control in human wound healing.

Poster Number 7

Goldman, Julian MD
Instructor, Anesthesia, Critical Care and Pain Medicine
jmgoldman@partners.org

Medical Device Clock Time Errors in the Hospital

Investigators: Julian Goldman, MD; Susan Whitehead; David Arney; Pratyusha Mattegunta, MS

Medical device integration is forcing healthcare technology management departments to focus on new challenges, and one of them is getting devices in sync when it comes to time. Time discrepancies can lead to patient care delays and inaccurate time stamps on data in patient records. Observation shows that medical device clocks are frequently not set to the correct time, due to multiple causes. Most medical devices lack automatic clock-setting capabilities and cannot set their clocks using a network time reference. Also, there is no adopted standard for medical device time management. Consequently, clocks are typically set manually twice yearly for Daylight Savings Time (DST).

Most electronic medical devices contain an internal clock that is used to time-stamp data. Depending on EHR configuration and the data source, the EHR may insert incorrectly time-stamped data into the wrong time slot or reject the data altogether. Therefore, asynchronous time stamps may undermine the integrity of EHR data and the accurate reconstruction of clinical events or device failures.

To explore the problem, we recorded a sample of medical device clocks from the operating rooms, ICUs, and Biomedical Engineering equipment storage facilities at Massachusetts General Hospital (Boston, MA). Device clocks were compared to the NIST Internet Time Service for clock consistency and to evaluate the deviance of the device clocks. Of 337 device clock-times we recorded, two displayed the wrong date and were eliminated from calculation of the mean offset of the devices in order to prevent skewing the data. Of the 335 remaining devices, 177 of them displayed in seconds: 53% had an offset of >1 min, 17% had an offset of >30 minutes, and 11% had an offset of >1 hour. The maximum offset was observed to be 3 hours 27 minutes on an infusion pump. The average offset was ~13 minutes, with a standard deviation of ~29 minutes.

This pilot study supports anecdotal data and first principles that erroneous clock times from medical devices are pervasive. Given the absence of automatic clock-setting capabilities in most medical devices, and typical clock drift, these findings are not surprising. However, these findings underscore the need for a solution that ensures accurately time-stamped device data in the EHR. We have extended this study to other top institutions in the US and to different care areas (e.g. emergency room). We have captured more detailed information about the status of these medical devices—if they are standalone or connected to a network, if they display accuracy in minutes or in seconds, and how often the clocks on these devices get updated—during repairs or twice every year during DST—in order to collect and analyze a sufficient body of data to document this important problem and to encourage consensus solutions by industry. Another part of this study will examine resources for adjusting clocks to a standard time, which is sorely lacking in the healthcare field now. We are also conducting an open survey with questions designed to capture data from other healthcare technology management professionals.

Poster Number 8

Hamarneh, Sulaiman MD
Research Fellow, Surgery
shamarneh@partners.org

Intestinal Alkaline Phosphatase Prevents Acute Alcohol-Induced Liver Injury in Mice

Investigators: Sulaiman R. Hamarneh[1], MD; Kanakaraju Kalliannan[1], MD; Mussa M. Rafat Mohamed[1], MD; Konstantinos P. Economopoulos[1], MD; Palak Patel[1]; Abeba Teshager[1], BS; Nondita S. Malo[1]; Seyed M. Abtahi[1], MD; Nur Muhammad[1], MD; Omeed Moaven[1], MD; Atri Raychowdhury; Sayeda N. Alam[1], MD; Atul K. Bhan[2], MD; Madhu S. Malo[1], MD; Richard A. Hodin[1], MD,
[1]Department of Surgery, Massachusetts General Hospital, Harvard Medical School, Boston, MA
[2]Department of Pathology, Massachusetts General Hospital, Harvard Medical School, Boston, MA

Bacterial endotoxin (LPS) plays a major role in the activation of Kupffer cells, production of inflammatory mediators and the pathogenesis of alcoholic liver injury. The brush-border enzyme intestinal alkaline phosphatase (IAP) dephosphorylates LPS, reduces endotoxemia and prevents LPS-induced inflammation. In this study, we sought to investigate whether oral IAP supplementation could protect against acute alcohol-induced liver injury. C57BL/6 female mice were treated with a single or multiple binge ethanol doses [6 or 5 g/kg body weight] by gastric gavage +/- pre-treatment, simultaneous treatment or post-treatment (n=5) with varying doses of IAP [100U or 200U/gavage]. Control mice were gavaged with dextran-maltose. Mice were sacrificed at different times and investigated for hematological, inflammatory and histopathological liver changes. In the single dose study, pretreatment with IAP resulted in significantly lower serum ALT than the ethanol group in a dose dependent fashion (38% inhibition with IAP 200U). Simultaneous-treatment with IAP (100U) also lowered serum ALT (EtOH vs. EtOH + simIAP= 110 ± 6.6 vs. 89.8 ± 5.7U/L, p=0.04). In contrast, there was no beneficial impact in the post-treatment group. In the 3 dose study, pretreatment with IAP (200U) significantly lowered serum LPS (EtOH vs. EtOH + IAP= 2.1 ± 0.35 vs. 1.0 ± 0.21EU/ml, p=0.027), serum ALT (EtOH vs. EtOH + IAP=114 ± 16.1 vs. 68.9 ± 6.7U/L, p=0.034) and protected against hepatic steatosis (EtOH vs. EtOH + IAP= 4 vs. 2, Hepatic Steatosis Score). Furthermore, hepatotoxicity due to acute ethanol administration was further evidenced by elevated liver TNF-alpha which was also attenuated by IAP (EtOH vs. EtOH + IAP= 80.44 ± 7.9 vs. 55.01 ± 7.0 pg/mg protein, p=0.035). Here we show that treatment with Oral IAP protected mice from acute alcohol-induced hepatotoxicity and steatosis. Oral IAP supplementation could represent a novel therapy to prevent against alcoholic liver disease in humans.

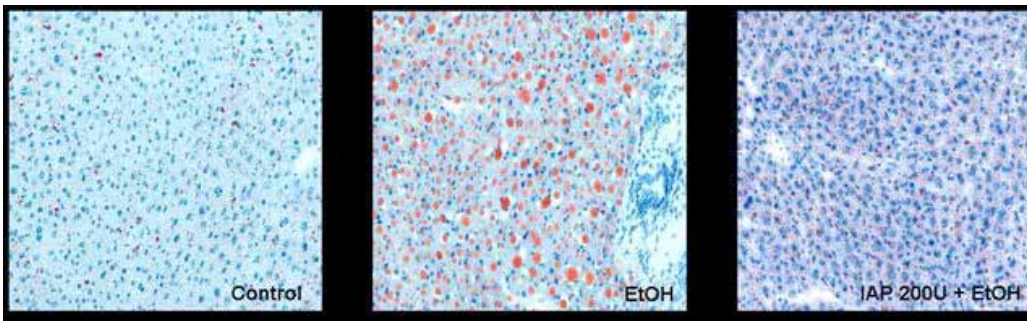

Figure 1. IAP protects from acute alcoholic liver steatosis

Hazan, Ronen PhD
Research Fellow, Surgery
hazan@molbio.mgh.harvard.edu

Poster Number 9

Auto-poisoning of the Respiratory Chain by secreted Molecule Leads to Beneficial bacterial Programmed Cell Death

Investigators: Ronen Hazan, PhD; Yok-Ai Que, PhD, MD; Benjamin Strobel, MA; Paul Anthony Majcherczyk, PhD; Laura Rose Hopper; Laurence G. Rahmea, PhD

Programmed cell death (PCD) in bacteria provides exceptionally strong evidence of multicellular behavior, wherein bacteria cells coordinate their actions to function like one organism. We found that 2-n-heptyl-4-hydroxyquinoline-N-oxide (HQNO), a Pseudomonas aeruginosa low-molecular-weight quorum-sensing regulated excreted molecule, triggers beneficial autolytic PCD. This self-induced PCD results from an inhibition of cytochrome b1 by HQNO and subsequent massive production of reactive oxygen species (ROS) that reduces membrane potential and disrupts membrane integrity. In turn, as a result of cell autolysis, cellular nutrients and DNA are released, allowing a subpopulation of cells to survive, re-grow, and form biofilms. The HQNO-dependent PCD mechanism described here is reminiscent of the opening of mitochondrial permeability transition (MPT) pores that initiates eukaryotic apoptosis and may suggest that the latter originated from a bacterial PCD mechanism.

Hou, Steven BS
Graduate Student, Radiology
shou@fas.harvard.edu

Poster Number 10

Whole body time-domain diffuse optical tomography of mice

Investigators: Steven S. Hou, BS; William L. Rice, PhD; Brian J. Bacskai, PhD; Anand T. N. Kumar, PhD

Near infrared (NIR) time-domain diffuse optical tomography (TD-DOT) is an attractive modality for non-invasive in vivo imaging in both clinical and pre-clinical (small animal model) settings. The use of TD-DOT is advantageous because of its use of non-ionizing, low energy NIR photons (wavelengths from 700 nm to 1000 nm), and its relative low cost compared to other imaging technologies such as X-ray computed tomography or magnetic resonance imaging. For quantitative measurements and tomographic reconstructions of intrinsic (oxy/deoxy hemoglobin) and extrinsic (fluorescence molecular imaging) contrast, an accurate knowledge of tissue optical properties and their distribution is essential. Previous studies of TD-DOT for optical property mapping have primarily focused on tissue mimicking phantoms, while most small animal tomography studies rely on assumptions of homogeneous optical properties throughout the animal.

Here we describe the development of a TD-DOT system with the capability of imaging the three dimensional distribution of intrinsic optical properties (absorption and scattering) in intact, living mice. This instrument captures time-resolved (picosecond to nanosecond scale) images of light from multiple point sources, transmitted though the mouse. This data is then used to reconstruct the distribution of the optical properties using the Gauss Newton method with photon propagation modeled by a full time-domain finite element method (FEM) solution to the diffusion equation.

We observe several orders of magnitude of variation in NIR light transmission across the mouse body, suggesting a large heterogeneity in intrinsic optical properties. This variation in transmission also results in a large dynamic range in the measured signal. To overcome this challenge, we modified the acquisition software to allow dynamic power adjustments. We have also incorporated spatial masking of detectors as a way to improve the overall measured signal quality. Our system was further calibrated using liquid phantoms of known optical properties. Preliminary optical property reconstructions of nude mice indicate a large variation in the 3D absorption/scattering distributions across regions that correspond to the heart, brain, lungs, liver and bladder. We will further explore the use of CT co-registered images to enhance the optical reconstructions. CT images will be used for both anatomical identification of organ specific optical properties and to provide structural priors for the optical reconstructions. We anticipate that the system and algorithms presented in this work will serve as a robust imaging tool for screening both intrinsic and extrinsic contrast in small animal models of disease.

Poster Number 11

Kulig, Katherine M. BS
Research Technician, Center for Regenerative Medicine
kkulig@partners.org

Biologic properties of surgical mesh materials derived from dermal ECM

Investigators: Katherine M. Kulig, BS; Xiao Luo, MD; Eric B. Finkelstein, PhD; Xiang-Hong Liu, PhD; Scott M. Goldman, MS; Cathryn A. Sundback, ScD; Joseph P. Vacanti, MD; Craig M. Neville, PhD

Surgical mesh scaffolds manufactured from donor human or animal tissue are increasingly being used to promote soft tissue repair and regeneration. The clinical product consists of the residual extracellular matrix remaining after a rigorous decellularization process. Optimally, the material provides both structural support during the repair period and cell guidance cues for effective incorporation into the regenerating tissue. Surgical mesh materials are available from several companies and are unique products manufactured by proprietary methodology. A significant need exists for a more thorough understanding of scaffold properties that impact the early steps of host cell recruitment and infiltration. In this study, a panel of in vitro assays was used to make direct comparisons of several similar, commercially-available materials: Alloderm, Medeor Matrix, Permacol, and Strattice. Differences in the materials were detected for both cell signaling and scaffold architecture-dependent cell invasion. Material-conditioned media studies found Medeor Matrix to have the greatest positive effect upon cell proliferation and induction of migration. Strattice provided the greatest chemotaxis signaling and best suppressed apoptotic induction. Among assays measuring structure-dependent properties, Medeor Matrix was superior for cell attachment, followed by Permacol. Only Alloderm and Medeor Matrix supported chemotaxis-driven cell invasion beyond the most superficial zone. Medeor Matrix was the only material in the chorioallantoic membrane assay to support substantial cell invasion. These results indicate that both biologic and structural properties need to be carefully assessed in the considerable ongoing efforts to develop new uses and products in this important class of biomaterials.

Poster Number 12

Mwizerwa, Olive BA
Research Technician, Center for Regenerative Medicine
omwizerwa@partners.org

Engineered Skeletal Muscle for Cranioaxillofacial Reconstruction

Investigators: Olive Mwizerwa, BA; Thomas Cervantes, BS; Katherine Kulig, BS; Jeffrey Widrick, PhD; Irina Pomerantseva, MD, PhD; Craig Neville, PhD; Cathryn Sundback, ScD

Military and civilian trauma can cause extensive damage to craniofacial tissue. A non-functional orbicularis oculi (eyelid) often leads to blindness. Surgical repair can be performed by allogeneic muscle transplantation, but it requires life-long immunosuppression. Engineered autologous skeletal muscle eliminates the risks associated with allogeneic sources but must be strong, highly vascularized and innervated to be functional. We established a prevascular network within engineered muscle tissue which anastomosed with the host vasculature upon implantation. We hypothesize that establishing neuromuscular junctions in vitro in the engineered skeletal muscle using embryonic spinal cords will facilitate innervation by the host when implanted. Furthermore, using electrical stimulation in vitro may create stronger and larger muscle constructs.

Skeletal muscles were engineered using primary myoblasts and fibroblasts on fibrin gel. Microvascular networks were engineered within the muscle using a vasculogenesis approach. HUVECs (human umbilical vein endothelial cells) and MSCs (mesenchymal stem cells) were co-cultured with myoblasts and fibroblasts, forming an endothelial-lined network within the muscle tissue. Vascularized engineered muscles were implanted into immunocompromised mice for periods of up to 21 days. Prior to harvest, the mice were injected with Evans blue or dextran FITC to assess maturation of the engineered vasculature. The vasculature was also characterized through immunohistochemistry against endothelial markers.

Neuromuscular junction (NMJ) formation was examined in vitro. E12 rat spinal cord explants were added to engineered muscles at either 0 d or 2 d differentiation. At 10 d differentiation, immunohistochemistry was performed to detect NMJs.

An electrical bioreactor was used to culture engineered muscles. At 10d of differentiation, muscle constructs were stimulated for 24 or 48hrs. The muscles' cross-section area and force production was measured before and after stimulation. Myotube alignment and hypertrophy were characterized through immunohistochemistry.

Vascularization, innervation and force production of engineered muscle were characterized. After implantation, the engineered human endothelial-lined networks successfully anastomosed with host vasculature and were perfused with blood by 1 d post-implantation. By 3 weeks, the engineered blood vessels had remodeled and matured to form a vasculature characteristic of native skeletal muscle.

Neurite outgrowth from E12 rat spinal cord explants formed NMJs in vitro in engineered muscles; innervation enhanced myotube hypertrophy and alignment. Electrically stimulated engineered muscles also had greater hypertrophy and better alignment. The stimulated muscles produced a significantly greater force than un-stimulated constructs.

Using vasculogenesis, an endothelial-lined network was established within the engineered muscle in vitro which was perfused in less than 1d post-implantation. Using embryonic spinal cords explants, NMJs were established within the engineered muscles, which will likely facilitate innervation of engineered muscle upon implantation. Electrically stimulating engineered muscles produced stronger constructs. Important milestones have been achieved toward developing functional replacement skeletal muscle for facial reconstruction.

Poster Number 13

Nichols, Alexander BA
Graduate Student, Wellman Center for Photomedicine
ajnichol@fas.harvard.edu

Mapping oxygen tensions in an avascular, 3D in vitro tumor model using novel optical oxygen sensors

Investigators: Alexander J. Nichols, BA; Emmanuel Roussakis, PhD; Conor L. Evans, PhD (Principal Investigator)

Recent work has suggested that hypoxic regions in cancerous tumors harbor a pernicious population of robust and therapy-resistant cells. These cells evade death during therapy and often go on to reform untreatable disease. Although hypoxia has been associated with therapeutic resistance, few tools currently exist that allow high-resolution spatial mapping of oxygen tension in living systems. Without such technology, it is difficult or impossible to quantitatively study the differences in therapeutic response between normoxic and hypoxic cancer cells and analyze how each population behaves in the hours, days, and weeks after therapy.

Although several methods can be used to image tissue oxygen, few are compatible with real-time in vivo applications; of these, only optical microscopy techniques are capable of providing cellular-level resolution. In one such technique, known as phosphorescence lifetime imaging (PLI), certain photoexcited emissive molecules, such as porphyrins, can be used to generate optical contrast through the oxygen sensitivity of the lifetime of their electronically excited state. These approaches thus require delivery of the oxygen sensing molecule throughout the area to be imaged–a challenging problem for imaging avascular, hypoxic regions deep inside tumors. Problematically, current commercially available porphyrin-based "dendritic" sensors, which contain a porphyrin core surrounded by "dendrons" which provide chemical functionality, are compatible only with intravascular imaging, rendering them inherently unable to penetrate into solid tumors that host hypoxic environments. Furthermore, the majority of PLI systems are slow, expensive, and incapable of providing the 3D, cellular-level resolution required to comprehensively understand oxygen distribution in tumors. In contrast, porphyrin sensors based on a ratiometric platform, in which the oxygen sensitive signal is referenced to an oxygen-independent emission generated by a different chromophore within the same dendrimer, can be imaged using straightforward confocal microscopy.

Our work aims to solve these problems through the development of a new class of tissue-permeable porphyrin dendrimers as well as the construction of custom optical imaging systems based on a ratiometric detection platform. In developing our sensors, we have adopted a bottom-up, modular approach which allows us to synthesize the appropriate oxygen sensing porphyrin core and functionalize it with custom-made, polycationic dendrons which serve both to enhance the core's sensitivity to oxygen as well as to allow it to move rapidly through avascular tissue regions. The porphyrins under development exhibit dramatically improved brightness relative to current sensors and emit in the near-infrared region of light, allowing for improved optical penetration through tissue.

To demonstrate proof-of-concept, we report the synthesis, characterization, and application of a near-infrared (NIR) oxygen sensor based on the well-characterized palladium(II)-tetrabenzoporphyrin core that is capable of penetrating into large in vitro 3D models of metastatic ovarian cancer. Using a custom-assembled laser scanning confocal microscope specially optimized to collect low-levels of NIR phosphorescence, we demonstrate fully calibrated ratiometric oxygen measurements in living cells.

Poster Number 14

Oto, Jun MD, PhD
Research Fellow, Anesthesia, Critical Care and Pain Medicine
joto@partners.org

A comparison of leak compensation in acute care ventilators during non-invasive ventilation; a lung model study

Investigators: Jun Oto, MD, PhD; Christopher Chenelle, BA; Andrew D. Marchese, BS; Robert M. Kacmarek, PhD, RRT

Ventilators used for non-invasive ventilation (NIV) must be able to synchronize in the presence of system leaks. We compared the ability of 8 ventilators to compensate for leaks during NIV.

Using an ASL5000 lung simulator, the Maquet Servo-i, Drager V500, Covidien PB840, General Electric Carestation, CareFusion Avea, Respironics V60, Hamilton C3 and Hamilton G5 were compared during increasing (n=6) and decreasing leaks (n=6). Leak levels used were: BL (baseline 3–4L/min), L1 (9–10L/min), L2 (26–27L/min) and L3 (35–36L/min). Lung model inspiratory and expiratory resistance were 10, and 20 cmH2O/L/sec with compliance 60 ml/cmH2O (COPD model) and inspiratory and expiratory resistance 5, and 5 cmH2O/L/sec with compliance 20 ml/cmH2O (ARDS model). Ventilator settings were non-invasive ventilation mode, pressure support, PEEP5, and 10 cmH2O and pressure support level 12 cmH2O. The number of breaths to synchronization was recorded for each leak scenario.

Servo I, PB840, C3, and V60 exhibited synchronization to increasing and decreasing leaks in both the COPD and ARDS models for all scenarios. G5, Carestation and V500 could not synchronize to leaks L2 and L3. Avea could not synchronize all leak scenarios. Number of breaths to synchronization for increasing leaks differed from decreasing leak with median breaths (25th, 75th) of 3 (1, 4) and 0 (0, 1) ($p < 0.001$) respectively. Significant differences were observed for number of breaths to synchronization between PEEP 5 cmH2O 1 (0, 3) and 10 cmH2O 2 (0, 4) ($p < 0.001$), but not with the COPD 2 (0, 4) and ARDS model 2 (0, 4) ($p=0.61$). PB840 required less breath to synchronize to increasing and decreasing leaks compared with all other ventilators ($p < 0.001$).

The leak compensation in non-invasive ventilation modes can correct partially or completely for leak interference within 4 breaths, but there are wide variations between ventilators.

Poster Number 15

Paunescu, Teodor PhD
Instructor, Medicine
tgp@partners.org

High resolution helium ion microscopy of the rodent kidney and epididymis

Investigators: Teodor G. Paunescu, PhD; Chuong Huynh, BS; Lorenz Lechner, PhD; Bernhard Goetze, PhD; Lewis Stern, MS; Sylvie Breton, PhD; Dennis Brown, PhD

Helium ion scanning microscopy (HIM) is a novel imaging technology that has the potential to produce nanometer resolution images of uncoated biological samples. We applied this technology to explore the epithelia of the rat and mouse kidney and male reproductive tract. We found that high contrast, high resolution imaging of the investigated epithelial tissues is possible with a relatively simple processing procedure that consists of transcardial perfusion with aldehyde fixatives, vibratome tissue sectioning, tissue dehydration with graded methanol solutions and careful critical point drying. HIM allows the visualization of fine cellular and plasma membrane details, including depressions suggesting endo- or exocytotic events, cilia, and microvesicles. In the kidney, membranous nanoprojections on podocytes and pores within the filtration slit diaphragm were seen in the glomerulus, and extensive apical microplicae of the intercalated cells in the collecting duct. In the epididymis, stereocilia in principal cells and microplicae in clear cells are clearly distinguishable, and high resolution imaging of sperm reveals their close interaction with the epithelium. We also demonstrated the use of colloidal gold probes for highlighting specific cell-surface proteins and found that 15 nm gold labels are both practical and easily distinguishable, indicating that external labels of various sizes can be used to detect multiple targets in the same tissue. In conclusion, this technology represents a major breakthrough in imaging of the topographical ultrastructure of biological samples and should provide significant advances in our understanding of cell surface structures and membrane organization. Funding sources: NIH DK42956, DK97124, and HD40793; Carl Zeiss Microscopy, LLC.

Poster Number 16

Reyes, Christopher BS
Research Technician, Orthopaedics
creyes5@partners.org

Oxidative Analysis of Surgically-Retrieved Moderately Cross-linked Acetabular Bearings

Investigators: Christopher R. Reyes, BS; Shannon L. Rowell, BS; Charles A. Engh, Jr., MD; Robert Hopper, PhD; Orhun K. Muratoglu, PhD

Total hip arthroplasty (THA) must replicate the ball and socket articulation of the acetabulum and the femoral head. A polymer known as ultra-high molecular weight polyethylene (UHMWPE) is the most commonly used bearing material in artificial joints. Conventional UHMWPE proved susceptible to high wear rates in vivo, leading to particulate-induced osteolysis and eventual implant revision. Radiation cross-linking was developed to improve wear resistance. Unless stabilized, free radicals formed during the irradiation process lead to oxidative degradation of the material. Post-irradiation melting is one method used to eliminate these free radicals. Irradiated and melted UHMWPE is considered oxidatively stable and has shown excellent clinical results and low wear up to 10 years in vivo. However, it has recently been discovered that lipids absorbed from synovial fluid in the joint are able to induce oxidation in otherwise oxidatively-stable materials. Therefore, the aim of this study was to investigate any in vivo oxidative changes that may be occurring in a subset of surgically-retrieved irradiated and melted UHMWPE acetabular bearings. Twenty-nine surgically-retrieved 50kGy -irradiated and melted UHWMPE MarathonTM acetabular liners with in vivo durations up to ten years were analyzed along with one never-implanted liner. Material properties of these liners were analyzed using (i) infrared microscopy to determine lipid absorption, oxidation and oxidation potential, (ii) differential scanning calorimetry to measure crystallinity and (iii) gravimetric swelling to assess cross-link density. We discovered that the irradiated/melted acetabular liners maintained their overall oxidative stability up to 10 years in vivo, but had begun to show subsurface material property changes associated with low level oxidation. These changes need to be monitored at longer in vivo durations to assess clinical implications over the next decade of in vivo service.

Poster Number 17

Rice, William PhD
Research Fellow, Radiology
wrice@nmr.mgh.harvard.edu

Fluorescence lifetime contrast for whole body imaging of multiple fluorophores

Investigators: William L. Rice, PhD; Anand T.N. Kumar, PhD

Fluorescent proteins have proven to be an invaluable tool in microscopy for highlighting proteins and cell types of interest. Currently these proteins are emerging as highly specific markers for whole body imaging.

While the use of spectrally different fluorescent proteins, such as Green and Red fluorescent protein offers the ability to measure multiple tissue and tumor types within the same animal, in practice, most fluorescent proteins have broad, overlapping excitation and emission spectral profiles. This, in addition, to the spectrally broad tissue autofluorescence in the visible spectrum has proven to be a significant impediment for whole body imaging of fluorescent proteins, requiring multiple spectral measurements and limiting the number of fluorescent proteins that can be reliably imaged simultaneously within the same animal.

Here we demonstrate that fluorescence lifetime contrast can be used for quantitative, non-invasive monitoring of spectrally similar fluorescent protein expressing tumor cells. Tissue autofluorescence exhibits a characteristic non-exponential decay that is distinct from the single exponential decay of fluorescent protein fluorescence. We show that this enables the quantification of low levels of FP cells from implanted pellets under the skin of a mouse cadaver.

We next apply lifetime unmixing to distinguish spectrally similar fluorescent proteins in cells expressing the red fluorescent proteins : mCherry, dsRed, and tdTomato placed subcutaneously in a mouse cadaver based on their measured lifetimes of 1.51 ns , 2.23 ns, and 2.69 ns respectively.

Currently we are exploring the use of lifetime based contrast to quantitatively monitor the growth of a mixture of GFP (2.5 ns) and mCherry (1.51 ns) mouse mammary tumors in vivo with a single excitation and emission wavelength pair. These two spectrally distinct fluorescent proteins are used so that our measurements can be verified ex vivo by flow cytometry.

The fluorescence lifetime based whole body imaging techniques presented here are applicable across a wide range of fluorescent protein tagged animal disease models and study designs, from planar imaging of multiple fluorescent proteins to fluorescence molecular tomography and the no-invasive tracking of metastasis throughout the animal.

Poster Number 18

Schuemann, Jan PhD
Instructor, Radiation Oncology
JSchuemann@partners.org

Nano-dosimetric Monte Carlo simulations of the bystander effect

Investigators: J. Schuemann, PhD; H. Paganetti, PhD; K.D. Held, PhD

The Radiation-Induced Bystander Effect is the phenomenon in which unirradiated cells exhibit irradiated effects as a result of signals received from nearby irradiated cells. The onset of the bystander effect depends on radiation type, lineal energy transfer, dose and cell type. However, the mechanisms producing this effect are still not understood. Recent cell experiments performed at the Brookhaven National Laboratory have investigated the bystander effect for AG01522 human diploid cells with different radiation modalities (protons and heavy ions) and fluences.

We utilize the Monte Carlo simulation tool TOPAS to investigate the radiation effects on the sub-cellular level. TOPAS, layered on top of the multi-purpose Geant4 simulation toolkit, is being developed by a team at MGH, SLAC Stanford Linear Accelerator and the University of California San Francisco. This tool aims to make Monte Carlo simulations accessible and easy-to-use for researchers and clinicians. We extended TOPAS to include track structure Monte Carlo simulations abilities through the Geant4-DNA package to investigate the effects of different radiation modalities at the nanometer scale.

We reconstructed the setup of the cell experiments in TOPAS. A 6-well plate is placed in a uniform beam of 300 MeV/u or 1GeV/u Fe ions or 1GeV protons (left figure). The AG01522 cells are approximated by 800 µm3 (40x20x1µm) voxels, their nucleus by 100 µm3 (10x10x1µm) voxels. Fluences of the incident particles matching the experimental setup were simulated for as low as 100 incident particles per cm2 and up to 5 million protons and 225,000 iron ions per cm2. Ion irradiations are found to cause radiation effects in more than just the traversed cell due to higher energetic delta electrons (middle figure), while proton irradiation effects were contained within a single cell.

In the cell experiments, bystander effects were observed starting at fluences of 200 (2000) iron ions of 300 MeV/u (1GeV/u) and 200,000 protons of 1GeV. Iron radiation caused higher energy deposition density and dose inside a cell.

Here we show that the onset of the bystander effect is found to have two dependencies, the number of cells receiving dose and the amount of energy deposited inside a cell (right figure). Due to the limited amount of experimental data points, the data of our simulations is not sufficient to draw a final conclusion. However, for the first time we could correlate the onset of the bystander effect to simulated radiation properties at the cell level, for all three data sets the bystander effect starts at a threshold value Bth = N D^2 > 3 µGy^2, where D is the dose deposited in a cell and N the number of cells receiving the dose. More cell experiment data is necessary to conclusively establish this threshold.

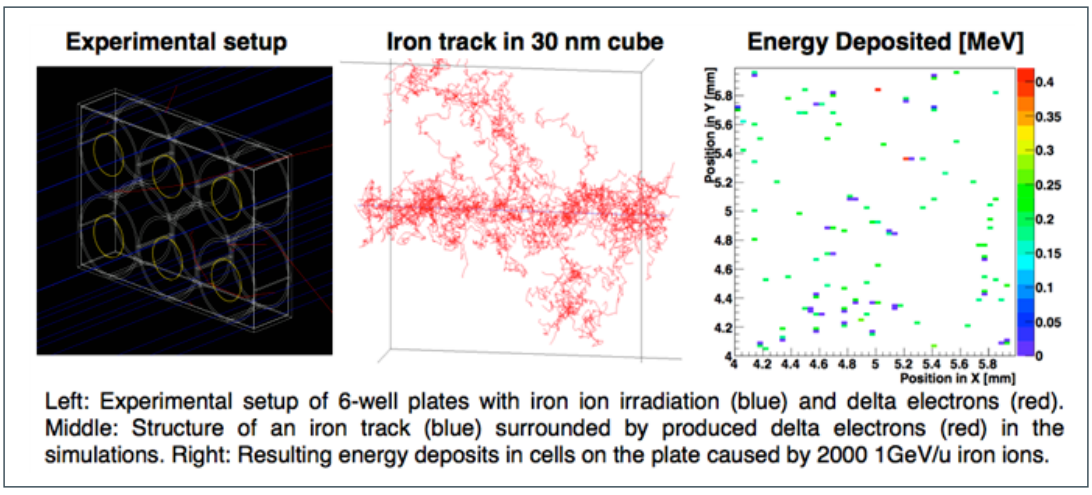

Left: Experimental setup of 6-well plates with iron ion irradiation (blue) and delta electrons (red). Middle: Structure of an iron track (blue) surrounded by produced delta electrons (red) in the simulations. Right: Resulting energy deposits in cells on the plate caused by 2000 1GeV/u iron ions.

Poster Number 19

Silberstein, Lev MD, PhD
Instructor, Center for Regenerative Medicine
lsilberstein1@partners.org

In-vivo single cell RNA-Seq analysis of osteolineage cells within the HSPC niche identifies interleukin-18 as a novel hematopoieitic regulator

Investigators: Lev Silberstein, MD, PhD; Peter Kharchenko, PhD; Mastake Osawa, PhD; Youmna Kfoury, PhD; Francois Mercier, MD; Charles P. Lin, PhD; David Scadden, MD

Despite substantial experimental evidence suggesting that osteolineage cells (OLCs) regulate hematopoietic stem and progenitor cell (HSPC) behavior, the molecular nature of OLC-HSPC cross-talk remains largely unknown. We hypothesized that OLCs adjacent to transplanted HSPC represent a distinct "niche OLC" population, which is enriched for HSPC-regulating molecules. We set out to define the molecular signature of this population in-vivo by comparative single cell RNA-Seq analysis of the individual col2.3GFP+ OLCs located proximally (<2 cell diameters) and distally (>5 cell diameters) from a single transplanted HSPC.

In order to address this question, we established a novel method of targeted single cell retrieval, which enabled micromanipulator-assisted aspiration of HSPC-proximal and HSPC-distal OLCs into a glass micropipette directly from live unfixed sections of neonatal mouse bone (Figure A).

We found that HSPC-proximal OLCs had a distinct transcriptional signature, both at the level of top 200 differentially expressed genes and genome-wide, as determined by using a blind classifier software (Figure B). HSPC-proximal OLCs were enriched for membrane-bound and secreted factors, consistent with their role in inter-cellular communication. Specifically, these cells displayed immature OLC phenotype (osteocalcinlow osterix +) and expressed higher level of known HSPC quiescence-inducing molecules (CXCL12, angiopoietin 1) and cell surface proteins CD106/VCAM1 and Embigin. Notably, the Q-PCR profile of FACS-sorted col2.3GFP+Embigin+CD106+ cell isolated from adult mouse bones recapitulated that of an individually picked single HSC-proximal niche OLCs (Figure C), indicating that despite massive amplification, the molecular differences detected by the single cell RNA-Seq assay can be reproduced at the cell population level.

We also noted that HSPC-proximal OLCs expressed a higher level of interleukin-18, a pro-inflammatory cytokine whose role in HSPC regulation has not been previously investigated in-vivo. We found that IL18 is involved in extrinsic control of HSPC quiescence. Under homeostatic conditions, IL18 KO mice had a decrease in the proportion of HSPCs in the G0 phase of the cell cycle (82% vs 87%), which was associated with a small (1.4-fold) reduction in the frequency of HSPCs in the bone marrow, presumably due to their loss through excessive proliferation. Upon transplantation, IL18-deficient microenvironment conferred significantly faster short-term reconstitution ability to WT bone marrow cells; this effect was further enhanced in secondary transplant recipients (Figure D). IL18 acted in a non-cell-autonomous manner, since we observed no difference in short-term reconstitution kinetics between IL18-deficient or normal bone marrow upon transplantation into WT recipients.

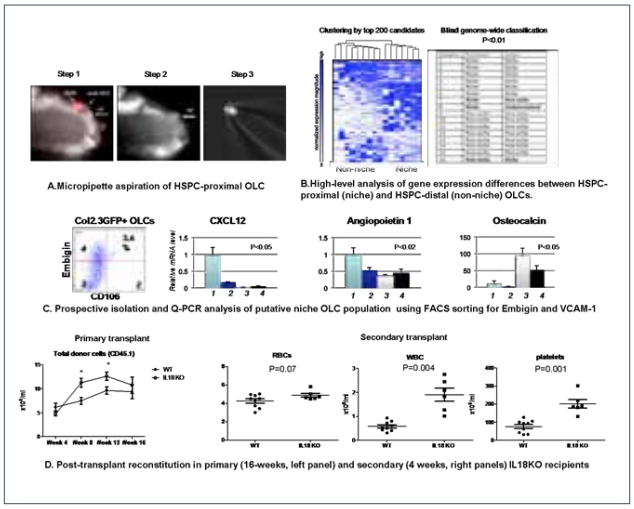

We conclude that our approach identified a rare population of niche OLCs which is likely to control HSPC quiescence. Furthermore, we uncovered a previously unknown role of IL18 as an HSPC quiescence regulator, and our data suggest that attenuating IL18 signaling may be clinically relevant in accelerating post-transplantation bone marrow recovery. More generally, our studies established and validated a novel experimental approach to the study of heterologous cell interactions in-vivo at the single cell level, and demonstrated—to our knowledge, for the first time—that single cell RNA-Seq assay can be used as a discovery tool for novel mediators of inter-cellular communication.

Poster Number 20

Spencer, Joel PhD
Research Fellow, Wellman Center for Photomedicine
spencer.joel@mgh.harvard.edu

Characterization of Bone Marrow pO2 by Two-photon Phosphorescence Quenching Method

Investigators: Joel A. Spencer, PhD; Francesca Ferraro, MD; Emmanoulis Yousakis, PhD; Alyssa Klein; Juwell Wu, PhD; Luke Mortensen, PhD; Clemens Alt, PhD; David Scadden, MD; Sergei Vinogradov, PhD; Charles P. Lin, PhD

Hematopoiesis is the process by which all blood cells and platelets originate from primitive hematopoietic stem cells (HSCs) and their committed progenitors. HSCs reside in specialize bone marrow (BM) compartments called 'niches' where they are retained in a quiescent state. Spontaneous failure along any point in the hematopoietic cascade can lead to dysfunction of the blood cell lineages and eventually to hematopoietic disorders such as leukemia and lymphoma. HSC maintenance and proliferation is dependent on intrinsic factors and extrinsic cues such as soluble molecules secreted by supporting cells such as osteoblastic, endothelial, and perivascular cells. One of the environmental cues thought to play a major role in hematopoiesis is molecular oxygen.

To date, quantitative measurement of BM vascular partial pressure of oxygen (pO2) has not been possible due to technical limitations. Here we show a system capable of high-resolution quantitative pO2 measurement in the vascular and extravascular compartments of the BM without damaging the native environment. We built an intravital two-photon imaging/oxygen sensing system capable of measuring in vivo BM pO2, and we used this tool to characterize BM vascular and extravascular pO2 in living mice. We found a steep drop in vascular pO2 as blood vessels enter the bone marrow, and as a result the BM vasculature is hypoxic compared to other vascular beds.

Furthermore, we found a decreasing pO2 gradient away from the endosteal zone toward the sinusoidal region of the BM. Thus, the osteoblastic niche near the endosteal surface, commonly thought to be the HSC niche, is not the most hypoxic region of the BM. Rather, the lowest pO2 reside in the perisinusoidal region away from the endosteum. Interestingly, preconditioning of BM with radiation or chemotherapy both lead to significant elevation of BM pO2, suggesting that the transplanted HSC is exposed to a microenvironment that is very different from the homeostatic situation, and the elevated pO2 may be an important determinant of HSC activity in the post-transplant microenvironment.

Poster Number 21

Sprinkhuizen, Sara PhD
Research Fellow, Radiology
sara@nmr.mgh.harvard.edu

Trabecular Bone Quality Measurements in Human Spine using MRI

Investigators: Sara M. Sprinkhuizen, PhD; Jerome L. Ackerman, PhD; Yi-Qiao Song, PhD

The microstructure of trabecular bone is an important measure for bone quality. For example, in osteoporosis, bone loss is reflected in microstructural changes of trabecular bone. However, the currently used bone screening modality, dual energy x-ray absorptiometry (DXA), does not account for the trabecular microstructure, since it assesses bone mineral density only.

An MRI technique that provides information on the microarchitecture of porous materials is the Decay due to Diffusion in the Internal Field (DDIF) technique. The DDIF-MRI technique allows for measuring bone microstructure, by probing the diffusion of water protons through the pore space of trabecular bone. Internal magnetic field gradients are present in the pores. These magnetic field gradients are caused by the magnetic susceptibility difference between the pore space (marrow) and the solid part (bone) and therefore depend on the microstructure of the bone. Diffusion of water through these magnetic gradient fields leads to MR signal decay. The amount of water signal decay has been shown to relate to the microstructure of trabecular bone in ex vivo bone samples on non-clinical MRI systems. Smaller pore spaces are reflected in stronger DDIF signal decay for water. Fat molecules have a significantly smaller diffusion constant and therefore do not exhibit the DDIF effect.

We have implemented the DDIF technique on a clinical MRI system for evaluation in human subjects. Our first aim was to test the hypothesis that the DDIF signal decay rate in trabecular bone correlates inversely with subject age in healthy volunteers, since larger trabecular pore spaces are known to occur in older people. Twenty generally healthy subjects between 18 and 80 years old are included in the experimental cohort. At this time 4 subjects between 23 and 62 years old have been scanned. The DDIF sequence was run on L2 vertebra in all subjects. Water and fat signal decays were analyzed separately. Fat did not show a DDIF effect, as expected. The DDIF decay rate for water varied amongst subjects and its relation with age will be determined at the end of the study.

Poster Number 22

Toiber, Deborah PhD
Research Fellow, Cancer Center
dtoiber@partners.org

SIRT6 recruits SNF2H to sites of DNA breaks, preventing genomic instability through chromatin remodeling

Investigators: Debra Toiber; Fabian Erdel; Dafne M. Silberman; Lei Zhong; Peter Mulligan; Karim Bouazoune; Carlos Sebastian; Claudia Cosentino; Barbara Martinez-Pastor; Sofia Giacosa; Agustina D'Urso; Anders Naar; Robert Kingston; Karsten Rippe; Raul Mostoslavsky

SIRT6 is a chromatin-bound protein from a family of NAD(+)-dependent deacetylases with roles in DNA damage, metabolism and cancer. Cells deficient in SIRT6 exhibit genomic instability, sensitivity to genotoxic damage and defects in DNA repair. However, the precise molecular mechanisms underlying these phenotypes remain unclear. Furthermore, whether SIRT6 may influence DNA repair as a modulator of chromatin accessibility remains poorly understood. In this study, we find that SIRT6 is one of the earliest factor recruited to sites of Double Strand Breaks (DSBs), serving two critical functions: SIRT6 recruits SNF2H, a member of the ISWI ATP-dependent chromatin remodeling family, and deacetylates histone H3 at lysine K56. Lack of SIRT6 and/or SNF2H impairs chromatin remodeling and increases sensitivity to genotoxic damage through epistatic pathways. These defects in chromatin remodeling inhibit recruitment of downstream repair factors, such as 53BP1. Remarkably, SIRT6 deficient mice have lower levels of chromatin-associated SNF2H in specific tissues such as brain, a phenotype accompanied by increased signs of DNA damage. Our results demonstrate that SIRT6 plays a critical role in recruiting a chromatin remodeler as an early step in the DNA damage response, indicating that proper unfolding of chromatin plays a rate-limiting role in this process. DNA damage accumulation has been linked to multiple human diseases, such as cancer, neurodegeneration and senescence. Our results indicate that Sirt6 may function in mammalian organisms to counteract environmental stressors to prevent DNA damage, offering putative therapeutic strategies against DNA damage dependent diseases.

Poster Number 23

Tran, Thanh-Nga MD,PhD
Instructor, Dermatology Service
ttran2@partners.org

Cutaneous Delivery of siRNAs for Dermatologic Applications

Investigators: Thanh-Nga T. Tran, MD, PhD; Eric Boyer; Garuna Kositratna, MD; Mehdi Khaled, PhD; Kevin Love; Suprabha Devi; Daniel Anderson, PhD; Dieter Manstein, PhD; Robert Langer, PhD; David E. Fisher, MD, PhD

Delivery of therapeutics to the skin has long been proven to be a very attractive option to treat a variety of skin diseases. By direct application of medication to the disease site of interest, the drug is rendered effective only locally, thus preventing systemic side effects. With new advances in biotechnology, new therapies are being developed to treat a variety of skin diseases recalcitrant to current treatment modalities. One of the newest and most exciting therapies is the use of small RNA molecules, called small interfering RNAs or siRNAs, to inhibit the expression of a gene involved in a disease pathway. These molecules can turn off many genes such as those involved in skin cancers, pigmentation disorders, and genetic skin diseases, thus allowing for a novel, powerful way to treat common and uncommon skin diseases. Unfortunately, the stratum corneum (SC) is a formidable barrier to drug delivery. Hence, the aim of our project is to use nanotechnology and state-of-the art drug delivery techniques to deliver siRNAs to the epidermis and dermis, the layers of skin most commonly affected in dermatologic diseases.

The most challenging aspect of cutaneous delivery of siRNAs is designing a delivery system that can pass through the stratum corneum. The second challenge involves the vehicle that can help siRNAs penetrate cells. Cells do not take up naked siRNAs effectively, so the siRNAs must be encapsulated in a vehicle that allows for effective cellular penetration. Finally, another challenge is to design a model that can best approximate human skin in vitro and in vivo as mouse skin is a poor substitute for human skin in terms of thickness of the epidermis and SC. We have exploited a naturally occurring compound that cleaves the extra-cellular portion of desmoglein 1, a desmosomal protein that binds corneodesmosomes together, as a potential way to remove the SC. For delivery into cells, our unique approach involves a library of small lipid-like molecules that can be quickly and efficiently synthesized to provide for a diverse group of carriers for the siRNAs. These can be screened in parallel to obtain the best delivery vehicle for the cells in the epidermis, primarily keratinocytes and melanocytes. Lastly, we have successfully developed an in vitro model of human skin using discarded breast reduction skin or abdominal surgery skin. We can grow this human skin in tissue culture as well as engraft the human skin onto immunodeficient mice. These mice will provide a useful model prior to testing in patients. We have shown effective delivery of siRNAs in an in vitro model of pigmentation, and also in xenografted mice. Our technique will hopefully open up a new frontier in treating skin diseases and can lead directly to clinical trials that will benefit patient care.

Poster Number 24

Wang, Shaobai PhD
Instructor, Orthopaedics
swang17@partners.org

Compensatory Scoliosis due to Coupled Bending Motion in the Dynamic Lumbar Twisting Motion–3D Analysis using Dual Fluoroscopic Image System

Investigators: Shaobai Wang, PhD; Jae-Hyuk Shin, MD; Qi Yao, MD; Jing-Sheng Li, MD; Thomas Cha, MD; Kirkham Wood, MD; Guoan Li, PhD

It is known that vertebral segments function synergistically to maintain the stability of the human spine. However, there is no data that have been reported on the coupled motions of the spine during functional dynamic motion. The purpose of this study is to investigate the characteristic motion patterns of human lumbar spine during dynamic human body twisting motion.

Eight asymptomatic subjects (M/F : 7/1; Age : 40-60 years old) were recruited with IRB approval. The lumbar segments of each subject was MRI scanned for construction of 3D models of the vertebrae from L2 to S1. The lumbar spine was then imaged using a biplane fluoroscopic system while the subject performed a dynamic twisting from maximal left to maximal right in a standing position. The in-vivo vertebral motion was reproduced using a 3D to 2D registration protocol. In this study, we analyzed the primary right-left twisting rotation and the couple right-left bending rotation of each vertebral segment with respect to the corresponding distal segment.

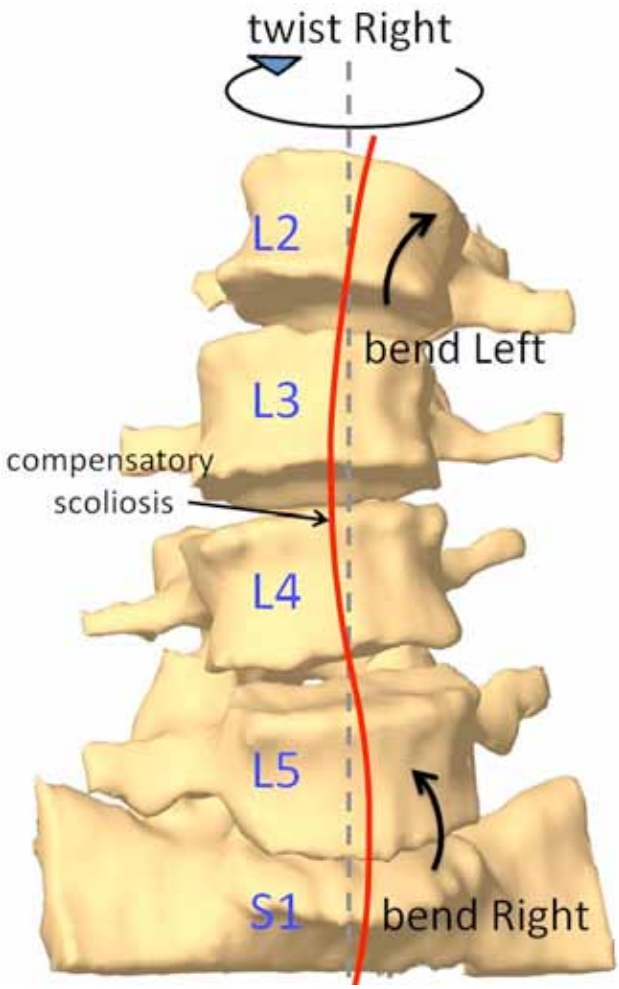

The primary axial rotations of all segments followed the direction of body twisting. The range of rotation of each segment were between 4.5°±1.2° to 6.7°±3.0° from maximum left to maximum right body twisting. The coupled bending ROMs were in general smaller than the primary twisting. The upper segments of L2-3 and L3-4 demonstrated a coupled contralateral bending towards the opposite direction of the twisting, while the lower segments of L4-5 and L5-S1 demonstrated a coupled ipsilateral bending motion toward the same direction of the twisting (Fig. 1). Strong correlation between the primary twisting and the coupled bending was found at each vertebral level with correlation coefficients $R2 > 0.5$ ($p<0.05$).

This balanced coupling pattern of multiple lumbar segments could create a de novo 'compensatory scoliosis', implying a coordination of the global balance of the whole body posture in diverse positions of the vertebrae. The different bending coupling could also result in varied shear deformation in the discs at different vertebral levels, implying a biomechanical mechanism that may be related to increased pathology in the lower levels. The data on coupling motion pattern could be further applied for advancement of exercise-based physiotherapy for low back pain and for optimization of a lumbar implant design that could better adapt to the physiologic lumbar motion.

Poster Number 25

Wang, Ying-Hua PhD
Instructor, Center for Regenerative Medicine
wang.ying-hua@mgh.harvard.edu

The Role of Glycolytic Metabolism in Hematopoiesis and Leukemogenesis

Investigators: Ying-Hua Wang, PhD; William Israelsen, BA; Dong-Jun Lee, PhD; Matthew Vander Heiden, MD, PhD; Clary B Clish, PhD; David Scadden, MD

It has been increasingly realized that different cell states employ different metabolic modes. Whether the metabolic mode is a determinant of cell state is unclear, but studies in cancer cells suggest that specific metabolic pathway is required for cancer cell survival and growth. Cancer cells metabolize glucose into lactate even in the presence of oxygen, a phenomenon known as aerobic glycolysis or the Warburg effect. Normal somatic cells thought to also preferentially use glycolytic metabolism are tissue stem cells, particularly the self-renewing hematopoietic stem cells (HSC) resident in the hypoxic microenvironment of the bone marrow. Recently the molecular basis for the Warburg effect in cancer cells has been identified as due to a specific isoform of pyruvate kinase M2 (PKM2). In contrast, normal tissues that rely on oxidative phosphoryation express the alternatively spliced isoform PKM1. Interestingly, we observed that cells in the hematopoietic lineage, including HSC, predominantly express PKM2. To understand the role of glycolytic metabolism in HSC as well as in hematological malignancy, we have developed genetically modified mouse strains that allow conditional deletion of PKM2 and LDHa. Our data show deletion of PKM2 leads to upregulation of PKM1, accompanied with decreased glycolysis and increased oxidative phosphorylation specifically in the hematopoietic stem/progenitor population. Under homeostatic conditions, no apparent changes in normal hematopoiesis were observed in PKM2-/- mice. Loss of PKM2, however, appears to compromise the long-term hematopoiesis as evidenced by the decreased reconstitution capacity in serial transplantation assay. Moreover, we also observed that deletion of PKM2 markedly disadvantaged the establishment of leukemia in mice when hematopoietic cells express human leukemogenic alleles. Similar phenotype was observed in mouse with depletion of LDHa, the enzyme converting pyruvate to lactate. These data suggest important roles of glycolytic metabolism in both normal hematopoiesis and leukemogenesis.

Poster Number 26

Yu, Binglan PhD
Instructor, Anesthesia, Critical Care and Pain Medicine
byu1@partners.org

Inhaled Nitric Oxide Attenuates the Adverse Effects of Transfusing Stored Syngeneic Red Blood Cells in Mice with Endothelial Dysfunction after Hemorrhagic Shock

Investigators: Binglan Yu, PhD; Chong Lei, MD, PhD; Mohd Shahid, PhD; Arkadi Beloiartsev, MD; Kenneth D. Bloch, MD; Warren M. Zapol, MD

Background: Transfusion of red blood cells (RBCs) stored for prolonged periods is associated in some retrospective and prospective studies with adverse clinic outcomes in patients. We investigated whether transfusion with stored RBCs would increase tissue injury, inflammation, oxidative stress and mortality (adverse effects of transfusing stored RBCs) in a murine model of hemorrhagic shock. We tested whether the adverse effects associated with transfusing stored RBCs were exacerbated by endothelial dysfunction (reduced bioavailability of nitric oxide) and ameliorated by inhaling nitric oxide.

Methods: We studied mice fed a high-fat diet (HFD-fed, 60% of calories from fat to induce endothelial dysfunction) or a standard diet (10% of calories from fat) for 4-6 weeks. Mice were subjected to 90 min of hemorrhagic shock, followed by resuscitation with leukoreduced syngeneic RBCs stored for less than 24 h (fresh RBCs) or stored for 2 weeks (stored RBCs).

Results: In standard diet-fed mice at 2 h after resuscitation, transfusion with stored RBCs increased tissue injury more than transfusion with fresh RBCs. The adverse effects of transfusing stored RBCs were more marked in HFD-fed mice and associated with increased lactate levels and short-term (up to 12 h) mortality. Compared with fresh RBCs, resuscitation with stored RBCs was associated with a reduction in P50 (increased oxygen affinity), increased plasma hemoglobin levels, and increased indices of inflammation and oxidative stress, effects that were exacerbated in HFD-fed mice. Inhaled nitric oxide reduced tissue injury, lactate levels, and indices of inflammation and oxidative stress, as well as improved short-term survival in HFD-fed mice resuscitated with stored RBCs.

Conclusions: Resuscitation with stored RBCs adversely impacts outcome in mice with hemorrhagic shock, an effect which is exacerbated in mice with endothelial dysfunction (e.g. HFD-fed mice). Inhaled nitric oxide reduces tissue injury and improves short-term survival in HFD-fed mice resuscitated with stored RBCs after hemorrhagic shock.

Poster Number 27

Yu, Vionnie PhD
Research Fellow, Center for Regenerative Medicine
vyu1@partners.org

Bone Cell Governance of T Lymphopoiesis

Investigators: Vionnie W.C. Yu, PhD; Sutada Lotinun, PhD; Borja Saez, PhD; Colleen Cook, BSc; Rushdia Yusuf, MD; Francesca Ferraro, MD; Stefania Lymperi, PhD; Marc Raaijmakers, MD; Joy Wu, MD; Henry M. Kronenberg, MD; Roland Baron, DDS, PhD; David T. Scadden, MD

Mesenchymal cell direction of parenchymal cell activity is hypothesized to be critical for adult tissue function, but remains poorly defined. We examined how specific subsets of osteolineage mesenchymal cells affect parenchymal hematopoietic cells in the bone marrow by a method of selective cell depletion. Here we report that mature bone cells expressing Osteocalcin (Ocn+) are unexpectedly critical for T lymphopoiesis through the modulation of cells destined for thymic emigration. Specific depletion of Ocn+ cells reduced the number of adult bone marrow T-lymphoid biased progenitors by reduced endosteal Delta-like Ligand (DLL4) production and hematopoietic progenitor Notch activation. Thymic emigrants were compromised in association with reduced C-C Chemokine Receptor 7 (CCR7) expression, yet were capable of normal T lineage differentiation upon adoptive transfer to the thymus. B cell, myeloid progenitor cell and hematopoietic stem cell numbers were unperturbed. Therefore, mature osteolineage cells have a highly constrained hematopoietic cell specific effect, altering T cell production by regulation of thymic emigrants and their ability to translocate to the site of maturation. These data suggest a new role for bone in the homeostasis of the immune system.

Poster Number 28

Buvall, Lisa PhD
Research Fellow, Medicine
Buvall.Lisa@mgh.harvard.edu

Proteasomal regulation of Nck1 but not Nck2 controls actin dynamics

Investigators: Lisa Buvall, PhD; Priyanka Rashmi, PhD; Astrid Weins, MD, PhD; Anna Greka, MD, PhD; Peter Mundel, MD

The kidney podocyte possesses a highly dynamic actin cytoskeleton, which is vital for the maintenance of the glomerular filtration barrier. The SH2/SH3 domain containing adapter protein family Nck has been shown to interact with proline rich effector molecules to regulate cytoskeletal dynamics. Podocyte-specific double deletion of Nck1 and Nck2 in mice causes a severely disrupted podocyte actin cytoskeleton, and a leaky filtration barrier manifest as proteinuria. While Nck1 and Nck2 are widely expressed and share high amino acid identity, which has promoted the notion that they are redundant, here we show that Nck1 and Nck2 play distinct roles in the regulation of the actin cytoskeleton. Using the podocyte as a model system, we specifically show that differences in the proteasomal regulation of Nck1 and Nck2 account for their distinct effects on the actin cytoskeleton. Through an interaction with the proline rich actin-associated protein synaptopodin, Nck1, but not Nck2, is protected from E3 ligase c-Cbl-mediated ubiquitination and subsequent proteasomal degradation. This is in keeping with our prior work showing that synaptopodin prevents the E3 ligase Smurf-1 from degrading the small Rho protein RhoA, thus revealing a generalized role for synaptopodin in the inhibition of E3 ligases. Gene silencing of synaptopodin in podocytes causes loss of stress fibers and reduction of Nck1 abundance. Overexpression of a ubiquitination-resistant mutant of Nck1 promotes actin polymerization and stress fiber formation in a Rho-associated protein kinase-dependent manner in synaptopodin knockdown podocytes. These findings reveal proteasomal regulation as a key mechanism to distinct and non-redundant Nck protein effects on actin dynamics.

Poster Number 29

Chandrachud, Uma PhD
Research Fellow, Center for Human Genetic Research
chandrachud@chgr.mgh.harvard.edu

Chemical genetic dissection of an autophagic defect in a neuronal cell model of JNCL

Investigators: Uma Chandrachud, PhD; Sasja Heetveld, MS; Pavlina Wolf, MS; Anton Petcherski, MS; Stephanie Norton, PhD; Stephen Haggarty, PhD; Susan L. Cotman PhD

Abnormal accumulation of undigested macromolecules is a major feature of lysosomal storage disorders and in neurodegenerative disease. In juvenile onset neuronal ceroid lipofuscinosis (JNCL), like most other forms of NCL, the primary component of the storage material is the mitochondrial ATPase subunit c protein. We have previously demonstrated that there is a defect in autophagy in an accurate genetic model of JNCL, which is likely to be responsible for the build-up of the subunit c protein. Because a healthy autophagy pathway is particularly important to neuronal function, we sought to gain an improved understanding of the root cause of the autophagy defect in the JNCL model system, and we sought to identify candidate drugs or target pathways to improve the autophagy defect that arises through CLN3 dysfunction. In order to achieve this goal, we developed a cell-based screening assay to monitor autophagy via GFP-LC3, and performed focused and unbiased small molecule modifier screens. In line with published data from other cell culture systems, the majority of compounds from the unbiased library that were displayed activity in the GFP-LC3 screen in the JNCL neuronal cells function through modulation of intracellular calcium levels. Consistent with these results, upon screening a focused set of ion channel blockers, we found that an unexpectedly high percentage of the calcium channel blockers, 78%, showed activity in the assay, while comparatively fewer of the potassium and sodium channel blockers showed significant activity (26% and 18%, respectively). In particular, thapsigargin, which inhibits the SERCA calcium pump and effectively increases intracellular calcium levels, and at the same time has been reported to disrupt late steps in the autophagy pathway, specifically autophagosome-lysosome fusion, was highly active in our JNCL mutant cells, more-so than in wild-type cells. Moreover, calcium chelation by BAPTA-AM reversed the effect of thapsigargin, confirming the mechanism of action on the GFP-LC3 autophagy marker was mediated by calcium. We also observed that thapsigargin treatment worsened the hallmark NCL storage of the subunit c protein in our cell culture system. These data therefore further strengthen the hyopthesis that CLN3 dysfunction impacts a late step in the autophagy pathway and highlight a possible role for calcium in this process. Further analyses of intracellular calcium stores and the role of the autophagy-lysosomal system in JNCL cell and mouse models are ongoing to better understand the role of calcium in the JNCL disease process. Since calcium is a key molecule in neuronal communication and neuronal function, targeting calcium pathways may be beneficial in JNCL, if calcium signaling is disrupted in JNCL brain.

Poster Number 30

Kesler, Cristina T. PhD
Research Fellow, Radiation Oncology
ckesler@steele.mgh.harvard.edu

Vascular endothelial growth factor-C enhances radiosensitivity of lymphatic endothelial cells

Investigators: Cristina T. Kesler, PhD; Angera H. Huo, PhD; Shan Liao, PhD; Hon Kit Wong, PhD; Kathy D. Held, PhD; Timothy P. Padera, PhD

The incidence of lymphedema is strongly correlated with axillary lymph node dissection and regional radiotherapy. Current lymphedema treatments provide little relief for many patients. Thus, it is critical to develop methods to prevent and reverse the formation of lymphedema. While information on the radiosensitivity of many tissues is available, the effects of radiation on adult lymphatic endothelial cells (aLECs) and lymphatic vessels have been largely unreported. Using clonogenic survival assays, we determined the radiosensitivity of LECs over the range of 0 to 8 Gy. We then used standard colony formation assays to test whether known lymphangiogenic growth factors alter the radiosensitivity of LECs. Neither VEGF nor bFGF altered radiosensitivity; however, VEGF-C reduced colony formation by 15% at 2 Gy and 30% at 6 Gy when present prior to radiation. Cell cycle analysis revealed a higher fraction of VEGF-C-treated LECs in S and G2/M prior to and 24 h after radiation relative to control. Using phospho-H2AX as a marker for DNA double strand break repair, we measured an increase in the number of pH2AX nuclear foci inVEGF-C-treated cells relative to control. Together, these data suggest that abundant VEGF-C and lymphangiogenesis may predispose patients to radiation-induced lymphatic damage and lymphedema.

Poster Number 31

Marangoni, Francesco PhD
Research Fellow, Medicine
marangoni.francesco@mgh.harvard.edu

Multiphoton Intravital Microscopy Analysis of Signaling in T Cells Reveals Persistent NFAT Activation During Dynamic APC Scanning

Investigators: Francesco Marangoni, PhD; Thomas T. Murooka, PhD; Teresa Manzo, PhD; Edward Y. Kim, PhD; Esteban Carrizosa, PhD; Natalie M.C. Elpek, MSc; Thorsten R. Mempel, MD, PhD

The Ca2+ dependent activation and nuclear shuttling of the cytoplasmic transcription factor NFAT is a hallmark of productive T cell receptor (TCR) triggering. However, the kinetics of NFAT activation and the relationship to the Ca2+ dependent migratory stop signal has not been explored in vivo.

We used Multiphoton Intravital Microscopy (MP-IVM) to visualize the subcellular dynamics of a fluorescent reporter of NFAT signaling (NFAT-GFP) in hemagglutinin (HA)-specific cytotoxic T cells during their antigen-dependent interactions with various APC in lymph nodes (LNs) and in tumor tissue in vivo.

During interactions with HA peptide-loaded B cells representing optimal APC in LNs, t1/2 of NFAT nuclear translocation was 1 minute. Relocation to the cytoplasm upon contact cessation occurred with a slower t1/2 of ~20 minutes. We therefore hypothesized that NFAT may facilitate the integration of TCR signals received through serial APC contacts. To test this in vivo, we performed MP-IVM to visualize contacts between cytotoxic T cells and tumor cells expressing HA, representing suboptimal APCs. We observed that among T cells with continuously nuclear NFAT, 30% remained motile while engaging in transient, serial contacts with multiple tumor cells. Therefore, our data indicate that nuclear NFAT constituted a short-term imprint of transient TCR signals ("NFAT memory").

We next investigated whether NFAT target genes were transcribed during the "NFAT memory" phase. We found that this was the case for the T cell tolerance gene Egr2, but not for the effector gene Ifng, which required continuous TCR triggering and ERK activity for expression.

Finally, we hypothesized that the "NFAT memory" behavior of CTLs may be predominant during establishment of immunological tolerance in vivo. To test this, we induced immunological tolerance to the tumor by injection of HA-specific T regulatory cells, and found that tumor-infiltrating HA-specific CTLs preferentially operated under "NFAT memory".

Taken together, our data indicate that sustained NFAT activation after cessation of TCR triggering ("NFAT memory") may result in the preferential induction of tolerogenic gene expression programs in T cells, and may be one of the mechanisms involved in the establishment of immunological tolerance.

Poster Number 32

Meynard-Sautet, Delphine PhD
Instructor, Center for Systems Biology
dmeynard-sautet@partners.org

Inflammation Regulates Tmprss6 Expression Via Stat5 In Human Cells And Mice

Investigators: D. Meynard, PhD; C.C. Sun, PhD; W. Chen, PhD; Q. Wu, PhD; S Chen; C.N. Nelson, PhD; student M.J. Waters, PhD; J.L. Babitt, MD; H.Y. Lin, MD, PhD

TMPRSS6 is a regulated gene, with a crucial role in the regulation of iron homeostasis by inhibiting hepcidin expression. Mutations in TMPRSS6 gene result in an Iron Refractory Iron Deficiency Anemia (IRIDA). The liver antimicrobial peptide hepcidin, the main regulator of iron homeostasis, also has a role in immunity, and is upregulated by inflammation.

In this study, we studied whether TMPRSS6 was also regulated by inflammation and explored the mechanism of this potential regulation. In addition, we also determined if the regulation of TMPRSS6 by inflammation was part of the mechanism leading to the increase of hepcidin expression in response to inflammation.

We demonstrated that IL-6 treatment of Hep3B cells down-regulates TMPRSS6 expression and matriptase 2 activity. We also showed that LPS injection in wild-type mice leads to a decrease in Tmprss6 expression. In addition, injection of LPS in Hjv-/- mice (BMP-SMAD pathway inhibited) also induced a down-regulation of Tmprss6 expression indicating that the down-regulation of Tmprss6 by inflammation in mice is not dependent on the Bmp-Smad pathway.

Interestingly, in wild-type mice the phosphorylation of Stat5 is decreased by inflammation with the same time course as the decrease in Tmprss6 expression. Moreover, by electrophoretic mobility shift assay, we established that Stat5 binds to a Stat5 element located on the mouse Tmprss6 promoter. We then supported this result with two in vitro assays. First, we showed that over-expression of Stat5 positively regulates Tmprss6 expression by binding to a Stat5 element located on the mouse Tmprss6 promoter, using a mouse wild-type Tmprss6 promoter luciferase reporter construct in comparison with the same construct but with a mutation in the STAT5 element, Second, we demonstrated that silencing of STAT5 expression in Hep3B cells results in a decrease of TMPRSS6 expression. Altogether, these results indicate that TMPRSS6 is regulated by inflammation and that this regulation occurs through a decrease in Stat5 phosphorylation.

Importantly, our results suggest that the inflammatory modulation of TMPRSS6 expression is part of the regulation of hepcidin by inflammation. Indeed, we demonstrated that silencing of TMPRSS6 expression during IL-6 treatment potentiates the increase in HAMP caused by inflammation in Hep3B cells. In addition, we also showed that TMPRSS6 over-expression reduces the increase of HAMP-promoter activity induced by IL-6 treatment in Hep3B cells.

These results indicate that inflammation regulates TMPRSS6 expression, and that in turn TMPRSS6 has a functional role in mediating the inflammatory regulation of hepcidin regulation.

Poster Number 33

Schaldecker, Thomas
Graduate Student, Medicine
thomasschaldecker@gmail.com

Essential role for TRPC5 channels in the initiation of immune and non-immune mediated kidney disease

Investigators: Thomas Schaldecker; Sookyung Kim; Dequan Tian, PhD; Constantine Tarabanis; Lisa Buvall, PhD; Samy Hakroush, MD; Astrid Weins, MD, PhD; Philip Castonguay; Wooin Ahn, MD, PhD; Hanna Wallentin, PhD; Peter Mundel, MD; Anna Greka, MD, PhD

Proteinuria, the result of a leaky kidney glomerular filter, is an early marker of kidney disease. More importantly, proteinuria is an independent predictor of cardiovascular diseases such as stroke and myocardial infarction, independent of underlying kidney disease.

Podocytes are highly specialized cells of the kidney glomerulus and their function is crucial for the maintenance of the filtration barrier.

Transient Receptor Potential Classical (TRPC) channels are calcium permeable cationic channels with diverse functions. We have previously shown that calcium influx through TRPC5 and TRPC6 regulates the actin cytoskeleton in an antagonistic fashion. Furthermore, TRPC5 channels were shown to activate the small Rho protein Rac1 to mediate maladaptive cytoskeletal rearrangements in podocytes.

Here we show that TRPC5 knockout mice are protected from Lipopolysaccharide (LPS) induced proteinuria. Our electrophysiology studies reveal that LPS increases TRPC5 open channel probability (Po). Intriguingly, we show that TRPC5 knockout mice injected with Protamine Sulfate (PS), a well-established non-immune model of proteinuria, are protected from PS-mediated glomerular changes. In electrophysiology and calcium imaging studies, PS is shown to enhance TRPC5 channel activity. Finally, in an independent genetic approach, the podocyte-specific inducible expression of TRPC5 in podocytes in vivo leads to proteinuria within four weeks of induction. In further in vitro studies, we show that these immune and non-immune signals converge on TRPC5 and the podocyte actin cytoskeleton to confer susceptibility to cellular injury. Specifically, TRPC5 (over)activity leads to increased Rac1 activation and a disrupted actin cytoskeleton.

In conclusion, our data reveal TRPC5 as an essential mediator of immune and non-immune proteinuric kidney disease, and thus, an attractive target for novel therapies for which there is a great need in the clinic.

Poster Number 34

Wein, Marc N. MD
Clinical Research Fellow, Medicine
mnwein@partners.org

Control of PTH signaling in osteocytes by class IIa HDACs

Investigators: Marc N. Wein, MD, PhD; Shigeki Nishimori, MD, PhD; Jordan Spatz, BS; John Doench, PhD; Paola Pajevic-Divieti, MD, PhD; Henry Kronenberg, MD

Parathyroid hormone (PTH) is a peptide hormone with a major role in calcium metabolism. A recombinant form of PTH (1-34, teriparatide) is the only FDA-approved anabolic therapy for osteoporosis. We do not fully understand the mechanisms whereby teriparatide increases bone mass. It is likely that PTH receptors in osteocytes play a crucial role. Osteocyte-derived sclerostin is a potent inhibitor of bone formation. When osteocytes sense PTH, sclerostin is rapidly down-regulated. The molecular details of how signaling through the PTH receptor leads to sclerostin inhibition are not known. Here we show that class IIa HDACs play a crucial role in PTH-mediated sclerostin down-regulation. PTH leads to the dephosphorylation and nuclear translocation of HDAC4 in osteocytes. shRNA-mediated reductions in class IIa HDAC levels blunts PTH-mediated sclerostin down-regulation. Studies are now ongoing to further characterize the mechanisms whereby class IIa HDACs participate in PTH-mediated sclerostin inhibition.

Poster Number 35

Zumbrennen-Bullough, Kimberly PhD
Research Fellow, Medicine
bullough.kimberly@mgh.harvard.edu

microRNA-130a downregulates hepcidin expression during iron deficiency by targeting ALK2

Investigators: Kimberly Zumbrennen-Bullough, PhD; Qifang Wu, PhD; Wenjie Chen, PhD; Jodie Babitt, MD

Systemic iron homeostasis is primarily controlled by the liver through the secretion of the peptide-hormone hepcidin, which regulates intestinal iron absorption and hepatocyte and macrophage iron sequestration. Hepcidin expression is upregulated via a canonical BMP-SMAD signaling pathway during iron-replete conditions and results in the downregulation of intestinal iron uptake and cellular iron export. Here we show that microRNA-130a (miR-130a) specifically targets members of the BMP-SMAD pathway to downregulate hepcidin expression during iron deficiency. Using miRNA microarray and qRT-PCR analysis, we found miR-130a upregulated in iron deficient and anemic mouse livers. Web-based miRNA target-prediction programs identified potential miR-130a targets within the BMP-SMAD pathway including the BMP type I receptor ALK2 and the intracellular signaling molecule SMAD5. Using luciferase reporter constructs containing the 3′ untranslated region (3′ UTR) of the putative target transcripts, we found reduced luciferase activity in the presence of miR-130a mimic for both ALK2 and SMAD5 3′ UTRs. Mutation of the putative miR-130a target sites in the ALK2 and SMAD5 3′ UTRs restored luciferase activity. Hep3b cells treated with miR-130a mimic showed reduced levels of endogenous ALK2 mRNA while endogenous SMAD5 mRNA and protein levels remained unchanged. Using actinomycin D to inhibit cellular transcription, we found the half-life of ALK2 mRNA was significantly decreased in miR-130a mimic treated cells. miR-130a mimic-transfected cells also showed reduced levels of phosphorylated SMAD1/5/8 protein (a marker of BMP-SMAD signaling) and hepcidin mRNA in response to BMP stimulation. These data indicate that miR-130a is upregulated in iron deficient conditions and targets ALK2, and potentially SMAD5, to downregulate hepcidin expression. We hypothesize that miR-130a functions to fine-tune hepcidin synthesis after iron deficiency by reducing the signaling capacity of the BMP-SMAD pathway, thereby increasing iron availability.

Poster Number 36

Baliga, Sunanda PhD
Research Fellow, Heart Center
sbaliga@partners.org

ephb4 regulates notch signaling during zebrafish angiogenesis

Investigators: Sunanda Baliga, PhD; Joanna Yeh, PhD

Angiogenesis is an intricate process that requires the careful coordination of several signaling pathways. The VEGF pathway has been extensively studied for decades, thereby serving as the basis of anti-angiogenic therapeutics. The increasing importance of the Notch signaling pathway in angiogenesis has opened up another target for the development of anti-angiogenesis compounds; however, the few commercially available Notch inhibitors induce severe side effects and cannot be utilized to their full capacity. Thus, compounds that converge with the VEGF and/or Notch pathways would prove useful. EphB4—a receptor tyrosine kinase—is overexpressed in several cancers and promotes tumor advancement in breast and ovarian cancers, although the precise mechanisms are not well established. EphB4 also plays a role in angiogenesis during development; it is highly expressed in venous cells. Embryonic zebrafish are an excellent model to study Ephb4 signaling because they allow the visualization of vessel dynamics in vivo, and vascular development in the zebrafish is similar to that in higher vertebrates. We generated an ephb4 knockout zebrafish line (ephb4-/-) using zinc finger nuclease technology. Using confocal imaging, we found a significantly higher number of arterial-venous shunts, stunted intersegmental vessels, and vessel patterning defects in ephb4-/- embryos. Surprisingly, we found that notch1b is upregulated in the mutants, whereas notch2 and notch3 were decreased in ephb4-/- embryos. Further, ectopic expression of notch in the zebrafish generates angiogenic defects remarkably similar to the ephb4-/- phenotype, suggesting that hyperactive notch signaling is responsible for the vessel patterning defects seen in the ephb4-/- embryos. Treatment of ephb4-/- embryos with compound E, a pan notch inhibitor is able to rescue the angiogenic defects. Our data collectively suggest that the ephb4 and notch signaling pathways converge in the zebrafish and might present a novel target in the development of anti-angiogenic therapies.

Poster Number 37

Etchegaray, Jean-Pierre PhD
Research Fellow, Cancer Center
Etchegaray.Jean-Pierre@mgh.harvard.edu

The histone deacetylase SIRT6 plays a critical role in mouse embryonic stem cell differentiation

Investigators: Jean-Pierre Etchegaray, PhD; Jiho Choi, PhD; Cesar Sommer, PhD; Yun Huang, PhD; Defni Silberman, PhD; Konrad Hochedlinger, PhD; Gustavo Mostoslavsky, MD, PhD; Anjana Rao, PhD; Raul Mostoslavsky, MD, PhD

Embryonic Stem (ES) cells can self-renew indefinitely and upon stimulation they are able to differentiate into the three primary germ layers: ectoderm, mesoderm and endoderm. We found that the mammalian histone deacetylase SIRT6 plays a critical role in embryogenesis. Sirt6 knockout mice from C57BL/6 strain are born at significantly lower Mendelian ratios, which highlight a developmental defect. Upon differentiation, ES as well as induced Pluripotent Stem (iPS) cells derived from SIRT6 deficient mice generate smaller embryonic bodies (EBs) with underdeveloped endoderm and mesoderm, but overdeveloped neuroectoderm. This morphological phenotype is recapitulated in human EBs with downregulated SIRT6. In support of a SIRT6-dependent regulation of stem cell differentiation, we found teratomas obtained from mouse ES cells lacking SIRT6 to be of significantly smaller size and enriched in neuroectodermal tissue. We found the expression of the core pluripotent factors OCT4, SOX2 and NANOG to be upregulated in SIRT6 depleted EBs. This upregulation correlates with an increased acetylation of H3K56, a mark for active transcription, at the promoters of these pluripotent genes, indicating that SIRT6 functions as an histone deacetylase to repress pluripotent genes during ES cell differentiation. Remarkably, we find bulk genomic levels of 5-hydroxymethylcytosine (5hmC), an epigenetic hallmark for pluripotency, to be increased in SIRT6 deficient ES cells along with elevated levels of the hydroximethylases TET1 and TET2. Importantly, downregulation of TET1 or TET2 fully rescues the differentiation defect in SIRT6 deficient EBs, indicating that this particular epigenetic mark plays a critical role during early embryo differentiation. Therefore, we proposed a model where the deacetylase activity of SIRT6 causes the transcriptional repression of Oct4 and Sox2, which in turn regulates the expression of Tet1 and Tet2 as an epistatic pathway required for proper embryogenesis. Here we show that SIRT6 plays a critical role during embryonic differentiation as a modulator of an epigenetic cross-talk that includes: 1) repression of pluripotency by deacetylation of H3K56 on the core pluripotent genes Oct4, Sox2 and NanoG; and 2) downregulation of an epigenetic mark (5hmC) via Oct4-Sox2/Tet protein levels.

Poster Number 38

Lee, Jungwoo PhD
Research Fellow, Surgery
lee.jungwoo@mgh.harvard.edu

Implantable microenvironments to attract hematopoietic stem/cancer cells

Investigators: Jungwoo Lee, PhD; Matthew Li; Jack Milwid, PhD; Joshua Dunham; Claudio Vinegoni, PhD; Rostic Gorbatov; Yoshiko Iwamoto; Fangjing Wang, PhD; Keyue Shen, PhD; Emmet McCormack, PhD; Benjamin L. Ebert, MD, PD; Ralph Weissleder, MD, PhD; Martin L. Yarmush, MD, PhD; Biju Parekkadan, PhD

The environments that harbor hematopoietic stem and progenitor cells are critical to explore for a better understanding of hematopoiesis during health and disease. These compartments often are inaccessible for controlled and rapid experimentation, thus limiting studies to the evaluation of conventional cell culture and transgenic animal models. Here we describe the manufacture and image-guided monitoring of an engineered microenvironment with user-defined properties that recruits hematopoietic progenitors into the implant. Using intravital imaging and fluorescence molecular tomography, we show in real time that the cell homing and retention process is efficient and durable for short- and long-term engraftment studies. Our results indicate that bone marrow stromal cells, pre-coated on the implant, accelerate the formation of new sinusoidal blood vessels with vascular integrity at the microcapillary level that enhances the recruitment hematopoietic progenitor cells to the site. This implantable construct can serve as a tool enabling the study of hematopoiesis.

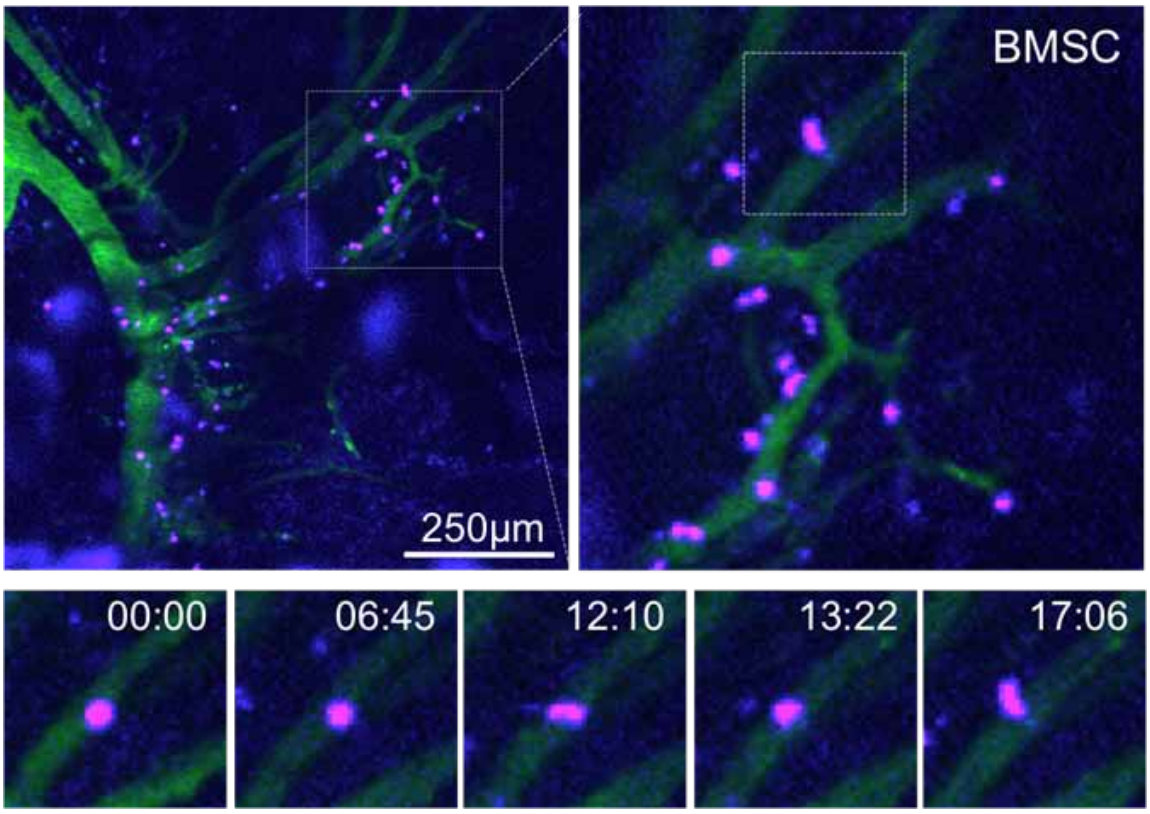

Poster Number 39

Moore, Finola PhD
Research Fellow, Cancer Center
femoore@partners.org

The Role of the Tumor Suppressor PHF6 in Blood and Leukemia

Investigators: Finola E. Moore, PhD; David M. Langenau, PhD

Cancers of blood coopt normal hematopoietic differentiation pathways to create tumor cells. Plant Homeodomain Finger 6 (PHF6) is a tumor suppressor of unknown function in blood malignancies such as T cell Acute Lymphoblastic Leukemia (T-ALL), Acute Myeloid leukemia (AML), and Chronic Myeloid Leukemia (CML). PHF6 contains two zinc finger-like PH domains and localizes to the nucleus where it may play a role in chromatin remodeling. PHF6 is expressed broadly with notably higher expression in lymphoid cells in human and mice. The goal of this project is to understand the function of the leukemia tumor suppressor PHF6, in both hematopoiesis and leukemogenesis. Zebrafish will be used to study hematopoiesis and hematological malignancy due to the remarkable conservation of molecular pathways that regulate blood development and cancer, ease of performing gain-of-function and loss-of-function experiments, and ability to observe embryonic development over a short window of time. We hypothesize that loss of PHF6 will cause an expansion of blood cell progenitors, similar to the over proliferation of lymphocytes observed in leukemias with PHF6 mutations. Here we determined the effect of PHF6 loss on blood progenitor specification by knocking down PHF6 by morpholino and knocking out PHF6 in mutants generated by TALEN designer nucleases. PHF6 mutants will also be examined as potential modifier of Myc-induced T-ALL in zebrafish. The results of this work, the first in vivo characterization of PHF6 function, will provide powerful insights into the role of PHF6 in human hematological disease, potentially providing drug targets for therapies in the future.

Poster Number 40

Nishimori, Shigeki MD,PhD
Research Fellow, Medicine
snishimori@partners.org

Parathyroid hormone-related peptide (PTHrP) regulates Histone Deacetylase (HDAC) 4 to inhibit chondrocyte hypertrophy

Investigators: Shigeki Nishimori, MD, PhD; Forest Lai, BA; Henry M. Kronenberg, MD

The existence of parathyroid hormone-related peptide (PTHrP) was first predicted by Fuller Albright in an MGH CPC (NEJM, 1941) when he noted that a tumor might produce PTH to induce hypercalcemia in a cancer patient. Later studies showed that PTHrP shares homology with PTH primarily within its first 13 residues (Suva, Science, 1987), but that PTHrP binds a common PTH/PTHrP receptor with high affinity (Jüppner, JBC, 1988).

In addition to PTH-like endocrine action in cancer patients, the physiological roles of PTHrP as a paracrine and autocrine factor have been recognized in multiple tissues. The PTHrP knockout (KO) mouse dies immediately after birth from respiratory failure due to defective rib cage formation (Karaplis, G&D, 1994). Studies using the PTHrP KO and a transgenic (Tg) mouse overexpressing PTHrP in chondrocytes (PTHrP Tg) (Weir, PNAS, 1996) showed that PTHrP inhibits chondrocyte hypertrophy.

Class II Histone Deacetylases (HDAC4, 5, 7, 9) are transcriptional repressors of Myocyte Enhancer Factor 2 (Mef2), a key transcription factor for muscle development. The HDAC4 KO mouse exhibits a dramatic chondrocyte phenotype involving accelerated chondrocyte hypertrophy and dies around eight days after birth (Vega, Cell, 2004). Later study showed that the HDAC4 phenotype resulted because normally HDAC4 blocks the action of Mef2C to stimulate chondrocyte hypertrophy (Arnold, Dev. Cell, 2007).

Thus, both PTHrP and HDAC4 inhibit chondrocyte hypertrophy, but the molecular mechanisms of these processes have not been clarified. Here we provide in vivo genetic and molecular evidence that PTHrP regulates HDAC4 to inhibit chondrocyte hypertrophy.

Our genetic tests support the hypothesis that PTHrP and HDAC4 work in a common pathway: (1) The HDAC4 KO mouse shows a phenotype similar to that of the PTHrP KO mouse; (2) Even though the PTHrP heterozygous (HET) mouse and the HDAC4 HET mouse have normal growth plates at birth, the double HET mouse exhibits accelerated chondrocyte hypertrophy; and (3) The complete suppression of chondrocyte hypertrophy in the PTHrP Tg mouse is blocked by knocking out the HDAC4 gene in this Tg mouse.

HDAC4 binds Mef2 and also has phosphorylation-dependent binding sites for the cytoplasmic chaperon protein, 14-3-3. HDAC4 translocates into nucleus through dephosphorylation of the sites that bind 14-3-3, and then represses the action of Mef2C. In the PTHrP KO, confocal microscopy, combined with immunohistochemistry, shows that most of the HDAC4 is cytoplasmic; in the PTHrP Tg, in contrast, most of the HDAC4 is in the nucleus. Immunohistochemistry specific for phosphorylated serine-246 of HDAC4 similarly showed high levels of phosphorylated HDAC4 in the PTHrP KO, but low levels in the PTHrP Tg chondrocytes.

These in vivo studies are consistent with a recent in vitro study that used a chondrocyte cell line and chick primary chondrocytes to show that PTHrP activates protein phosphatase 2A, leading to dephosphorylation of HDAC4 and movement of HDAC4 to the nucleus to block Mef2C action (Kozhemyakina, MCB, 2009).

In conclusion, these findings reveal that PTHrP inhibits chondrocyte hypertrophy by inducing HDAC4 dephosphorylation and subsequent nuclear translocation.

Poster Number 41

Ramasamy, Selvi PhD
Instructor, Cancer Center
sramasamy2@partners.org

Mice deficient for Tle1 display poor survival, delayed development, abnormal hematopoesis and an enhanced inflammatory response

Investigators: Selvi Ramasamy, PhD; Borja Saze, PhD; Subhankar Mukhopadhyay, PhD; Daching Ding, MD, PhD; Xi Chen, MD, PhD; David Sweetser, MD, PhD

TLE1 belongs to the Groucho/TLE family of co-repressors that act as master regulators during development affecting segmentation, neurogenesis, myogenesis, and multiple cell fate decisions. TLE1 modulate several major signaling pathways including Wnt and Notch, and specifically interacts with multiple transcription factors involved in hematopoiesis such TCF/LEF, HES1, RUNX1/AML. TLE1 has also been implicated in Crohn's disease via its interaction with NOD2, a regulator of NFkB. Our laboratory identified TLE1 as a likely AML tumor suppressor gene, commonly deleted in subgroups of AML, and others have shown its role as a tumor suppressor gene in myeloid and other hematopoietic malignancies. To better understand the role of TLE1 in hematopoiesis and leukemogenesis we created a line of Tle1 null mice.

Tle1 null mice are born normally, but become progressively growth retarded by 3 days of life, with only 50% survival by 4 weeks as compared to heterozygous and wild type littermates. Abnormalities are observed in several organs systems including the hematopoietic system. We characterized the hematopoietic system in Tle1 knock out mice between two and 12 weeks of age. The bone marrow cellularity in the Tle1 knock out mice is comparable to the wild type mice at all time points examined. However, frequency of granulocyte macrophage progenitors in bone marrow mononuclear cells is significantly higher in the Tle1 knockout bone marrow compared to heterozygous and wild type mice. The proportion and number of myeloid cells as evidenced by Gr1, Mac1 expression are significantly higher in the bone marrow, spleen and blood of these knockout mice. There were significantly lower B-cells (B220+ cells) in the Tle1 knockout mice compared to heterozygous and wild type.

In colony forming assays there was a trend towards higher number of CFU-GM (7.66 vs 5), p=0.07) and CFU-M (27.16 vs 12.5, p=0.05) colonies from Tle1 null bone marrow as compared to wild type bone marrow. The spleens from four week and 17 months old Tle1 knockout mice had higher frequency of Gr1-negative, Mac1-positive and F4/80 positive macrophages. We also observed a significantly higher production of the inflammatory cytokines IL6 and TNFa from peritoneal macrophages harvested from Tle1 null mice as compared to those from wild type mice in response to TLR ligand stimulation. The Tle1 null mice are more sensitive to the treatment of inflammatory compound 2-O-tetradecanoylphorbol-13-acetate (TPA), and the Tle1 null produced increased inflammatory response than the wild type mice.

In summary this work demonstrates that the lack of Tle1 expression biases hematopoiesis towards myeloid differentiation, a finding of potential relevance given the inactivation of TLE1 seen in subsets of myeloid malignancies. We further show that inactivation of Tle1 leads to an increase in macrophages primed to release increased inflammatory cytokines and enhanced response to inflammatory stimuli . This is notable given the recent observation that TLE1 may modulate the effects of NOD2 in the pathogenesis of Crohn's disease. These Tle1 null mice will allow the investigation of the potential role of TLE1 as a modulator of a variety of other inflammatory diseases.

Poster Number 42

Zulauf, Courtney BA
Clinical Research Fellow, Psychiatry
czulauf@partners.org

Substance and Nicotine Use in Young Adults with Bipolar Disorder: 5-Year Findings of a Controlled Longitudinal Study

Investigators: Timothy E. Wilens, MD; Courtney A. Zulauf, BA; MaryKate Martelon, MPH

Background: Bipolar Disorder (BPD) is an increasingly recognized, serious psychopathologic condition affecting children and adolescents. Few data exists evaluating the course of BPD from adolescence into young adulthood focusing on comorbid substance dependence. We looked to evaluate the risk for comorbid substance dependence in young adults with BPD. We hypothesized that young adults with BPD would have higher levels of substance dependence than young adults in our control group.

Methods: study design, setting, population, measures and analytic procedures.): These data are based on a midpoint analysis of an ongoing 5 year follow-up study. Subjects were 57 BPD (mean age: 19.5 + 2.8 years) and 76 control probands (19.0 + 2.5 years) who received 5 year follow-up structured diagnostic interviews as part of an ongoing case-control family study of an initial cohort of adolescents with BPD and adolescents without a mood disorder.

Results: BPD was endorsed by 66% of probands within the past year. There were no statistically significant differences between the BPD and control probands for age or sex distribution (p values>0.05). We did detect a significant difference in socioeconomic status (p=0.001). As a result all analyses were adjusted for SES. There was a marked increase in the risk for substance use disorders that occurred during the follow-up period. At follow-up, lifetime rates of alcohol dependence (22% vs. 5%, p<0.01), drug dependence (29% vs. 9%, p=0.01), and cigarette smoking (46% vs. 16%, p<0.001) were greater in BPD probands compared to controls.BPD probands had significantly higher rates of ADHD, conduct and oppositional defiance disorders, severe major depression, multiple anxiety disorders, panic disorder, and agoraphobia compared to control probands (all p values <0.001). We found high rates of nicotine and SUD in young adults with persistent BPD compared to non-persistnet BPD and controls.

Conclusion: Results from a five-year follow-up study of BPD probands now in young adulthood found BPD was associated with much higher risk for comorbid cigarette smoking, alcohol and drug use disorders compared to controls. Those with persistent BPD were at a heightened risk for SUD. At follow-up, BPD continued to be associated with other psychopathology including ADHD, disruptive disorders, anxiety disorders, and serious depression compared to adolescents without a mood disorder.

Fig 1. Difference in substance dependence between BPD and Control probands: Baseline and 5-year follow-up data presented

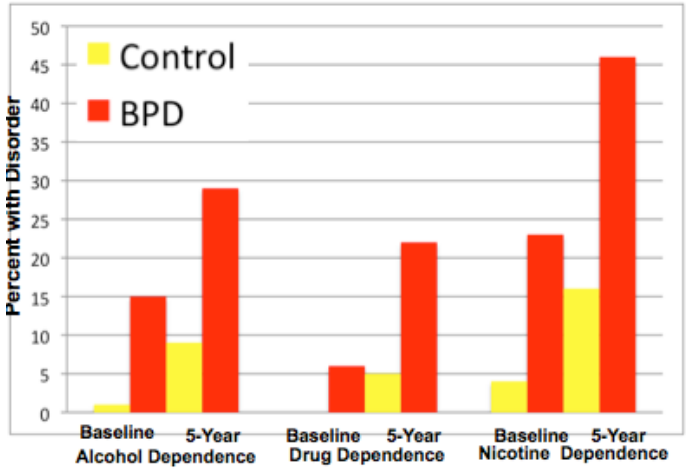

Poster Number 43

Buys, Emmanuel PhD
Assistant Professor, Anesthesia, Critical Care and Pain Medicine
ebuys@partners.org

Soluble guanylate cyclase: an emerging therapeutic target in open angle glaucoma

Investigators: Emmanuel S. Buys, PhD; Yu-Chieh Ko, MD; Clemens Alt, PhD; Sarah R. Hayton; Alexander Jones; Laurel T. Tainsh; Ruiyi Ren; Andrea Giani, MD; Maeva Clerté, MD; Emma Abernathy; Robert E.T. Tainsh; Dong-Jin Oh, PhD; Rajeev Malhotra, MD; Pankaj Arora, MD; Nadine De Waard, Binglan Yu, PhD; Raphael Turcotte; Daniel Nathan; Marielle Scherrer-Crosbie, MD, PhD; Stephanie J. Loomis; Jae H. Kang, DSc; Charles P. Lin, PhD; Haiyan Gong, MD, PhD; Douglas J. Rhee, MD; Peter Brouckaert, MD, PhD; Janey L. Wiggs, MD; Meredith Gregory, PhD; Louis R. Pasquale, MD; Kenneth D. Bloch, MD; Bruce Ksander, PhD

Primary open angle glaucoma (POAG) is a leading cause of blindness in the US and worldwide. As of yet, there is no cure for POAG and although available therapies delay disease progression, they offer incomplete protection. The molecular signaling involved in the pathogenesis of POAG remains unknown.

Here, we report that mice lacking the α1 subunit of the nitric oxide (NO) receptor soluble guanylate cyclase (sGCα1-/- mice) represent a novel and translatable animal model of POAG, characterized by thinning of the retinal nerve fiber layer (RNFL) and loss of optic nerve axons in the context of an open iridocorneal angle. The optic neuropathy associated with sGCα1–deficiency was accompanied by modestly increased intraocular pressure (IOP, currently the only risk factor amenable to treatment) and retinal artery dysfunction. Moreover, a candidate gene association study of POAG with paracentral vision loss, a POAG subtype thought to be associated with vascular dysregulation, identified a variant in the locus containing the genes encoding the α1 and β1 subunits of sGC. Together, these results highlight the relevance of sGC (and our animal model) in the pathogenesis of POAG.

This study provides new insights into the pathogenesis and genetics of POAG and represents a paradigm shift in POAG research. Our findings suggest that therapies that do not focus on lowering IOP (e.g. targeting retinal vascular dysfunction) constitute a complementary approach to treating POAG. In addition, our observations are the first to unequivocally identify perturbation of a well-characterized signaling pathway (NO-cGMP signaling) as a key mechanism in the etiology of POAG using data from a novel murine gene knockout model of POAG and genetic data from a subgroup of POAG patients. Identifying sGC as a potential therapeutic target for POAG suggests new therapeutic strategies for POAG and may inform the clinical development of existing cGMP-elevating therapeutic compounds (currently being tested in clinical trials for various cardiovascular diseases, including pulmonary arterial hypertension) for the treatment of POAG.

Poster Number 44

Do, Ron PhD
Research Fellow, Center for Human Genetic Research
dron@broadinstitute.org

Exome sequencing as a tool to understand the inherited basis for myocardial infarction, a common complex disease

Investigators: Ron Do, PhD[1, 2]; Nathan O. Stitziel, MD, PhD[2, 3]; Christopher O'Donnell MD[4, 5]; David Altshuler MD, PhD[1, 2]; Stacey Gabriel PhD[2]; Sekar Kathiresan MD[1, 2]
[1]Center for Human Genetics Research, Massachusetts General Hospital, Boston, MA, United States. [2]Broad Institute, Cambridge, MA, United States. [3]Cardiovascular Medicine, Brigham and Women's Hospital, Boston, MA, United States. [4]National Heart, Lung, and Blood Institute's Framingham Heart Study, Framingham, MA, United States. [5]Division of Intramural Research, National Heart, Lung, and Blood Institute, Bethesda, MD, United States.

Introduction: Myocardial infarction (MI) is a complex disease that commonly causes death and disability around the world. Prior genetic association studies have discovered more than 30 common DNA sequence variants associated with risk for MI. Here, we test the hypothesis that rare DNA sequence variants contribute to MI risk.

Methods: In order to test this hypothesis, we deeply sequenced the protein-coding regions of ~18,500 genes—the exomes—in each of 1,027 individuals with MI at an early age and 946 individuals without MI. We followed up rare variants and genes from this study in a much larger number of individuals using three approaches—statistical imputation (n=66,809), genotyping (n=17,302), and targeted re-sequencing (n=12,319).

Results: Here, we report that a low-frequency missense variant in the phosphofructokinase, muscle (PFKM) gene decreases risk for MI (PFKM R696H, 1.7% frequency, odds ratio (OR) 0.61, P=5 x 10-7). In addition, we find that a burden of rare, non-synonymous mutations in the apolipoprotein A5 (APOA5) gene increases risk for early-onset MI, with 1.4% of cases and 0.6% of controls carrying a rare variant (OR 2.2, P=1.2 x 10-6). These rare APOA5 mutations contribute not only to early-onset MI but also to increased plasma triglyceride concentrations.

Conclusion: Taken together, our study demonstrates for the first time that exome sequencing can be used to discover rare variants contributing to risk for a common, complex disease.

Lane, Jacqueline PhD
Research Fellow, Anesthesia, Critical Care and Pain Medicine
lane@chgr.mgh.harvard.edu

Poster Number 45

Functional assessment of genetic variants using a targeted circadian luciferase assay

Investigators: Lane J.M., PhD; Tare A.M.S.; Winn P, Cowan, CA, PhD; Saxena R., PhD

In recent genome-wide association studies genetic variants in circadian genes are associated with complex disease (e.g. depression, prostate cancer, bipolar disorder, anxiety, breast cancer, type 2 diabetes). It is unknown if changes to circadian timing mediate disease risk associated with circadian gene loci. Current challenges to evaluating the functional impact of disease risk variants on circadian characteristics include: 1) limited number and diversity of human tissue biopsies to determine whole body circadian characteristics 2) lack of serial tissue biopsies to evaluate circadian characteristics over time 3) mixed genetic background of samples bearing genotypes of interest. To overcome these challenges, our goal is to create a novel circadian luciferase assay in human pluripotent cells to test the impact of genetic variants on circadian timing in an isogenic background across a panel of tissue types. Our circadian assay marks the first all human, endogenous circadian cellular reporter assay. To achieve this we used transcription activator-like (TAL) effector nucleases (TALENs) to target integration of a single copy of luciferase in the cellular human genome in the stop codon of the core molecular clock gene PER2. First we designed, cloned, and tested each TALEN pair for efficacy. Next, to integrate luciferase into the genome of pluripotent cells, we co-transfected our TALEN pairs with a donor plasmid bearing genomic homology arms flanking a luciferase cassette. We then screened for integration positive clones. To test for circadian luminescence output, pluripotent cells were differentiated into mesenchymal progenitor cells and luciferase expression from each clone was measured over 48 hours. Using this approach we created a novel circadian assay in human pluripotent cells. Moving forward, introduction of genetic variants into our assay by genome-editing techniques will allow for the isogenic evaluation of functional circadian consequences in multiple tissue types.

Majithia, Amit MD
Clinical Research Fellow, Molecular Biology
amajithia@partners.org

Poster Number 46

High throughput functional analysis of coding variants identified in population scale genome sequencing: a paradigm for mapping genes underlying human metabolic diseases

Investigators: Amit R. Majithia, MD; David Altshuler MD, PhD

Genome scale sequencing of large, clinically phenotyped cohorts enables the identification of genes underlying human disease traits. As part of several large type 2 diabetes (T2D) sequencing collaborations, we are sequencing >17,000 individuals. Thus far, we have observed a large number of non-synonymous variants in most genes across the genome. Some of these variants, by affecting the biological function of their gene products, will impact human metabolic phenotypes and T2D. Identifying a few biologically functional variants among many neutral variants is a key challenge. Adipocyte function and expansion play important roles in metabolic homeostasis; impaired adipocyte function and differentiation have been implicated in insulin resistance and T2D. As such, we have developed an experimental platform for the rapid and parallel introduction of candidate mutations into human SGBS pre-adipocytes that can be flexibly combined with a variety of phenotypic assays. In this work, we combine high content microscopy and automated image analysis to create a high throughput, quantitative adipocyte differentiation assay. As a proof-of-principle, we show that our platform can accurately identify previously known gain and loss-of-function (LOF) mutations in human PPARG. We then apply our platform to functionally characterize novel, non-synonymous variants in PPARG found from human sequencing and identify new LOF variants spanning both the DNA and ligand binding domains. We score these LOF variants for dominant negative activity by titrating levels of wildtype, endogenous PPARG. With the set of biologically functional PPARG variants we will perform genotype-phenotype correlations for T2D, blood pressure, and insulin resistance.

Our strategy of variant discovery, high-throughput experimental characterization, and subsequent genotype-phenotype correlation is a paradigm for identifying new disease relevant genes from genomic sequencing.

Poster Number 47

Mouro Pinto, Ricardo PhD
Research Fellow, Center for Human Genetic Research
rmouropinto@chgr.mgh.harvard.edu

Genetic mapping in HD knock-in mice exposes MutLγ as a critical modifier of CAG somatic expansion

Investigators: Ricardo Mouro Pinto[1]; Ella Dragileva[1]; Andrew Kirby[1, 2]; Jason St. Claire[1]; Tammy Gillis[1]; Edith Lopez[1]; Jolene R. Guide[1]; Alejandro Lloret[1]; Gagan B. Panigrahi[3]; Caixia Hou[4]; J. Kim Holloway[5]; Winfried Edelmann[6]; Paula E. Cohen[5]; Guo-Min Li[4]; Christopher E. Pearson[3]; Mark J. Daly[1, 2]; Vanessa C. Wheeler[1]

[1]Center for Human Genetic Research, Massachusetts General Hospital, Boston, Massachusetts, United States of America; [2]Program in Medical and Population Genetics, Broad Institute of MIT and Harvard, Cambridge, Massachusetts, United States of America; [3]Program of Genetics and Genome Biology, The Hospital for Sick Children, Department of Molecular Genetics, University of Toronto, Toronto, Canada; [4]Graduate Center for Toxicology and Markey Cancer Center, University of Kentucky College of Medicine, Lexington, Kentucky, United States of America; [5]Department of Biomedical Sciences, Cornell University, Ithaca, New York, United States of America; [6]Department of Cell Biology, Albert Einstein College of Medicine, Bronx, New York, United States of America

Huntington's disease (HD) is a fatal, dominantly inherited neurodegenerative disease, which is caused by the hyperexpansion of a CAG repeat within exon 1 of the HTT gene. The presence and length of the CAG repeat tract are the primary determinants of whether and when a person will exhibit HD, respectively, where repeat length is inversely correlated with the age of onset. However, the variability of disease manifestations implies the contribution of additional factors, including genetic. The identification of such genetic factors would potentiate novel therapeutic interventions that could modify the nature and/or pace of the HD-associated pathogenic process.

Here we report the first genetic mapping study using an accurate genetic knock-in mouse model of HD (HdhQ111), in which we have mapped a QTL that modifies the somatic expansion of the HTT CAG repeat, using as few as 70 F2 intercross mice. This QTL strongly implicated the Mlh1 gene, a member of the DNA mismatch repair (MMR) pathway, as the modifier gene underlying the strain-specific difference in HdhQ111 CAG instability. As a role for other MMR genes had previously been demonstrated in mouse models of HD we hypothesized that Mlh1 also modified somatic instability. Gene knockout experiments of Mlh1 and Mlh3, a binding partner of MLH1, demonstrated that both of these genes are essential for somatic HTT CAG expansion in HdhQ111 mice. Further, we showed that Mlh1 is an enhancer of nuclear mutant huntingtin accumulation/epitope accessibility, a dominant, CAG length-dependent and medium-spiny striatal neuron-selective phenotype.

The mechanism(s) by which MMR proteins mediate somatic CAG/CTG expansion is unclear. In this study, we found that MLH1 and MLH3 (MutLγ) are as critical to somatic HdhQ111 CAG expansion as the DNA binding proteins MSH2 and MSH3 (MutSβ). Importantly, this is the first evidence in support of a role for additional MMR proteins downstream of MutSβ, arguing against proposed mechanisms whereby expansions occur as a consequence of inhibition of the MMR pathway following MutSβ binding to repeats.

In summary, our findings highlight the critical role of mismatch repair genes in HTT CAG-dependent events, and further support somatic expansion as an enhancer of the pathogenic process in target cell types in HdhQ111 mice.

Pinter, Stefan PhD
Research Fellow, Molecular Biology
pinter@molbio.mgh.harvard.edu

Poster Number 48

Spreading of X-chromosome inactivation by defined Polycomb binding sites

Investigators: Stefan Pinter, PhD; Ruslan Sadreyev, PhD; Eda Yildirim, PhD; Yesu Jeon, PhD; Toshiro Ohsumi, PhD; Mark Borowsky, PhD; Jeannie Lee, MD, PhD

Loss of function mutations in many of the roughly 1000 genes on the X chromosome are known to cause over 50 X-linked human diseases. These include Rett syndrome, Fragile X syndrome (FMR1), hemophilia A and B (FVIII, FVIX), and Duchene muscular dystrophy (DMD). Some of these diseases manifest not only in males and homozygous females, but also in heterozygous females due to random inactivation of one X chromosome (XCI), resulting in varied degrees of severity depending on the proportion of cells that silenced the wild-type allele.

A classic example in epigenetics, XCI achieves dosage balance in mammals by completely silencing one of two X chromosomes in female embryos. Although XCI has been studied for over 50 years now, there are many aspects that remain poorly understood, first and foremost the mechanism by which XCI spreads and silences genes across an entire chromosome. During XCI, the long non-coding RNA Xist recruits repressive Polycomb proteins to the inactive X (Xi), and recent work from our lab has shown that XCI originates from a nucleation center inside the Xist gene itself. A major unresolved problem, however, pertains to the cis-specific and long-range action of Xist RNA. In particular, how are silencing complexes anchored to the Xi and how are they spread throughout the chromosome? One hypothesis suggests that repetitive elements of the LINE1 class facilitate spreading. However, this hypothesis has been difficult to test directly, as the task of linking repeats to locus-specific function has been complicated by their nature of being repetitive. We herein devise a strategy that overcomes this problem and examine allele-specific binding of Polycomb repressive complex 2 (PRC2) and changing chromatin composition during XCI at nucleosome-resolution. Our chromosome-wide profiles of Xi and Xa (active X) allow us for the first time to examine the spreading of silencing factors and loss of active transcription during XCI. In addition, we also identify genes subject to or escaping XCI and develop testable hypotheses to dissect the mechanism of XCI spreading in the future. Our data suggest a model by which XCI is governed by a hierarchy of defined Polycomb stations that spread silencing along gene-rich domains of the Xi.

Reyon, Deepak BS, PhD
Research Fellow, Department of Pathology
dreyon@partner.org

Poster Number 49

High-throughput genome editing using FLASH assembled TALENs

Investigators: Deepak Reyon, PhD; Shengdar Q. Tsai, PhD; Cyd Khayter, BS; Jennifer A. Foden, BS; J. Keith Joung, MD, PhD

Engineered transcription activator-like effector nucleases (TALENs) are quickly becoming a widely adopted technology for genome editing because they have been shown to work robustly in several organisms, cells types, and both human somatic and pluripotent stem cells. We recently described Fast Ligation-based Automatable Solid-phase High-throughput (FLASH), a public available TALEN assembly platform that enables a single researcher to build up to 96 sequence verified TALEN encoding DNA constructs in one week (Reyon & Tsai et al., Nat Biotechnol. 2012). In this study we used FLASH to generate 48 TALEN pairs that bind to target sites of varying length (from 10 to 21 base pairs) along an integrated EGFP reporter gene. Using this strategy we identified optimal binding site lengths that result in active engineered TALENs. Furthermore, we identified that, excluding the 5' thymine, the activity of a TALEN is not dictated by the sequence composition of the target site as suggested by previous studies. Encouraged by these results we proceeded to build 96 TALEN pairs to target endogenous sites within genes that have been implicated in cancer or epigenetic regulation. Of these 96 TALEN pairs tested, we could detect varying rates of mutagenic NHEJ events (from 2.5% to 55.8% of alleles) in 84 sites. These results, along with the FLASH platform, demonstrate that TALENs are robust reagents that can be used routinely for both simple genome editing project and in high-throughput for large-scale genome editing.

Poster Number 50

Saxena, Richa PhD
Assistant Professor, Center for Human Genetic Research
rsaxena@chgr.mgh.harvard.edu

PER2 Polymorphism Influences Slow-Wave Sleep

Investigators: Anne-Marie Chang, PhD; Orfeu M. Buxton, PhD; Charles A. Czeisler, PhD, MD; Jeanne F. Duffy, PhD, M.BA; Steven W. Lockley, PhD; Frank A.J.L. Scheer, PhD; Richa Saxena, PhD

Introduction: Slow wave sleep (SWS), defined by EEG brain activity in the low-frequency range (0.5-4.5 Hz), is a marker of deep sleep. SWS has been associated with growth hormone release, memory consolidation, and is considered to be the more restorative stage of sleep. Suppression of SWS is associated with impaired glucose tolerance. Recent studies have shown genetic associations between SWS measures and common genetic variants.

Methods: Using a candidate gene approach, we genotyped 129 single nucleotide polymorphisms (SNP) tagging common variation and rare missense variants from circadian genes (CLOCK, CRY2, DEC2, PER2) and type 2 diabetes gene MTNR1B in 104 young healthy adults in whom sleep was recorded in the laboratory. Genetic analysis was initiated in a discovery cohort (n=64) where sleep was recorded during 8-h episode on the 3rd baseline night. Association with PER2 SNP rs6753456 was then tested in another cohort (n=40) which included 8-h sleep recordings collected during the 1st baseline night. Both groups were independent with no overlap of individuals, and the replication cohort was selected apriori.

Results: rs6753456 was associated with SWS duration in the 3rd baseline night group (n=50 whites, p=3.42 x10-5, empirical p=0.002). SWS time was reduced by 36 minutes/night in those carrying the risk allele. This association was not replicated in the 1st baseline night group (n=27 whites p=0.56) but meta-analysis of both groups (n=77 whites) showed a 26 minute/night decrease of SWS (p=3.49 x10-5).

Conclusion: We found that a common polymorphism in the human PER2 gene had an effect of 36 minutes in the amount of SWS. The risk allele was highly prevalent in our cohort (MAF 0.37). Lack of replication in the 1st night group may be due to power and/or increased variability of PSG during the 1st night in the laboratory. These results support the mounting evidence showing that objective measures of sleep, such as those from PSG, have a genetic basis.

Support: National Institute of Health (NIH) grant DK089378; and in part by NIH grants HL080978 and MH045130, the National Space Biomedical Research Institute (NSBRI) grant HPF01601, and the CTSC (NIH UL1 RR025758).

Poster Number 51

Slaugenhaupt, Susan A. PhD
Associate Professor, Center for Human Genetic Research
slaugenhaupt@chgr.mgh.harvard.edu

Creation of a new mouse model for the mRNA splicing disease familial dysautonomia

Investigators: Elisabetta Morini, PhD; Paula Dietrich, PhD; Ioannis Dragatsis, PhD; Susan A. Slaugenhaupt, PhD

Recent studies emphasize the importance of splicing mutations as causative agents of human genetic disease. 50% of point mutations responsible for genetic disorders are predicted to affect splicing. Familial dysautonomia (FD) is a good disease model for studying new strategies to correct splicing defects. FD is a recessive neurodegenerative disease caused by a splice mutation in the IKBKAP gene which leads to variable skipping of exon 20. The fact that FD patients retain the capacity to make normal mRNA and protein have made this disorder an attractive candidate for development of therapies aimed at increasing splicing efficiency and normal protein levels. We found that the small molecule kinetin, a plant cytokinin, can correct the IKBKAP splicing defect and increase the amount of normal mRNA and protein in FD cell lines. We have also shown that kinetin can increase the level of functional IKAP protein in mice following oral dosing in all tissues tested, including brain. Kinetin has also been shown to improve exon inclusion in neurofibromatosis type I. Despite these remarkable advances, including our demonstration of in vivo efficacy in human FD patients, we still do not know if increasing protein expression will result in correction of phenotype.

In order to create a phenotypic model of FD in which we can study the effect of drugs aimed at correcting splicing defect, we introduced an FD transgene (TgFD9) into the Ikbkap delta20/flox mouse model by sequential mating. The Ikbkap delta20/flox mouse model shows and accurately models many phenotypes of the human disease. Here we show that these mice exhibit the same tissue-specific mis-splicing of the IKBKAP transgene, which results in the correct temporal-spatial pattern of IKAP protein expression. At the same time the introduction of human IKAP from the transgene attenuates the severe FD phenotype observed in Ikbkap delta20/flox mouse, but does not result in complete rescue. Our results demonstrate that the new TgFD9 Ikbkap delta20/flox mouse accurately models both disease phenotype and mRNA mis-splicing. The creation of this new model will allow us to perform detailed clinical trial of kinetin and other therapeutics and, thus, to develop therapies not only for familial dysautonomia, but also for other genetic disorders caused by aberrant mRNA splicing.

Poster Number 52

Tabach, Yuval PhD
Research Fellow, Molecular Biology
tabach@molbio.mgh.harvard.edu

Small RNA pathway genes identified by patterns of phylogenetic conservation and divergence

Investigators: Yuval Tabach; Allison C. Billic; Gabriel D. Hayesa; Martin A. Newman; Or Zuk, Harrison Gabel; Ravi Kamath; Keren Yacoby; Brad Chapman; Susana M. Garcia; Mark Borowsky; John K. Kim; Gary Ruvkun

Genetic and biochemical analyses of RNA interference (RNAi) and microRNA (miRNA) pathways have revealed proteins such as Argonaute/PIWI and Dicer that process and present small RNAs to their targets. Well validated small RNA pathway cofactors, such as the Argonaute/PIWI proteins show distinctive patterns of conservation or divergence in particular animal, plant, fungal, and protist species. We compared 86 divergent eukaryotic genome sequences to discern sets of proteins that show similar phylogenetic profiles with known small RNA cofactors. A large set of additional candidate small RNA cofactors have emerged from functional genomic screens for defects in miRNA- or siRNA-mediated repression in C. elegans and D. melanogaster1,2 and from proteomic analyses of proteins co-purifying with validated small RNA pathway proteins3,4. The phylogenetic profiles of many of these candidate small RNA pathway proteins are similar to those of known small RNA cofactor proteins. We used a Bayesian approach to integrate the phylogenetic profile analysis with predictions from diverse transcriptional coregulation and proteome interaction datasets to assign a probability for each protein for a role in a small RNA pathway. Testing high-confidence candidates from this analysis for defects in RNAi silencing, we found that about half of the predicted small RNA cofactors are required for RNAi silencing. Many of the newly identified small RNA pathway proteins are orthologues of proteins implicated in RNA splicing. In support of a deep connection between the mechanism of RNA splicing and small RNA-mediated gene silencing, the presence of the Argonaute proteins and other small RNA components in the many species analysed strongly correlates with the number of introns in that species.

Poster Number 53

Tare, Archana MS
Research Technician, Center for Human Genetic Research
tare@chgr.mgh.harvard.edu

Impact of BDNF obesity variants on circadian phenotypes in humans

Investigators: Archana Tare, MS; Charles A. Czeisler MD, PhD; Jeanne F. Duffy, PhD; Sean W. Cain, PhD; Anne-Marie Chang, PhD; Richa Saxena, PhD

Brain-derived neurotrophic factor (BDNF) is a growth factor that influences proliferation, differentiation, and survival of neuronal cells. It has been found to be a potent modulator of circadian rhythms. Recent genome-wide association studies have identified that two independent variants, rs6265 and rs925946 (r2 =0.135), in BDNF are associated with obesity. Disruption of circadian rhythms has been previously shown to be associated with increased body fat and altered metabolism. Also, heterozygous BDNF knock out mice have been found to have altered intrinsic periods, with an endogenous day length that is ~30 minutes shorter than in wild-type mice. However, the relationship between BDNF variants, circadian rhythms and obesity remains unclear. Here, we investigated the association of missense polymorphism rs6265 (Val66Met) and rs925946 with circadian phenotypes in humans. The study sample consisted of participants in forced-desynchrony in-lab protocols at the Division of Sleep Medicine at BWH. Two hundred sixty subjects were genotyped for rs6265 and rs925946 using Taqman genotyping assays. An additive and recessive genetic model with age, gender and 10 principal components to adjust for ancestry was used to test for genetic association between BDNF variants and 16 circadian phenotypes. The analysis was performed with European Americans only. We observed that humans with the Met/Met genotype had an average endogenous period of temperature and melatonin that was ~18 minutes shorter than subjects with the Val/Val of Val/Met genotype ($P<0.025$). The effect of the Met allele is recessive, with no difference between Val/Val and Val/Met subjects. Moreover, humans with Met/Met genotype had 1.53 hr phase advance, measured using core body temperature, compared to the subjects with Val/Val and Val/Met genotypes ($P<0.025$). Genetic variation in BDNF contributes to circadian period, phase and obesity, suggesting there may be shared genetic mechanisms. This study identifies the first common polymorphism having a powerful influence on circadian period and phase in humans which require additional validation in larger samples.

Poster Number 54

Thomas, Brett P. BA
Research Technician, Center for Human Genetic Research
bthomas@atgu.mgh.harvard.edu

xBrowse: a fast, intuitive interface for genomic data from Mendelian disease families

Investigators: Brett P. Thomas, BA; Monkol Lek, PhD; Elaine Lim; Andrew Kirby; Mark J. Daly, PhD; Daniel G. MacArthur, PhD

Exome sequencing, which provides high-quality sequence data for the majority of protein-coding bases in the human genome, is a powerful tool for discovering the causes of Mendelian genetic disorders. However, many exome studies of monogenic disease families do not immediately identify an unambiguous genetic cause. We have developed a software platform, xBrowse, that aims to improve the interpretation and outcomes of exome sequencing studies.

There are two primary reasons that exome sequencing can fail to identify the genetic cause of a Mendelian disease. One possibility is that a cause is simply undiscoverable—the underlying mutations may lie outside protein-coding regions, or the disorder may not follow Mendelian inheritance. Another possibility is that a genetic cause is present in the exome, but current methods fail to identify it. This latter category has been our focus. We have identified three targets for improvement in current methods: better quality control and variant filtering; streamlined variant annotation; and creating phenotype-rich reference datasets.

We have developed a set of methods and best practices for each area above, but for these efforts to be useful in a clinical research setting it is essential that results be made accessible in an intuitive format. As a result, we developed a software platform, xBrowse, that provides researchers with solutions to many of these challenges at once. xBrowse allows researchers to load the raw results from a Mendelian family sequencing study, along with basic information about the pedigree structure, and receive automated variant calling, sample quality control, and variant annotation. xBrowse then provides a web-based graphical interface for researchers to search for potential causal variants under a variety of inheritance models and to prioritize the results from these searches based on other functional data. Individual variants can be compared to variation from over 10,000 control exomes in multiple reference populations. For phenotypes that have known disease-causing genes, variants can be cross referenced with known disease genes, and candidate genes prioritized using protein-protein interaction and tissue expression data.

We describe the application of this platform to exome sequencing data from over 100 families affected by a wide variety of rare diseases - highlighting several published collaborations within the MGH community in which novel genetic disorders were identified. We are actively seeking collaborations with clinical researchers in the MGH community for beta testing the application of xBrowse to other rare disease families.

Poster Number 55

Acharya, Mridu PhD
Research Fellow, Mass General Hospital *for* Children
acharya.mridu@mgh.harvard.edu

Regulation of B Cell Tolerance by Alpha (v) Integrins and Selective Autophagy

Investigators: Mridu Acharya, PhD; Anna Sokolovska, PhD; Kara Konway, PhD; Elahna Paul, MD, PhD; Richard Hynes, PhD; John Savill, PhD; Lynda Stuart, MD, PhD; Ramnik Xavier, MD, PhD; Adam Lacy-Hulbert

Complex networks modulate immune cell signaling, to ensure appropriate immune response to pathogens while limiting responses to self-antigens. Failure of mechanisms that limit excessive immune signaling are thought to drive chronic systemic autoimmune diseases such as systemic lupus erythematosus (SLE). SLE is characterized by production of high titers of autoantibodies to DNA and RNA, and is often associated with increased immune responses to remnants from apoptotic cells. Excessive signaling through nucleic acid sensing toll-like receptors (TLRs) such as TLR9 and TLR7 is known to drive the activation and expansion of autoreactive B cells. However, the mechanisms by which B cell activation to self-antigens, such as those derived from dying cells, is regulated to avoid autoimmunity are still poorly understood.

Integrins are adhesion molecules that modulate signaling via other receptors and the αv family of integrins are known to bind apoptotic cells and have important role in immune cell functions. I have found that mice lacking αv integrins in B cells have increased activation of potentially autoreactive subsets of B cells in the marginal zone (MZ) and B1 B cell compartment and develop autoantibodies. In preliminary experiments I have discovered a novel mechanism by which αv integrins can regulate TLR signaling in MZ and B1 B cells using the process of autophagy. Based on my preliminary data, I hypothesize that αv integrins induce selective autophagy of immune signaling molecules through ubiquitylation, and that this limits activation of self-reactive effector B cells, preventing autoimmunity.

IMMUNOLOGY & INFLAMMATION

Poster Number 56

Alves, Anna-Maria MS
Research Technician, Mass General Hospital *for* Children
aalves4@partners.org

Studying the Expression of the Transcription Factor HLH-30 under Alternative Promoters in C. elegans

Investigators: Anna-Maria F. Alves, MS; Orane Visvikis, PhD; Amanda C. Wollenberg, PhD; Javier E. Irazoqui, PhD

C. elegans is a powerful tool in studying innate immunity to Staphylococcus aureus infection. During infection, S. aureus induces a transcriptional response that we have shown to be largely dependent on the transcription factor HLH-30. HLH-30 expression is induced by S. aureus. Knocking out HLH-30 makes animals susceptible to S. aureus, suggesting that HLH-30 is a critical component of host defense. Like its human counterpart TFEB, HLH-30 has three alternative promoters. Focusing on one of these promoters, we have shown that HLH-30 is expressed in the vulva, rectal cells, pharynx and the intestine. We have also shown that under this promoter, expression of HLH-30 is sufficient to rescue the hypersusceptibility of hlh-30 mutants to S. aureus. However, we know very little about the role and relevance of the other two HLH-30 promoters and it is still unknown which of these promoters is responsible for the induction of HLH-30 in response to S. aureus. We have focused our research on three questions. , we are interested in knowing (a) whether the expression pattern of HLH-30 changes under different promoters, and (b) whether all of the promoters are induced during infection with S. aureus. To address these questions, we are creating transcriptional fusions of GFP under the control of one of the two alternative promoters. We will look at GFP localization and levels both before and after exposure to S. aureus using fluorescence microscopy. Lastly, we are interested in the functional relevance of the alternative promoters during S. aureus infection. To address this question, we will create translational fusions that express GFP-tagged HLH-30 under the control of the two alternative hlh-30 promoters. We will determine whether these constructs can rescue hlh-30 mutants by performing killing assays comparing the differences in median toxic dose of the rescued versus the non-rescued hlh-30 mutants. In this poster, we will present our preliminary findings and discuss directions for future research.

Poster Number 57

Becker, Christine PhD
Research Fellow, Mass General Hospital *for* Children
cbecker2@partners.org

A lysosomal resident GTPase that interacts with caspase-1 and is important for regulating trafficking in the innate immune system

Investigators: Christine Becker, PhD; Anna Sokolovska, PhD; WK Eddie Ip, PhD; Ashish Sarraju, BSc; Daniel R. Caffrey, PhD; Nicholas Paquette, PhD; Antoine Tanne, PhD; Emma M. Creagh, PhD; Katherine A. Fitzgerald, PhD; Adam Lacy-Hulbert, PhD; Luke A.J. O'Neill, PhD; Lynda M. Stuart, PhD

Differential compartmentalisation of receptors and their adaptors dictates which ligands are recognised, as well as the downstream signals that are generated. The innate immune system relies on a variety of trafficking networks to ensure correct delivery of the receptors and their ligands to these compartments. These networks are comprised of proteins that include Rab and Rho GTPases. There are over 60 Rab GTPases currently identified and proteomic analysis has previously shown that many of these Rab proteins are localised to phagosomes and endolysosomal compartments and therefore may be important in host defense. Here we describe Rab39a as a GTPase protein with important functions in the innate immune system. We show that Rab39a binds caspase-1 and contains an evolutionary conserved caspase-1 cleavage site. Rab39a is cleaved by recombinant caspase-1 and during inflammasome activation. Our previous work has shown that Rab39a participates in IL-1b secretion. Current work focuses on the role of Rab39a in other trafficking events in the innate immune system. In resting macrophages Rab39a localises with LAMP1 positive tubular lysosomes and vesicles, identifying it as a lysosome-resident Rab. Rab39a is also a phagosome–associated Rab and is recruited to phagosomes containing S. aureus, C. albicans or latex beads. Our results suggest that by controlling many steps of trafficking in the innate immune system Rab39a plays an important role in host defense.

Poster Number 58

Causton, Benjamin PhD
Research Fellow, Medicine
bcauston@partners.org

CARMA3 Links the Innate and Adaptive Immune Responses in Allergic Asthma

Investigators: Benjamin Causton, PhD; Ravisankar A. Ramadas, PhD; Benjamin D. Medoff, MD

Innate immune responses by airway epithelial cells (AECs) help initiate and propagate the adaptive immune response associated with allergic airway inflammation in asthma. Activation of the transcription factor NF-κB in AECs by allergens or secondary mediators via G-protein-coupled receptors (GPCRs) is an important component of this multifaceted inflammatory cascade. The CARMA family of proteins (CARMA1, 2, and 3) are molecular scaffolds required for the assembly of multi-protein complexes involved in the activation of NF-κB and thus mediate cell- and pathway-specific NF-κB activation. Whereas CARMA1 and CARMA2 are predominantly expressed in lymphocytes and placenta respectively, CARMA3 is expressed in a wide range of non-hematopoietic cells, including AECs. Here we demonstrate that lentiviral knockdown of CARMA3 in normal human bronchial epithelial cells reduces the production of pro-asthmatic mediators IL-8, TSLP, CCL20/MIP-3α and GM-CSF in response to asthma-relevant GPCR ligands, including lysophosphatidic acid (LPA), adenosine triphosphate (ATP) and house dust mite (HDM) allergen.

We have also generated a mouse strain that has deletion of CARMA3 specifically in AECs and utilizing a murine model of allergic airways disease, we demonstrate that these mice develop reduced airway eosinophilia and pro-inflammatory cytokine production compared to control mice. In addition, we show that in mice deficient in CARMA3 in AECs that there were reduced mature myeloid DCs in the lung compared to the control mice and that the DCs from mice lacking CARMA3 in AECs had impaired antigen presentation.

In conclusion, we show that CARMA3 helps mediate allergic airway inflammation, and that CARMA3 is a critical signaling molecule bridging the innate and adaptive immune responses. These data suggest that CARMA3 could be a promising therapeutic target to reduce airway inflammation in asthma.

Poster Number 59

Climov, Mihail MD
Research Fellow, Surgery
mihail.climov@tbrc.mgh.harvard.edu

Immune regulation of allogeneic antibody responses

Investigators: Raimon Duran-Struuck, DVM, PhD; Mihail Climov, MD; Ashley Gusha; Edward Harrington; Abraham J. Matar; Rebecca L. Crepeau; Thomas R. Spitzer, MD; David H. Sachs, MD; Christene A. Huang, PhD

Background: Durable multi-lineage chimerism and allograft tolerance without graft versus host disease can be readily achieved in mice, dogs and pigs, but has proved difficult to achieve in the clinic. Protocols using combined hematopoietic cell and renal transplantation have demonstrated feasibility of allograft tolerance induction despite loss of detectable peripheral blood chimerism in non-human primates (NHP) and in patients. The mechanism of allograft tolerance induced through such transient chimerism in these recipients remains unclear. Using miniature swine as a large animal model with demonstrated clinical relevance, we have developed a novel mild conditioning protocol for allogeneic hematopoietic cell transplantation (HCT) that preserves immune function and results in stable stem cell engraftment across MHC barriers without graft versus host disease. The quality and frequency of stem cells within the donor hematopoietic cell source used for transplantation is important for consistent stable stem cell engraftment when using this protocol. During optimization of the donor stem cell mobilization strategy, some recipient animals developed only transient multi-lineage peripheral blood chimerism that became undetectable within the first 3 months post transplantation similar to the transient chimerism seen in NHP and patients. This study assessed the cellular and humoral status of HCT treated animals in correlation with loss of chimerism.

Methods: Ten HCT recipients lost detectable donor cell chimerism in the peripheral blood and were included in this study. All animals received 30 days of cyclosporine (CyA) beginning two days prior to HCT with taper until day 45. In addition to CyA, animals received low-dose total body irradiation (100cGy TBI) and partial recipient T cell depletion using a porcine specific CD3 immunotoxin (pCD3-IT). The dose of donor cells given as part of the HCT ranged from 0.5 – 15 billion cells/kg recipient body weight. Six animals received cytokine mobilized donor leukapheresis product and 4 animals received un-mobilized donor peripheral blood mononuclear cells. Control animals were exposed to allogeneic cells without any immunosuppression. Cellular immune responses to donor cells were assessed by Mixed Lymphocyte Reactivity (MLR) and Cell Mediated Lympholysis (CML) assays. Donor specific allo-antibody was assessed by flow cytometry and complement dependent antibody mediated cytotoxicity assays.

Results: Loss of chimerism coincided with return of donor specific MLR and CML responses suggestive of rejection. Despite the loss of chimerism and return of anti-donor cellular proliferative and cytotoxic responses, no anti-donor antibody could be detected in these recipients. Upon further investigation, we observed that allo-antibody responses were not induced even after a second exposure to donor cells without immunosuppression through donor leukocyte infusion (DLI) (n=10) or following donor skin graft rejection (n=3). Attempts to further immunize some of these animals (n=6) with multiple subcutaneous injections of donor cells with or without complete Freund's adjuvant also failed to induce donor specific antibody. In contrast, control animals exposed to donor cells without conditioning had sustained allo-antibody responses detectable within two weeks following either intravenous (n=2) or subcutaneous (n=2) injection of cells as well as following skin graft rejection.

Conclusions: These results suggest that exposure to donor cells following mild conditioning and with a short course of CyA can result in robust immune modulation of antibody responses to allogeneic cells. B cell unresponsiveness is stable and does not depend on persistence of unresponsiveness at the T cell level or the persistence of donor cells. We speculate that this mechanism of immune modulation of B cell responses by allogeneic cells may play an important role in facilitating induction of transplantation tolerance through HCT.

Poster Number 60

Germana, Sharon MS
Lab Manager, Surgery
sgermana@partners.org

Role of MHC Class II in Treg-Mediated Tolerance to Allogeneic Transplants

Investigators: Sharon Germana, MS; Paulo Martins, MD; PhD Christian LeGuern, PhD

Transfer of donor MHC class II genes (MHCII) in the bone marrow of recipients of allografts induced tolerance spreading to all alloantigens. Tolerance was donor MHCII-specific tolerance, transferable only via host CD4 Tregs and was selectively induced by MHCII gene therapy. Studies on the fate of transgenic MHCII molecules revealed that both the α and β chains provided peptides presented on the MHCII of bone marrow-derived antigen-presenting cells (APCs). Transgene-matched graft MHCII was critical for survival as donor MHCII-treated recipients promptly rejected MHCII-deficient transplants. Next, the role of thymic transgenic MHCII peptides on Treg development was studied in a model recapitulating MHCII peptide presentation: the IEα 52-68 peptide/IAb complexes recognized by the YA-e mAb and TEa transgenic TCR. With this model we showed that 1) the highly conserved IEα sequence was dominantly exposed on all dendritic cells located in the thymic medulla, the birthplace of Tregs, and 2) transfer of the IEα peptide into IEneg mice via bone marrow transplantation, converted host IEα-specific CD4 T cells into CD4+ CD25hi CD25+ Foxp3+ Tregs. These data are consistent with a dominant role of MHCII peptides in shaping Treg TCR specificity and differentiation. They also propose a mechanism for MHCII-tolerance: MHCII-specific Tregs would require activation by cognate MHCII peptide provided by MHCII-matched transplants prior to suppressing alloreactive T cells of different TCR specificity

Poster Number 61

Grigoryeva, Lubov BS
Research Technician, Center for Systems Biology
grigoryeva.lubov@mgh.harvard.edu

Postnatal development of mononuclear phagocytes in the mouse epididymis

Investigators: Lubov S. Grigoryeva, BS; Eric Hill, BS; Nicolas Da Silva, PhD

The establishment of male fertility requires tightly regulated interactions between the immune and reproductive systems. The epididymis, which is the primary site of sperm maturation and storage, is a long and convoluted tubule lined by a complex pseudostratified epithelium. We have shown previously that the epididymal tubule is surrounded by a dense and heterogeneous network of mononuclear phagocytes (MPs, expressing various levels of dendritic cells and macrophage markers) that establish intimate contact with adjacent epithelial cells. The functions of epididymal MPs are currently unknown, but their antigen-presenting capabilities and their abundance in the proximal epididymis suggest that they might play an active role in the modulation of immunity and/or tolerance during the early stages of sperm maturation. To gain insight into the possible functions of epididymal MPs, we mapped their distribution in the epididymis during the postnatal development using microscopy analysis of CD11c-EYFP and CX3CR1-GFP mice, two models that have been used extensively by other groups to identify and study mononuclear phagocytes in other mucosal systems.

CD11c+ and CX3CR1+ cells were present in the epididymis as early as 1 week after birth. At that time, MPs were rare and distributed randomly throughout the interstitial space. Until week 3, MPs were mostly ovoid or elongated/bipolar and did not establish intimate contact with the maturing epididymal tubule. The number of epididymal MPs gradually increased and, between week 4 and week 5 (which corresponds to puberty in the C57BL/6 mouse background), they underwent major morphological changes. In the proximal epididymis, CD11c+ and CX3CR1+ cells progressively acquired a stellate/dendriform morphology and relocated in the peritubular region. Cellular bodies and lateral extensions were located at the base of the epithelium, while slender dendrites extended between epithelial cells toward the lumen. This reorganization of the mononuclear phagocyte network coincided with the arrival of sperm and luminal hormones in the epididymis, as well as the increase of circulating androgens. At week 5, the epididymal MP had acquired the overall appearance described previously in adult mice: dendriform cells with numerous intraepithelial dendrites were abundant in the most proximal region of the epididymis, while the most distal segments were populated by peritubular and interstitial phagocytes. Interestingly, the peritubular region of the vas deferens (VD, located immediately downstream of the epididymis) was heavily populated by CD11c+ and CX3CR1+ MPs during the early stages of postnatal development, long before the arrival of testicular luminal factors and spermatozoa in the lumen.

Our preliminary results indicate that mononuclear phagocytes start populating the epididymis shortly after birth and are modulated by factors released at puberty. The specific roles of luminal and circulating hormones, as well as spermatozoa, will be further investigated. In addition, phagocytes might populate the distal segments of the excurrent duct (including VD) very early to prevent ascending pathogens from infecting the maturing epididymis and testis. Our data will help elucidating the nature of the intricate relationships between the immune system and the reproductive system during the development of the male reproductive tract.

Huang, Christene PhD
Associate Professor, Surgery
christene.huang@tbrc.mgh.harvard.edu

Poster Number 62

Histological Assessment of Cutaneous Acute Graft-Versus-Host Disease in a Preclinical Swine Model of Hematopoietic Cell Transplantation and Vascularized Skin Flap Tolerance

Investigators: George F. Murphy, MD; Raimon Duran-Struuck, DVM, PhD; Evan Farkash, MD; Mihail Climov, MD; David Leonard, MD; Curtis L. Cetrulo, Jr., MD; Thomas R. Spitzer, MD; David H. Sachs, MD; Christene A. Huang, PhD

Graft-versus-host disease (GVHD) remains a frequent complication of hematopoietic cell transplantation with skin being a principal target organ. Murine models have provided some insight into the mechanisms of this complex disease process. However, mouse skin differs from human skin, and results of studies in rodents may not translate well to the clinic. Miniature swine is a well-recognized animal model for preclinical studies of skin including dermal toxicology, transdermal drug delivery and wound healing. Unlike skin of rodents, dogs or non-human primates, porcine skin is similar to human skin in terms of structure of epidermal rete ridges (Figure 1A), hair follicle structure and density, and presence of sweat glands and subcutaneous fat.

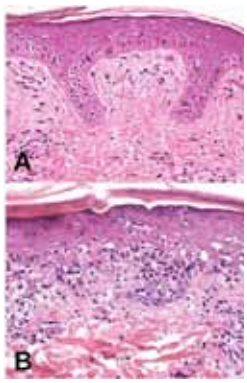

Figure 1: Comparison of normal porcine skin (A) resembling epidermal and dermal layers of human integument, and (B) recipient skin 34 days post DLI, showing brisk superficial lymphoid infiltrate associated with basal layer epidermal apoptosis.

We have developed a miniature swine model of haploidentical hematopoietic cell transplantation that results in stable stem cell engraftment, hematopoietic chimerism and donor skin flap tolerance without GVHD. Swine leukocyte antigen (SLA)ad animals receive 100cGy total body irradiation and T cell depletion using porcine CD3 immunotoxin prior to cytokine mobilized peripheral blood hematopoietic cell transplantation from a haploidentical SLAac donor. Daily cyclosporine is administered at doses adjusted to maintain serum levels between 400-800 ng/ml starting one day prior to transplantation and continued for 30 days with taper until day 45.

Mixed hematopoietic cell chimerism persists in these animals and donor vascularized skin flaps are accepted without the need for maintenance immunosuppression regardless of whether they are placed at the time of hematopoietic cell transplantation or greater than 100 days later. Despite the initial resistance to GVHD in this model, acute cutaneous GVHD could be induced through infusion of a high dose of donor leukocytes (DLI) including 15 million donor T cells/kg recipient body weight administered 463 days post hematopoietic cell transplantation and 314 days post vascularized donor skin flap transplantation. Conversion to full donor hematopoiesis was observed between 3-4 weeks post DLI. At this time a mild skin rash was evident in both donor and host skin which appeared to progress specifically within host skin. The presence of both donor and host skin on a tolerant animal whose peripheral blood consists of a mixture of both donor and host derived hematopoietic cells provides a novel model to evaluate specific targets of acute GVHD.

In this study we assess histologically the manifestations of acute GVHD in both donor and host skin and compare it to typical histological manifestations of acute GVHD observed in patients. Specifically, recipient skin developed superficial lymphoid infiltrates that progressed to confluence along the dermal-epidermal junction by day 21. These infiltrates were associated with intraepidermal migration, prominent basal cell layer keratinocyte apoptosis, and satellitosis virtually indistinguishable from grade 3-4 human cutaneous acute GVHD (Figure 1B). Superficial portions of hair follicles were involved, as also seen in human disease. Of interest, mild disease was detected in the donor skin grafts by day 62 post-DLI, where selective lymphoid infiltration in the tips of the epidermal rete ridges and in association with target cell apoptosis/satellitosis was documented, a finding remarkably similar to early targeting events in humans.

These findings emphasize the value of the porcine model for translational studies of cutaneous GVHD. Preliminary data suggest differences in cellular targeting between recipient and donor skin whereby the latter may be triggered by the presence of chimeric recipient-derived hematopoietic elements that have populated donor grafts. Further studies are now possible to explore the effector-target cell interactions in this clinically-relevant model of human cutaneous GVHD.

Poster Number 63

Jain, Nitya PhD
Research Fellow, Center for Computational and Integrative Biology
njain@ccib.mgh.harvard.edu

Understanding neonatal immunity: Does the evolving intestinal microbiota influence neonatal T cell development?

Investigators: Nitya Jain, PhD; Slim Sassi, PhD; Lyn Bry, MD, PhD; Brian Seed, PhD

The neonatal period is a unique ontological stage that is characterized by a largely immature immune system prone to tolerogenic responses. While beneficial for thwarting inappropriate autoreactivity, the lackluster immune responses in neonates has poor prognosis for successful pathogen-specific immunity as well as vaccinations. Interestingly, while newborns and infants are more susceptible to infectious diseases, infants in developed countries have become increasingly sensitive to developing allergies and asthma and there has been a recent striking elevation in the incidence of autoimmunity such as Type 1 Diabetes (T1D) and Inflammatory Bowel Disease (IBD) in children less than 5 years of age.

Post-natal microbial colonization of the sterile gut and the establishment of a symbiont microbial community are critical for the development and maturation of the neonatal mucosal immune system. Alterations in intestinal microbiota or dysbiosis have been associated with precipitation of several diseases such as IBD and T1D in adults. While dysbiosis can be brought about by various factors such as feeding regimens and antibiotic exposure, dramatic changes in gut microbial compositions also occur naturally during the post-natal period. Whether neonatal adaptive immunity perceives changes to the intestinal microbial environment and how it impacts the development and effector function of T cells is largely unknown. We hypothesize that the developing neonatal gut environment influences thymic T cell development by imprinting distinct effector and regulatory potentials that impacts peripheral T cell tolerance. Using cutting-edge, high-resolution RNA-sequencing technology, we show here that the molecular profile of developing T cell subsets in the thymus of neonate and adult mice are distinct. Maximal differences in gene expression are found at the DN2A and DN3A stages of T cell development suggesting that the key developmental events of commitment to the T cell and $\alpha\beta$ lineages respectively may be differentially impacted in neonates and adults. Further, neonatal mice raised in a germ-free environment have altered expression of regulatory transcription factors in thymic CD4SP and CD8SP cells that impacts effector T cell function in the periphery.

Our data suggest that thymic programming of effector $\alpha\beta$ T cell function is influenced by evolving gut microbiota in neonates. Understanding how the neonatal immune system first interacts with and normally tolerates fluctuations in the microbiota will help dissect the events of pediatric autoimmunity resulting from genuine dysbiosis. Further, mechanistic insights into the evolution of neonatal T cell responses will aid in the improved design of infant vaccine strategies as well as immune-directed therapies.

Jung, Keehoon PhD
Research Fellow, Wellman Center for Photomedicine
keehoonjung@gmail.com

Poster Number 64

Endoscopic time-lapse imaging of immune cells in infarcted mouse hearts

Investigators: Keehoon Jung, PhD; Pilhan Kim, PhD; Florian Leuschner, MD, PhD; Rostic Gorbatov, BS, PhD; Jun Ki Kim, PhD; Takuya Ueno, MD, PhD; Matthias Nahrendorf, MD, PhD; Seok Hyun Yun, PhD

High-resolution imaging of the heart in vivo is challenging due to the difficulty in accessing the heart and the tissue motion caused by the heartbeat. Here, we describe a suction-assisted endoscope for visualizing fluorescently labeled cells and vessels in the beating heart tissue through a small incision made in the intercostal space. A suction tube with a diameter of 2-3 mm stabilizes the local tissue motion safely and effectively at a suction pressure of 50 mmHg. Using a minimally invasive endoscope integrated into a confocal microscope, we performed fluorescence cellular imaging in both normal and diseased hearts in live mice for an hour per session repeatedly over a few weeks. Real-time imaging revealed the surprisingly rapid infiltration of CX3CR1+ monocytes into the injured site within several minutes after acute myocardial infarction (MI). The time-lapse analysis of flowing and rolling (patrolling) monocytes in the heart and the peripheral circulation provide evidence that the massively recruited monocytes come first from the vascular reservoir and later from the spleen. The imaging method requires minimal surgical preparation and can be implemented into standard intravital microscopes. Our results demonstrate the applicability of our imaging method for a wide range of cardiovascular research.

Kim, James PhD
Assistant Professor, Surgery
jkim35@partners.org

Poster Number 65

Transplantation tolerance that depends on regulatory T cells induced by TGF-beta-producing regulatory B cells

Investigators: James I Kim, PhD; Kang Mi Lee, PhD; Gaoping Zhao, MD; Ryan Stott, BS; Julie SooHoo, BS; Moh Moh Lian, MD,; Wei Xiong, MD; Lindsey Fitzgerald, BS; Heidi Yeh, MD; Shaoping Deng, MD; James F Markmann, MD, PhD

Regulatory B cells (Bregs) have been shown to play a critical role in immune homeostasis and in autoimmunity models. We have recently demonstrated that combined anti-TIM-1 and anti-CD45RB antibody treatment generates regulatory B cells necessary for long-term mouse islet allograft survival in a full MHC-mismatch donor-recipient pair. Here we provide evidence that the induction of tolerance by regulatory B cells requires regulatory T cells. Specifically, adoptive transfer of Bregs results in an increase in absolute number of Tregs in grafted recipients and depletion of Tregs abrogates transplant tolerance conferred by adoptive transfer of regulatory B cells. We hypothesize that Bregs induce the expansion of Tregs, and demonstrate that Bregs from transplanted but not naive mice express TGF-beta complexed to latency-associated peptide (LAP). Furthermore, Bregs but not naive B cells induce Foxp3 expression in CD4+CD25- T cells by adoptive transfer in vivo and Breg mediated graft prolongation is abrogated by neutralization of TGF-beta activity. Collectively, these findings suggest that in this model antibody induced Bregs promote tolerance by inducing Tregs, possibly via TGF-beta production.

IMMUNOLOGY & INFLAMMATION

Poster Number 66

Kirienko, Natalia PhD
Research Fellow, Molecular Biology
kirienko@molbio.mgh.harvard.edu

Pseudomonas aeruginosa infection of Caenorhabditis elegans disrupts iron homeostasis, causing hypoxic response and death

Investigators: Natalia V. Kirienko, PhD; Daniel R. Kirienko, PhD; Jonah Larkins-Ford, BS; Frederick M. Ausubel, PhD

The opportunistic human pathogen Pseudomonas aeruginosa is a serious risk to patients who have burn wounds, medical implants, cystic fibrosis, or are immunocompromised. The nematode Caenorhabditis elegans is a valuable host for investigating P. aeruginosa infection, as many innate immune pathways are conserved between C. elegans and humans. In addition, multiple bacterial virulence factors necessary for human infection play roles in C. elegans pathogenesis. Here we describe a virulence mechanism for P. aeruginosa strain PA14 in a liquid-based, C. elegans infection model.

PA14-mediated killing in this model does not depend upon known quorum sensing pathways. Moreover, killing does not require either accumulation of P. aeruginosa cells in the C. elegans intestine or phenazine intoxication. To gain insight into pathogenic mechanisms that may be responsible, we used the liquid C. elegans–PA14 assay to carry out a high-throughput chemical genetics screen using compounds from the ICCB-Longwood/NSRB collection. Hits from this screen included known antimicrobials and chemotherapeutics. We also identified several compounds that appear to act as anti-infectives. Finally, one particular hit, the metal chelating agent ciclopirox olamine, suggested the importance of iron for infection and pathogenesis. This implicated pyoverdin, an iron-scavenging siderophore, as a crucial factor in the host-pathogen interaction. Our research sheds light on a function for pyoverdin directly in pathogenesis, rather than in nutrient acquisition and growth. Scavenging iron from the host triggers hypoxia and, subsequently, death. Finally, this C. elegans model allows further investigation of pyoverdin pathogenesis, which is crucial for virulence in mammals.

Poster Number 67

Lan, Yuk Yuen PhD
Research Fellow, Medicine
ylan@partners.org

Lysosomal Dnase2a is required for the autophagic clearance of self-damaged nuclear DNA

Investigators: Yuk Yuen Lan, PhD; Diana Londoño, MD, PhD; Nir Hacohen, PhD

Deficiencies in nucleases that degrade DNA lead to accumulation of self DNA, activation of innate immune responses and development of autoimmune disorders, including systemic lupus erythematosus and Aicardi-Goutiéres syndrome in humans, and autoimmune arthritis, nephritis and myocarditis in mice. How undegraded DNA accumulates and leads to immune responses in these deficiencies is not well understood. Here, we investigate the cell type specificity, source and sub-cellular localization of accumulated DNA in the absence of the major lysosomal DNA degradation enzyme, Dnase2a. Deletion of this nuclease results in inflammation and chronic polyarthritis that resembles human. We find that high levels of undegraded DNA accumulate in both phagocytic and non-phagocytic cells of Dnase2a-deficient mice. This excess DNA is of nuclear origin and co-localizes outside the nucleus with γ-H2AX, a protein that binds ends of damaged double-stranded DNA, and increases in abundance after induction of DNA damage. DNA appears to escape from the nucleus via nuclear buds and speckles and requires autophagosomes and lysosomes for degradation. A deficiency in autophagy leads to higher levels of extranuclear DNA. Furthermore, an innate immune response is induced in either Dnase2a-deficient or autophagy-deficient cells, but is abolished upon depletion of the Sting-mediated cytosolic nucleic acid sensing pathway. Our results reveal a process by which damaged nuclear DNA is transported via nuclear buds and autophagosomes from the nucleus to the lysosome where it is degraded by Dnase2a, thus preventing accumulation of DNA and activation of innate immune responses. Such a process may help explain how inflammation is regulated in diverse conditions, including cancer, chemotherapy and aging when damaged DNA is generated at high levels.

Poster Number 68

Lee, Kang Mi PhD
Research Fellow, Surgery
klee28@partners.org

Spontaneous Acceptance of B cell-deficient Mouse Islet Allografts Is Associated with Donor-derived Plasmacytoid Dendritic Cells

Investigators: Kang Mi Lee; Moh Moh Lian; Ryan Stott; Heidi Yeh; Shaoping Deng; James I Kim; James F. Markmann

Spontaneous acceptance of grafts can demonstrate novel mechanisms of drug-free transplantation tolerance. Mouse renal allografts as well as rat liver allografts in certain strain combinations survive spontaneously without immunosuppression. Here we demonstrate that mouse islet allografts from B cell-deficient donors have a remarkable ability to survive when transplanted to fully MHC mismatched B cell-deficient recipients. Wild-type Balb/c islets into B cell-deficient μMT-/- B6 recipients and B cell-deficient JH islet into wild-type B6 recipients were all rejected by 20 days post transplantation. Strikingly, islet allografts from JH mice survived long-term in 5 out of 6 μMT-/- B6 recipients without the need for any immunosuppression. Adoptive transfer of donor B cells caused allograft rejection quickly in all μMT-/- B6 recipients bearing JH islets, but this effect was not observed in recipients receiving B6 B cells which suggests donor B cells are more pathogenic in early immune processes of mouse islet rejection compared to recipients B cells. Interestingly, flow cytometry analysis showed a significantly increased proportion of plasmacytoid dendritic cells (pDC) in isolated islets, spleens and bone marrow from naive B cell-deficient mice compared to naive wild-type mice. Moreover, adoptive transfer of pDC purified from JH mice delayed allograft rejection upon transfer to untreated, grafted μMT-/- B6 recipients suggesting a tolerogenic effect of donor pDC. These results demonstrate that donor islets include cellular populations exerting contradictory roles: B cells represent critical players in the pathogenesis of graft rejection and pDCs contribute to tolerance. This study will help developing novel therapies targeting donor B cells and pDC to induce indefinite transplant survival.

Poster Number 69

Lee, Soyoung MD
Research Fellow, Transplant Center
slee84@partners.org

Renal allograft tolerance can be achieved in non-human primates via delayed mixed-hematopoietic chimerism and Alefacept treatment.

Investigators: Soyoung Lee, MD[1]; Yohei Yamada, MD[1]; Svjetlan Boskovic, MD[1]; Muhammad Atif[1]; Makoto Tonsho, MD; Ognjenka M. Nadazdin, MD[1]; Georges Tocco, MD[1]; Rex-Neal Smith, MD[2]; Robert B. Colvin, MD[2]; A. Benedict Cosimi, MD[1]; Joren C. Madsen, MD, D-Phil[1]; James S. Allan, MD[1]; Gilles Benichou, MD[1]; Tatsuo Kawai, MD[1]
[1]Transplant Surgery, Massachusetts General Hospital, Boston, Massachusetts, United States
[2]Pathology, Massachusetts General Hospital, Boston, Massachusetts, United States

Background: Renal allograft tolerance has been achieved in MHC-mismatched non-human primates (NHPs) and patients via the mixed-chimerism approach. To extend the applicability to deceased donor transplantation, we recently developed a novel approach, the "delayed protocol" in which donor bone marrow cells are infused 4 months after kidney transplantation. We have previously shown that activation/expansion of donor-reactive CD8+ effector memory T cells (TEMs) occurring after kidney transplantation (KTx) represents a major barrier to tolerance induction using our delayed mixed chimerism protocol. In this study, we tested whether, Alefacept, a fusion protein composed of IgG Fc portion and LFA-3, known to deplete selectively CD2highCD8+ TEMs could promote tolerance to kidney allografts in our model.

Method: 20 Cynomolgus monkey recipients underwent KTx from MHC mismatched donors with a triple drug immunosuppressive regimen (tacrolimus, mycophenolate mofetil and prednisone). Four months after KTx, recipients received a nonmyeloablative conditioning regimen (low dose TBI, thymic irradiation, ATGAM, anti-CD40L mAb) with or without additional treatment against CD8 TEM and received donor bone marrow transplantation from the kidney donor. The recipients were then treated with a one-month course of cyclosporine after, after which no immunosuppression (IS) was administered. Recipients were divided into three groups according to the additional treatment : Group A (control, n=5), B (anti-CD8 mAb, n= 12), C (LFA3-Ig, n=3).

Results: In Group A, all recipients failed to develop chimerism and lost their allograft due to rejection. In Group B, 10/12 developed chimerism and 6/10 survived long term without IS, 3 died due to EBV related lymphoma or BK virus infection and the last monkey due to acute rejection. Two failed chimerism and developed acute rejection. In Group C, all recipients developed multilineage chimerism without infectious complication or lymphoma and survived long-term without IS. The Alefacept treatment significantly delayed the expansion of CD2 high cells including CD8+ TEM while it did not affect the recovery of CD8+ naïve T cells. All transplanted monkeys maintained stable normal renal function (creatinine <2.0mg/dl) for more than 300 days.

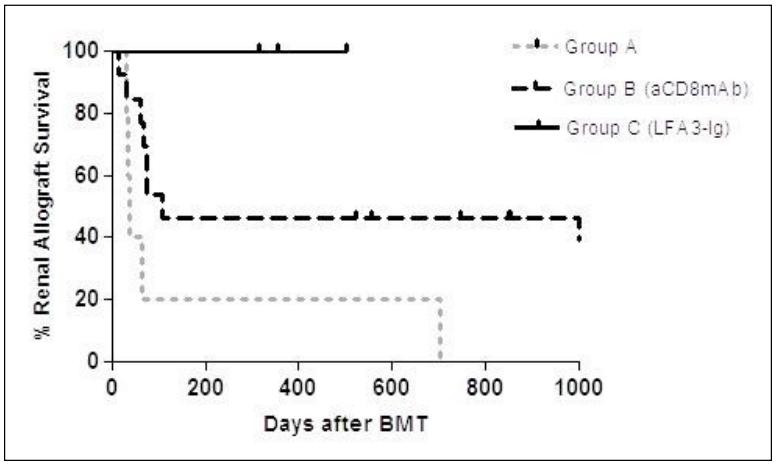

Conclusion: Alefacept successfully enhanced induction of chimerism and promoted renal allograft tolerance presumably via elimination of deleterious alloreactive CD8+ TEMs. Therefore, targeting of CD2high T cells represents a promising approach to overcome the expansion/activation of donor-reactive TEM thus promoting tolerance induction to allografts in primates.

Lin, Tian MD,PhD
Instructor, Pediatric Service
tlin7@partners.org

Poster Number 70

Identification of hemopexin as an anti-inflammatory factor that inhibits hemoglobin synergy with HMGB1 in sterile and infectious inflammation

Investigators: Tian Lin, MD, PhD; Fatima Sammy; Huan Yang, PhD; Sujatha Thundivalappil; Kevin J. Tracey, MD; H. Shaw Warren, MD

In numerous clinical settings such as trauma, infections and other hemorrhagic diseases, multiple endogenous substances are released into the extracellular space, including hemoglobin (Hb) and HMGB1, a pro-inflammatory intracellular DNA-binding protein in present in injured cells. We studied the effect of Hb and HMGB1 on the activation of macrophages. In the supernatant of cultured bone marrow-derived macrophages from C57BL/6 or C3H/HeN mice, significantly increased levels of pro-inflammatory cytokines (TNF and IL-6) were detected if Hb was added with HMGB1 as compared to culture with HMGB1 alone ($P < 0.01$), while Hb itself did not induce detectable TNF or IL-6. This synergistic effect was also present in the culture of TLR2 knockout and TLR4 deficient (C3H/HeJ) macrophages. Addition of hemopexin (Hx), an endogenous heme-binding plasma protein, significantly decreased TNF and IL-6 induced by Hb and HMGB1 ($P < 0.01$). Co-incubation of microbial ligands LPS or Pam3Cys with Hb and HMGB1 in the culture resulted in further dramatic increases of TNF and IL-6 that were also significantly decreased by Hx ($P < 0.01$). These findings suggest that Hb may play an important role in amplifying sterile as well as infectious inflammation, and that endogenous Hx may play a role in controlling it. Administration of Hx could be a beneficial strategy in clinical settings where extracellular Hb and HMGB1 are both present.

Madariaga, Maria Lucia L. MD
Resident, Surgery
lucia.madariaga@tbrc.mgh.harvard.edu

Poster Number 71

Kidney-Induced Cardiac Allograft Tolerance Across A Full MHC-Barrier In Miniature Swine

Investigators: Maria Lucia L. Madariaga, MD; Sebastian G. Michel, MD; Masayuki Tasaki, MD; Vincenzo Villani, MD; Evan A. Farkash, MD; Glenn M. La Muraglia II; James S. Allan, MD; David H. Sachs, MD; Kazuhiko Yamada, MD; Joren C. Madsen, MD

We have previously demonstrated that a kidney allograft has the ability to confer tolerance on a co-transplanted heart allograft procured from a class I-mismatched donor. However, kidney-induced cardiac allograft tolerance (KICAT) has not been tested in a fully MHC-disparate strain combination. The purpose of this study was to determine whether tolerance could be induced in heart/kidney transplant recipients across a more clinically relevant full-MHC barrier. Heart allografts (n=3) or heart/kidney allografts (n=5) were transplanted heterotopically into fully mismatched recipients that were treated with high-dose tacrolimus for 12 days. All isolated heart allografts rejected by POD 40. In contrast, all heart/kidney allografts survived for >100 days, with no evidence of rejection on serial cardiac biopsies. Heart/kidney recipients lost donor-specific responsiveness in CML and MLR assays, and did not develop alloantibody. These results show that KICAT can be extended to fully mismatched allografts in a consistent and robust manner. Elucidating the renal element responsible for KICAT could provide mechanistic information that leads to protocols aimed at inducing tolerance in recipients of isolated heart allografts.

Poster Number 72

Mansour, Michael MD,PhD
Instructor, Medicine
mkmansour@partners.org

The beta-1,3-glucan receptor, Dectin-1, controls fungal phagosome maturation

Investigators: Michael Mansour, MD, PhD; Jenny Tam, PhD; Nida Khan, BS; Sravanthi Puranam, Michael Seward; Peter Davids; Jatin Vyas, MD, PhD

The number of life-threatening fungal infections has risen as a result of the increased use of chemotherapeutics and immunosuppressive agents. Host defenses against invasive fungal infections require prompt recognition and phagocytosis by macrophages and dendritic cells. Following phagocytosis, these fungal-containing compartments, or phagosomes, dictate the subsequent maturation or specific recruitment of host cellular machinery such as lysosomes in a process termed phagosomal maturation. The initial recognition of fungal pathogens occurs through conserved pattern-recognition receptors including C-type lectins such as Dectin-1. Dectin-1 recognizes a common fungal cell wall carbohydrate constituent, β-1,3-glucan, found on many pathogenic fungi including Candida albicans, and Aspergillus fumigatus. Defects in Dectin-1 have been isolated in patients suffering from recurrent Candida infections demonstrating the essential role of carbohydrate recognition in eliciting protective immunity. In the following work, we sought to characterize the subsequent intracellular steps following β-1,3-glucan recognition, and phagocytosis by macrophages. We used our previously described fungal-like particle system (FLP) consisting of a polystyrene bead platform covalently conjugated to β-1,3-D-glucan that mimics the geometry and surface of a fungal pathogen. Following incubation with FLP, macrophages expressing GFP-Dectin-1 were lysed and contents subjected to discontinuous sucrose gradient to recover purified phagosomes. Using RAW cells expressing GFP-Dectin-1, we show that there is translocation of Dectin-1 from the surface to the phagosome with an off-rate of 2 hours after phagocytosis. In order to explore the contribution of pH to Dectin-1 egress from the phagosome, bafilomycinA1, a VTPase inhibitor, was used and showed significantly increased retention. Following Dectin-1 binding spleen tyrosine kinase (Syk) is activated. To understand the role of Syk signaling in phagosomal pH and subsequent Dectin-1 retention, a tyrosine to phenylalanine substitution was introduced within the Dectin-1 cytoplasmic ITAM-like motif responsible for the activation of Syk (Dectin-1-ΔY15). Raw cells expressing GFP-Dectin-1-ΔY15 were unable to phosphorylate Syk and showed prolonged retention of Dectin-1 to the phagosome when compared to wild-type Dectin-1. Raw cells expressing GFP-Dectin-1 pretreated with chemical inhibitors of Syk activation also show increased retention of Dectin-1 to β-glucan-containing phagosomes. We next explored subsequent phagolysosomal maturation milestones such as acidification and acquisition of LAMP-1. Phagosomes positive for Dectin-1-ΔY15 were unable to recruit LAMP-1 or acidify and remained Rab5B positive, an early endosome marker, indicating that Syk-activation is critical for phagosomal maturation. Using Candida albicans, similar blockade of phagosomal maturation was also seen. These data suggest a novel role for Dectin-1, not only as the initial surface receptor for β-glucan recognition, but also as a master controller for subsequent fungal phagosomal maturation through activation of a Syk-dependent process.

Poster Number 73

Mohamed, Mussa MD
Research Fellow, Surgery
mmohamed2@partners.org

Intestinal Alkaline Phosphatase is An Endogenous Anti-inflammatory Factor

Investigators: Mussa Mohamed, MD; Konstantinos P. Economopoulos, MD; Palak Patel, BA; Nur Muhammad, MD; Omeed Moaven, MD; Angela K. Moss, MD; Abeba Teshager, BA; Kanakaraju Kaliannan, MD; Seyed M. Abtahi, MD; Sayeda N. Alam, MD; Nondita S. Malo, BA; Sulaiman Hamarneh, MD; Madhu S. Malo, MD; Richard A. Hodin, MD

Introduction: Intestinal alkaline phosphatase (IAP) is an intestinal brush border enzyme known to have the ability to detoxify in-vitro many pro-inflammatory bacterial components, including lipopolysaccharides (LPS), lipoteichoic acid (LTA), flagellin, CpG-DNA and uridine diphosphate (UDP). Gastrointestinal tract inflammation and endotoxemia due to elevated bacterial toxic components in the gut and disruption of intestinal permeability play a crucial role in the development and progression of a wide spectrum of diseases. In this study we sought to determine whether the endogenous IAP enzyme functions as an anti-inflammatory factor.

Methods: We established a novel intestinal loop model to study the impact of endogenous IAP on the inflammatory activity of different bacterial components within a physiologic in vivo environment. The model was set up in wild type (WT) vs. IAP knockout (KO) mice of approximately 25 grams (n=5 for all groups). In another setting, we applied a fast (48 hours) vs. fed mouse model. Under general anesthesia, a 5 cm segment of proximal jejunum was carefully tied off at the proximal and distal ends, to isolate the loop. Different concentrations of LPS (100 ng/ml), LTA (5 µg/ml), flagellin (100 ng/ml), CpG-DNA (100 µg/ml) or UDP (1 mM) were injected into the loop and the luminal content was collected 2 hours later. Then, the supernatants were applied to RAW264.7 murine macrophage cells in triplicate and incubated overnight. LPS, LTA, Flagellin, CpG-DNA or UDP were directly applied to the cells as positive controls and endotoxin-free water was applied as a negative control. Tumor necrosis factor-alpha (TNF-α) levels were subsequently measured by sandwich ELISA.

Results: All studied bacterial components induced a marked increase in TNF-α levels from the RAW264.7 cells, whereas little TNF-α was seen in the case of endotoxin-free water alone. The luminal contents from the WT mice resulted in significantly lower TNF-α levels compared to the luminal contents from the KO mice for all studied bacterial toxins: LPS (600.9±75.47 vs. 946.2±55.99 pg/ml, p= 0.006), LTA (223.1±62.85 vs. 536.2±54.64 pg/ml, p= 0.005), flagellin (679.9±60.05 vs. 1008.8±61.15 pg/ml, p= 0.005), CpG-DNA (638.7±61.81 vs. 949.6±57.36 pg/ml , p= 0.006) and UDP (212.5±15.77 vs. 312.6±26.60 pg/ml, p= 0.012). Luminal contents from fed mice resulted in lower TNF-a levels compared to fasted mice for LPS (585.4±76.35 vs. 900.2±63.62 pg/ml, p=0.013).

Conclusions: IAP detoxifies and prevents the inflammatory effects of LPS, LTA, flagellin, CpG-DNA and UDP in the gut. The loss of IAP expression that occurs with fasting could be responsible for the systemic sepsis syndrome seen in critically ill patients.

IMMUNOLOGY & INFLAMMATION

Poster Number 74

Paidassi, Helena PhD
Research Fellow, Mass General Hospital *for* Children
hpaidassi@partners.org

αv integrins and orchestration of intestinal immune responses by dendritic cells

Investigators: Helena Paidassi, PhD; Ailiang Zhang, MS; Mridu Acharya, PhD; Subhankar Mukhopadhyay, PhD; Manjae Kwon; Lynda Stuart, MD, PhD; John Savill, MD, PhD; Adam Lacy-Hulbert, PhD

In the gastrointestinal tract, the immune system must protect against potential pathogens whilst preventing destructive inflammatory responses to the host commensal microflora. This is achieved in part through a complex and active network of specialized immune cells and regulatory cytokines. Breakdown of this dynamic balance between immune response and regulation is likely to be a major contributor to Inflammatory Bowel Disease. The importance of regulatory populations of lymphocytes in maintaining intestinal immune homeostasis is well established, but the contribution of innate immune cells, particularly macrophages and dendritic cells (DCs), is less well understood. The cytokine TGF-β is central to the generation and function of immune regulatory cells, and is present at high levels in the intestinal lamina propria. TGF-β is ubiquitously expressed but is synthesized in an inactive form and must be activated before it can signal, activation that is mediated by αv integrins.

We have found that deletion of αv integrins in DCs and macrophages causes colitis and autoimmunity in mice, and this is associated with loss of TGF-β dependent regulatory T cells (Tregs) and Th17 cells in this intestine. Based on these and other data, we have proposed a model in which αvβ8 integrin expressed by DCs binds and activates TGF-β during antigen presentation to T cells, promoting differentiation to Tregs and Th17 cells. Here we show that indeed restricted β8 expression effectively defines the population of DCs with the preferential ability to induce TGF-β-dependant regulatory T cells and control intestinal inflammation. Preliminary data will be also presented showing how intestinal DCs through expression of αv integrins acquire the ability to activate TGF-β and thus orchestrate intestinal immunity.

Poster Number 75

Paquette, Nicholas PhD
Research Fellow, Pediatric Service
npaquette1@partners.org

Characterization and Modification of Immunomodulating Bacterial-Effectors.

Investigators: Nicholas Paquette, PhD; Cammie Lesser, MD, PhD; Lynda Stuart, MD, PhD

The innate immune system acts as our first line of defense during a microbial infection. Bacterial effector proteins, particularly those secreted via type 3 secretion systems, such as those found in Yersinia sp., Pseudomonas sp., and Shigella sp., are typically thought of as virulence factors which play an essential role in immune inhibition, increasing the pathogenic potential of a microorganism. Intriguingly, work in plants and mammals, has demonstrated that some effectors function as 'avirulence' genes, protecting the host during infection by eliciting 'effector triggered immunity' (ETI). Thus, in co-evolved systems, pathogens may contain effectors that both positively and negatively regulate immune responses. This project focuses on understanding the mechanisms by which these effector proteins modulate innate immune signaling. Although evolutionarily distant, the innate immune signaling pathways of Drosophila show a great deal of homology to those found in mammals. Using the Drosophila model system we have generated GFP immune reporter cell lines that can detect both immune activation and inhibition. Utilizing the Drosophila metallothionein promoter, which allows even the most lethal of proteins to be inducibly expressed with very little background expression, we are currently examining the immune modulatory properties a panel of bacterial effectors proteins. Understanding of the molecular mechanism of these microbial effectors is likely to provide insights into critical regulatory hubs in host immune signaling pathways, as well as identify potential new targets for antimicrobial agents.

Poster Number 76

Porichis, Filippos PhD
Research Fellow, Ragon Institute
fporichis@partners.org

PD-1, IL-10, IFN-γ and IL-12 form a network to regulate HIV-1-specific CD4 T cell and antigen-presenting cell function

Investigators: Filippos Porichis, PhD; Lucie Barblu, PhD; Douglas S. Kwon, MD; Meghan Hart; Jennifer Zupkosky; Gordon J. Freeman, PhD; Daniel G. Kavanagh, PhD; Daniel E. Kaufmann, MD

Background: PD-1 and IL-10 blockade can restore antigen-specific T cell functions in chronic infections and cancer. However, not all subjects respond to inhibition of either pathway, the potential differences in functions restored by these interventions are unknown, and mechanistic interactions between these pathways are poorly understood.

Methods: We investigated 45 subjects with HIV-1 infection with different disease status. We used CFSE assays to measure proliferation of HIV-1-specific CD4 T cells and Luminex arrays to analyze IFN-*g*(Th1), IL-2(Th0), IL-13(Th2) and IL-12 secretion in supernatants of CD8-depleted PBMC stimulated for 48h with Gag peptide pools in the presence of isotype control antibody, anti-PD-L1 and/or anti-IL--0R*a*, anti-IFN-γ or anti-IL-12. We used flow cytometry to evaluate the role of IFN-*g* in regulating PD-L1, HLA-DR, HLA-ABC and CD86 expression by monocytes.

Results: Whereas PD-L1 blockade had a balanced impact on proliferation and cytokine secretion by HIV-1-specific CD4 T cells, anti-IL-10R*a* preferentially restored IFN-γ production. Combined blockade resulted in a dramatic 9.8-median-fold increase of IFN-γ, contrasting with the moderate effect of single blockade (2.5 median-fold). Antigenic stimulation of HIV-1-specific CD4 T cells upregulated PD-L1, HLA-DR and HLA-ABC on monocytes through an IFN-γ-dependent mechanism. Combined PD-L1/IL-10R*a* induced a striking increase in IL-12 production by antigen-presenting cells (APCs) that was governed by IFN-γ derived from the Thelper cells. Neutralization of IL-12 reduced the dramatic effect of combined blockade on IFN-γ, demonstrating a positive feedback loop between IFN-γ produced by HIV-1-specific CD4 T cells and IL-12 produced by APCs.

Conclusion: These data provide important evidence on the therapeutic potential of combined interventions on the PD-1 and IL-10 pathways to restore HIV-1-specific CD4 T cell and antigen-presenting cell function. We provide mechanistic insight on the mode of action of dual blockade by showing that IFN-γ produced by HIV-1-specific CD4 T cells and IL-12 secreted by APCs regulate each other in a positive feedback loop.

Poster Number 77

Shinoda, Kazunobu MD,PhD
Research Fellow, Transplant Center
kshinoda@partners.org

Depletion of both recipient and donor Foxp3+ cells can break tolerance of skin or heart allografts induced by mixed chimerism in mice

Investigators: Kazunobu Shinoda, MD, PhD; Takurin Akiyoshi, MD, PhD; Catherine M Chase; Evan A. Farkash, MD, PhD; Paul S. Russell, MD; Joren C. Madsen, MD, PhD; Alessandro Alessandrini, PhD; Robert B. Colvin, MD

Background: Donor-specific transplant tolerance has been achieved by induction of mixed chimerism in both mice and humans and evidence for both deletion (mouse) and regulation (human) exists. To address the role of regulatory T cells in the mouse, we employed the C57/B6.Foxp3DTR+/y strain that allows for the specific depletion of Foxp3+ cells by diphtheria toxin (DT).

Methods: DBA/2 mice were bred to C57/B6.Foxp3DTR+/+ and bone marrow (BM) from these H2d/b F1 mice was transplanted into recipients, treated with 3 Gy TBI and mAb to CD4, CD8 and CD154. Three groups were created: A, male F1 to C57/B6.Foxp3DTR+/y; B, male F1 to male wild type B6; and C, female F1 to C57/B6.Foxp3DTR+/+. Skin and heart transplants from sex-matched DBA/2 were then performed in each mouse 5 weeks and 12-19 weeks after BM transplant, respectively, followed by 2 doses of DT treatment (50 µg/kg) 4 weeks after heart transplant. Viability of the skin and heart grafts and peripheral blood chimerism were monitored.

Results: Substantial Foxp3+ cell depletion in Group A (n=8), in which both donor and recipient carried the Foxp3DTR knock- in gene, resulted in the rejection of 7 and 6 skin and heart allografts, respectively, 41 days after DT treatment (Figure 1). In Group C (n=7), in which the donor BM was heterozygous for the Foxp3DTR knock-in, blood Foxp3 depletion never exceeded more than 50% and skin and heart graft survived greater than 89 days. In Group B (n=2), only the donor Foxp3 cells carried the Foxp3DTR knock-in, and no rejection of skin and heart grafts was observed. In all groups mixed chimerism was maintained.

Conclusion: This study provides new evidence that maintenance of tolerance of skin or organ allografts in murine mixed chimerism is Foxp3+ cells dependent, and can be maintained by either donor or recipient Foxp3+ cells. Mixed chimerism itself, in contrast, is robustly resistant to Foxp3+ cells depletion. These results suggest that regulatory mechanisms are important in mixed chimerism in mice as they are in humans.

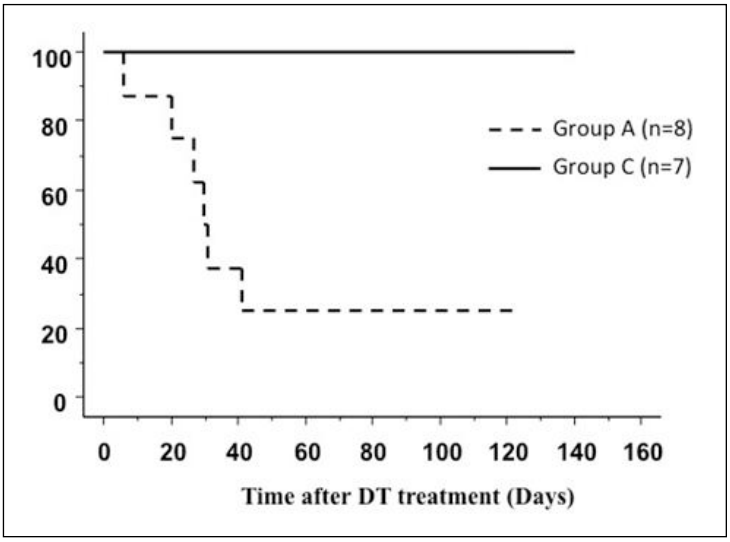

Sihag, Smita MD
Resident, Surgery
mmadariaga@partners.org

Poster Number 78

Mitigating Lung Ischemia-Reperfusion Injury in Miniature Swine

Investigators: Smita Sihag, MD*; Maria Lucia L. Madariaga, MD*; James D. Gottschall; Evan A. Farkash, MD; Michael S. Haas, PhD; Michael C. Carroll, PhD; James S. Allan, MD;
*Both authors contributed equally to this work.

Background: Lung ischemia-reperfusion injury (LIRI) is one of the leading causes of primary graft dysfunction, which limits graft survival in lung transplant recipients. To date, there is no specific therapeutic intervention for LIRI. In other models, autoimmunity to the N2 epitope of the heavy chain of non-muscle myosin has been shown to be an important mechanism underlying the inflammatory response to reperfusion injury. The objective of our study is to see whether a novel mimeotopic peptide that blocks activation of the N2 pathway can mitigate LIRI in miniature swine, a pre-clinical large-animal model.

Methods: Four miniature swine underwent 2 or 4 hours of left lung ischemia. Prior to reperfusion, animals were treated with either the N2 peptide or normal saline (NS). Serial open lung biopsies and blood sampling were performed throughout a 24-hour period of reperfusion. Serum was analyzed for biomarkers of acute lung injury (IFN-gamma, CXCL-10, MCP-1) and tissue biopsies analyzed by a pathologist blinded to the intervention.

Results: After 4 hours of ischemia, N2-treated swine demonstrated significantly decreased alveolar and interstitial edema compared to NS-treated swine at 6, 12, and 18 hours of reperfusion. N2 peptide also decreased levels of IFN-gamma and MCP-1 during the reperfusion period. Two hours of ischemia were not sufficient to demonstrate differences between the treatment and control animals.

Conclusion: This preliminary study demonstrates that blocking the N2 pathway in a pre-clinical model of LIRI decreases the inflammatory response and tissue injury. Further investigation is needed to characterize the role of N2 pathway blockade in this and other models of ischemia-reperfusion injury.

Sokolovska, Anna PhD
Research Fellow, Mass General Hospital *for* Children
Sokolovska.Anna@mgh.harvard.edu

Poster Number 79

Activation of caspase-1 by the NLRP3 inflammasome regulates NOX2 to control phagosome function

Investigators: Anna Sokolovska, PhD; Christine E. Becker, PhD; WK Eddie Ip, PhD; Vijay A.K. Rathinam, PhD; Mathew Brudner, BS; Nicholas Paquette, PhD; Antoine Tanne, PhD; Sivapriya K. Vanaja, PhD; Kathryn J. Moore, PhD; Katherine A. Fitzgerald, PhD; Adam Lacy-Hulbert, PhD; Lynda M. Stuart, MD, PhD

Phagocytosis is a fundamental cellular process that is pivotal for immunity as it coordinates both microbial killing and activation of innate and adaptive immune pathways. Phagosomes are newly formed upon engulfment of pathogens and rapidly remodelled by the sequential fission with components of the endolysosomal system to generate a mature and microbicidal compartment. A requisite step for the optimal function of these vacuoles is acidification, which regulates the activity of pH-sensitive enzymes required to destroy internalized microbes. Here we report that the microbicidal activity of phagosomes containing Gram-positive bacteria is regulated by the NLRP3 inflammasome and caspase-1. Once delivered, caspase-1 acts locally to regulate the NADPH oxidase to control the phagosome pH and hence the microbicidal activity of the organelle. These data establish a new function for NLRP3/caspase-1 in cellular defense and provide insight into a mechanism by which innate immune signals act to modify the function of phagosomes.

Poster Number 80

Stromp Peraino, Jaclyn BSc
Research Technician, Transplant Center
jaclyn.peraino@tbrc.mgh.harvard.edu

A New Potent Reagent for Depleting Porcine Tregs: Diphtheria Toxin-Based Bivalent Porcine IL-2 Fusion Toxin

Investigators: Jaclyn Stromp Peraino, BSc; Guoying Li, MD; Huiping Zhang, MD; David H. Sachs, MD; Christene A. Huang, PhD; Zhirui Wang, PhD

Regulatory T cells (Tregs) are suppressive of immune reactivity and are therefore frequently considered in studies investigating autoimmunity and transplantation. Tregs constitutively express CD25 on their surface; a high affinity receptor molecule for the cytokine Interleukin 2 (IL-2), which when bound to CD25 induces cellular proliferation. Our laboratory uses a unique large animal model, the MGH-MHC-defined miniature swine for pre-clinical studies investigating transplantation tolerance and immune regulation. In this study, we have successfully developed an extremely potent porcine fusion toxin that promises to be highly effective for depleting porcine Tregs in vivo.

Our new porcine IL-2 fusion toxin consists of an N-terminal truncated diphtheria toxin (DT390) genetically linked to a C-terminal porcine IL-2 molecule. It functions by first binding to CD25 on the cell surface via interaction with the porcine IL-2 domain, DT390 then facilitates internalization followed by protein synthesis inhibition, resulting in cell death. In order to find the best functional isoform, we constructed four versions of this reagent: 1. Monovalent glycosylated porcine IL-2, DT390-pIL-2-Gly (Gly), 2. Monovalent non-N-glycosylated porcine IL-2, DT390-pIL-2-NonGly (NonGly), 3. Bivalent glycosylated porcine IL-2, DT390-Bi-pIL-2-Gly (Bi-Gly) and 4. Bivalent non-N-glycosylated porcine IL-2, DT390-Bi-pIL-2-NonGly (Bi-NonGly). We determined these products to be functional in vitro through CD25 binding analysis using flow cytometry and an assay which measures an ability to inhibit protein synthesis by tritium incorporation. We found that the bivalent, non-N-glycosylated isoform is the most potent reagent and thus, the best candidate for in vivo use in our large animal model. This reagent has been found to be more potent by a factor of four logs than the FDA approved reagent, ONTAK®, for in vitro depletion of porcine T cells.

Poster Number 81

Tanne, Antoine PhD
Research Fellow, Mass General Hospital *for* Children
atanne@partners.org

Understanding the viral co-infection effect on bacterial infection

Investigators: Antoine Tanne, PhD; Lynda Stuart, MD, PhD

Co-infection between virus and bacteria leads to a dramatic prognosis and suggests that antiviral polarization of the innate immune response may interfere with proper antibacterial responses. During a flu infection (epidemic or pandemic) many people develop secondary bacterial infections, which results in serious respiratory disease and significantly increases the risk of death. The antiviral response is characterized by a strong induction of the interferon pathway, which regulates a large family of interferon-associated genes such as the Interferon Inducible Trans-Membrane Proteins (IFITM).

IFITM genes have been shown to be essential to control different viral infections such as those caused by Influenza Viruses (Flu), Flaviviruses (Dengue), Filoviruses (Ebola) and Coronavirus (Severe Acute Respiratory Syndrome). The IFITMs are thought to interfere with endosomal trafficking or, alternatively, can make these compartments unsuitable for essential membrane fusion of the restricted viruses. However, disruption of maturation of the endolysosomal compartment by these antiviral effectors may alter antibacterial responses.

We have tested the role of the IFITM upon bacterial and viral infection in macrophages. We have better characterized the antiviral functions of the IFITM and we have demonstrated that they could differentially interfere with the antibacterial innate immune response. We have shown that the IFITM are differentially regulated upon bacterial and viral infection. After bacterial infection they are recruited from the cytoplasm to the cell membrane and to the late phagosome. The recruitment of IFITM1,2,3 to the viral vacuole contributes to the cell protection whereas we have shown that some IFITM differentially affect the antibacterial response upon S.aureus (Gram+) or Enterohaemorrhagic E.coli (EHEC) infection (Gram-). We have shown that the IFITM functions in the antiviral response and in the regulation of the antibacterial response could be related to an immuno-regulatory function such as by modulating the inflammasome pathway. Thus IFITMs appear to be proteins related to the cellular innate immune response and can differentially affect the antiviral and antibacterial response. The functions of IFITMs remain yet to be better understood and our work will help to decipher how these proteins can interact with the endolysosomal pathway. The study of co-infection models with Influenza Viruses and S. aureus may increase our understanding of co-infections and may help explain why people with viral infection such as Flu or HIV have a higher susceptibility to bacterial infection.

Poster Number 82

Tonsho, Makoto MD
Research Fellow, Transplant Center
mtonsho@partners.org

Effect of Kidney Cotransplantation on Induction of Cardiac Allograft Tolerance in Nonhuman Primates (NHPs)

Investigators: M. Tonsho, MD; G. Benichou, PhD; S. Boskovic, MD; O. Nadazdin, MD; N.R. Smith, MD; R.B. Colvin, MD; D.H. Sachs, MD; A.B. Cosimi, MD; T. Kawai, MD, PhD; J.C. Madsen, MD; D. Phil

Background: Tolerance has been achieved in NHP and human recipients of kidney transplants using a mixed chimerism approach. However, the same protocol has failed to induce tolerance in NHP recipients of heart allografts. Based on earlier studies, we asked whether tolerance to cardiac allografts could be achieved by heart and kidney allograft cotransplantation.

Methods: Allogeneic hearts or heart and kidneys from the same donor were transplanted into cynomolgus macaques infused with donor bone marrow cells. All recipients received a peri-transplant nonmyeloablative conditioning regimen consisting of 3 Gray total body irradiation, 7 Gray thymic irradiation, equine anti-thymocyte globulin, anti-CD154 monoclonal antibody and a 28 day course of cyclosporine. The alloimmune response was monitored through ELISPOT, mixed lymphocyte reaction (MLR) and alloantibody production assays. Graft rejection was assessed by serial biopsies.

Results: All recipients developed transient multilineage chimerism. The four recipients of isolated heart allografts demonstrated severe rejection as early as 69, 70, 78, 82 days posttransplantation. In contrast, recipients of heart/kidney cotransplants (n=5) demonstrated no evidence of rejection for over 300 days (>566, >356, >335, >315, >315 days). IFN gamma-ELISPOT and MLR assays performed in the cotransplanted monkeys revealed donor specific T cell hyporesponsiveness. Although donor-reactive antibodies were detected in some monkeys, they were not specific for donor MHC antigens. Expansion of regulatory T cells was observed in the peripheral blood and in the kidney allografts of tolerant monkeys. Removal of the donor kidney transplants in the tolerant monkeys (at day 315 post-transplant) resulted in acute rejection of the heart transplant.

Conclusions: Tolerance to heart allografts has been achieved for the first time in NHPs using a mixed chimerism induction protocol and kidney cotransplantation from the same donor. The presence of the kidney allograft is necessary for the induction and maintenance of tolerance. Work is in progress to elucidate the renal element that is responsible for conferring unresponsiveness on cardiac allografts.

Poster Number 83

Visvikis, Orane PhD
Research Fellow, Mass General Hospital *for* Children
ovisvikis@partners.org

C. ELEGANS HLH-30/CeTFEB ORCHESTRATES CYTOPROTECTIVE AND ANTIMICROBIAL HOST RESPONSES TO INFECTION

Investigators: Orane Visvikis, PhD; Nnamdi Ihuegbu, PhD; Anna-Maria F. Alves; Lyly G. Luhachack; Amanda C. Wollenberg, PhD; Gary D. Stormo, PhD; Javier E. Irazoqui, PhD

The human pathogen Staphylococcus aureus can infect and kill Caenorhabditis elegans, where we showed that S. aureus triggers a pathogen-specific transcriptional host response. To identify signaling components that orchestrate this host response, we performed bioinformatic analyses and found that an evolutionarily conserved E-box motif is over-represented in the promoters of S. aureus induced genes. This E-box motif has been described as the binding sequence of the HLH-30 transcription factor, the C. elegans homolog of human TFEB.

To confirm the role of HLH-30 in triggering the host response to S. aureus, we performed RNA-seq to identify downstream targets of HLH-30 induced upon infection. We found that ~80% of the S.aureus-induced genes require HLH-30 for their induction, thus revealing that HLH-30 plays a key role in the host response. Additionally, fluorescence microscopy analysis of HLH-30::GFP from transgenic animals reveal the acute activation of HLH-30, which is targeted to cell nuclei early during infection. Consistently, we found that hlh-30(-) mutants exhibit enhanced susceptibility to S. aureus-mediated killing, a phenotype which is rescued by over-expressing HLH-30::GFP. Therefore, we conclude that the transcriptional defect observed in hlh-30(-) animals is biologically significant for host defense.

Furthermore, among the HLH-30 dependent genes, we found an over-representation of cytoprotectives genes and immunity genes. We verified by qRT-PCR and in vivo reporter analysis that HLH-30 induces the expression of autophagy/lysosomal and antimicrobial genes upon infection, and that autophagy itself and expression of specific lysozymes are required for host defense. Human TFEB is known as a major regulator of autophagy in mammalian system in the context of starvation. Altogether, these results indicate that HLH-30 plays a critical role in C. elegans host defense, and suggest that TFEB might play similar role in mammalian host defense by regulating both autophagy and immunity genes during infection.

Poster Number 84

Wollenberg, Amanda PhD
Research Fellow, Mass General Hospital *for* Children
wollenberg.amanda@mgh.harvard.edu

Molecular and phenotypic characterization of interactions between a model host (Caenorhabditis elegans) and bacterial isolates collected from its natural environment

Investigators: Amanda C. Wollenberg, PhD; Anna-Maria Alves, MS; Orane Visvikis, PhD; Marie-Anne Felix, PhD; Javier E. Irazoqui, PhD

The nematode Caenorhabditis elegans is best known as a genetic model for developmental biology, but as a natural bacterivore, it also serves as a tractable system in which to investigate interactions between bacteria and the eukaryotic digestive tract. In the past decade, the use of C. elegans to study the invertebrate immune system has yielded considerable information about the molecular crosstalk between nematodes and medically relevant pathogens. However, until the recent and pioneering work of Dr. M.A. Felix demonstrated that wild C. elegans populations are most often found on rotting fruit, it was unclear what types of microbial communities would be naturally encountered by C. elegans and what sorts of beneficial and detrimental interactions might occur between C. elegans and bacteria in the wild. We are beginning to address these questions using a panel of 46 bacterial isolates that were collected by Dr. M.A. Felix at seven microsites in France (e.g. a rotting apple) where C. elegans populations were also found. The isolates have been assigned to 20 genera on the basis of 16S rDNA sequencing and represent 2 Gram-positive phyla (Actinobacteria, Firmicutes) and 4 Gram-negative phyla (Alphaproteobacteria, Betaproteobacteria, Gammaproteobacteria, Bacteroidetes). Our hypothesis is that this collection of bacterial isolates will include not only potential pathogens, but also potentially beneficial microbes able to protect nematodes from more pathogenic bacteria, perhaps via colonizing the intestine or by priming the immune system. We will present data showing that these isolates vary in their effect on the lifespan of adult animals and in their capacity to elicit immune responses such as induction of putative antimicrobial genes. Importantly, of the isolates that elicit an immune response, not all are lethal pathogens, and we are investigating the possibility that some of these non-lethal isolates can prime the nematode immune system for future pathogen exposure. Additionally, we are investigating how combinations of isolates influence the nematode response. Because nothing is currently known about the natural microbiota that inhabit the C. elegans intestine, our work is likely to generate novel insights. Furthermore, because nematodes are an excellent model for intestinal immunity, our findings will shed light on the medically relevant issue of host-bacterial interactions at epithelial tissues.

Yonker, Lael MD
Research Fellow, Pediatric Service
lyonker@partners.org

Poster Number 85

Feasibility of an RNAi screen in neutrophils

Investigators: Lael M. Yonker, MD; Abdul Hakkim, PhD; David Sykes, MD, PhD; Lynda Stuart, MD, PhD

Although neutrophils have been implicated in numerous disease states, relatively little is known about the molecular pathways involved in these processes. Neutrophils are known to phagocytose and kill bacteria, release neutrophil granules that are rich in antimicrobial peptides and hydrolytic enzymes, and sterilize the inflamed site by the release of large amounts of reactive oxygen species. Furthermore, neutrophils have been found to undergo an additional, unique form of cell death: NETosis, whereby neutrophils expel their lysosomal and DNA contents into the extracellular space, creating sticky webs called 'neutrophil extracellular traps' (NETs). Although normally protective immune processes, neutrophils and their NETs have been implicated in numerous diseases including cystic fibrosis, Wegener's granulomatosis and lupus. Understanding the molecular basis of the pathways involved in NETosis and neutrophil function has proven difficult. The major limitation has been the fact that neutrophils have proved refractory to modern genetic approaches: primary neutrophils are short lived and readily activated to undergo degranulation, making any RNAi or cDNA screens impossible, and prior neutrophil cell lines have proven inadequate surrogates for primary neutrophils. However, a murine myeloid progenitor cell line that is immortalized by estrogen-regulated Hoxb8 but can be differentiated into mature neutrophils by estrogen withdrawal have allowed for advances in the understanding of neutrophil pathways. Here we show that, for the first time, we are able to apply modern genetic techniques to interrogate neutrophil function, including NETosis. Using these ER-hoxb8 neutrophil precursors, we have successfully performed viral transduction with GFP and thus established that RNAi with short-hairpin RNA is feasible in these cells. Furthermore, the transduced green GFP-containing ER-hoxb8 neutrophil precursors undergo normal differentiation into neutrophils and display expected NETosis that is indistinguishable from that in primary neutrophils. Not only will this genetic manipulation allow for better understanding of pathways involved in normal neutrophil pathways, but it will allow us insight into numerous disease processes.

Poster Number 86

Arimon, Muriel PhD
Research Fellow, Neurology Service
marimon@partners.org

Local increase in oxidative stress in vivo triggers local increase in the Abeta42/40 ratio due to changes in presenilin1/gamma-secretase conformation

Investigators: Muriel Arimon, PhD; Shuko Takeda, PhD; Kathryn L. Post, MSc; Bradley, T. Hyman, MD, PhD; Alberto Serrano-Pozo, MD, PhD; Oksana Berezovska, PhD

Presenilin-1 (PS1) is the catalytic subunit of γ-secretase, an enzyme that cleaves amyloid precursor protein (APP) to generate amyloid-beta peptide (Aβ) of different lengths. While Aβ40 is the most abundant isoform, Aβ42 is the most prone to aggregation, and is the main constituent of amyloid plaques in Alzheimer's disease (AD) brain. An increased Aβ42/40 ratio, rather than absolute Aβ levels, is crucial for the development of AD, and is elevated in both sporadic AD and normal aging brain. Moreover, Aβ deposits have been detected in the brain of aging adults prior to cognitive decline, suggesting the presence of age-related stressors that are upstream of Aβ accumulation. We have previously confirmed that increase in the Aβ42/40 ratio strongly correlates with the changes in PS1 conformation, although factors that may affect PS1 conformation in the brain remain unclear. Some recent data from our group suggest that familial-AD-like PS1 conformational changes (i) do also occur in sporadic AD, (ii) PS1 conformation is selectively altered in the vicinity of amyloid plaques, and (iii) similar PS1 conformational changes occur during normal aging.

Here we report that oxidative stress triggers a change in PS1 conformation towards more closed, "pathogenic" state in vitro, compared to that in neurons treated with vehicle control. To assess whether these conformational changes also occur in the brain and correlate with altered Aß generation, we used in vivo microdialysis to locally induce oxidative stress and to collect interstitial fluid (ISF) Aß in the brain of living mice. A microdialysis probe was implanted in the hippocampus of wild-type mice and 4,4'-dithiodipyridine (DTDP), a strong oxidizing agent, or 4-hydroxynonenal (HNE), a product of lipid peroxidation, was delivered via reverse microdialysis. Aß quantified from the collected ISF of awake animals showed increase in the Aβ42/40 ratio in mice treated with DTDP or HNE vs. mice treated with vehicle. The brains of mice used for the microdialysis were immunostained to assess PS1 conformation by means of Fluorescence Lifetime Imaging Microscopy. PS1 conformation in the brain of DTDP/HNE-treated mice was more "closed" (shorter PS1-NT to -CT distance) as compared to that in vehicle-treated mice.

In summary, we provide direct evidence of the relationship between oxidative stress, PS1 conformation and altered Aβ42/40 ratio in vivo. A deeper knowledge of the processes taking place before amyloid deposition and better experimental models would help to design and test more effective therapeutic strategies able to prevent amyloidosis and neurotoxicity associated with AD.

Blasi, Francesco PhD, PharmD
Research Fellow, Radiology
fblasi@partners.org

Poster Number 87

Notch3 gene deletion worsens tissue outcome and cognitive impairments in a mouse model of subcortical white matter stroke

Investigators: Francesco Blasi, PharmD, PhD; Michael A. Moskowitz, MD

Ischemic stroke is leading cause of death and permanent disabilities worldwide. The failure of most recent stroke clinical trials is driving the scientific community to work on more translational and clinically relevant models, but no one yet fully mimics the neuropathological events of human stroke. In particular, the subcortical white matter (SWM) is often affected by ischemic strokes, but most part of preclinical animal studies mainly focus on large cortical and striatal strokes, especially involving the grey matter. Here we show how a selective, endothelin-induced, white matter lesion at the peri-ventricular level is associated with longstanding cognitive impairments in mice. The ischemic damage features many of the early (cerebral blood flow deficit, blood brain barrier opening) and late (myelin and axonal degeneration, microglia/macrophages infiltration, reactive astrogliosis) hallmarks of a human white matter stroke. Interestingly, stroke mice don't show any evident motor anomaly, but display a protracted (up to 4 weeks) deficit in novel object recognition test when compared with sham-operated animals. Moreover, tissue outcome and cognitive impairments are worsen in mice lacking Notch3, a transmembrane receptor involved in vascular smooth muscle cells (vSMCs) maturation and linked to ischemic stroke susceptibility. Taken together, these data show the association between white matter damage and cognitive deficit in a mouse model of selective SWM stroke, and provide new hints toward understanding the role of Notch3 in cerebrovascular pathologies.

Cagsal-Getkin, Ozge DVM, MS
Research Technician, Molecular Biology
ocagsal-getkin@partners.org

Poster Number 88

Analysis of Exosomal microRNAs in Cerebrospinal Fluid from Alzheimer's Disease Patients

Investigators: Ozge Cagsal-Getkin, DVM, MS; Charles R. Vanderburg, PhD; Meredith Banigan

Alzheimer's disease (AD), the most common type of aging associated dementia, is characterized by progressive accumulation of extracellular amyloid plaques comprised of amyloid β-peptide (Aβ) produced by processing of amyloid precursor protein (APP), and intracellular neurofibrillary tangles composed of aggregates of abnormal hyperphosphorylated microtubule associated protein tau. Plaques and tangles are accompanied by neuron degeneration and predominantly affect regions of the basal forebrain, hippocampus, and association cortices. To date, the only available treatments have modest effects on disease progression and on relieving symptoms possibly due to delayed diagnosis and treatment initiation and AD related changes in the brain are well advanced by the time the symptoms of dementia appear. Thus, understanding the early pathogenesis of the disease and discovering a reliable early diagnostic test or biomarker for AD before the clinical symptoms occur, might increase the likelihood to attenuate AD disease progression before there is a significant neuronal loss. Recent evidence suggests that microRNAs (miRNAs), short non-coding RNA molecules that regulate gene expression, may play a critical role in AD. miRNAs are present in exosomes and can be used as diagnostic markers. The objective of this study was to determine if exosomes are present in human CSF, and if these exosomes contained any miRNA. In addition, the goal was also to test the hypothesis that the exosomal miRNA content of human AD CSF differs from the content of non-demented controls. Results presented here show the presence of miRNA in human CSF and differences in the CSF exosomal miRNA content between AD patients and non-demented controls. The particular profile of AD CSF exosomal miRNA could potentially be used as a biomarker. The findings from this study could serve as the basis for new research approaches that can, not only increase our knowledge of the disease process, but also establish novel diagnostic biomarkers.

Poster Number 89

Dzhala, Volodymyr PhD
Instructor, Neurology Service
vdzhala@partners.org

Progressive chloride accumulation and anticonvulsant resistance during post-traumatic epileptogenesis in vitro

Investigators: Volodymyr Dzhala, PhD; Michelle Mail, BS; Kevin Staley, MD

Traumatic brain injury is a major cause of acquired epilepsy. Seizures may occur because of the acute injury or progressive post-traumatic changes in brain metabolism, blood flow and homeostasis. Phenytoin is effective in treatment of acute seizures but failed to prevent post-traumatic epilepsy (PTE). Anticonvulsant efficacy of Phenobarbital is low with a greater risk of developing PTE. Understanding the mechanisms of anticonvulsant resistance and development of PTE is a critical for understanding the epilepsy and development of more efficient therapy for prevention and prophylaxis of PTE. Currently, we developed in vitro model of post-traumatic seizures in organotypic hippocampal slice cultures. Extracellular field potential recordings, two-photon imaging of Clomeleon, lactate and lactate dehydrogenase production assays were used to monitor neuronal network activity, intracellular chloride concentration and neuronal cell death. Hippocampal slices were incubated for six-seven weeks, during which a latent one-two week period was followed by spontaneous seizure activity and electrical status epilepticus. Phenytoin exerted powerful acute concentration-dependent anticonvulsive effects. Chronic anticonvulsive efficacy of phenytoin progressively decreased demonstrating no antiepileptic action in this model. Phenobarbital was much effective at controlling post-traumatic seizures at the earlier stage of epileptogenesis. Anticonvulsive efficacy of phenobarbital decreased from 60-70 % to 0-10% during four-five weeks of epileptogenesis. Anticonvulsive efficacy of phenobarbital was correlated with intracellular chloride concentration and GABA action. We found a correlation between seizure severity and frequency, increases in neuronal chloride and phenobarbital efficacy. Bumetanide, a sodium-potassium-chloride (NKCC1) co-transporter blocker, significantly increased anticonvulsive efficacy of phenobarbital. High concentration of furosemide (NKCC1 and potassium-chloride (KCC2) co-transporter blocker) controlled acute seizures at all stages of epileptogenesis, but failed to reduce interictal epileptiform discharges and prevent epilepsy. In conclusion, our data suggest a complex mechanism of anticonvulsant resistance that involves chronic post-traumatic chloride accumulation and alterations in GABA-mediated inhibition. More effective prevention of post-traumatic and seizure-induced neuronal chloride accumulation may comprise a new strategy for both anticonvulsive and antiepileptogenic therapy.

Poster Number 90

Elmariah, Sarina B. MD, PhD
Instructor, Dermatology Service
sbelmariah@partners.org

Neural recruitment and dynamism in the pathogenesis of atopic dermatitis

Investigators: Sarina B. Elmariah, MD, PhD; Vemuri B. Reddy, PhD; Ethan A. Lerner, MD, PhD

Atopic dermatitis is a common and frequently disabling cutaneous disorder characterized by pruritus and inflammation. In addition to defective barrier function and immune dysregulation, alterations in neural innervation and neurogenic inflammation appear to play little recognized but important roles in atopic dermatitis pathogenesis. In this study, we characterize changes in neural innervation in eczematous skin and determine when changes in sensory innervation patterns occur. We performed in vivo confocal imaging of fluorescently labeled peripheral sensory nerves in mice during epicutaneous sensitization to ovalbumin, an allergic mouse model that produces eczematous skin lesions. Visualization of the same cutaneous nerve branches sequentially over time revealed that specific subpopulations of peripheral sensory nerves are highly dynamic throughout eczema development, eventually resulting in higher innervation density and arbor complexity. Neural sprouting and retraction occurred early in the evolution of the dermatitis, within hours to days of ovalbumin sensitization, and continued throughout epicutaneous sensitization. Increases in the average length of primary and secondary branches, as well as in the number of branch points, were observed in ovalbumin-treated skin compared to baseline or saline-treated controls. Moreover, these changes occurred prior to the development of a rash or increased scratching behavior. Our results suggest that cutaneous inflammation may promote re-organization of sensory innervation patterns early in atopic dermatitis pathogenesis and that different neural populations may contribute to the development of eczema.

Poster Number 91

Hennig, Krista PhD
Research Technician, Center for Human Genetic Research
hennig@chgr.mgh.harvard.edu

Targeting Chromatin-Modifying Complexes Important to Memory and Mood: Class I HDAC Complexes Purified from Mouse Brain Reveal Differential Inhibitor Sensitivity

Investigators: Krista Hennig, PhD; Surya Reis, PhD; Wen-Ning Zhao, PhD; Chelsea Groves Kuhnle, BA; Thomas Nieland, PhD; Nadine Joseph, MSc; Jennifer Gale, PhD; Mike Lewis, PhD; Kelly Dennehy, BA; F. Al Schroeder, PhD; Emily Ricq, BSc; Balaram Ghosh, PhD; Ralph Mazitschek, PhD; Yan-Ling Zhang, PhD; Florence Wagner, PhD; Edward Holson, PhD; Tracey Petryshen, PhD; Daniel Fass, PhD; Li-Huei Tsai, PhD; Stephen Haggarty, PhD

Modulation of chromatin structure by players such as histone acetyl transferase (HAT) and histone deacetylase (HDAC) enzymes is a powerful means by which gene expression can be regulated and in turn affect neuroplasticity. While recent studies highlight the potential use of HDAC inhibitors to treat a range of psychiatric conditions in humans, they have also raised a number of important mechanistic questions in terms of the in vivo selectivity of the compounds, role of different HDAC complexes, and relevant downstream target genes. To address these questions, we have begun to dissect in detail the protein complexes and downstream genes affected by the HDAC inhibitors that are active in memory and mood behavioral models. We have determined the in vitro isoform selectivity, in vivo histone acetylation and transcriptome-wide gene expression effects of a series of benzamide-class inhibitors generated through medicinal chemistry efforts to target the different combinations of the class I HDAC isoforms selectively. In addition, by using distinct immunoprecipitated HDAC1/2, and HDAC3 complexes from adult mouse brain in our biochemical HDAC activity assays, we have been able to profile, for the first time, the differential potency of a subset of HDAC inhibitors towards the different class I HDAC complexes. Specifically, we find that the benzamide inhibitors designed for HDAC1/2-selectivity and reported by our colleagues to be most active in rodent mood behavioral models, preferentially target the HDAC2-LSD1-CoREST complex over the mSin3A- or MTA1/2/3-containing HDAC2 complexes. This selectivity is observed to varying degrees across all benzamide inhibitors examined, while the well-characterized hydroxamic acid SAHA and the carboxylic acid butyrate affect the different HDAC2 complexes similarly. Comparison of the genome-wide transcriptional profiles of a subset of benzamide inhibitors with differential selectivity for the HDAC2-CoREST complex has allowed the potential identification of CoREST complex target genes whose regulation may play a mechanistic role in behavioral efficacy. Current efforts are focused on the validation of these putative CoREST complex targets through chromatin immunoprecipitation. Our studies have thus provided insight into the mechanism of action of novel, HDAC1/2-selective benzamide HDAC inhibitors displaying superior behavioral efficacy and a decreased side effect profile in rodent models.

Poster Number 92

Im, Maesoon PhD
Research Fellow, Neurosurgery
Im.Maesoon@mgh.harvard.edu

ON-OFF Directionally Selective Retinal Ganglion Cells Detect Motion and Suppress Luminance Responses During Natural Viewing

Investigators: Maesoon Im, PhD; Shelley I. Fried, PhD

Directionally selective (DS) retinal ganglion cells generate robust spiking in response to movement of a stimulus in one (preferred) direction but spike little or none to movement of the same stimulus in the opposite (null) direction. Although numerous studies have investigated the performance and mechanism of DS cells using artificial stimuli such as high-contrast moving bars, the ability of DS cells to extract motion from complex natural stimuli is not well understood. Increased complexity of the stimulus is known to reduce the preferred direction response raising the question of how efficiently these cells can extract motion from complex natural scenes. ON-OFF DS cells also respond strongly to sudden changes in luminance (ON and OFF responses to flashes) raising the question of how the brain distinguishes between spikes arising from motion and spikes arising from luminance changes. Here, we measured the response of DS cells to natural movies that contained complex motion as well as a wide range of luminance changes.

Cell-attached patch clamping was used to record spikes from ganglion cells in the isolated rabbit retina. Ganglion cells were classified as ON or OFF cells by their response to stationary flashes ranging from 100 um to 1000 um in diameter, and as DS or non-DS by their response to moving bars (300 um×1800 um at 600 um /sec) in 12 directions. After cell type classification, a natural scenes movie (2 mm diameter, 20 frames/sec, and 18 sec duration) was presented 12 times to a targeted ganglion cell; between each presentation the movie was rotated by 30 degrees. We recorded the movie responses of ON-OFF DS cells (n=14), non-DS ON cells (n=7), and non-DS OFF cells (n=8).

The response of DS cells varied considerably with the angle of rotation of the movie. Responses were strongest for a given scene when the rotation of the movie was such that the motion (within that scene) was aligned with the cell's preferred direction. Directional indices for such scenes were comparable to those elicited by laboratory stimuli. In contrast, responses of ON and OFF cells changed little for rotations of the movie. Surprisingly, the responses to movie scenes that contained luminance changes without significant motion were highly suppressed in DS cells, but not in non-DS cells.

Our results indicate that ON-OFF DS cells effectively extract motion from complex natural movies. In contrast to their motion detection capability, DS cells elicited very weak responses in response to luminance changes suggesting that DS cells may somehow suppress the luminance responses, possibly so that only motion information gets reported to the brain.

Poster Number 93

Jung, Joo Eun PhD
Research Fellow, Radiology
garvy76@gmail.com

STATs regulate transcription of 12/15-LOX in mouse cortical neurons under glutamate-induced oxidative stress

Investigators: Joo Eun Jung, PhD; Klaus van Leyen, PhD

Oxidative stress during reperfusion following cerebral ischemic stroke causes neuronal death and various forms of cerebrovascular injury. 12/15-lipoxygenase (12/15-LOX) is a major contributor to these processes; however, the regulation of 12/15-LOX expression in the ischemic brain is still unknown. In this study, we investigated the transcriptional regulation of 12/15-LOX in primary cortical neurons subjected to oxidative stress. Immature cortical neurons were treated with glutamate. Western blots were performed for analysis of 12/15-LOX protein level and phosphorylation of STAT1 and 6 in response to glutamate stimuli. Primary mouse cerebral cortical neurons were transfected with small interfering RNA probes targeted to STAT1 or 6 and were used for real time RT-PCR for analysis of changes in 12/15-LOX mRNA level, and cell viability assay following glutamate treatment. In preliminary screening of putative transcriptional factors on the promoters of mouse and human 12/15-LOX genes, we detected multiple putative binding motifs for STATs in the promoters of 12/15-LOX. Following glutamate treatment of primary cortical neurons, phosphorylation of STAT1 (Y701) and STAT6 (Y641), as well as 12/15-LOX protein levels, were significantly increased. Importantly, we found significant increases in mRNA levels of 12/15-LOX in mouse cerebral cortices subjected to ischemia reperfusion, which was paralleled in glutamate-treated primary cortical neurons. Gene silencing of STAT1 or 6 by siRNA transfection in primary cortical neurons reduced the levels of both 12/15-LOX mRNA and protein under glutamate-induced oxidative stress. Moreover, inhibition of STAT1 or 6 by siRNA transfection protected primary cortical neurons against glutamate-induced oxidative stress. This study increases our understanding of the transcriptional regulation of the 12/15-LOX gene in cerebral ischemic injury and oxidative stress, which will be important to guard against neuronal cell death. Identifying regulators of 12/15-LOX transcription may suggest new molecular targets for stroke therapy.

Poster Number 94

Jung, Yookyung PhD
Research Fellow, Wellman Center for Photomedicine
Jung.Yookyung@mgh.harvard.edu

Visualizing axon regeneration through whole sciatic nerve after cut injury and repair by tissue clearing

Investigators: Yookyung Jung, PhD; Joanna Ng, MD; Cameron P. Keating, MD; Prabhu Senthil-Kumar, MD; Amanda Meppelink, BS; Jonathan N. Soriano, BS; Mark A. Randolph, M.A.S.; Jonathan M. Winograd, MD; Conor L. Evans,PhD

While the majority of nerve research has been focused on the central nervous system, in part because of injury severity and the inability of central nerves to regenerate, improved peripheral nerve injury therapies will impact hundreds of thousands of patients and cannot be overlooked. Unlike central nerve injuries, peripheral nerve injury research has the potential to yield powerful and clinically applicable results due to the inherent regenerative capacity of peripheral nerves. However, our current inability to visualize how the thousands of nerves regenerate through an injury or surgical site is a fundamental gap in our research toolkit and renders us unable to answer critical questions: How do axons regenerate through injured nerves? Can regenerated axons re-innervate the original tube (endoneurium) that guides axons to target tissues? Without the ability to see what is happening in the injured nerve with axonal resolution, evaluating and developing improved treatments is exceedingly difficult.

The depth penetration limit of optical imaging in tissue arises from light scattering, which occurs at the boundaries of objects where a change in optical refractive index occurs. Tissue is composed of numerous cells and connective layers containing water, lipids and other proteins. Light passing through tissue undergoes numerous scattering events that act to make the tissue opaque. In tissue clearing, chemicals are infused into tissue that dispel water and other tissue components to homogenize the index of refraction. This refractive index matching reduces scattering significantly and increase the transparency of the tissue, which enables deep tissue optical imaging.

This presentation introduces a new protocol to visualize whole sciatic nerves with subcellular resolution after cut or crush injury and repair. By combining tissue clearing and confocal fluorescence microscopy, this work demonstrates uncovering and visualizing the complex three-dimensional axonal structure in healthy and surgically repaired nerves. Once optimized and established, this method will enable comprehensive, microscale evaluation of axon regeneration, opening the door to research for improved therapies and recovery.

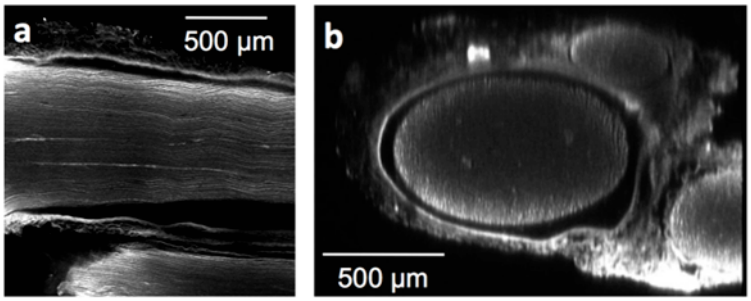

Figure. a) Longitudinal and b) transverse cross section images of the tissue cleared sciatic nerve of a rat. The linear structure of individual nerve fibers (axons) can be seen in figure a). Be advised on the scale bars of the figure. While conventional optical microscopy has a depth limit of 100~200 µm, tissue clearing method enables visualizing whole nerve with cellular resolution.

Poster Number 95

Kil, Kun-Eek PhD
Research Fellow, Radiology
kkil@nmr.mgh.harvard.edu

Radiosynthesis of 3-[I-123]iodo-5-(pyridine-2-ylethynyl)benzonitrile ([I-123]IPEB) for metabotropic glutamate receptor subtype 5 (mGluR5) and its preclinical evaluation with normal rat

Investigators: Kun-Eek Kil, PhD; Ji-Kyung Choi, PhD; Chunyu Gong, MD; Sreekanth Kura, MS; Kimmo Jokivarsi, PhD; Alana Ross, BS; Anna-Liisa Brownell, PhD

Backgrounds: Recent development of PET radiotracers for mGluR5 enables us to elucidate the role of mGluR5 in neurodegenerative diseases such as Alzheimer's disease, Parkinson's disease, and Huntington's disease in vivo. Those successes will bring more demand for mGluR5 radiotracers in the future. However, short half-life of PET isotope and limited number of PET radiochemistry facilities will not be able to catch up with the future demands for mGluR5 research and clinical application. Those problems can be solved by the development of SPECT radiotracers for mGluR5. Recently several promising iodine compounds were proposed as mGluR5 negative allosteric modulators. Here, we report the radiosynthesis of [I-123]IPEB and its preliminary SPECT-CT imaging with normal rat brain.

Chemistry: Bromo-precursor of [I-123]IPEB was prepared by Sonogashira coupling between 2-ethynylpyridine and 3,5-dibromobenzonitrile with 64% yield. The bromine of the precursor was converted into iodine via tributylstannyl group to synthesize nonradioactive IPEB. Radioiodine displacement reaction with [I-123]iodide and bromo-precursor mediated by copper (I) catalyst produced [I-123]IPEB up to 40% radiochemical yield with >98% radiochemical purity.

SPECT Imaging: Dynamic SPECT-CT scan for min was carried out using a normal Sprague Dawley rat. [I-123]IPEB did cross blood brain barrier, and showed major uptake in hippocampus, striatum, cerebellum, and olfactory bulb which corresponded with previous studies with mGluR5 PET radiotracers. Time-activity curves showed fast uptake and slow wash-out in hippocampus and striatum.

Conclusion: We developed promising SPECT radiotracer for mGluR5 with 2 steps synthesis. [I-123]IPEB displayed major uptake in the brain regions where mGluR5 is abundant. Specificity and selectivity with other mGluR are needed to be validated by further study.

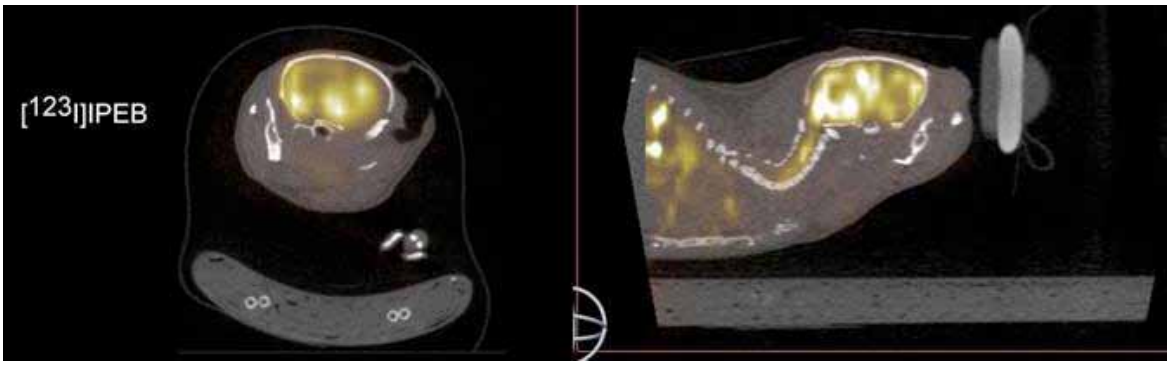

Poster Number 96

Lee, Jonghwan PhD
Research Fellow, Radiology
jonghwan@nmr.mgh.harvard.edu

Microscopic Imaging of Neuro-Capillary Coupling in Brain Cortex

Investigators: Jonghwan Lee, PhD; Weicheng Wu, MD; David A. Boas, PhD

The brain consumes energy. Energy supply regulation is essential for normal functioning of the brain. Oxygen and glucose should be supplied to meet spatiotemporally varying metabolic needs, location by location, moment to moment. They are mainly supplied by cerebral blood flow (CBF) and are used for maintaining ionic balance in the presence of underlying synaptic currents and action potentials in neurons. When this energy supply regulation does not work, neurons and glia become injured or die. As such an inadequate supply occurs in various disorders of the brain, understanding the mechanisms is a prerequisite for developing therapies to correct defects in blood flow control occurring in stroke, hypertension, and Alzheimer disease. The current paradigm for understanding this energy supply regulation is neurovascular coupling, which focuses on how local neuronal activity adjusts arteriolar tone (and thus local CBF) to meet metabolic needs. This paradigm, however, has recently been challenged by a concept of neuro-capillary coupling that cerebral capillaries also contribute to the blood flow regulation in response to neuronal activity. Recent studies showed that contractile cells called pericytes can control the diameter of capillaries, but regulation of blood flow at the capillary level has been demonstrated only in vitro.

Here we demonstrate in vivo capillary flow regulation in response to neural activation. For this purpose, we developed novel optical coherence tomography-based technology that enables us to measure the blood flow speed over hundreds of capillaries at the same time. We repeated, with ~1 s temporal resolution, imaging of the blood flow pattern of the cerebral capillary network in the cranial window preparation of rats while applying electrical stimulation to the forepaw. The mean flow speed averaged across capillaries increased in response to neural activation, only at the region close to the activated center. Interestingly, the standard deviation of the capillary flow decreased, commonly across three animals. Furthermore, this flow homogenization occurred significantly earlier than both the mean flow increase and the arterioles' supply increase, supporting the active capillary control of blood flow. The observed flow homogenization may support the theoretical hypothesis that the tissue oxygen extraction is higher with a more homogeneous flow network. These results provide a direct in vivo evidence of neuro-capillary coupling.

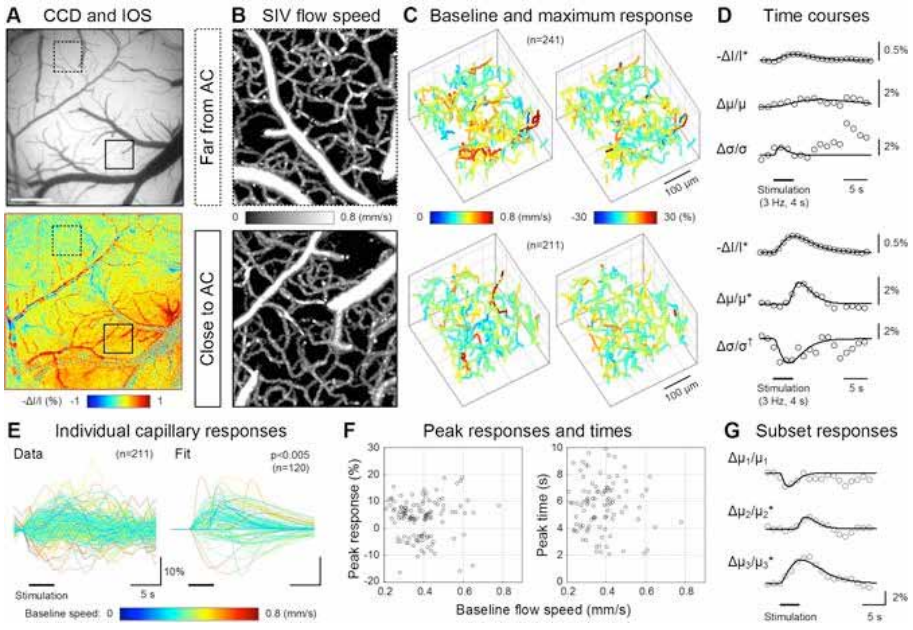

Poster Number 97

Liang, Minrui MD
Research Fellow, Pediatric Service
mliang6@partners.org

Receptor Interacting Protein Kinase 1 Is a Positive Regulator of Inflammatory Signaling in Microglia

Investigators: Minrui Liang, MD; Qiong Liu, MD, PhD; Jianhua Qiu, MD, PhD; Xingfen Su, MD; Nicholas Peters, BA; Micheal Whalen, MD

Background: Receptor-interacting protein kinase 1 (RIPK1) mediates cell death and inflammation in cultured cells and in systemic inflammatory disorders. Previous studies show that inhibition of RIPK1 protects neurons form death, reduces learning and memory deficits, and markedly inhibits microglial activation after acute traumatic brain injury (TBI). These previous findings suggest a link between chronic microglial activation and pathogenesis of learning and memory deficits after TBI that might be targetable by drug therapy. In this study, we investigated whether RIPK1 mediates TBI-related inflammation in microglial cells.

Methods: Mouse primary microglia and the microglial cell lines BV2 and N9 cells were subjected to a classic pro-necrosis stimulus used to produce cell death in sensitive cell lines (tumor necrosis factor alpha, 10 ng/ml in the presence of the pan-caspase inhibitor ZVAD, 50 uM). Gene expression was assessed by quantitative real time PCR and protein expression by Western blot and immunoprecipitation using well validated anti-RIPK1 and anti-RIPK3 antibodies. Necrostatin-1 (30 uM) was used to specifically inhibit the kinase activity of RIPK1.

Results: Tumor necrosis factor alpha (TNF-α)/ zVAD-fmk (zVAD) induced assembly of a RIPK1-TRADD-FADD-CYLD complex in the absence of cell death in BV2 cells. RIPK3, a key mediator of necrotic cell death, was not detectable in primary microglial cells by Western blot. The RIPK1 signaling complex assembly was prevented by pretreatment with necrostatin-1. TNF/zVAD induced upregulation of proinflammatory cytokines (il-1β, il-1α, tnf-α, il-6) and chemokines (ccl2, ccl3, ccl4, ccl7, cxcl1, cxcl2) in microglial cell lines and primary mouse microglia cultures. Necrostatin-1 efficiently inhibited induction of all of these gene products including the prototypic proinflammatory mediator interleukin-1 beta (Il-1β). Genetic knockdown of RIPK1 using specific siRNA also inhibited TNF-α/zVAD induced upregulation of Il-1β. However, necrostatin-1 did not block LPS-induced upregulation of IL-1β in BV2 cells suggesting specificity of TNF/zVAD signaling.

Conclusion: Our study indicates that RIPK1 plays a key role in inflammatory signaling in microglia following classical inducers of programmed necrosis. Lack of programmed necrosis in microglial cells may be related to their absence of detectable RIPK3, a key mediator of programmed necrosis. Importantly, RIPK1 signaling is a strong inducer of pro-inflammatory signaling in microglia, suggesting a link between protection against cognitive deficits by necrostatin-1 and the ability of necrostatin-1 to reduce microglial activation after experimental traumatic brain injury. RIPK1 may therefore be a therapeutic target to limit inflammation and improve functional outcome after traumatic brain injury.

Poster Number 98

Liu, Qiong MD, PhD
Research Fellow, Pediatric Service
qliu11@partners.org

Novel roles for Akt and mTOR in neuronal programmed necrosis

Investigators: Qiong Liu, MD, PhD; Michael J. Whalen, MD

Necroptosis is a newly described form of regulated necrosis mediated by serine-threonine kinases RIPK1 and RIPK3, which contribute to neuronal cell death in experimental models of stroke and brain trauma. Although much work has been done elucidating initiating and effector mechanisms, signaling events governing necroptosis remain largely unexplored. Akt is a pro-survival factor that is well known to inhibit apoptotic neuronal cell death. mTOR is a direct substrate of Akt that initiates protein synthesis. We previously reported that dual inhibition of Akt and mTOR reduced acute cell death and improved long term cognitive deficits after controlled cortical impact in mice. These findings raised the possibility that Akt/mTOR might regulate necroptosis, opposite to their role in apoptotic cell death. To test this hypothesis we induced necroptosis in primary mouse cortical neurons or the hippocampal neuronal cell line HT22 using concomitant treatment with TNF alpha and the pan-caspase inhibitor ZVAD (to simulate inflammation), or hemin (to simulate blood products). Necroptosis was confirmed by electron microscopy, HMGB1 release, plasmalemma damage, inhibition by necrostatin-1 (a specific RIPK1 inhibitor) and butylated hydroxyanisole (BHA, a reactive oxygen species inhibitor), and genetic knockdown of RIPK3 ($p < 0.05$). TNF/ZVAD induced RIPK1-RIPK3 assembly (assessed by immunoprecipitation and Western blot), mitochondrial complex I reactive oxygen species production, and phosphorylation of Thr308 and Thr473 of AKT and its direct substrate GSK-3β, as well as phosphorylation of mTOR and its direct substrate S6 kinase, suggesting activation of Akt/mTOR pathways. Pretreatment with Akt inhibitor VIII and rapamycin inhibited Akt and S6 phosphorylation events, mitochondrial ROS production ($p < 0.05$), and necroptosis by over 50% ($p < 0.05$ vs. vehicle for cell death) without changing RIPK1-RIPK3 complex assembly. These data were confirmed using a genetic approach with siRNA-mediated knockdown of AKT1/2 and mTOR ($p < 0.05$ for cell death vs. inactive siRNA). All of the aforementioned biochemical events were inhibited by necrostatin-1 including Akt and mTOR phosphorylation and RIPK1-RIPK3 complex assembly. The data suggest a novel, heretofore unexpected role for Akt and mTOR in necroptosis signaling in neuronal cells. Further studies are needed to translate these findings in CNS injury models in vivo to identify new therapeutic targets for stroke and traumatic brain injury.

Poster Number 99

Malik, Wasim Q. PhD
Instructor, Anesthesia, Critical Care and Pain Medicine
wmalik@partners.org

Design of an Autonomous Brain-Body Interface for Neurorehabilitation

Investigators: Wasim Q. Malik, PhD; Robert Ajemian, PhD; Neelakantan Sunder, MD; Jonathan M. Winograd, MD; Emery N. Brown, MD, PhD; Emilio Bizzi, MD, PhD

The pathophysiology of neuromuscular injury or disease is characterized by an inability of the central nervous system to exert functional control over the peripheral musculature. In many cases of spinal cord injury or late-stage neuromuscular disease, specific end-effectors are completely immobilized. When these devastating conditions occur, clinicians and patients are deeply frustrated by the dichotomy that arises between the patient's capacity for action and the ability to realize that action. The cognitive faculties of these patients, their full affective range, and even motor memories of complex learned behaviors often persist; yet, because of damage to the spinal cord and/or degradation of motor neurons, the patients are unable to implement even rudimentary movements.

Neural prosthetics is an area of research that holds much promise for developing improved means of rehabilitation for these patient populations. Within this discipline, researchers are attempting to tap into neural control signals and use them to establish new, artificial pathways for controlling actuators. In order to do this, control of prosthetic arms must be fluid, natural, and effective. Current neuroprosthetic devices do not meet these specifications. We suggest an alternative approach to the approaches that have been used so far. Specifically, our research differs from most other research in neural prosthetics by virtue of the fact that the devices we construct are fully autonomous: all of the learning occurs in the brain, and none of it occurs in a decoder or machine learning algorithm. Given the considerable challenge of the native brain developing a high level of control over a newly introduced actuator on the timescale of a single laboratory session, we initially simplify our experimental preparation to address the problem of control of a single degree-of-freedom.

Here we show that an ultrasound-guided nerve blocking technique together with surgical manipulation of the peripheral neuroanatomy can be used to establish a pure motor block of elbow flexion in a non-human primate model. Although active elbow flexion is impossible, all other motor degrees-of-freedom are in tact, as well as most forms of tactile feedback. The block is fully reversible when the anesthetic wears off and can be maintained indefinitely with multiple injections. This non-human primate model can be used as a testbed for restoring motor function to a single degree-of-freedom using neuroprosthetic control of stimulating electrodes that activate a paralyzed muscle.

Poster Number 100

Nilbratt, Mats PhD
Research Fellow, Center for Human Genetic Research
nilbratt@chgr.mgh.harvard.edu

Using Human iPS cells to Model Tissue-Specific Splicing and Peripheral Nervous System Development

Investigators: Mats Nilbratt, PhD; Gabsang Lee, DVM, PhD; Susan A. Slaugenhaupt, PhD

Familial Dysautonomia (FD), or Riley-Day syndrome, is an autosomal recessive disorder with extensive sensory and autonomic nervous system perturbations. The disorder has been described with symptoms including recurrent episodes of hypertension with tachycardia, nausea and vomiting, as well as impaired thermoregulation, and deceased sensitivity to pain and temperature.

The clinical features of FD are due to a genetic mutation in the IKBKAP gene that results in reduced IKAP expression and begins during development and show progressive degeneration throughout life. Neuropathological examination has shown that there are reduced number of neurons in the dorsal root ganglion in FD patients. These findings indicate that IKAP is critical for the development of afferent baroreflex pathways which explains their characteristic sensory loss and labile blood pressure.

All FD patients have an intronic splice site mutation in the IKBKAP gene, the scaffolding member of the Elongator protein complex involved in transcriptional elongation. This mutation results in tissue-specific skipping of exon 20 in the mRNA with aberrant splicing most pronounced in neuronal tissues. The alternative splicing defect leads to reduced production of normal IKAP protein in FD patients. In addition, complete embryonic loss of Ikbkap in mice causes early embryonic lethality, suggesting that this gene is required for effective transcription of genes involved in very early neural development.

Methods to model human development of the sensory and autonomic nervous system in a controlled, defined manner from induced pluripotent stem (iPS) cells have considerable potential to enable functional studies of the human development of the peripheral nervous system. Here we show directed differentiation of iPS cells from FD-patient fibroblasts to neural progenitors followed by the formation of human peripheral neurons. Gene expression analysis in FD-iPS cell lineages revealed tissue-specific mis-splicing of IKBKAP in vitro. Furthermore, by testing and validating candidate compounds for FD treatment, the aberrant splicing of IKBKAP was reversed.

In summary, our data suggest that our system enables studies of human tissue-specific splicing in disease-relevant cell types for disease modeling and therapeutic purposes.

Poster Number 101

Pham, Loc-Duyen MSc
Research Technician, Radiology
lpham1@partners.org

Radical scavenger edaravone protects oligodendrocyte precursor cells both in vitro and in vivo

Investigators: Loc-Duyen D. Pham, MSc; Nobukazu Miyamito, MD, PhD; Ken Arai, PhD

Background and Purpose: During brain injury, reactive oxygen species (ROS) is produced and released to cause further damage, especially under the acute phase. In case, where the region of injury involves the white matter area, the severity of ROS damage may be critical because white matter consists of lipid-rich myelin sheathes and is an enormous source of ROS. Oligodendrocyte precursor cells (OPC) are one of the major cell types in the white matter. After white matter is damaged, they proliferate and differentiate into mature oligodendrocytes as a compensative response. However, OPCs are intrinsically vulnerable to oxidative damage, and thus far, there has been no clinically proven reagent to protect OPCs under pathological conditions. In this study, we investigate the OPC-protective effects of edaravone, a radical scavenger, which is used in clinic as an acute stroke therapy in Japan, using in vivo and in vitro white matter injury models.

Methods and Results: A mouse model of prolonged cerebral hypoperfusion was prepared by bilateral common carotid artery stenosis. This animal model was previously shown to have similar pathological features as vascular dementia, such as white matter lesion. As expected, white matter myelins were broken down over time after the stress onset, and importantly, immunostaining confirmed that the number of damaged OPCs was increased at day 14. Notably, edaravone treatment (3 mg/Kg, i.p. twice/week) significantly decreased the death of OPC at day 14. Next, we prepared cultured rat OPCs from neonatal rat cortex to examine the OPC-protective effects of edaravone in vitro. OPC cultures were treated with pyocyanin (PCN), which is known to generate ROS. The DCF assay confirmed that PCN treatment increased the ROS levels in our OPC cultures, and co-treatment of edaravone (10 uM) significantly reduced the oxidative stress. Correspondingly, edaravone treatment protected OPC cultures against the PCN-induced damage.

Conclusions: Taken together, our data show that edaravone has OPC-protective effects under oxidative stress conditions. OPCs play pivotal roles on white matter repairing after brain injury, and hence, ROS suppression therapy could be a promising therapeutic approach for white matter related diseases, such as vascular dementia and stoke.

Poster Number 102

Rennekamp, Andrew J. PhD
Research Fellow, Medicine
arennekamp@cvrc.mgh.harvard.edu

Can we use zebrafish to identify new antipsychotics?

Investigators: Andrew J. Rennekamp, PhD; Samir Patel, BS; David Kokel, PhD; Randall T. Peterson, PhD

The target-centric approaches of cell-based and in vitro high-throughput screens have the potential to miss systems-modulating compounds, which may be useful for the treatment of complex polygenic diseases such as schizophrenia. New classes of antipsychotics have remained elusive, despite intense research effort, in part due to the lack of a systems-wide approach to neuroactive drug discovery. Zebrafish larvae are neurocompetent organisms exhibiting complex behavioral phenotypes with neurophysiology remarkably similar to humans, yet they are also well-suited for in vivo, high-throughput screening. We have discovered a reproducible zebrafish behavior that is specifically modulated by drugs known to be either anti-psychotic or hallucinogenic in humans, such as dopamine antagonists and NMDA receptor blockers. Importantly, this behavior is amenable to high-throughput assaying. We then used the zebrafish as a tool for the identification of novel small-molecules that perturb fish behavior in a manner similar to the human drugs. These screening hits are now lead compounds for preclinical assessment of antipsychotic activity.

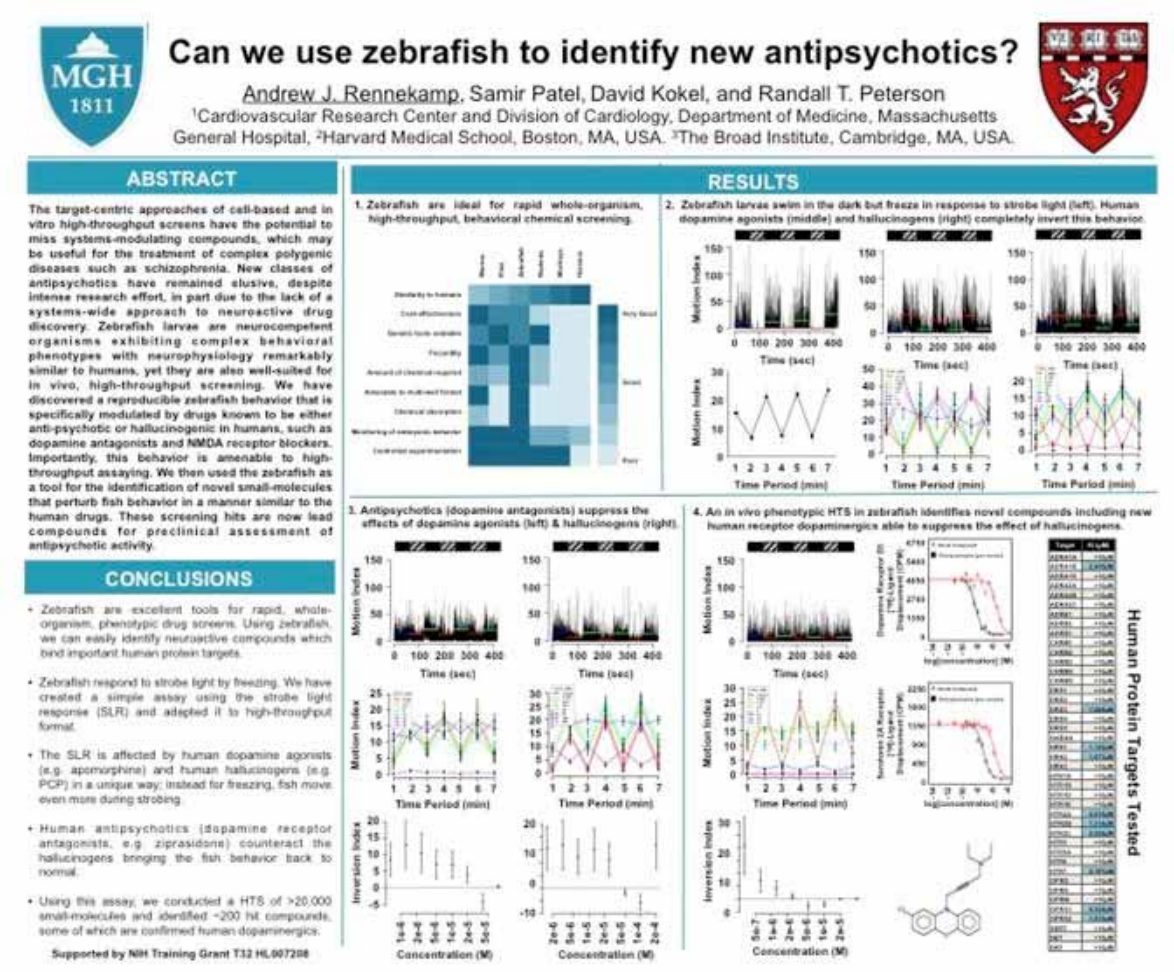

NEUROSCIENCES

Poster Number 103

Sadri-Vakili, Ghazaleh PhD
Assistant Professor, Neurology Service
gsadrivakili@partners.org

Epigenetic inheritance of a cocaine-resistance phenotype

Investigators: Fair M. Vassoler, PhD; Samantha L. White, BS; Heath D. Schmidt, PhD; Shayna B. Darnell, BS; Gavin R. Sangrey, BS; R. Christopher Pierce, PhD; Ghazaleh Sadri-Vakili, PhD

A rat model was developed in order to delineate a heritable phenotype resulting from the self-administration of cocaine. Male, but not female, offspring of sires that self-administered cocaine had delayed acquisition and reduced maintenance of cocaine self-administration relative to the offspring of yoked saline controls. Previous work showed that increased brain derived neurotrophic factor (BDNF) in the medial prefrontal cortex (mPFC) blunts the behavioral effects of cocaine. The current results showed increased association of acetylated histone H3 associated with BDNF promoters in both the sperm of cocaine experienced sires as well as the mPFC of male offspring, which represents an epigenetic mechanism whereby cocaine self-administration by sires confers resistance to cocaine reinforcement in their male offspring. Collectively, these results indicate that voluntary paternal ingestion of cocaine reprograms the germline resulting in profound effects on mPFC gene expression and behavior among their male progeny.

Poster Number 104

Saponjian, Yero BS
Graduate Student, Neurology Service
saponjian.yero@mgh.harvard.edu

A moderate-throughput in vitro screen for antiepileptogenic compounds

Investigators: Yero Saponjian, BS; Yevgeny Berdichevsky, PhD; Waldemar Swiercz, PhD; Kevin Staley, MD

The accelerated course of epileptogenesis in the in vitro organotypic hippocampal slice culture model of post-traumatic epilepsy was utilized to conduct a moderate-throughput screen of an array of drugs to study their antiepileptic and neuroprotective effects and ultimately identify antiepileptogenic compounds. Organotypic hippocampal slice cultures (350 µm) were prepared from postnatal day 6 or 7 Sprague-Dawley rats and were maintained for 28 days in vitro on a rocking platform in a 37oC, 5% CO2, humidified incubator in culture medium consisting of Neurobasal-A, B27, 0.5 mM GlutaMAX, and 30 µg/ml Gentamicin. Spent culture medium was collected at media changes every 3-4 days and stored at -80oC until analysis. Drugs, obtained primarily from the NINDS Custom Collection of compounds, were dissolved in DMSO (final concentration 0.1%) and added to the culture media starting on DIV 3. All experiments included control slice cultures derived from the same animals as experimental ones. Lactate concentration in collected culture media was strongly correlated with electrographic seizure activity and used in subsequent experiments as an assay for epileptic activity. Lactate dehydrogenase (LDH) release into culture media was correlated with propidium iodide assays for cell death and used in subsequent experiments as an assay for neuroprotection. Measurement of lactate and LDH concentrations in spent culture media from organotypic hippocampal slice cultures allows for rapid analysis of chronic application drug effects on seizure activity and cell death. Lactate and LDH concentrations were plotted as cumulative values of 28 days in vitro. We have screened over 100 drugs, with most drugs screened at multiple concentrations. Several drugs exhibited significant dose-dependent anticonvulsive or proconvulsive effects, as well as neuroprotective or neurotoxic effects. Reduction in ictal cell death likely underlined the correlation between anticonvulsant and neuroprotective effects. Drugs with significant antiepileptic and neuroprotective effects are being retested, including 10-day wash-out experiments, to differentiate anticonvulsant from antiepileptogenic effects.

Poster Number 105

Staropoli, John F. MD,PhD
Research Fellow, Center for Human Genetic Research
jstaropoli@partners.org

Human iPS-based models of neuronal ceroid lipofuscinosis capture pre-storage pathology in multiple cellular compartments

Investigators: John F. Staropoli, MD, PhD; Xenia Lojewski, PhD; Sunita Biswas, PhD; Larissa Haliw, MS; Steven Sheridan, PhD; Martin K. Selig, MS; Chad Cowan, PhD; Stephen J. Haggarty, PhD; Katherine B. Sims, MD; Alexander Storch, MD; Susan L. Cotman, PhD

The neuronal ceroid lipofuscinoses (NCLs) comprise a group of at least 12 distinct lysosomal storage diseases (LSDs) with overlapping clinical features including progressive motor and cognitive decline, pigmentary retinal degeneration and visual loss in most cases, seizures, movement disorder, and eventual premature death. Collectively, the NCLs comprise the major Mendelian cause of neurodegeneration among children, affecting as many as 1 in 12,500 live births. Of these, the most common forms are classic late-infantile NCL (CLN2), caused by loss-of-function mutations in TPP1, which encodes the soluble lysosomal enzyme tripeptidyl peptidase-1, and juvenile NCL (CLN3), caused by loss-of-function mutations in CLN3, which encodes a transmembrane endosomal/lysosomal protein with orthologs from yeast to mammals. The histopathologic features common to the NCLs, including lysosomal accumulation of autofluorescent, electron-dense material composed of oxidized lipids and undigested proteins, in particular, subunit c of the mitochondrial ATP synthase complex, suggest a final common pathway that may include incomplete clearance of mitochondria targeted to lysosomes.

Studies using lower mammalian and other eukaryotic disease models suggest that defects in endocytic trafficking, autophagy, lipid processing, and cytoskeletal organization are major components of NCL pathogenesis, particularly in juvenile NCL. Cerebellar cell lines derived from a genetically precise murine model of CLN3 have shown that subunit c storage is preceded by endosomal-lysosomal trafficking defects, impaired autophagy, and mitochondrial abnormalities. While these and other models offer useful guiding principles, it remains unknown whether these observations are valid in human neurons or recapitulate critical aspects of the human disease. For this reason, induced pluripotent stem cells (iPSCs) derived from patients and redifferentiated to cell types of interest have emerged as powerful, if imperfect, tools for human disease modeling and therapeutic screening. Although subject to the limitations of any in vitro model system, iPSCs and their derivatives from patients with Mendelian disorders provide the precise genetic lesion and genetic background for testing mechanistic hypotheses and potential therapies in a genotype-specific manner.

Here we characterize iPSC lines, and their neuronal derivatives, obtained by 4-factor retroviral reprogramming of fibroblasts from CLN2 and CLN3 patients. We demonstrate striking pre-storage pathology in multiple subcellular compartments in both forms of NCL. In the CLN3 lines, a defect in endosomal or lysosomal maturation was appreciated as early as the iPSC stage, and persisted through neuronal and astrocytic differentiation, whereas mitochondrial pathology, including distension and loss of cristae, did not appear until the neuronal precursor stage. By contrast, CLN2 cells showed lysosomal and ER pathology beginning at the neuronal precursor stage but did not show disruption of mitochondrial architecture until the mature neuronal stage. In most cell lines, characteristic lysosomal storage material did not appear until differentiation of neuronal precursor cells into mature neurons. In mature neurons carrying the common nonsense mutation in TPP1, c.622C>T/p.Arg208X, the nonsense suppressor PTC124 markedly attenuated subunit c accumulation, demonstrating the value of this marker as a screening tool for compounds that modify NCL disease in neuronal populations.

Poster Number 106

Sweadner, Kathleen J. PhD
Associate Professor, Neurosurgery
sweadner@helix.mgh.harvard.edu

A new mutant mouse with symptoms of dystonia

Investigators: Kathleen J. Sweadner, PhD; Y.B. Liu, MA; J.S. Salameh, MD; L.J. Ozelius, PhD; A. Brashear, MD

Objective: To obtain a mouse model that exhibits consistent symptoms of dystonia for future pathway analysis and testing of drugs and interventions.

Background: While there are many mutant mice with measurable motor deficits, it has been difficult to obtain mice with obvious symptoms of dystonia. Some display paroxysmal dystonia only when treated with drugs; others have severe neuropathological features or are difficult to keep alive. A useful mouse would have reliable symptoms, but require no special care. More than 20 spontaneous mutations cause dystonia in humans.

Methods: A new mutation arose spontaneously in a colony of C57BL/6 mice. Genetic inheritance was established by breeding with a sibling, then by additional crosses to affected offspring and to wild type mice. The genetic locus was determined by SNP marker mapping in hybrids. Dystonic movements and postures were documented with video in pilot motor behavioral studies.

Results: The new mutant proband was the only affected mouse out of 28 siblings. Inheritance is dominant and 100% penetrant on the C57BL/6 strain background. All affected mice have identical hindlimb symptoms that resemble posturing types of dystonia. Excessive contraction of extensors results in caudal and lateral hyperextension that is seen upon awakening and moving around the cage. Hindlimb hyperextension continues during sitting, and the feet jut forward and laterally. However, the mice can also walk well, albeit often with hindleg hyperextension. Most notably, they can run quite well on a wheel, running for hours a night and at ~80% of the speed of unaffected littermates in preliminary experiments. They maintain weight; breed readily; show exploratory behavior; and climb voluntarily despite hindlimb problems. EMG recordings from opposing hindlimb muscles show co-contraction, a cardinal feature of dystonia. Rotarod testing, beam crossing, and swimming are impaired.

Conclusions: Importantly, the ability to execute wheel-running suggests intact upper motor neurons, spinal pattern generators, and segmental motor and sensory innervation. We propose that the primary impairment is supra-spinal. The mouse's ability to override dystonic postures to walk and run may be analogous to sensory tricks in human dystonia. This mouse merits study of its genetics, neuropathology, and physiology to determine if it is a useful model of dystonia.

Wang, Zemin MD, PhD
Research Fellow, Neurology Service
zwang15@partners.org

Poster Number 107

Long-term modification of Electrical Synapses by activating mGluRs

Investigators: Zemin Wang, MD, PhD; Baltazar A. Zavala, BS; Ryan Neely, BS; Carole E. Landisman, PhD

Gap junctions extensively exist in mammalian brain, which function as electrical synapses between neurons and play an important role in development, physiological and pathological conditions. GABAergic interneurons in the thalamic reticular nucleus (TRN) mainly communicate using gap junction-mediated electrical synapses (Landisman et al., 2002), and activation metabotropic glutamate receptors (mGluRs) in TRN, either by brief tetanus of corticothalamic feedback fibers or by applying non-specific mGluR agonist (ACPD), can cause long-term depression (LTD) of gap junctional coupling strength (Landisman and Connors, 2005). But, the underlying mechanisms of this modulation are unknown. mGluR3 mRNA is highly expressed in adult rat TRN, as well as less highly-expressed mRNA of several other specific group I and II mGluRs (Neto, et al., 2000). Activation of mGluRs by agonist application can cause opposite effects in TRN interneurons, where mGluR I activation causes depolarization, and mGluR II activation causes hyperpolarization (Cox and Sherman, 1999). Furthermore, group I and group II mGluRs converge on the same intracellular signaling pathway (AC – cAMP – PKA) after activation, but with opposite effects (Hermans and Challiss, 2001; Hughes and Crunelli, 2006; Wang and Landisman, 2009, 2010).

To study this pathway in depth, we used dual whole-cell recording in rat thalamocortical slices combined with pharmacological and calcium imaging methods. We found that bath–application of the mGluR3 agonist NAAG can cause long-term potentiation of gap junctional coupling strength (eLTP), and the group II antagonist LY 341495 occludes this eLTP; In addition, activation of the G-protein Gi/o, which is triggered by mGluR3 stimulation, also causes eLTP. By contrast, application of the group I mGluR agonist DHPG causes eLTD. The AC activator Forskolin causes eLTD; and activation of PKA by the cAMP analog 8-Bromo-cAMP also cause eLTD. Finally, inhibition of PKA by KT 5720 induces eLTP. After exposure to KT 5720, the fluorescence of un-patched cells shows a significant increase that is tightly correlated to stimulation of the patched cell compared to control; furthermore, significantly more neurons are activated by stimulation of the patched neuron in the presence of KT 5720 than under control conditions. Thus, similar to their chemical counterparts, electrical synapses undergo both strengthening and weakening forms of plasticity, which should play a significant role in thalamocortical function.

Poster Number 108

Wey, Margaret Chia-Ying PhD
Research Fellow, Psychiatry
mwey@partners.org

Role of Glutamatergic Circuitry in Pediatric Compulsive Disorders: Translating Preclinical Results into Therapies

Investigators: Margaret Chia-Ying Wey, PhD; Mai Saito, BS; Jeremiah Scharf, MD, PhD; Tracey Petryshen, PhD

Compulsive disorders, including obsessive-compulsive disorder (OCD) and Tourette Syndrome (TS), are characterized by uncontrollable, repetitive, and ritualized behaviors one feel compelled to perform. OCD is one of the most prevalent neuropsychiatric disorders affecting about 1 – 3 % of the population worldwide. Disease onset is rare at very young ages, but the rate increases with age and affects 1 % of children and adolescents. Only up to 60 % of patients do not respond to current pharmacological regimens. Lack of effective treatments for compulsive disorders may due to limited knowledge about the neurobiology of the disease. Genetic studies suggest that familial inheritance plays an important role in compulsive disorders including OCD and TS, furthermore, OCD and TS have been shown to be genetically related. Evidence from animal model and genetic association studies suggests that the SLITRK gene family may play a role in disease risk. There are six members of the SLITRK gene family (SLITRK1 – 6) that were identified as neuronal transmembrane proteins that control neurite outgrowth. The function of SLITRKs has not been precisely elucidated, but it is predominantly expressed in neurons in the cortex and striatum, where it may function in neuronal development. Human genetic analyses have shown that SLITRK1 is associated with TS. Scharf et. al. (2012) recently discovered a SNP located within the intergenic region of SLITRK1 and SLITRK6 may increase the risk of TS. A knockout (KO) mouse model in which the Slitrk5 gene is disrupted was reported to exhibit compulsive behaviors. The Slitrk5 KO mice also exhibit altered glutamate receptor expression, suggesting abnormal glutamatergic circuit function which has been implicated in human compulsive disorders. We hypothesize that impaired Slitrk5 function is associated with elevated glutamatergic signaling in compulsive disorders. The hypothesis is tested by assessing the effect of reduced glutamate signaling via pharmacological intervention in a juvenile animal model of compulsive disorders with the aim to pilot efficacy and toxicity for subsequent translation into clinical trials in children. Mice were treated for 21 days after weaning (6-9 weeks old; N = 8 males per group) with glutamate modulating agents, riluzole or memantine, to antagonize glutamate signaling. Drug efficacy in reversing compulsive phenotypes of Slitrk5 KO mice compared to wild-type littermates are assessed using the behavioral readouts of including over-grooming, marble burying, spontaneous alternation. After behavioral testing, mechanistic protein assays will be performed in striatum, orbitofrontal cortex, and thalamus brain regions involved in compulsive disorders of Slitrk5 KO mice to assess glutamatergic circuitry, including expression of glutamate receptor subunits (NR2A, NR2B, GluR1 and GluR2) by Western blot using commercial antibodies. This study provides evidence of pharmacologic strategies as a therapeutic approach to treatment of compulsive disorders which would aid understanding of disease pathophysiology and development of better treatment.

Poster Number 109

Wheeler, Vanessa PhD
Associate Professor, Center for Human Genetic Research
Wheeler@chgr.mgh.harvard.edu

A single mutant HTT allele is sufficient to elicit neuronal phenotypes in a knock-in mouse model of Huntington's disease

Investigators: Austen Milnerwood, PhD; Marina Kovalenko, PhD; Jeff Carroll, PhD; Jolene R. Guide, BA; Tiffany Lydon, BA; Jason St. Claire, BA; Marcy E. MacDonald, PhD; Lynn Raymond, PhD; Vanessa Wheeler, PhD

Huntington's disease (HD) is a dominantly inherited neurodegenerative disease caused by the expansion of a CAG repeat in the HTT gene encoding huntingtin. While mutant huntingtin has been found to impact many brain regions and peripheral tissues, medium-spiny neurons (MSNs) in the striatum are exquisitely vulnerable. Successful disease-modifying therapy for Huntington's disease (HD) will likely require intervention very early in the pathogenic process. To increase the likelihood of identifying early responses to mutant huntingtin that are relevant to the disease process in patients we are using accurate genetic knock-in mouse models of the CAG expansion mutation that causes HD. These allow us to delineate phenotypes that result from the expression of a single allele's worth of the full-length mutant huntingtin protein, as occurs in the majority of HD patients.

We probed MSNs in heterozygous HdhQ111/+ mice by performing immunohistochemistry with an antibody against DARPP-32. DARPP-32 is expressed specifically in MSNs within the striatum and is believed to play a role in integrating neuronal signaling in these neurons. DARPP-32 immunostaining intensity was significantly decreased in heterozygous HdhQ111/+ mice compared to wild-type controls at 10 months of age, indicating a potential functional deficit of the MSNs. To explore a functional deficit we used acute slice electrophysiology to analyze glutamatergic transmission from the cortex to the MSNs. As early as 1.5 months of age HdhQ111/+ mice exhibited a slowed decay of evoked NMDA receptor-mediated postsynaptic currents compared to wild-type controls. At 5 months of age HdhQ111/+ mice exhibited elevated extrasynaptic NMDA currents as well as altered AMPA receptor-mediated spontaneous postsynaptic currents. Extrasynaptic NMDA currents are thought to signal cell death pathways rather than pro-survival pathways that are signaled through synaptic NMDA receptors. Together, these electrophysiological data provide evidence for alterations at the cortico-striatal synapse in HdhQ111/+ mice. To begin to investigate the molecular underpinnings of these functional alterations we have performed preliminary RNAseq analyses of HdhQ111/+ and wild-type striata. Consistent with synaptic alterations these data indicate alterations in a number of pathways related to neurotransmission.

Further experiments are needed to better elucidate the temporal sequence of these phenotypes and their underlying mechanism(s). Nevertheless, these data strongly indicate that the expression of endogenous levels of full-length mutant huntingtin expressed from a single expanded allele is sufficient to elicit phenotypes consistent with neuronal dysfunction at an early age.

Poster Number 110

Zhang, Martin MD, PhD
Instructor, Neurology Service
Zhang.Can@mgh.harvard.edu

Characterization of novel gamma-secretase modulators in processing of the amyloid-beta precursor protein and in the therapeutics of Alzheimer´s disease

Investigators: Martin Zhang, MD, PhD; Sean Miller, BS; Rudolph Tanzi, PhD

Background: Alzheimer's disease (AD) is a devastating neurodegenerative disease with no cure. Considerable genetic, biochemical and molecular biological evidence support the "amyloid-hypothesis" in the pathogenesis of AD, stating that the excessive accumulation of a small peptide, amyloid-beta (Abeta), is the primary pathological event leading to AD. Abeta is generated through a sequential proteolytic cleavage from the amyloid-β precursor protein (APP) via beta- and gamma-secretase. Since the establishment of the Abeta hypothesis, a major strategy for AD treatment and prevention has focused on specifically modulating APP processing and decreasing Abeta levels. One class of promising drugs is known as gamma-secretase modulators (GSMs), a group of small molecules that modulate the cleavage activity of gamma-secretase in the processing of APP and specifically lowering Abeta levels without altering cleavage of other substrates, e.g. Notch. Our recently published study reported the development and characterization of a series of aryl 2-aminothiazole GSMs with biologically beneficial properties. These GSMs bind directly to gamma-secretase complex, decreasing the levels of longer Abeta species (e.g. Abeta42 and Abeta40) and increasing the levels of shorter Abeta species (e.g. Abeta38 and Abeta37). However, one disadvantage of those original GSMs is their low aqueous solubility, making them poor candidates for clinical development.

Methods and Findings: A novel series of GSMs were developed and characterized with desirable safety-profile and high aqueous solubility, based on the our previous study. We showed these novel GSMs with vastly improved aqueous solubility and strong potency. Moreover, cell and animal-based studies showed that these GSMs significantly modulated gamma-secretase processing of APP and lowered both Abeta42 and Abeta40 levels. Importantly, we also showed that these GSMs did not affect the processing of Notch, an essential protein involved in development.

Conclusion and Significance: These data provide further in-depth support of the "amyloid-hypothesis" in the pathogenesis of AD and provide the mechanism-of-actions utilizing these novel GSMs to lower Abeta levels in the therapeutics of AD. Our results warrant follow-up characterization of these GSMs in animal-based neurobehavioral studies and further strongly support them as excellent candidates in clinical development.

Poster Number 111

Ager, Eleanor PhD
Research Fellow, Radiation Oncology
eager@steele.mgh.harvard.edu

Inhibition of MMP14 activity slows the growth of orthotopic murine breast carcinoma and can synergize with radiation therapy

Investigators: Eleanor Ager, PhD; Sergey Kozin, PhD; Nathaniel Kirkpatrick, PhD; Matija Snuderl, MD; Shom Goel, BMMS, PhD; David Kodack, PhD; Dan Dransfield, PhD; Yves Boucher, PhD; Dai Fukumura, MD, PhD; Rakesh Jain, PhD

Background: Matrix metalloproteinase (MMP)-14 expression is frequently upregulated in cancer and can facilitate angiogenesis and metastasis. Vascular normalization induced by anti-angiogenic agents or changes in nitric oxide can improve response to radiation therapy. We aimed to determine the effect of blocking MMP-14 on primary tumor growth, angiogenesis, and response to radiation therapy as well as the formation of lung metastases.

Methods: We used DX-2400, a specific MMP-14 inhibitory antibody, combined with radiation therapy in two orthotopic murine models of breast cancer (4T1 and E0771). We assessed tumor growth, lung metastasis, and vascular parameters (vessel density and diameter, tumor perfusion, and pericyte and basement membrane coverage). The role of inducible nitric oxide synthase (iNOS) was examined with an iNOS-selective inhibitor (1400W) and NOS2-/- C57BL6 mice.

Results: DX-2400 and radiation therapy each inhibited primary tumor growth. In the 4T1 tumor model, we found synergy between DX-2400 and radiation while in E0771 tumors the growth delay was additive. Vascular normalization, including increased vessel diameter and perfusion, and an upregulation of iNOS were evident with DX-2400. These effects were more pronounced in the 4T1 model than in the E0771 model. The effects of DX-2400 in combination with radiation on tumor growth were reduced, but not completely ameliorated, by pharmacological and genetic blockade of iNOS. Finally, compared to radiation therapy alone, the formation of spontaneous lung metastases was reduced by concurrent DX-2400 treatment.

Conclusions: Here we show that DX-2400 can slow primary tumor growth and synergize with radiation therapy. This improved radiation response is mediated by DX-2400 induced vascular normalization and increased iNOS/NO expression.

Poster Number 112

Antoszczyk, Slawomir PhD
Research Fellow, Neurosurgery
santoszczyk@partners.org

Efficacy of Receptor Tyrosine Kinase Inhibitors in Sciatic Nerve MPNST Models

Investigators: Slawomir J. Antoszczyk, PhD, Brain Tumor Research Center, Massachusetts General Hospital and Harvard Medical School, Boston MA; Samuel D. Rabkin, PhD, Brain Tumor Research Center, Massachusetts General Hospital and Harvard Medical School, Boston MA

Molecular targeted therapies, including receptor tyrosine kinase inhibitors (TKI), are an increasingly important class of cancer therapeutic that targets selective oncogenic signaling pathways operative in individual tumors, including malignant peripheral nerve sheath tumors (MPNST). Two recently approved TKI are imatinib mesylate (Gleevec) and sunitinib malate (Sutent) that inhibit plateled-derived growth factor receptor (PDGFR) and c-KIT (CD117). PDGFR and c-KIT are overexpressed in many NF1 tumors, as well as in tumor stromal cells. In these studies, we evaluate the efficacy of Gleevec and Sutent in mouse and human MPNST models.

We have developed an orthotopic sciatic nerve MPNST model. Mouse MPNST cell lines derived from spontaneously-arising tumors in Nf1/Trp53 heterozygous mice (obtained from L Parada, Southwestern Medical School, Dallas, TX) are implanted into syngeneic mice, and human MPNST stem-like S462 cells are implanted into immune-deficient mice. The stem-like S462 cells were isolated by non-adherent culture of S462 cells in neurosphere media with EGF and bFGF (without serum). As tumors grow in the sciatic nerve, mice develop neurologic deficits, quantified with a neurologic scoring system, which occur earlier than external tumor detection. Mouse MPNST M2 (37-3-18-4) and human stem-like S462 cells form sciatic nerve tumors with different kinetics. M2 tumors are vascular, as determined by anti-CD31 staining, with mast cells present in the periphery.

The in vitro effects of Gleevec or Sutent on M2 and human stem-like S462 cell viability were determined using MTT or MTS assays, respectively. Sutent was more effective than Gleevec at equivalent doses in reducing cell viability. Mice displaying neurologic deficits, when tumors are established, were treated by gavage with Gleevec or Sutent daily. With mouse M2 tumors, 20 mg/kg/day of Sutent significantly inhibited tumor growth, decreased neurological deficits and extended survival in comparison to control and Gleevec-treated mice. In the human stem-like S462 model, Sutent (50 mg/kg/day) was somewhat better than Gleevec (100 mg/kg/day) at slowing the decrease in neurologic score. These studies demonstrate the value of the sciatic nerve MPNST model for testing novel therapeutics and suggest that Sutent warrants consideration for clinical testing in patients with MPNST.

Badr, Christian E. PhD
Research Fellow, Neurology Service
badr.christian@mgh.harvard.edu

Poster Number 113

Obtusaquinone, a small molecule targeting cancer cells through oxidative stress

Investigators: Christian E. Badr, PhD; Stephanie Van Hoppe, MSc; Hawasatu Dumbuya, BSc; Bakhos A. Tannous, PhD

Cancer therapeutics exploiting the biochemical changes in cancer such as high levels of oxidative stress could provide a powerful treatment strategy. Through a cell-based small molecule drug screening assay, we identified a natural compound, Obtusaquinone (OBT), exhibiting selective cancer-related toxicity towards different malignant glioma cell lines and primary cells as well as on twelve different cancer cell lines. OBT induced rapid increase in intracellular ROS levels, downregulation of cellular glutathione levels as well as DNA damage, subsequently leading to apoptosis. Along with the oxidative stress effect, the stabilization of p53 protein levels as well as the activation of Erk1/2 and c-Jun, were also detected in OBT treated glioblastoma cells. Co-treatment of cells with antioxidants protected against the OBT-induced cell-death suggesting that oxidative stress is the main mechanism through which this compounds targets cancer cells. OBT was well tolerated in mice and its therapeutic efficacy was validated in subcutaneous, intracranial glioma, as well as mammary tumor models. OBT slowed tumor growth and prolonged survival in treated mice compared to the control group. To our knowledge, this is the first report describing the antineoplastic effect of OBT in different cancer cell lines/models.

Balaj, Leonora PhD
Research Fellow, Neurology Service
lbalaj@partners.org

Poster Number 114

Heparin affinity purification of extracellular vesicles

Investigators: Leonora Balaj, PhD; Nadia A. Atai, MA; Weilen Chen; Bakhos A. Tannouss, PhD; Johan Skog, PhD; Xandra O. Breakefield, PhD; Casey A. Maguire PhD

Extracellular vesicles (EVs) are membrane vesicles released by cells. They carry active biomolecules including DNA, RNA, ncRNA, protein and lipids which can be transferred to recipient cells and cause downstream effects. Isolation and purification of EVs from in vitro and in vivo biofluids is still a major challenge and the most widely used isolation method still remains ultracentrifugation (UC) which requires expensive equipment and only partially purifies EVs due to co-precipitation of proteins. Affinity purification of biomolecules is an efficient way to achieve high purity without requiring expensive equipment. Previously we have shown heparin to block EV uptake in mammalian cells. Here we show that we can purify EVs from conditioned media using heparin-coated agarose beads. We directly compared heparin-purified EVs to UC EVs for the following characteristics: (1) purity by silver-stained SDS PAGE gels, (2) morphology by transmission electron microscopy (TEM), (3) EV markers by immunoblot and RNA analysis, and (4) functionality by labeled EV uptake into mammalian cells. Heparin-purified EVs were of a higher purity than UC EVs. Furthermore, they retained the RNA content, morphology, and functionality of UC EVs. In conclusion, we have discovered a simple and effective way to isolate a highly pure population of EVs using their apparent affinity for heparin.

ONCOLOGY

Poster Number 115

Batista, Ana PhD
Research Fellow, Radiation Oncology
abatista@steele.mgh.harvard.edu

Placental Growth Factor/Neuropilin-1 Signaling is a Therapeutic Target in Pediatric Medulloblastoma

Investigators: Ana Batista, PhD; Matija Snurdel, MD; Nathaniel Kirkpatrick, PhD; Carmen Almodovar, PhD; Lars Riedemann, MD; Peter Carmeliet, MD, PhD; Rakesh Jain, PhD

Medulloblastoma is the most common malignant brain tumor of childhood. Although current therapies improve survival, these regimens are highly toxic and associated with significant morbidity. Here, we show that Placental growth factor (PlGF) is expressed in the majority of medulloblastomas independent of their morphologic or molecular subtype; and that expression of PlGF receptor neuropilin 1 (Nrp1) correlates with poor overall survival of children with medulloblastoma. We demonstrate that PlGF and Nrp1 are required for the growth and spread of medulloblastoma. Moreover, we show that blockade of PlGF or Nrp1 results in direct antitumor effects in vivo, which result in medulloblastoma regression, decreased metastatic burden, and increased survival—even in an interventional setting. Finally, we reveal that PlGF production is stimulated in the cerebellar stroma by Sonic hedgehog (Shh) ligand secreted by medulloblastomas, and that PlGF acts through Nrp1—and not VEGFR1—to convey pro-survival signals in the medulloblastoma cells. The critical role of this tumor-stroma interaction mediated by Shh, PlGF, and Nrp1 across pediatric medulloblastoma genetic subtypes supports the development of novel therapies targeted at PlGF and/or Nrp1.

Poster Number 116

Blackburn, Jessica PhD
Research Fellow, Cancer Center
jsblackburn@partners.org

Single cell evolution of AKT pathway activation drives T-cell acute lymphoblastic leukemia relapse

Investigators: Jessica Blackburn, PhD; Sali Liu,BS; Kimberly Dobrinski, PhD; Sarah Martinez, BS; Jayme Ranali, BS; Finola Moore, PhD; Riadh Lobbardi, PhD; Charles Lee, PhD; David Langenau, PhD

The aggressive and unpredictable behavior of relapsed T-cell acute lymphoblastic leukemia (T-ALL) presents a major clinical challenge, with >70% of children and >90% of adults unable to survive relapsed disease. Relapsed T-ALL often acquires mutations that are not found in the primary malignancy that allow clones to survive treatment and enhance relapse growth. In order to identify the genes and pathways responsible for T-ALL relapse, we have developed a transgenic zebrafish model of relapsed T-ALL where single fluorescently-labeled cells are transplanted into genetically identical recipient fish and functionally assessed for differences in relapse growth. Using serial transplantation of single T-ALL cells and >6,000 recipient animals, we have followed single-cell evolution of T-ALL and identified critical drivers of relapse potential. These experiments showed that 6 of 49 individual T-ALL cells significantly increased their ability to form relapse over time, and analysis of T-ALL clones pre- and post-evolution showed that AKT pathway activation was correlated with increased relapse potential. Subsequent studies utilizing transgenic zebrafish that over-expressed activated AKT in developing T-ALL demonstrated that AKT signaling increased relapse potential 10-fold. Further, transgenic epistatic experiments revealed that AKT signaling plays two distinct roles in T-ALL relapse: the AKT/mTORC1 pathway directly enhanced relapse potential, while AKT mediated stabilization of the Myc protein increased T-ALL aggressiveness. Moreover, small molecule inhibition of AKT signaling reduced T-ALL relapse potential in vivo by 25-fold and synergized with Dexamethasone, a common cytotoxic chemotherapy, to significantly enhance cell killing in both zebrafish and human T-ALL. Activation of AKT signaling is associated with poor prognosis and drug resistance in human T-ALL, which, together with our work, suggests that AKT will be a useful molecular target in T-ALL treatment. In total, our experiments have documented the functional heterogeneity of single leukemic cells and identified AKT as a critical driver of T-ALL aggression, relapse formation, and insensitivity to therapy. These are first studies performed in any model to follow single cell evolution as it relates to relapse, opening new and exciting avenues of study to uncover genetic pathways that drive cancer malignancy.

Poster Number 117

Guo, Yanyan PhD
Research Fellow, Radiology
guo.yanyan@mgh.harvard.edu

High Efficiency Diffusion Molecular Retention Tumor Targeting

Investigators: Yanyan Guo, PhD; Hushan Yuan, PhD; Hoonsung Cho, PhD; Darshini Kuruppu, PhD; Kimmo Jokivarsi, PhD; Aayush Agarwal, MS; Khalid Shah, PhD; Lee Josephson, PhD

Here we introduce diffusion molecular retention (DMR) tumor targeting, a technique that employs PEG-fluorochrome shielded probes that, after a peritumoral (PT) injection, undergo slow vascular uptake and extensive interstitial diffusion, with tumor retention only through integrin molecular recognition. To demonstrate DMR, RGD (integrin binding) and RAD (control) probes were synthesized bearing DOTA (for 111In3+), a NIR fluorochrome, and 5 kDa PEG that endows probes with a protein-like volume of 25 kDa and decreases non-specific interactions. With a GFP-BT-20 breast carcinoma model, tumor targeting by the DMR or IV methods was assessed by surface fluorescence, biodistribution of [111In] RGD and [111In] RAD probes, and whole animal SPECT. After a PT injection, both probes rapidly diffused through the normal and tumor interstitium, with retention of the RGD probe due to integrin interactions. With PT injection and the [111In] RGD probe, SPECT indicated a highly tumor specific uptake at 24 h post injection, with 352 %ID/gm tumor obtained by DMR (vs 4.14 %ID/gm by IV). The high efficiency molecular targeting of DMR employed low probe doses (e.g. 25 ng as RGD peptide), which minimizes toxicity risks and facilitates clinical translation. DMR applications include the delivery of fluorochromes for intraoperative tumor margin delineation, the delivery of radioisotopes (e.g. toxic, short range alpha emitters) for radiotherapy, or the delivery of photosensitizers to tumors accessible to light.

Poster Number 118

He, Lei PhD
Instructor, Cancer Center
lhe1@partners.org

Mcl-1 and FBW7 control a dominant survival pathway underlying HDAC and Bcl-2 inhibitor synergy in squamous cell carcinoma

Investigators: Lei He, PHD; Kristine Torres-Lockhart; Nicole Forster, PHD; Saranya Ramakrishnan; Patricia Greninger; Mathew J. Garnett, PHD; Ultan McDermott, PHD; S. Michael Rothenberg, MD; Cyril H. Benes, PHD; Leif W. Ellisen, PHD, MD

Effective targeted therapeutics for squamous cell carcinoma (SCC) are lacking. Here we uncover Mcl-1 as a dominant and tissue-specific survival factor in SCC cell lines and primary tumors, providing a roadmap for a new therapeutic approach. The Mcl-1 axis is disabled by the HDAC inhibitor vorinostat, which regulates Bcl-2 family member expression to induce apoptosis in SCC cells. Although Mcl-1 dominance renders SCC cells extremely resistant to the BH3 mimetic ABT-737, vorinostat primes them for sensitivity to ABT-737 by shuttling Bim from Mcl-1 to Bcl-2/Bcl-xl, resulting in dramatic synergy for this combination and sustained tumor regression in vivo. Moreover, cell line and primary tumor analysis shows that somatic FBW7 mutation in SCC is associated with stabilized Mcl-1 and high Bim levels, resulting in a poor response to standard chemotherapy but a robust response to HDAC inhibitors and enhanced synergy with combination vorinostat/ABT-737. Together, our findings provide a biochemical rationale and predictive markers for the application of this therapeutic combination in SCC.

Poster Number 119

Huang, Yuhui PhD
Research Fellow, Radiation Oncology
yhuang@steele.mgh.harvard.edu

Vascular normalization: a strategy to recondition the tumor immune microenvironment for immunotherapy

Investigators: Yuhui Huang, PhD; Jianping Yuan, PhD; Elda Righi, MD; Peigen Huang, MD; Dan G. Duda, DMD, PhD; Dai Fukumura, MD, PhD; Mark C. Poznansky, MD, PhD; Rakesh K. Jain, PhD

The recent approval of a prostate cancer vaccine has re-energized the research on cancer immunotherapy. A critical barrier for immunotherapies remains the immunosuppressive tumor microenvironment, which is due to abnormal tumor vasculature, hypoxia and tumor-infiltrating myeloid suppressors. Judiciously used anti-angiogenic agents have the potential to modulate the tumor immune environment to improve immunotherapy, but they are often used at high doses in the clinic aiming to prune tumor vessels. However, this has been shown to compromise other concurrent therapies, e.g., chemotherapy. Here, we demonstrate that anti-vascular endothelial growth factor receptor 2 (VEGFR2) antibody treatment at lower, "vascular normalizing" dosesbut not high "anti-vascular" dosesresults in a more homogeneous distribution of functional tumor vessels and reduces hypoxia. As a result, the lower doses are superior to the high doses at polarizing tumor-associated macrophages from immune inhibitory M2-like towards immune stimulatory M1-like phenotype, and in facilitating CD4+ and CD8+ T cell tumor infiltration. These findings indicate that vascular normalizing doses of anti-VEGFR2 antibody can reprogram the tumor immune microenvironment from suppressive to stimulatory. Based on this mechanism, synchronizing vascular normalization with T cell activation induced by a whole cancer cell vaccine therapy enhanced anti-cancer efficacy in a CD8+ T cell-dependent manner in both immune tolerant and immunogenic murine breast cancer models. Given that the combinations of high doses of bevacizumab with chemotherapy have not improved overall survival of breast cancer patients, our study suggests a new strategy to more effectively use anti-angiogenic agents with active immunotherapy and potentially other anti-cancer therapies in a clinical setting.

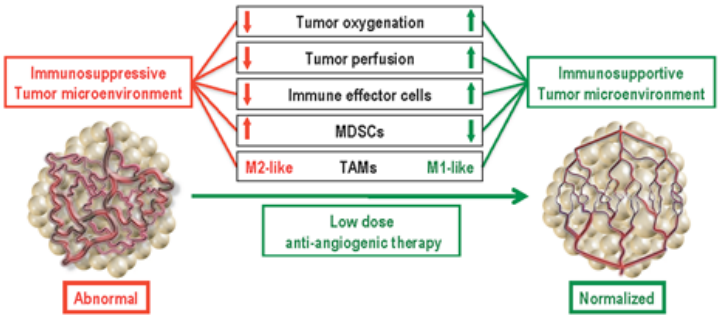

Schematic: Lower "Vascular normalizing" dose of anti-angiogenic treatment reprograms the tumor microenvironment from immunosuppressive to immunosupportive.

The abnormal tumor vasculature creates a hypoxic tumor microenvironment, which impedes T effector cell infiltration into tumors and polarizes tumor-associated macrophages (TAMs) to the immune inhibitory M2-like phenotype to suppress T effector cell function. Lower dose anti-angiogenic treatment normalizes the tumor vasculature and generates a homogeneous distribution of perfused tumor vessels, facilitating the infiltration of T effector cells while reducing myeloid-derived suppressor cell (MDSC) accumulation. In addition, improved vascular perfusion polarizes TAMs to an immune stimulatory M1-like phenotype. Thus, vascular normalization could be an effective strategy to alleviate the immunosuppressive tumor microenvironment and enhance cancer immunotherapy. (Adapted from Huang et al, PNAS, 2012 and Jain, Nature Medicine, 2001).

Poster Number 120

Khaled, Saman PhD
Research Fellow, Radiation Oncology
skhaled@partners.org

Time lapse microscopy as a cancer drug screening method for personalized radiation medicine: effects of chloroquine on A549 non-small cell lung cancer cells

Investigators: Saman F. Khaled, PhD; Matthew Flagg; Ashley Kern; Meng Wang, PhD; Henning Willers, MD; Jason A. Efstathiou, MD; DPhil, Kathryn D. Held, PhD

It is becoming increasingly clear that the effectiveness of cancer treatment is patient specific; hence, there is need for assays to determine response of cells from individual tumors to chemotherapy drugs and radiation. While static assays are efficient in determining levels of cell death, they are restricted to assaying cells at specific time points and may be limited by the assay selected for a specific cell response. Time lapse microscopy surmounts those shortcomings in three ways: 1) It shows the kinetics of drug/ radiation actions on the cell. 2) It allows for the visualization of different modes of cell death and cellular behavior, i.e., autophagy, senescence, apoptosis, and necrosis. 3) It keeps cells alive in conditions that more closely mimic an in vivo setting. The result is a platform that confers a wealth of cell and treatment-specific information. The purpose of this project is to develop a time lapse microscopy methodology capable of assaying tumor cell response to different cancer therapies, thereby establishing a screening method geared towards personalized radiation medicine. As an initial test of efficacy we treated A549 cells, a non small cell lung cancer cell line, with chloroquine, an autophagy inhibitor. We show that chloroquine treatment induces increased cleavage of caspase 3/7. A549 cells were plated in 12-well plates in the presence of Magic Red® (Immunochemistry), a caspase 3/7 substrate that fluoresces upon cleavage by the activated caspase, or DMSO as a control. The cells were treated with 10 μM chloroquine. An hour later, half the plate was irradiated with 2 Gy X-rays. The plate was then placed on a Nikon Eclipse TE2000-S fluorescence microscope surrounded by a 37 degree C, 5% CO2 incubator. Images were collected for 72 hours using Nikon Elements® software. Fluorescence intensity of Magic Red increases with time in both irradiated and unirradiated A549 cells treated with the autophagy inhibitor. 60 hours into the assay, fluorescence significantly increases in chloroquine treated, 2-Gy irradiated cells. By the end of 72 hours, Magic Red fluorescence intensity in irradiated cells is 2-fold higher than in unirradiated cells. However, although caspase 3 activation is generally a late step before morphological appearance of apoptosis, A549 cells do not show normal apoptotic cell morphology, rather they show increased vacuolization and size with time. This is not seen in untreated cells. In control cells, cell number increases 2-3-fold over the 72- hour assay period, with approximately 50% of the total cell population mitotically active and few spontaneous apoptotic or necrotic events occurring over the course of time lapse study. In contrast, ~60% of chloroquine treated cells were mitotically inactive, 25% were mitotic, and 5-10% formed giant cells, indicating overall stalled cell growth. These data show compelling evidence that time lapse microscopy can provide important information on the dynamic nature of cellular behavior following treatment with drugs and radiation.

Li, Chunjie MD, PhD
Research Fellow, Radiation Oncology
cli16@partners.org

POSTER NUMBER
121

The Radiation-induced Bystander Effect in Human Colon Cancer Cells

Investigators: : Chunjie Li, MD, PhD; Kathryn D. Held, PhD

Background: The radiation-induced bystander effect is the expression of damage in unirradiated cells when their neighboring cells are irradiated. It occurs in most normal cell types tested to-date, but its occurrence in cancer cells varies with cancer type. Little is known about the bystander effect in colon cancer, one of the most common cancers in the US, especially under exposure to low-dose and charged particle irradiations that are believed to be tumorigenic. Additionally, most bystander data have been obtained in vitro with monolayer cultures, while data in cancer tissue are limited.

Objective: To compare the magnitude and timing of the radiation-induced bystander effect in colon cancer cells in monolayer culture and a 3-dimensional tissue model.

Methods: In monolayer, bystander human colon cancer Caco2 cells shared media with irradiated cells immediately post-exposure to X-rays or charged particles, the latter irradiations performed at the NASA Space Radiation Laboratory at Brookhaven National Laboratory. The incidence of micronuclei (MN) and 53BP1 foci, at different time points, were detected. In 3D experiments, the artificial tissue construct consisted of AG01522 human fibroblasts embedded in collagen gel with Caco2 cells grown on the gel surface. Each 3D construct was cut into two pieces before irradiation. One piece was X-irradiated then promptly placed in contact and co-cultured with the other bystander piece. The incidence of 53BP1 foci was examined at different time points.

Results: In monolayer, MN levels in bystander CaCo2 cells after co-culture with 0.5 Gy, 1 Gy and 2 Gy X-irradiated cells were 15.3%, 19.1% and 19.4%, respectively, all higher than 6.3% in controls. Similar results were seen in bystander cells post-exposure to proton, silicon and iron ions. 53BP1 foci in Caco2 cells exposed to 0.5 Gy, 1 Gy and 2 Gy X-rays reached maximal levels, which were 55.5%, 73.1% and 82.7%, at 5 hours and decreased afterward. In bystander cells, however, the fraction of cells with 53BP1 foci increased more gradually, and the peak occurred at 12 hours with foci levels of 15.1%, 16.2% and 18.0%, followed by a decline at 24 hours. Similar results were observed post-exposure to iron ions. In the 3D studies, 53BP1 foci in Caco2 cells irradiated with 0.5 Gy and 1.0 Gy X-rays were higher than in control, reaching 26.5% and 50.8% at 5 hours, and dropped dramatically to control level thereafter. Nevertheless, 53BP1 foci in bystander cells not only were higher than in controls but also kept increasing until 12 hours when they were 14.5% and 18.3%, then recovered to control level at 24 hours. Hence, compared to monolayer culture, the fraction of cells with 53BP1 foci in irradiated 3D constructs appeared higher but there was no significant difference between levels in bystander cells.

Conclusions: Here we show that the bystander effect was observed in Caco2 cells in both monolayer culture and a 3D tissue model post-exposure to X-rays and charged particle irradiations. Although Caco2 cells appeared to be more radioresistant in 3D compared to monolayer culture, the bystander effect might be independent of culture method.

Poster Number 122

Martin, John BS
Graduate Student, Radiation Oncology
jmartin@steele.mgh.harvard.edu

Causes, consequences, and remedies for growth-induced solid stress in murine and human tumors

Investigators: Triantafyllos Stylianopoulos, PhD; John D. Martin, BS; Vikash P. Chauhan, PhD; Saloni R. Jain, BS; Benjamin Diop-Frimpong, PhD; Nabeel Bardeesy, PhD; Barbara L. Smith, MD; Cristina R. Ferrone, MD; Francis J. Hornicek, MD, PhD; Yves Boucher, PhD; Lance L. Munn, PhD; Rakesh K. Jain, PhD

The presence of growth-induced solid stresses in tumors has been suspected for some time, but these stresses were largely estimated using mathematical models. Solid stresses can deform the surrounding tissues and compress intratumoral lymphatic and blood vessels. Compression of lymphatic vessels elevates interstitial fluid pressure, whereas compression of blood vessels reduces blood flow. Reduced blood flow, in turn, leads to hypoxia, which promotes tumor progression, immunosuppression, inflammation, invasion, and metastasis and lowers the efficacy of chemo-, radio-, and immunotherapies. Thus, strategies designed to alleviate solid stress have the potential to improve cancer treatment. However, a lack of methods for measuring solid stress has hindered the development of solid stress-alleviating drugs. Here, we present a simple technique to estimate the growth-induced solid stress accumulated within animal and human tumors, and we show that this stress can be reduced by depleting cancer cells, fibroblasts, collagen, and/or hyaluronan, resulting in improved tumor perfusion. Furthermore, we show that therapeutic depletion of carcinoma-associated fibroblasts with an inhibitor of the sonic hedgehog pathway reduces solid stress, decompresses blood and lymphatic vessels, and increases perfusion. In addition to providing insights into the mechanopathology of tumors, our approach can serve as a rapid screen for stress-reducing and perfusion-enhancing drugs.

Poster Number 123

Ramsey, Haley PhD
Research Fellow, Wellman Center for Photomedicine
heramsey@partners.org

Loss of IEX-1 predisposes to therapeutically induced Myelodysplastic Syndrome

Investigators: Haley Ramsey, PhD; Qi Zhang, PhD; Mei Wu, MD, PhD

As the incidence of myelodysplastic syndromes (MDS) continues to rise alongside an aging population, few developments have been made towards a cure, possibly due to the heterogenic nature of the disease, complicating the development of empirical research models. MDS represents a progressive array of blood disorders, all of which are established within structural and functional mutations of hematopoietic stem cells (HSCs) and myeloid cells, however, the mechanism whereby these cells attain a high rate of mutations is largely unknown.

MDS may originate de novo or from therapeutic measures due to pre-existing cancer, such as alkylating agents or irradiation, thus called therapeutically induced MDS (tMDS), accounting for an increasing 10% of yearly diagnosed MDS cases. Currently, MDS patient data reveals high baseline levels of reactive oxygen species (ROS), a phenomenon questioned as having a bystander or causative role in MDS. As ROS have documented abilities to affect the homeostasis and genetic stability of HSC and myeloid precursors, one must question contribution of dysfunction of antioxidant genes in the genesis of tMDS.

Clinical studies have shown significantly decreased levels of immediate early responsive gene X-1 (IEX-1) in MDS patient HSCs. IEX-1 is a cell survival gene and targets mitochondrialF1F0-ATPase for degradation, thereby reducing ROS formation. In line with the "second hit leukemogenesis" theory, we believe that IEX-1 bone marrow (BM) with an already increased baseline of ROS, may be unable to assuage any further increase in ROS caused by therapeutic irradiation or other environmental agents.

With this in mind, we developed an inducible model of tMDS by subjecting our IEX-1 Knockout mice to 3 Gy of Total Body Irradiation (TBI), a non-myeloablative dose commonly used for therapeutics. It was found that the increased levels of ROS accompanying IEX-1 loss are heavily exacerbated by irradiation, leading to long-term decreased stem cell counts and progenitor function, accompanied by thrombocytopenia and paradoxal bone marrow hypercellularity alongside multiple dysplasias seen in MDS. The protective role of IEX-1 in the processes of thrombopoiesis and erythropoesis, through reduction of ROS, became further apparent as post irradiative treatment with MitoQ, a mitochondrial antioxidant, allowed for the return of normal platelet levels and red blood cell parameters in IEX-1 KO mice.

Through these data, we not only provide a novel and stringent model of murine inducible MDS, but also provide mechanistic detail on the roles of IEX-1 in thrombo- and erythropoesis. We find our IEX-1 KO mice excellent in the role of producing the first murine model of inducible tMDS, a model which could become a powerful asset to the field of MDS research.

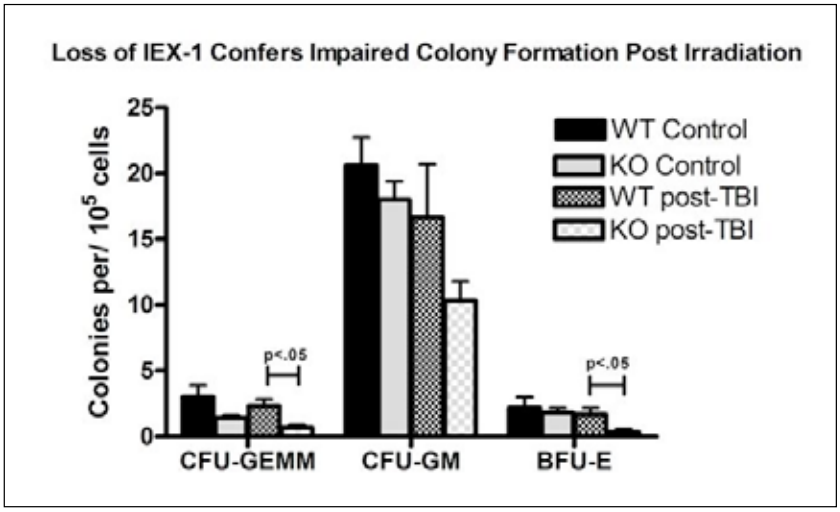

Poster Number 124

Sabbatino, Francesco MD
Research Fellow, Surgery
fsabbatino@partners.org

Targeting cancer initiating cells in pancreatic ductal adenocarcinoma

Investigators: Francesco Sabbatino, MD; Ravin Poudel, BS; Matteo Ligorio, MD; Yangyang Wang, MD; Xinhui Wang, MD, PhD; Soldano Ferrone, MD, PhD;Cristina R. Ferrone, MD

Even after surgical resection the 5 year overall survival of patients with pancreatic ductal adenocarcinoma (PDAC) is less than 20%. This clinical finding emphasizes the urgency to develop novel therapeutic strategies for PDAC. To be effective, a therapeutic strategy must eliminate not only differentiated PDAC cells but also PDAC cancer initiating cells (CICs). According to the cancer stem cell theory, CICs play a key role in disease recurrence and metastatic spread. Furthermore, an effective therapeutic strategy must target PDAC cells with multiple effector mechanisms in order to counteract the multiple escape mechanisms utilized by PDAC cells to avoid destruction. To this end, we have combined the recently developed human monoclonal antibody (mAb) W9 with LDE225, a novel oral available sonic hedgehog (SHH) pathway inhibitor, and with radiation. mAb W9 targets an extracellular epitope of the glucose-regulated-protein 94 kDa (Grp94), a member of the heat shock protein 90 family. This unique epitope is selectively expressed on malignant PDAC cells, including PDAC CICs. Our aim was to investigate in vitro whether mAb W9 in combination with LDE225 and radiation could eradicate PDAC differentiated cells as well as PDAC CICs.

The human PDAC2 cells were established in culture from ascites fluid of a metastatic PDAC patient. CICs were identified as aldehyde-dehydrogenase1A1 bright (ALDHbright) cells. The percentage of ALDHbright cells was determined by flow cytometry using the ALDEFLUOR kit. PDAC2 cells were treated with mAb W9 (10μg/ml), LDE225 (10μM), and/or radiation (20Gy). Following a 24 hour incubation, cells were stained with Annexin V/PI to determine the percentage of apoptotic cells by flow cytometry. The percentage of ALDHbright cells was determined after a 72 hour treatment. Lastly, the effect of mAb W9, LDE225 and/or radiation on signaling pathways associated with cell proliferation and survival was assessed by testing cell lysates with mAb in a western blot.

Treatment with mAb W9 enhanced the pro-apoptotic activity of LDE225 and radiation. Furthermore, the combination of mAb W9, LDE225 and radiation induced apoptosis to a significantly ($P<0.02$) greater extent than either one or two agents (Fig.1). Treatment of PDAC2 cells with mAb W9, LDE225 or radiation also significantly reduced the percentage of ALDHbright cells from the basal value of 11% to 7.4% ($p<0.02$), 7.1% ($p<0.02$) and 9% ($p<0.02$), respectively. The reduction in CICs was more marked when mAb W9 was combined with LDE225 (5.9%, $p<0.02$) or with radiation (5.8%, $p<0.02$). Lastly, mAb W9, LDE225 and radiation in combination decreased CIC percentage (1.2%) to a significantly ($P<0.02$) greater extent than one or two agents (Fig. 2). Western blot analysis demonstrated that treatment with mAb W9, LDE225 and radiation in combination inhibited posphorilated-ERK, posphorilated-AKT and GLI1 expression more than single or double agents.

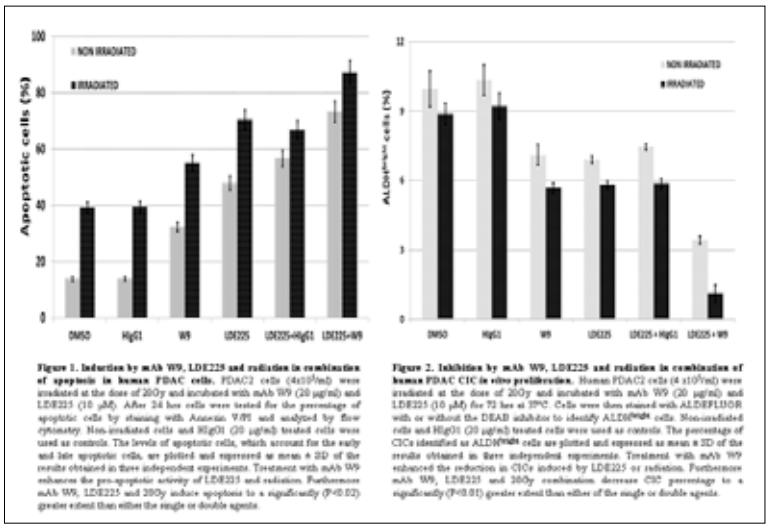

Figure 1. Induction by mAb W9, LDE225 and radiation in combination of apoptosis in human PDAC cells. PDAC2 cells ($4x10^5$/ml) were irradiated at the dose of 20Gy and incubated with mAb W9 (20 μg/ml) and LDE225 (10 μM). After 24 hrs cells were tested for the percentage of apoptotic cells by staining with Annexin V/PI and analyzed by flow cytometry. Non-irradiated cells and Hg01 (20 μg/ml) treated cells were used as controls. The levels of apoptotic cells, which account for the early and late apoptotic cells, are plotted and expressed as mean ± SD of the results obtained in three independent experiments. Treatment with mAb W9 enhances the pro-apoptotic activity of LDE225 and radiation. Furthermore mAb W9, LDE225 and 20Gy induce apoptosis to a significantly ($P<0.02$) greater extent than either the single or double agents.

Figure 2. Inhibition by mAb W9, LDE225 and radiation in combination of human PDAC CIC in vitro proliferation. Human PDAC2 cells ($4 x10^5$/ml) were irradiated at the dose of 20Gy and incubated with mAb W9 (20 μg/ml) and LDE225 (10 μM) for 72 hrs at 37°C. Cells were then stained with ALDEFLUOR with or without the DEAB inhibitor to identify $ALDH^{bright}$ cells. Non-irradiated cells and Hg01 (20 μg/ml) treated cells were used as controls. The percentage of CICs identified as $ALDH^{bright}$ cells are plotted and expressed as mean ± SD of the results obtained in three independent experiments. Treatment with mAb W9 enhanced the reduction in CICs induced by LDE225 or radiation. Furthermore mAb W9, LDE225 and 20Gy combination decrease CIC percentage to a significantly ($P<0.01$) greater extent than either of the single or double agents.

Our in vitro experiments demonstrate that mAb W9-based immunotherapy in combination with SHH pathway inhibitors and radiation effectively eliminate differentiated PDAC cells and PDAC CICs by modulating signaling pathways involved in proliferation, survival, and apoptosis. If corroborated by preclinical model results, they provide a strong rationale for the use of the described combinatorial strategy for PDAC treatment.

Poster Number 125

Sebastian, Carlos PhD
Research Fellow, Cancer Center
sebastian.carlos@mgh.harvard.edu

The Histone Deacetylase SIRT6, a novel tumor suppressor that regulates cancer cell metabolism

Investigators: Carlos Sebastián, PhD; Lei Zhong, PhD; Agustina d'Urso, B.S; Deborah Toiber, PhD; Dafne M. Silberman, PhD,; Jean-Pierre Etchegaray, PhD; Bárbara Martínez-Pastor, PhD; Claudia Cosentino, PhD; Sofia Giacosa, B.S; Jessica Truelove, PhD; Alex Guimaraes, MD; Raul Mostoslavsky, MD, PhD

Efficient glucose metabolism is critical for maintaining cellular viability. Under normal nutrient and oxygen conditions, glucose is converted to pyruvate, entering the mitochondria for oxidative phosphorylation and ATP production. Under hypoxia or nutrient stress, metabolism is switched to glycolysis, increasing lactate production and reducing mitochondrial respiration, a switch known to play an important role in cancer cells, as defined by Otto Warburg decades ago. Little is known whether chromatin plays a role in carbohydrate flux. The yeast Sir2 protein is an NAD-dependent histone deacetylase that senses the metabolic status of the cell and functions as a chromatin silencer to promote lifespan and genomic stability. Recently, we discovered that the mammalian SIRT6 is a chromatin factor that influences glucose metabolism and DNA repair. In mice, SIRT6-deficiency provokes a profound and lethal hypoglycemia that culminates in accelerated death. At the cellular level, SIRT6 inactivation leads to increased cellular glucose uptake, higher lactate production and decreased mitochondrial activity. Here, we show that SIRT6 deficient cells are tumorigenic and lead to tumor formation in SCID mice. Moreover, knock-down of pyruvate dehydrogenase kinase 1 (PDK1), a SIRT6-target gene and a key regulator of aerobic glycolysis, abrogates the tumorigenic properties of SIRT6 KO cells, indicating that SIRT6 suppress tumorigenesis by inhibiting glucose metabolism. Finally, we present some data showing decreased expression of SIRT6 in several human cancers. Together, all this data strongly indicates that SIRT6 is a novel tumor suppressor that regulates cancer cell metabolism.

Poster Number 126

Teng, Jian PhD
Research Fellow, Neurology Service
jteng@nmr.mgh.harvard.edu

Restoring sensitivity to temozolomide in orthotopic mouse glioblastoma model

Investigators: Jian Teng, PhD; Mark de Goojier, M.S.; Seyedali Hejazi1, MD; Bakhos A. Tannous, PhD

Glioblastoma multiforme (GBM) is the most common brain tumor and one of the most fatal and incurable cancers in humans. Current standard therapy for patients with newly diagnosed GBM includes maximal safe surgical resection, followed by a combination of radiation and chemotherapy with temozolomide (TMZ). Although this regimen is well tolerated and has been shown to provide modest clinical benefits, there has been little improvement in the survival of patients. A number of factors account for the poor response to therapy in the majority of patients, especially the intrinsic and/or acquired resistance against TMZ. GBM contains a population of cells that are suspected to be the origin of tumor. These stem-like cells can escape conventional treatments and contribute to tumor recurrence. Using a high-throughput screen setting based on Gaussia luciferase assay that was developed in our laboratory, we identified an FDA-approved compound having a strong sensitizing effect on TMZ in 4 sets of GBM cell lines (U87, U251, LNZ308, and HS683). Each set contains two different subpopulations of TMZ-resistant cells and the parent cells that the resistant cells were selected from. This hit was then validated in a panel of primary cultured GBM cells, as well as GBM stem-like cells grown in neurospheres (CSCs). The combination of this FDA-approved drug with temozolomide achieved a striking synergistic effect and effectively impaired the sphere formation ability of GSCs in vitro. We further investigated the mechanism of action and the signaling pathways involved in this combinational effect using microarray. This drug was found to inhibit the RRM2 subunit of ribonucleotide reductase, an enzyme involved in the reduction of ribonucleotides and induce the reduction of nicotinamide adenine dinucleotide (NAD+) and NAD phosphate (NADP+), to NADH and NADPH, respectively. This drug was also found to significantly inhibit -secretase, which activates Notch signaling pathway by releasing Notch intracellular domain (NICD) via intramembrane proteolysis.

This synergistic anti-glioma effect was then validated in vivo using an optimized orthotopic GBM xenograft model by transplanting a small number of FACS-purified CSCs into the brains of athymic mice. The FDA-approved compound was added to the regimen after tumors become resistant to TMZ treatment. Our study showed that this combination resulted in significant tumor recession (14±2% of control groups), revealed by monitoring the growth of implanted cells in live animals weekly using in vivo bioluminescence imaging. And the mice treated with combination of TMZ and this compound could survive significantly longer than those mice treated with only one drug (65 days on average versus 21, 27, 33 days in control, FDA-approved drug, and TMZ alone, respectively). We also found this compound promotes the penetration of TMZ across the blood-brain tumor barrier in tumor-bearing mouse pharmacokinetics models. Taken together, our study suggests that this FDA-approved small-molecule can be used to effectively restore the sensitivity to temozolomide in GBM models. These results are readily translatable to clinical trial and offer the potential for improved treatment outcomes for patients with glioblastoma.

Poster Number 127

Wheat, Justin BS, BA
Research Technician, Cancer Center
jwheat@partners.org

TLE4: A Principle Regulator of Both Normal Hematopoiesis and Leukemogenesis

Investigators: Justin C Wheat, BS, BA*; Daniela S. Krause, MD, PhD*; Jianfeng Wang, MD, PhD; Xi Chen, MD, PhD; and David Sweetser, MD, PhD

Our group had previously identified Transducin-like/Enhancer of Split 4 (TLE4), as a novel tumor suppressor gene suppressor lost in a subset of t(8:21) AML patients also harboring 9q deletion. The Tle/Groucho proteins are considered master developmental regulatory genes in Drosophila, controlling a variety of signaling pathways affecting cell fate decisions. However, the role of this gene family in vertebrate development and cancer has been poorly studied. TLE4 is known to interact with multiple highly conserved transcriptional complexes, including Hes1, Tcf/Lef, CSL, Runx1-3, and Pax5, all of which have been shown to be intimately connected to normal steady state hematopoiesis and deregulated in malignancy. Owing to its deletion in leukemia and its ability to confer functionality to a variety of signaling networks, our lab sought to investigate its role in hematopoiesis by generating a murine knockout model for Tle4.

While normal at birth, within 2-3 weeks of age knockout (KO) mice become runted and eventually moribund, with significant atrophy of the spleen and thymus and a litany of bone maturation defects. These mice also have a gradual clearing of the bone marrow itself, with 2 week old animals first showing evidence of cytopenia that then progresses to full marrow failure by 3-3.5 weeks of age. Through both transplant studies and in vitro assays, we have clearly illustrated roles for Tle4 in both cell intrinsic and extrinsic regulation of normal hematopoiesis. Fluorescence Activated Cell Sorting reveals striking alterations within mature white cell populations, particularly in the B lymphocyte lineage. Intriguingly, KO mice show severe reductions in the number of common lymphoid progenitors, cells at the first checkpoint of lymphocyte development from hematopoietic stem cells, while those cells committed to the myeloid lineage remain unaffected. Moreover, we show that hematopoietic stem cells derived from KO animals are able to induce a myeloproliferative disease spontaneously in transplanted animals. These parallel findings are incredibly exciting, as Tle4 knockout mice may delineate novel and sophisticated mechanisms of how hematopoietic stem cells fate decisions and leukemia development may intersect along common pathways and signals.

The unique spectrum of phenotypic consequences concomitant to Tle4 deletion argues for a complex yet fundamental role in the maintenance of the hematopoietic niche. Our work on Tle4 confirms the growing body of literature supporting the notion that hematopoiesis and lineage commitment are regulated in a heterotypic manner with interactions between the hematopoietic stems cells and their niche. Tle4, with its direct involvement in multiple highly conserved signaling pathways, offers an important addition to that paradigm. Considering its principal role in those pathways, continued efforts to investigate the function of the TLE family of corepressors may prove vital in reworking our understanding of how both normal hematopoiesis and leukemogenesis arise in the complex, multicellular compartment of the bone marrow niche.

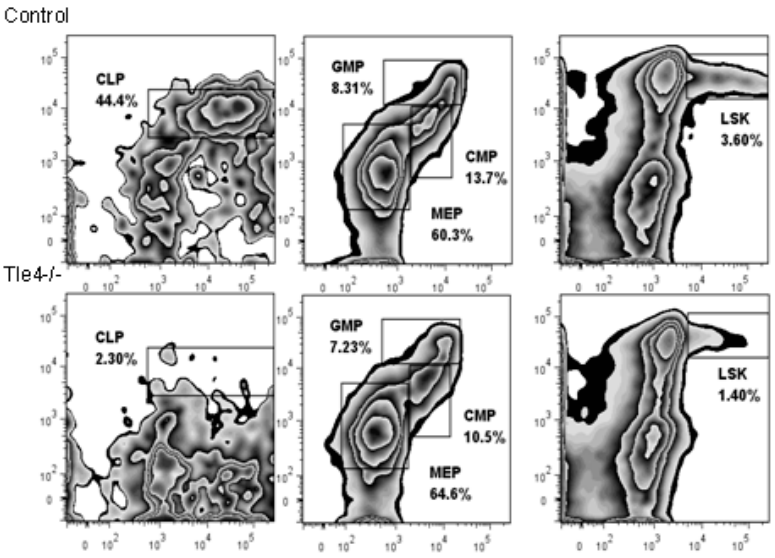

*These Authors Contributed Equally To This Work

Poster Number 128

Yang, Katherine PhD
Research Fellow, Center for Systems Biology
yang.katherine@mgh.harvard.edu

Single-cell and subcellular pharmacokinetic and pharmacodynamic imaging allows insight into drug action in vivo

Investigators: Katherine S. Yang, PhD*; Greg M. Thurber, PhD*; Thomas Reiner, PhD; Rainer H. Kohler, PhD; Peter Sorger, PhD ;Tim Mitchison, PhD; Ralph Weissleder, MD, PhD

Pharmacokinetic and pharmocodynamic analysis at the organ level provides insight into how drugs distribute throughout the body and affect tumor growth. However, most current methods do not have single cell or subcellular resolution, which ultimately is necessary to understand how drugs work and fail at the target level. Here we have developed tools for in vivo single cell pharmacokinetic and pharmacodynamic analyses of drugs and to model drug behavior under different conditions. We applied this approach to investigate the behavior of a promising class of drugs currently in clinical trials, PARP1 inhibitors (PARPi). Single-cell pharmacokinetic imaging (SCPKI) revealed for the first time a) the real-time intracellular kinetics of the model PARPi distribution, b) that the PARPi reached its cellular target compartment (the nucleus) within minutes in vivo and c) that it showed little distinction between cancer and host cells in different cancer models. Combined theoretical and experimental data indicates that tumor cells are exposed to sufficiently high PARPi concentrations (predicted both in mouse and humans with quantitative simulations despite microvascular heterogeneity), and provided evidence that failure observed in clinical trials is more likely related to proteomic heterogeneity or lack of cellular sensitivity mechanisms such as synthetic lethality with DNA repair lesions. Single-cell pharmacodynamic imaging (SCPDI) of a truncated 53BP1 DNA repair reporter is currently being developed to address the contribution of synthetic lethality to PARPi success and failure in breast, ovarian, and Ewing's sarcoma tumors. We believe that SCPKI and derived modeling combined with SCPDI can provide valuable information essential in understanding drug action at single cell resolution in vivo.

*These authors contributed equally to this work

Poster Number 129

Burns, Sean M. MD
Research Fellow, Molecular Biology
smburns@partners.org

High-Throughput Assays of Hormone Secretion Using Novel Propeptide-Luciferase Fusion Proteins

Investigators: Sean M. Burns, MD; Amedeo Vetere, PhD; Deepika Walpita, PhD; Vlado Dančík, PhD; Bridget K. Wagner, PhD; David Altshuler, MD, PhD

Peptide hormones regulate metabolism and play key roles in common disease, and insight into the pathways controlling their secretion could potentially inform drug development. However, high-throughput genetic and chemical screens of hormone secretion have historically been unfeasible due to a lack of suitable functional readouts. To overcome this bottleneck, we developed a series of luminescent hormone secretion reporters by internally fusing Gaussia luciferase within the precursor peptides of several key metabolic hormones. Luciferase was placed within inert portions of each prohormone, flanked by cleavage sites normally involved in prohormone maturation. Upon expression of each fusion protein in a relevant cell type, luciferase travels through the regulated secretory pathway, undergoes cleavage within the secretory vesicles and is co-secreted with mature hormone. To date, we have used this approach to track the secretion of insulin, amylin, glucagon and glucagon-like peptide-1 (GLP-1). In each case, we validated luciferase secretion as a close proxy for hormone secretion, with enzyme activity responding appropriately to known secretagogues and in tight correlation with hormone concentration as measured by ELISA. We adapted these reporters for high-throughput 384-well assays and applied our insulin secretion reporter in a proof-of-principle 1600-compound screen to identify novel glucose-dependent insulin secretagogues, including several with activity in human pancreatic beta cells. Our method is 50-fold faster and cheaper than standard ELISAs and may be generalizable to other disease-relevant secretory proteins, including hormones (e.g., PYY, ghrelin, PTH), cytokines (e.g., IL1B, TNFA, IFNG), growth factors (e.g., TGFB, PDGFA, NGF) and neuropeptides (e.g., proenkephalin, BDNF). In summary, propeptide-luciferase fusion reporters offer a fast, inexpensive and scalable approach for investigating disease-relevant regulatory pathways and for identifying small molecules to modulate protein secretion for therapeutic benefit.

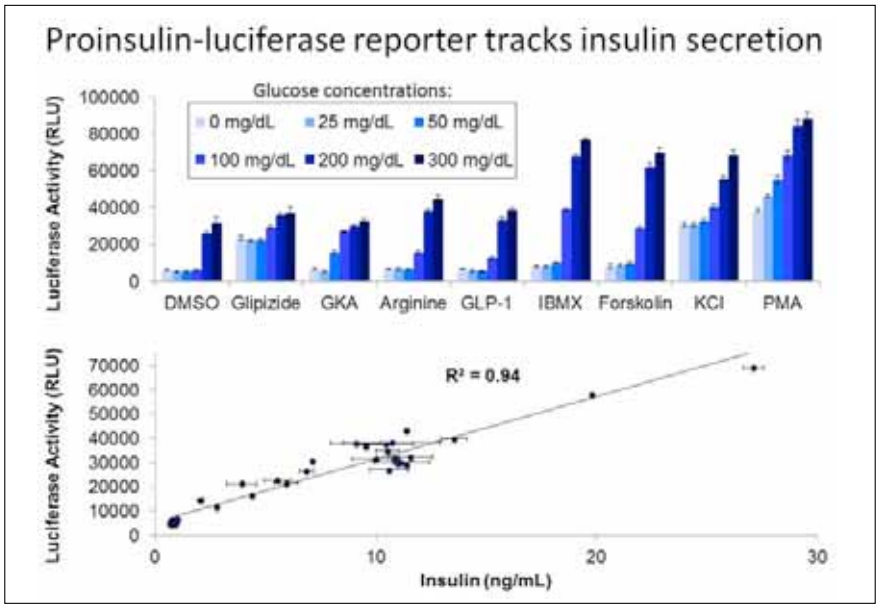

Poster Number 130

Dai, Ning PhD
Instructor, Molecular Biology
ning@molbio.mgh.harvard.edu

The function of IMP2 in metabolism

Investigators: Zhao Liping, PhD; Diedra Writing, PhD; David Altshuler, PhD, MD; Joe Avruch, MD

Susceptibility to Type 2 diabetes mellitus (T2DM) is strongly influenced by both environmental and genetic factors. Genome-wide association studies have identified single nucleotide polymorphisms (SNPs) in over 40 genes that are found more frequently in individuals with T2DM and encode elements that may influence risk for T2DM. One of the genes consistently identified to contain SNPs associated in excess with T2DM encodes IGF2 mRNA binding protein 2 (IMP2). The expression of IMP2 in the mouse embryo turns on at E10.5 and embryonic expression of IMP2 is largely extinguished by E16.5. However, the expression of IMP2 is widespread in the adult mouse such as pancreas, liver, fat and muscle. We examine the consequences of genetic inactivation of IMP2 expression in the mouse. IMP2 deficient mice appear normal up through weaning, but are slightly smaller and considerably leaner than wild type littermates in the rest of their lives. They gain much less weight on both NCD and HFD despite comparable intake, exhibit increased energy expenditure and remain insulin sensitive and glucose tolerant.

Poster Number 131

Economopoulos, Konstantinos MD
Research Fellow, Surgery
keconomopoulos@partners.org

Prevention of Antibiotic-Associated Obesity in Mice by Intestinal Alkaline Phosphatase

Investigators: Konstantinos P. Economopoulos, MD; Rizwan Ahmed, MD; Shahrad Hakimian, BA; Omeed Moaven, MD; Kanakaraju Kaliannan, MD; Abeba Teshager, BA; Sayeda N. Alam, MD; Nur Muhammad, MD; Sulaiman R. Hamarneh, MD; Seyed Abtahi, MD; Mussa M. Rafat Mohamed, MD; Palak Patel, BA; Atul K. Bhan, MD; Madhu S. Malo, MD; Richard A. Hodin, MD

Introduction: The administration of antibiotics in childhood is associated with increased rates of obesity in adult life, maybe through changes in gut microbiota composition. Intestinal alkaline phosphatase (IAP) maintains normal gut microbial homeostasis. We aimed to examine whether co-administration of IAP with antibiotics early in life may have a preventive role against obesity in mice

Methods: Groups of four-week old, C57BL/6 male mice (n=6-10) were treated with azithromycin (50 mg/kg/day) ± oral IAP (100 units/ml drinking water), and with no antibiotic ± IAP for three intermittent cycles. After the last course, the mice were administered regular diet for five weeks and subsequently were fed high-fat diet (HFD) for five weeks. Body weight and food intake were monitored weekly. Data were expressed as mean ± standard error and were analyzed by one-way analysis of variance with Tukey's multiple comparison post-tests. A significant difference was considered when $p<0.05$.

Results: The azithromycin-treated mice gained significantly more weight compared with the controls during the HFD period (10.9±0.49 vs 5.2±1.13 g; $p<0.001$). Food intake was similar among the groups ($p=0.849$). Azithromycin+IAP compared with the azithromycin only-treated group was associated with significantly less weight gain (4.7±1.15 vs 10¬.9±0.49 g; $p<0.001$), less visceral (1.5±0.35 vs 3.2±0.28 g; $p=0.001$) and subcutaneous fat weight (0.8±0.33 vs 2.1±0.24 g; $p=0.003$), fasting blood glucose levels (147.2±11.15 vs 241.5±22.83 mg/dl; $p=0.023$) and liver oil-red-O staining scores (2.7±0.20 vs 3.96±0.04, $p=0.002$) during the HFD period.

Conclusions: Co-administration of IAP with azithromycin early in life of mice could protect them from antibiotic-associated obesity in adult life. Oral IAP supplementation during antibiotic exposure may represent a novel therapeutic strategy to prevent antibiotic-associated obesity in humans.

Gillooly, Caitlin BS
Research Technician, Radiology
cgillooly@partners.org

Poster Number 132

Qualitative assessment of CSF drainage to the lymphatic system using Positron Emission Tomography in rats and nonhuman primates

Investigators: Caitlin Gillooly, BS; Vasily Belov, PhD; Elena Belova, PhD; Matthew Gagne, BA; James Titus; Mikhail Papisov, PhD

The cerebral spinal fluid (CSF) provides protection to the organs of the central nervous system (CNS). Furthermore, it can be an important drug delivery route to treat pathological conditions that involve the brain, spinal cord and meninges, such as neurodegenerative diseases, enzyme deficiencies, and cancer. In order to develop effective treatments for these diseases, it is necessary to understand the biokinetics of drugs after intra-CSF administration. This includes discovering the pathways by which drug molecules exit the leptomeningeal space and enter systemic circulation. Current literature suggests micron-range pores in arachnoid granulations as a primary pathway for CSF transfer directly into the blood. The clearance of drugs from the CSF through lymphatic uptake was also proposed; however, the extent and mechanism of this drainage is still widely debated and requires further investigation. Thus, the goal of the present study was to provide both qualitative and quantitative description of lymphatic uptake after intrathecal administration of radiolabeled test molecules in rats and nonhuman primates.

We administered various radiolabeled proteins and nanoparticles into the CSF of rats and nonhuman primates using surgically installed catheters in the lumbar spinal region. Using Positron Emission Tomography (PET), we assessed the extent of lymphatic drainage from the CSF using protein and particle uptake in the lymph nodes as a drainage marker. Our data indicates only minor uptake in the lymphatics, mainly in cervical lymph nodes, though differences appear across species. In rats, the total lymphatic uptake was much higher (4.3±2.0%ID, n=9) than in primates (0.27±0.20%ID, n=9), four hours after administration. However, the total amount accumulated in the nodes of both species was much less than some previously reported data would suggest. In primates, there does not appear to be any lymphatic drainage from the spinal CSF, with only minor lymphatic drainage from the cranial cavity. The literature suggests this drainage likely occurs through the cribiform plate and/or in the cervical nerve routes. Overall, our findings suggest that CSF drainage directly to the blood is the main pathway by which the vast majority of particles exit the CSF into systemic circulation. Additionally, the lymphatic route is insignificant physiologically and pharmacologically, at least in higher mammals, though it may facilitate the immune response to CSF-borne antigens.

Poster Number 133

Ran, Chongzhao PhD
Instructor, Radiology
cran@nmr.mgh.harvard.edu

Curcumin derivatives as imaging probes for interscapulae brown adipose tissue

Investigators: Xueli Zhang, BS; Hongbin Zhang, PhD; Yu-Hua Tseng, PhD; Anna-Liisa Brownell, PhD; Anna Moore, PhD; Chongzhao Ran, PhD

Brown adipose tissue (BAT), known widely as a 'good fat', has recently re-emerged as a target for research in a variety of diseases. BAT levels inversely correlate with body-mass index, particularly in the aged population, suggesting its potential role in obesity and diabetes of adults. PET imaging with 18F-FDG is currently the most commonly used method for visualizing BAT. However, stimulation of BAT by cold exposure or drug pretreatment is needed to obtain reproducible PET images. Through screening of a small library of fluorescent probes, we found that BAT can be imaged with curcumin derivatives using near infrared (NIR) optical imaging. One of the probes, CRANAD-2, clearly labeled the interscapular BATs in mice at 60 min after injection. By introducing an 18F and a minor structural modification, CRANAD-2 was then adapted into a PET probe. Both optical and PET images indicated that CRANAD-2 and its 18F analogue had high specificity towards BAT in mice. We also showed that spectral unmixing could be used to dissect fluorescence signals from BAT, WAT (white adipose tissue) and skin. In addition, we demonstrated that the selected probe could be used for monitoring the activation of BAT by norepinephrine treatment. The advantage of our probe is that no stimulation/pretreatment is needed. We believe our probe will be a very useful tool for imaging BAT.

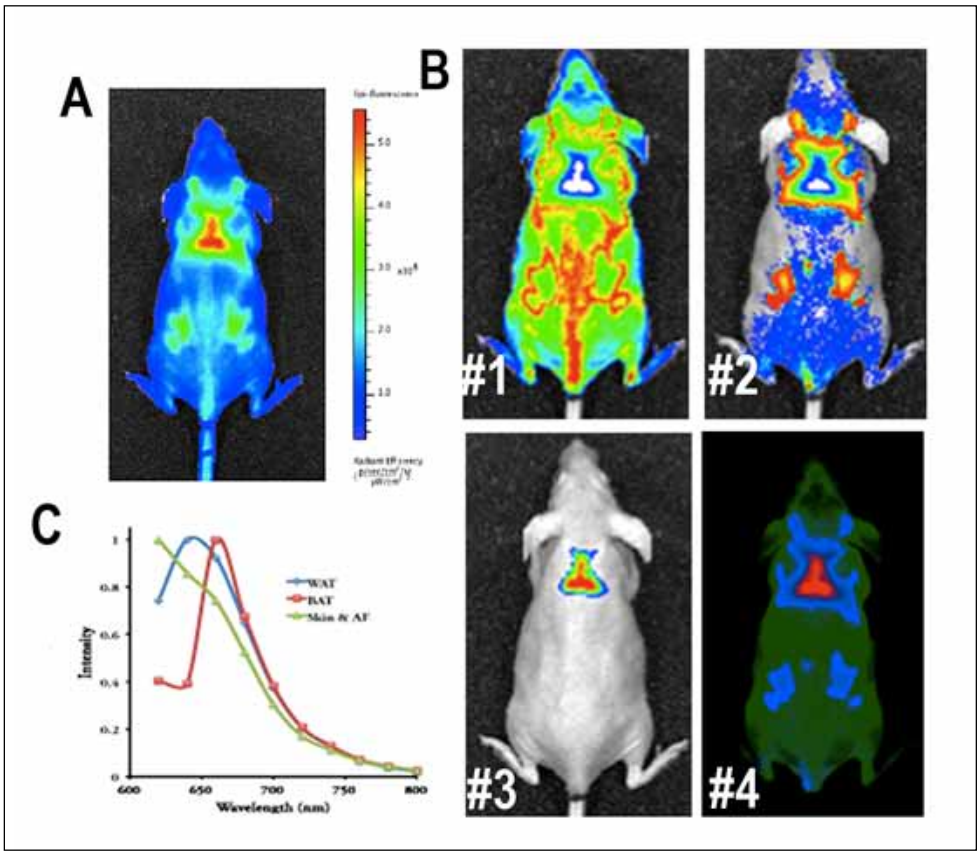

Poster Number 134

Sun, Chia Chi PhD
Research Fellow, Medicine
sun.chiachi@mgh.harvard.edu

A validated elisa for quantitating human serum hemojuvelin

Investigators: C.C. Sun[1]; W. Chen[1]; O. Gutierrez[2]; A. Pietrangelo[3]; J.L. Babitt[1]; H.Y. Lin[1]
[1]Program in Anemia Signaling Research, Division of Nephrology, Program in Membrane Biology, Massachusetts General Hospital, Harvard Medical School, Boston, MA, USA. [2]Division of Nephrology, Department of Medicine, University of Alabama at Birmingham, Birmingham, Ala, USA. [3]Laboratory of Hereditary and Metabolic Diseases of the Liver, "Mario Coppo" Liver Research Center, University Hospital of Modena and Reggio Emilia, Modena Italy

There is currently a clinical challenge in assessing the iron status of anemic patients with chronic kidney disease (CKD) and hemodialysis (HD) patients, and in those with anemia of chronic disease (ACD). These patients often have high serum ferritin levels, suggesting iron overload, but low transferrin saturation levels, suggesting iron deficiency, causing a dilemma for clinicians to determine whether intravenous iron should be administered to manage the anemia. Current clinical tools such as serum ferritin and transferrin saturation are insufficient in their differential diagnosis of true iron deficiency in these patients. Thus, new markers for iron status are needed and would be useful to guide iron therapy in these patients.

Hemojuvelin (HJV/RGMc/HFE2) is a glycosylphosphatidylinositol-linked (GPI) membrane bound protein expressed on hepatocytes that is required for maintaining systemic iron homeostasis. Membrane bound HJV can be released to generate soluble forms of HJV by proteases in vitro. It is thought that serum soluble HJV (sHJV) functions to inhibit expression of the main regulator of iron homeostasis, hepcidin.

Recent studies have suggested the utility of soluble hemojuvelin (sHJV) as a biomarker for iron deficiency in iron deficient-diet fed rodents and in human patients with anemia of chronic disease and anemia of chronic kidney disease. Assessing whether circulating sHJV has a role in physiology and in regulating hepcidin and iron status in humans requires a reliable validated sHJV assay.

We have developed a novel, specific and reliable two-site ELISA to measure sHJV concentrations in human serum. Our laboratory characterized a novel monoclonal anti-HJV antibody (C2G4), which we used as capture antibody and a polyclonal anti-HJV (RGMc) antibody (R&D Systems) as detection antibody. Our HJV ELISA has a low background and in contrast to the commercially available HJV ELISA, our assay can specifically detect human recombinant HJV/RGMc (R&D Systems) but not the closely related human RGMa or RGMb proteins (Figure 1 A, B). It was also able to detect sHJV in conditioned media from cells transfected with human HJV cDNA (Figure 1 C, D). Furthermore, as a negative control and to set the baseline, we validated the assay using serum from a HJV-null (G171R HJV mutation) patient. The lower limit of detection (LLOD) of our assay in human serum was 9 ng/mL. Our HJV-null patient sample was undetectable while serum from our normal healthy volunteers had measured sHJV levels ranging from 58 to 218 ng/mL, averaging 48 + 62 ng/mL (Figure 1 E). Thus, our two-site assay has improved sensitivity and specificity for sHJV in humans. Measurement of sHJV may provide insight into the physiological role of sHJV in hepcidin and iron regulation and may be useful to determine iron status in humans.

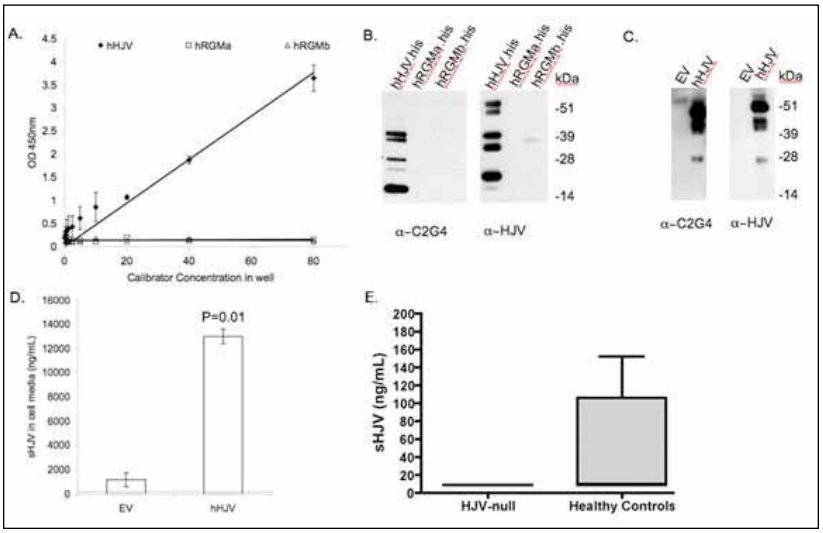

Poster Number 135

Tomas, Eva PhD
Instructor, Medicine
etomas-falco@partners.org

GLP-1-Derived Pentapeptide GLP-1(32-36)amide Increases Basal Energy Expenditure and Attenuates the Development of Obesity and Diabetes in Diet-Induced Obese Mice

Investigators: Eva Tomas, PhD; Violeta Stanojevic, M.S.; Rebecca R. Laudone, BS; Joel F. Habener, MD

Type 2 diabetes is associated with hyperinsulinemia and insulin resistance leading to elevated hepatic glucose production, hyperglycemia, and hyperlipidemia. Infusions of the C-terminal pentapeptide LVKGRamide, GLP-1 (32-36)amide, derived from glucagon-like peptide-1 (GLP-1), in high fat diet-induced obese mice for sixteen weeks curtailed the rate of weight gain as early as five weeks. At the end of the sixteen week infusion, body weights of mice infused with GLP-1(32-36) amide were decreased by 50% compared to vehicle control that correlated with a 40% decrease in fat mass with no significant difference in lean mass. Indirect calorimetric studies showed that in mice infused with GLP-1(32-36)amide the rate of oxygen consumption was significantly higher compared to vehicle control throughout the light and dark cycles, without differences in physical activity. These findings are consistent with an increase in basal energy expenditure. Moreover, GLP-1(32-36)amide attenuated the development of diabetes in high-fat fed mice since both plasma glucose and insulin were decreased close to values obtained in mice fed a control diet. Triglyceride levels in plasma and livers of peptide-treated mice were decreased to levels equivalent to triglyceride levels in control mice fed a low fat diet. These findings suggest a potential role for the C-terminal pentapeptide, GLP-1(32-36)amide, in the improvement of obesity-related diabetes, insulin resistance and hepatic steatosis. The pentapeptide might prove to be useful for the treatment of insulin resistance and metabolic syndrome.

Poster Number 136

Zhong, Lei PhD
Research Fellow, Cancer Center
lzhong@partners.org

The histone deacetylase SIRT6 is a critical modulator of transcription elongation in Metabolism

Investigators: Lei Zhong, PhD; Carlos Sebastian, PhD; Deborah Toiber, PhD; Dafne Silberman, PhD; Barbara Martinez, PhD; Jean-Pierre Etchegaray, PhD; Claudia Cosetino, PhD; Sofia Giacosa, BS; Raul Mostoslavsky, MD, PhD

Transcription is one of the most essential biological processes of all organisms. It consists of several highly regulated steps: initiation, pausing, elongation and termination. Multiple transcriptional factors are involved at each step. Uncontrolled transcription often leads to various diseases, such as diabetes and cancer. Although many transcriptional factors have been identified, gaps and holes still remain in our knowledge of transcription regulation.

SIRT6 is a member of the mammalian Sirtuin protein family. SIRT6-deficiency provokes pronounced genomic instability and metabolic defects resulting in profound hypoglycemia. Our previous work has demonstrated that SIRT6 is a master regulator of glucose metabolism, by repressing transcription of key genes in glycolytic pathway. However, the precise role SIRT6 plays in transcription regulation is largely unexplored. For example, how the presence of SIRT6, a histone deacetylase, affects the dynamics of transcription factors during transcription regulation is still unclear.

Here we present several lines of evidence that SIRT6 regulates transcription pausing and elongation steps. First, ChIP-Seq data show that SIRT6 resides on both the promoter regions and the intragenic regions of a large number of genes. Second, SIRT6 physically interacts with several key transcription factors, such as RNA polymerase II. Third, SIRT6 regulates the recruitment of NELF-E, a negative transcription factor, to the promoters of its target genes, thus promoting transcription repression. Under nutrient scarce conditions, inactivated SIRT6 allows NELF-E to be removed from the transcription complex and subsequent successful elongation.

It is the first time that a histone deacetylase is demonstrated to specifically modulates the transcription elongation. The knowledge gained from our study will give us a clearer picture of how transcription is regulated, especially with changes of nutrient availability. It is also expected to give us new pharmaceutical tools to fight diseases such as diabetes and cancer.

Poster Number 137

Fusco, Dahlene MD,PhD
Instructor, Medicine
dnfusco@partners.org

Identification of Interferon Alpha Effector Genes as New Targets for Antiviral Development Background and Rationale

Investigators: Dahlene N. Fusco, MD, PhD; Cynthia Brisac, PhD; Yi-Wen Huang, MD; Tiao Xie, MD; Hong Zhao, MD; Esperance Schaefer, MD, MPH; Pattranuch Chusri, BS; Nikolaus Jilg, MD; Du Tran MD, PhD; Lei Zhao, MD; Leiliang Zhang, PhD; Wenyu Lin, PhD; Lee Peng, MD, PhD; Abraham Brass, MD, PhD; Raymond T. Chung, MD

There is limited available treatment for most clinically relevant viruses. Interferon alpha (IFNa) is one of the broadest acting antivirals known. Agents that enhance the IFNa response may provide broad acting antiviral effects. However, identification of IFNa-enhancing agents has been limited by incomplete understanding of the mechanism of IFNa antiviral activity. Identification of the mechanism of IFNa antiviral activity has been limited by the lack of tools to systematically evaluate the hundreds of IFN-effector genes (IEGs) required for these antiviral effects. To systematically identify mediators of IFN's antiviral effects, we developed a high-throughput screening assay using an image based screening platform and fully infectious JFH1 HCV. Using this functional genomic approach, we performed a whole genome siRNA screen for anti-HCV IEGs.

Methods: Huh 7.5.1 hepatocytes are plated in 384 well plates and transfected with siRNA. 2d later, cells are treated with 100 IU/ml of IFNa. 1d later, cells are inoculated with JFH1 HCV. 2d post-infection, cells are stained with HCV core antibody and Hoechst nuclear stain, then imaged using an automated microscope to determine percent infected cells (Fig.1). Rescue from IFNa treatment is scored as 2-fold increase in percent infection above plate mean. Our positive control for IFN rescue, IFNa receptor 1 (IFNAR), rescues ~50% of HCV replication from IFNa suppression, and our negative control, non-targeting (NT3), does not rescue HCV from IFN compared to plate mean (Fig.1).

Results: Here we have identified several known HCV IFN stimulated genes (eg TYK2, ISGF3G) as well as previously unknown interferon effector genes, including P285, ALG10, and MYST1, as essential components of the IFNa mediated suppression of HCV. IFN stimulation analysis reveals that P285 is upregulated at the mRNA level by IFNa, but ALG10 and MYST1 are not. In addition, these genes appear to rescue HCV from IFNa at multiple steps of the HCV lifecycle. These results indicate that both IFNa stimulated genes (ISGs) and non ISGs are essential for the complete antiviral effects of IFNa. These candidate host factors, or IEGs, may be useful as a platform for novel antiviral design or to inform studies of host variation in antiviral defense.

Poster Number 138

Sha, Ky PhD
Research Fellow, Mass General Hospital *for* Children
ksha@partners.org

Transposon Mutagenesis Screen to Identify and Characterize Host-Encoded Antiviral Pathways

Investigators: Ky Sha, PhD; Li Chen, PhD; Marshall Karpel, BS; Adam Lacy-Hulbert, PhD; Lynda Stuart, MD, PhD

Ebola and Lassa viruses cause severe hemorrhagic fevers with high mortality rates. They are also potential bioterrorism threats. Despite their classification as Category A pathogens by the NIAID, our knowledge of how these viruses usurp host cells to complete their life cycles is limited. A better understanding of the host cellular machinery essential for these viruses to complete their life cycles would provide potential downstream therapeutic targets. Based on emerging data and our own preliminary studies, we hypothesize that host cells encode factors whose upregulation confers anti-viral immunity. Called restriction factors, such host-encoded factors could act to prevent virus entry into the host and/or prevent the virus from usurping the host cellular machinery.

To identify host restriction factors, we have adapted a transposon mutagenesis screening strategy that our lab previously developed and used successfully to identify chemotherapy drug resistance genes in cancer cells. Our strategy entails transposon mutagenesis of host cells using a modified version of the piggyBac transposon, followed by identification of virus-resistant cells. Candidate genes are transposon-tagged and are readily identified through sequencing. Here, we show that our method is an effective strategy to identify restriction factors. Transposon insertion is random and extensive, providing an unbiased genome-wide search for restriction factors. An initial screen has identified a handful of candidates (listed in poster body) in human A549 cells that confer resistance to vesicular stomatitis virus pseudotyped with the Ebola virus surface glycoprotein (Ebo-VSV). We continue to expand our screen on additional cell lines (Hec-1B, U2OS, and THP1), using Ebo-VSV as well as VSV pseudotyped with the Lasso virus glycoprotein. We will validate and characterize candidate genes to gain insights into host anti-viral pathways, with the hope that our work will provide starting points for the identification of therapeutics that promote host-encoded anti-viral immunity.

Poster Number 139

Abramowicz, Shelly DMD, MPH
Instructor, Oral and Maxillofacial Surgery
shelly.abramowicz@childrens.harvard.edu

Clinical Findings Associated with Active Temporomandibular Joint Inflammation in Children with Juvenile Idiopathic Arthritis

Investigators: Shelly Abramowicz, DMD, MPH; Harlyn Susarla, MPH; Susan Kim, MD, MMSc; Leonard B. Kaban, DMD, MD

Purpose: To identify clinical findings associated with active temporomandibular joint (TMJ) inflammation (i.e. synovitis) in children with juvenile idiopathic arthritis (JIA).

Patients and Methods: This was a retrospective study of children with JIA. Patients were included if they had confirmed diagnosis of JIA and had Magnetic Resonance Imaging (MRI) with contrast of TMJs. Medical records and imaging studies were reviewed to document demographic, clinical (facial asymmetry, joint noises, maximal incisal opening (MIO), deviation, excursions, occlusal cant), and MRI findings. Outcome variable was TMJ synovitis on MRI. Descriptive and bivariate statistics were computed. Multiple regression models were used to identify associations ($p < 0.05$ significance).

Results: There were 43 subjects with a mean age of 11.4 years who met inclusion criteria. Most common clinical findings were: limited MIO (N=29 subjects), facial asymmetry (N=15), deviation on MIO (N=10), joint noises (N=9), and occlusal cant (N=7). MRI demonstrated presence of synovitis in 27 patients. Limited MIO and deviation on opening were significantly associated with synovitis on MRI ($p=0.003$, 0.043, respectively). In a multiple regression model, subjects with limited MIO were 6.7 times more likely to have synovitis. Among subjects with limited MIO, deviation on opening was associated with presence of synovitis.

Conclusion: Results of this study indicate that in children with JIA, limited MIO and deviation on opening are indicative of TMJ synovitis. Measurement of MIO and deviation on opening should be an essential part of clinical exam and longitudinal follow up of children with JIA.

Poster Number 140

Battey, Thomas BS
Research Technician, Center for Human Genetic Research
battey@chgr.mgh.harvard.edu

FLAIR Ratio is a novel imaging biomarker for cerebral edema in stroke: Preliminary effect of RP-1127 in the GAMES-Pilot Trial

Investigators: Thomas Battey, BS; Hannah Irvine, BA; Albert Yoo, MD; Aneesh Singhal, MD; Kevin Sheth, MD; W. Taylor Kimberly, MD, PhD

Background: Malignant cerebral edema is a common complication following large ischemic stroke, conferring high morbidity and mortality on those affected. We sought to identify an imaging surrogate for cerebral edema in the GAMES-Pilot trial (NCT01268683), which evaluated the safety and feasibility of RP-1127 (glyburide for injection) in preventing cerebral edema following large ischemic stroke.

Methods: A quantitative signal intensity ratio on T2 fluid-attenuated inversion recovery (FLAIR) MRI sequence was developed. The region of interest (ROI) of the stroke was outlined and normalized to the unaffected contralateral hemisphere for each subject. We evaluated MRIs at acute presentation, 30 hours after stroke onset and 60 hours after stroke onset in GAMES-Pilot subjects (n=10) and historical controls (n=8) with similar stroke volume. The stroke ROI was also segmented into gray and white matter to explore the effect of study drug on these neuroanatomical regions.

Results: The acute FLAIR ratio was similar between the GAMES-Pilot and control cohorts at baseline, prior to initiation of study drug. At about 30 hours after stroke onset, the FLAIR ratio was 1.46 + 0.22 in GAMES-Pilot versus 1.81 ± 0.23 in controls (p = 0.003). This difference persisted at 60 hours after stroke onset, where GAMES-Pilot subjects had a FLAIR ratio of 1.56± 0.22 and controls 1.84± 0.11 (p=0.009). Segmentation of the stroke ROI into gray and white matter regions yielded similar results (gray matter in GAMES-Pilot: 1.60 ±0.24; Controls: 1.89± 0.13; p = 0.029), while there was a trend towards a difference in white matter (GAMES-Pilot: 1.47± 0.20; Controls: 1.66 ± 0.09; p =0.053).

Conclusions: Here, we show that the FLAIR ratio defined on MRI differs between cases and controls following acute stroke. FLAIR imaging is sensitive to tissue edema and this new quantitative imaging biomarker may provide further insight into both the development of cerebral edema as well as the mechanism of action of RP-1127 following ischemic stroke.

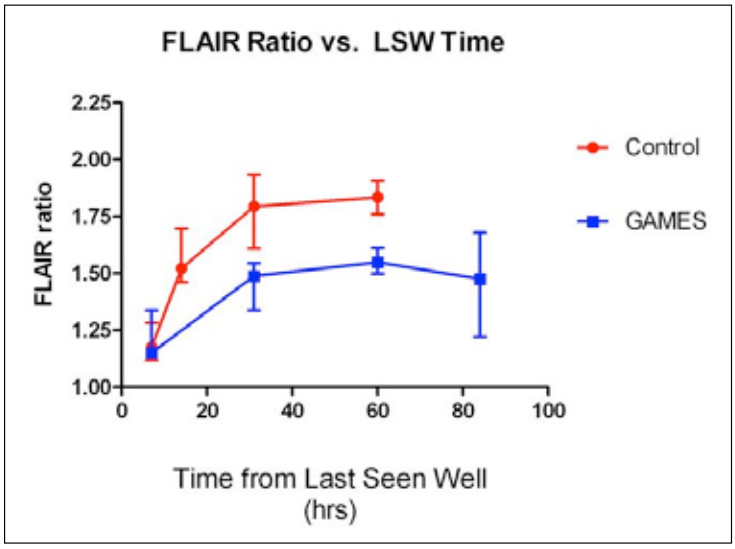

Poster Number 141

Bernstein, Emily BS
Research Coordinator, Psychiatry
eebernstein@partners.org

Mood Episodes and the Presentation of Comorbid Anxiety Symptoms

Investigators: Emily Bernstein, BS; Lori Eisner, PhD; Andrew Nierenberg, MD; Gustavo Kinrys, MD

Background: Anxiety includes psychic and somatic features, which can adversely affect treatment of comorbid mood disorders. The purpose of this study is to evaluate the impact of mood episodes on the presentation of anxiety in the general population.

Methods: We analyzed the National Epidemiologic Survey on Alcohol and Related Conditions. We included only participants who reported one lifetime general anxiety episode (N=1739). Participants were divided into three groups: those who experienced their anxiety episode during a low mood (N=501), high mood (N=147), or no mood episode (N=1091). We conducted ANOVAs to examine the relationship between concurrent mood episodes and psychic and somatic anxiety.

Results: Overall ANOVA revealed a difference in somatic anxiety symptoms reported by the groups ($p<.0001$); the high mood group ($M=7.94, SD=3.95$) and low mood group ($M=5.93, SD=3.55$) endorsed more somatic anxiety symptoms than the no mood episode group ($M=4.78, SD=3.25$) ($ps<.005$) and the high mood group more than the low mood group ($p=.015$). Groups also differed in number of psychic anxiety symptoms ($p<.0001$). High mood ($M=10.44, SD=2.35$) individuals experienced more psychic anxiety symptoms than the no mood episode ($M=7.43, SD=2.71$) group. Controlling for age and sex did not affect results.

Conclusion: Individuals experiencing concurrent mood symptoms endorsed more anxiety than those without mood symptoms; this effect was most robust for somatic anxiety. Results suggest that mood symptoms may worsen anxiety symptoms and support the literature describing the augmented clinical challenge of such prevalent comorbidities. We highlight the need for clinicians to assess concurrent symptoms and integrate these findings in treatment.

Poster Number 142

Brouwers, H. Bart MD
Clinical Research Fellow, Neurology Service
hbrouwers@partners.org

A Prediction Score for Hematoma Expansion Following Acute Intracerebral Hemorrhage

Investigators: H. Bart Brouwers, MD; Yuchiao Chang, PhD; Guido J. Falcone, MD, MPH; Alison M. Ayres, BA; Kristen A. McNamara, BA; Anastasia Vashkevich, BA; Thomas W. Battey, BSc; Valerie Valant, BA; Kristin Schwab, BA; Natalia S. Rost, MD, MPH; Javier M. Romero, MD; Anand Viswanathan, MD, PhD; Steven M. Greenberg, MD, PhD; Jonathan Rosand, MD, MSc; Joshua N. Goldstein, MD, PhD

Purpose: Hematoma expansion (HE) following acute intracerebral hemorrhage (ICH) is common and associated with poor outcome. Ongoing clinical trials therefore focus on restricting HE. In order to provide treatment options to the patients at highest risk of HE, we aimed to develop a prediction score for HE.

Methods: We performed a prospective cohort study of consecutive primary ICH patients presenting to a single center over a 12-year period, with available baseline and follow up CTs. HE was assessed using semi-automated software and defined as 6 mL or 33% growth. Our cohort was randomly divided in a 2/3 development and 1/3 validation cohort. Uni- and multivariate logistic regression was performed to assess clinical and neuroimaging covariates for relationship with HE. A prediction model was derived based on regression estimates, and this model was subsequently tested in the validation cohort.

Results: 817 ICH patients were included: 544 in the development cohort and 273 in the validation cohort. Overall, HE occurred in 156 patients (19%). In multivariate analysis, warfarin use (OR 2.09 [95%CI 1.24-3.52], p = 0.006), shorter time to CT (≤6 vs. >6 hours; OR 2.14 [95%CI 1.18-3.90], p = 0.013), baseline ICH volume (<30, 30-60, >60 mL; OR 1.90 [95%CI 1.01-3.55], p = 0.045), and the CT angiography spot sign (OR 3.59 [95%CI 1.77-7.29], p = 0.0004) were predictive of HE. The derived prediction score (0-9) showed a linear relation with the probability of HE and mortality (at discharge and 90 days), in both the development and the validation cohorts. The probability of HE in the validation cohort was 0%, 10%, 39%, and 54% for categorized scores 0, 1-3, 4-6, and 7-9, respectively. The c statistics were 0.69 for the development cohort and 0.78 for the validation cohort.

Conclusion: Warfarin use, presentation within 6 hours after ICH, larger ICH volumes at baseline, and the CT angiography spot sign are independent predictors of HE and mortality. Based on these findings, we developed a prediction score for HE. Since no therapy has demonstrated benefit in a randomized trial, our results open a path for individualized treatment and trial design in ICH, aimed at patients at highest risk of HE.

Poster Number 143

Erlwanger, Alison BA
Research Assistant, Medicine
aerlwanger@partners.org

Mobile HIV Screening in Cape Town, South Africa: Clinical Impact, Cost and Cost-Effectiveness

Investigators: Ingrid V. Bassett, MD, MPH; Darshini Govindasamy, BSc (BioMedSc), MPH, Alison S. Erlwanger, BA, Emily P. Hyle, MD, Nienke van Schaik, MBChB, MPH, Farzad Noubary, PhD, Robin Wood, BSc, BM, MMed, FCP (SA), Elena Losina, PhD, Linda-Gail Bekker, MBChB, FCP (SA), PhD, Kenneth A. Freedberg, MD, MSc

Background: Mobile HIV screening facilitates early HIV diagnosis. Our objective was to examine the value of adding a mobile screening unit to routine clinic-based HIV counseling and testing in Cape Town, South Africa.

Methods: We used a validated mathematical simulation model (CEPAC-International) to compare two HIV testing strategies in Cape Town: 1) clinic-based testing only; 2) the addition of a one-time HIV test and point-of-care CD4 count via mobile unit screening in the same community where clinic-based testing is available. Model outcomes included life expectancy, HIV transmissions, medical costs, and cost-effectiveness. Clinic-based testing was assumed to occur once every 4 years or at presentation with an AIDS-defining illness, and led to 100% linkage to care. Baseline input parameters were from a Cape Town-based mobile screening unit: undiagnosed HIV prevalence (10.3%), mean age of testers (32.7 years), mean initial CD4 count (males 422±236/μL, females 515±272/μL), HIV test acceptance rate (96.1%), CD4 count-dependent linkage to care rates for those newly diagnosed with HIV (males 31.4%-47.4%, females 51.0%-65.6%), mobile unit per person cost $45.25 (equipment and personnel cost of $510,000 amortized over 2 years), and mobile unit HIV test cost only ($1.66). The analysis accounted for a 3% annual discount rate. Incremental cost-effectiveness ratios (ICERs) below $8,100 (2011 South African per capita GDP) were considered very cost-effective. We conducted extensive sensitivity analyses on all major input parameters.

Results: With clinic-based testing alone, discounted life expectancy in those HIV-infected was 108.6 months; this increased to 115.4 months with the addition of the mobile unit (ICER $3,900/year of life saved (YLS), Table). Over a 5-year horizon, the mobile unit increased survival by 5.1% in the HIV-infected population and decreased HIV transmission by 9/1,000 HIV-infected individuals. Results of sensitivity analyses revealed that even at 10 times the mobile unit per person cost or an undiagnosed HIV prevalence as low as 0.5%, mobile HIV testing remained very cost-effective. Mobile testing remained the cost-effective strategy unless linkage to care was <18%.

Conclusion: The addition of a mobile screening unit to clinic-based testing improves survival, decreases HIV transmissions, and is very cost-effective in South Africa. Optimal outcomes depend on successful linkage. Identifying resources for mobile testing should be a major priority.

Poster Number 144

Fuenfer, Michael MD
Clinical Research Fellow, Pediatric Service
MFuenfer@partners.org

Lemiere Syndrome With Stroke Resulting From Parotiditis

Investigators: Michael M. Fuenfer, MD; Jennifer Munoz, MD; Sarah Murphy, MD

Introduction: Lemierre's Syndrome, a suppurative thrombphlebitis of the internal jugular vein is usually caused by oropharyngeal infections such as tonsillitis and dental infections. This condition is easily missed, and serious complications such as septic pulmonary emboli may lead to grave complications such as empyemea, lung cavitation, and hypoxemia.

Case Presentation: We present a case of a previously healthy 18 yrar old girl who developed Lemierre's Syndrome with a stroke following severe parotiditis, an inciting condition not previously reported. Her only medications were oral contraceptives. Initial symptoms of culture positive Group C streptococcus pharyntitis failed to resolve after a course of antibiotics, and was accompanied by onset of severe, painful swelling over her right neck and was treated with a course of prednisone and intravenous antibiotics (trimethoprim-sulfamethoxazole, and clindamycin). The following day she developed edema of the right eyelid, horizontal diplopia and inability to abduct her right eye psat the midline. An MRI revealed a subperiosteal abscess along the right lateral orbit with dural enhancement along the right temporal and frontal lobes, enhancement along the cavernous sinus without clear thrombosis, and multiple lobulated abscesses of the right parotid gland. The Fusobactyerium necrophorum was treated with vancomycin, clindamycin, meropenem and fluconazol. A follow-up MRI showd bilateral cavernous sinus infectious attenuation of the right and left internal carotid arteries. Systemic anticoagulation with unfractioned heparin was initiated. A subsequent MRI showed subacute punctate thromboembolic infarctions in the middle cerebral artery distribution. The pateint did not demonstrate focal neurological defitits. Upon complertion of five days of theratpeutic levels of intravenous heparin, the patient was transitioned to low molecular weight heparin and aspirin. Follow-up MRI/MRA studies demonstrated improvement in cerebral venous thrombosis and the bilateral carotid stentooclussive vasculitis. At a follow-up visit six weeks after discharge, the patient was doing well without residual neurologic sequellae.

Discussion: A diagnosis of Lemierre's Syndrome should be considered in any patient with an inflammatory process involving the neck, especially if in the vicinity of the carotid sheath. MRI provides accurate diagnosis. Early diagnosis and initiation of broad spectrum intravenous antibiotics is critical in decreasing the risk of potentially life-threatening compliations such as stroke.

Outcomes and cost-effectiveness of mobile unit HIV testing in Cape Town, South Africa

	Clinic-based testing only	Mobile unit intervention
HIV-infected population		
Undiscounted per-person life expectancy (months)	139.8	149.1
Discounted per-person life expectancy (months)	108.6	115.4
Discounted per-person costs ($)	10,660	12,500
5-year survival (%)	70.7	75.8
Total population		
Undiscounted per-person life expectancy (months)	458.5	459.5
Discounted per-person life expectancy (months)	250.8	251.5
Discounted per-person costs ($)	1,140	1,370
Incremental cost-effectiveness ratio[§] ($/YLS)	--	**3,900**

[§]ICERs < 1xSouth African per capita GDP ($8,100) considered very cost-effective as per WHO guidelines. Costs in 2011 US$.

Poster Number 145

Gill, Thomas IV MD
Associate Professor, Orthopaedics
tgill@partners.org

Rotator cuff tears in the setting of a stiff shoulder

Investigators: Thomas J. Gill IV, MD; Kaitlin Carroll, BS

Rotator cuff tears in the setting of a stiff shoulder are difficult problems to treat. To date, there is little data on the safety and efficacy of a single stage arthroscopic rotator cuff repair with concomitant arthroscopic capsular release for the treatment of rotator cuff tears in the setting of a stiff shoulder.

The purpose of this retrospective, consecutive series of patients treated by a single surgeon over a four year period is to report return of post-operative range of motion, elimination of pain, and level of patient satisfaction of patients treated with a single stage arthroscopic RCR and capsular release. These results are compared to a matched group of patients treated by the same surgeon who had an arthroscopic rotator cuff repair alone, with no pre-operative stiffness.

47 shoulders in 45 patients that underwent an isolated-RCR were compared to a combined RCR/ capsular release group of 27 shoulders in 27 patients at a mean follow-up of 1.5 years (range 1-5 years) in the RCR/capsular release and a mean follow-up of 1 year (range 1-3 years) in the isolated-RCR group. Patients completed the ASES shoulder score, Simple Shoulder Test (SST), and visual analog scale for pain (VAS), and Short Form 12 (SF12).

The mean age in both the isolated-RCR and RCR/ capsular release was 60 years. The isolated RCR had an average ASES score of 86.4, VAS 1, SST 10 and SF12 4.47. RCR/capsular release group had an average ASES score 85, VAS 0.33, SST 10, SF12 4.41. No significant differences between the groups were observed with respect to the ASES, VAS, SST, or SF12 scores. The isolated RCR group averaged 9.7 functions compared to 10 functions in the RCR/capsular release group on the SST. Average improvement in FF in the isolated-RCR group was 2.5 degrees compared to 18 degrees in the RCR/ capsular release group ($p=0.074$). Average improvement in ER in the isolated-RCR group was 0.7 degrees compared to 5 degrees in the RCR/capsular release group ($p=0.44$). Average difference in IR at neutral in the isolated-RCR group was a 0.5 decrease in vertebral levels compared to 1.86 increase in vertebral levels. Eight shoulders in the isolated RCR group had subsequent procedures (3 distal clavicle excisions, 2 biceps tenodeses, and 3 capsular releases) compared to zero shoulders in the RCR with capsular release. One patient in the isolated RCR group had a subsequent tear, but pursued conservative treatment.

The results of this study demonstrated that treatment of patients with a torn rotator cuff and concomitant stiff shoulder can be performed in a single stage. Specifically, a combined arthroscopic rotator cuff repair and arthroscopic capsular release is a successful procedure, with outcomes comparable to patients who undergo isolated arthroscopic rotator cuff repairs alone.

Poster Number 146

Gilman, Jodi PhD
Research Fellow, Psychiatry
jgilman1@partners.org

Neural Mechanisms of Social Influence in Young Adult Drug Use

Investigators: Gilman, J.M., PhD; Lee, S., BA; Kuster, J., MA; Kim, B.W., BA; Lee, M.J., MA; van der Kouwe, A., PhD; Blood, A.J., PhD; Breiter, H.C., MD

Background: Decades of research have demonstrated the importance of social influence in the initiation and maintenance of drug use. Peers play a pivotal role in introducing an individual to a drug, and most drug use occurs in social and recreational settings. Though social influence is a pivotal factor in drug use, however, little is known about neural mechanisms underlying social influence.

Methods: To better understand the role of social influence in drug use, we ran a study using a novel social decision-making paradigm in marijuana-using young adults (MJ) aged 18-25, and age and controls (CON) while they underwent functional magnetic resonance imaging (fMRI) scans. In this paradigm, subjects made a perceptual judgment after finding out how fictitious 'peers' had made the same judgment. They could either make a judgment that matched their peers (congruent) or one that went against their peers (incongruent). We performed an event-related design that allowed us to temporally separate events such as seeing a cue, seeing 'peer' judgments, making a choice, and receiving feedback. Participants were scanned using a 3T Siemens Trio scanner.

Results: We found a significant interaction between group (MJ or CON) and task behavior (congruent vs incongruent judgments) ($F = 3.98$, $p = 0.013$). Post-hoc Bonferroni tests indicated there was a significant difference only within the MJ group in the number of congruent vs incongruent choices ($p = 0.017$), indicating that MJ were more likely to make a judgment consistent with the group than were CON. We found no differences in neural activation between MJ and CON during congruent trials. During incongruent trials, MJ had significantly greater deactivation than CON in the bilateral nucleus accumbens (NAc), a region associated with social learning and reward processing.

Conclusion: MJ may experience more anxiety than CON when going against group decisions, which may be reflected in stronger conflict-related signals in the NAc. These results are consistent with data from a study showing that the NAc deactivated when subjects deviated from group opinion (Klucharez et al., 2009), and that deactivation of the NAc predicted conformity in future trials. The authors hypothesized that conformity was similar to reinforcement learning, in which deviation from group norms would trigger a neural response that signaled a 'mistake,' or a need to change behavior to be more in line with group norms. The MJ subjects may experience the deviation from group norms as an aversive event. The negative BOLD signal in the NAc during incongruent trials may either be a contributing factor to, or a result of, drug use behavior, and may be a possible biomarker in the development of addiction. A greater understanding of the neural mechanisms of peer influence may lead to the ability to predict who may be at highest risk for drug use in social situations, and allow clinicians to develop interventions to mitigate this risk.

Poster Number 147

Gilstrap, Lauren MD
Resident, Heart Center
lgilstrap@partners.org

Predictors of Survival to Orthotropic Heart Transplant in Patients with Light Chain Amyloidosis

Investigators: Lauren Gilstrap, MD; Khu Ton, MD, PhD; Jimmy Watts, MD; Raj Malhotra, MD; Megan Borase, BA; Marc Semigran, MD

Background: Light-chain amyloid patients with cardiac involvement and heart failure have limited treatment options. Orthotopic heart transplant (OHT) followed by myeloablative chemotherapy and stem cell transplant (SCT) can be successful, however the limited availability of cardiac donor organs causes a prolonged waiting period during which protein deposition with consequent organ dysfunction progresses. In cardiac amyloid patients on the waitlist, inotropes and mechanical support are either ineffective or associated with complications. The purpose of this study is to identify predictors of survival to OHT in this population and compare survival with other restrictive cardiomyopathy patients undergoing OHT.

Methods: From January 2000 to June 2011, 43 patients with light chain amyloidosis were evaluated for cardiac transplant at Massachusetts General Hospital including right heart catheterization and echocardiography. The Student's t-test or Mann-Whitney test was used to assess for differences between patients who survived to transplant and those that did not. Univariate and multivariate Cox regression analyses were performed to identify predictors of survival to OHT. Kaplan-Meier analysis was used to compare survival between MGH amyloid patients who did not undergo OHT, those that did undergo OHT and the Scientific Registry of Transplant Recipients (SRTR) database non-amyloid restrictive cardiomyopathy patients undergoing OHT.

Results: For those ultimately receiving transplants, the time from listing to transplant (wait list time) was 53 days ± 48 days.For those who died prior to OHT, average wait list time was 63 days ± 45 days p=0.58. There were no differences in hemodynamic or echocardiographic characteristics between those patients that survived to OHT and those that did not. There was no difference in pulmonary, renal, gastrointestinal or neurological amyloid involvement. There was also no difference in % plasma cells, light chain type or ratio. Univariate analysis identified only weight and body mass index (BMI) as predictors of survival to OHT. Multivariate analysis yielded BMI as the only significant predictor of survival to transplant (RR of Survival to OHT for patients with BMI above the median BMI of 26 = 0.8163, 95% CI = 0.6891-0.9670, p=0.0194). Survival of cardiac amyloid patients who were not eligible for OHT listing or died prior to OHT was markedly worse than those that underwent OHT (p<0.001). There was no difference in survival between cardiac amyloid patients undergoing OHT and other restrictive cardiomyopathy patients included in the SRTR database (p=0.989).

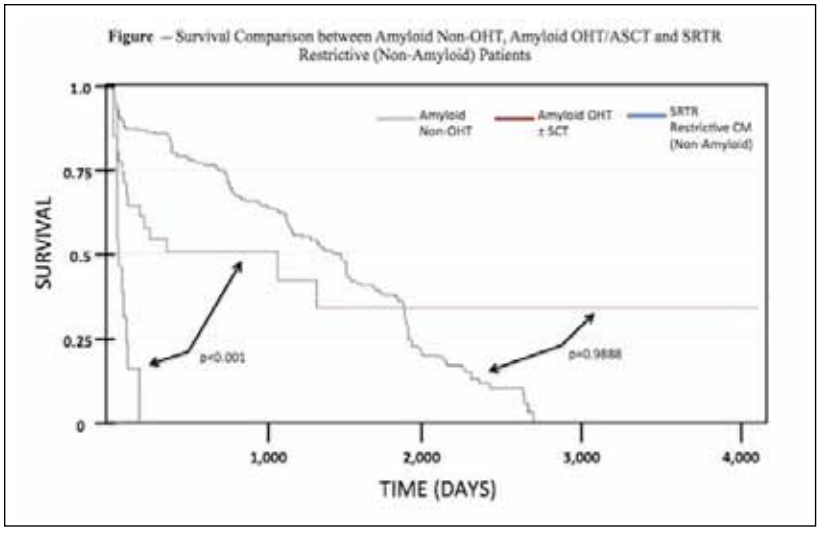

Discussion: This study showed that the only predictor of survival to OHT among cardiac amyloid patients was low BMI, which correlated with less wait list time. No other baseline demographic or hemodynamic variables predict survival to transplant. The type of amyloidosis and the extent of systemic disease do not affect the likelihood of survival to transplant. In addition, cardiac amyloid patient who underwent OHT followed by SCT had similar survival to other restrictive cardiomyopathy patients without amyloid. There was also a marked improvement in survival for amyloid patients undergoing OHT/SCT compared with those unable to receive a donor organ.

Poster Number 148

Hale, Timothy PhD
Research Fellow, Dermatology Service
tmhale@partners.org

Representation of Health Conditions on Facebook Pages

Investigators: Timothy M. Hale, PhD; Akhilesh S. Pathipati, BA; Shiyi Zan, BS; Joseph Kvedar, MD; Kamal Jethwani, MD, MPH

Introduction: The Internet has long been recognized as a primary source of health information. Google makes it possible to quickly search and find tens of thousands of sites listed in order of relevance. The introduction of Web 2.0, or social media technologies, has fueled the growth of social networking sites (SNS) like Facebook (FB) and new ways to find and share information. FB has not only become the most popular SNS but also the second most visited website in the world (second only to Google). Despite the rise in the popularity of FB, little is known about the representation of health conditions on this specific SNS, especially on FB pages. This study is a first step towards describing the health conditions found on FB pages, the content of these pages, and user engagement.

Methods: On July 24, 2012, we identified the 20 most searched for health conditions on Google using Google Insight. These 20 conditions provided the basis for subsequent searches on FB. We listed the first 50 FB page search results for each condition, recorded the number of 'Likes' for each page, and examined recent page content for condition-relevancy. We then categorized the type of content on the page into one of seven types (patient support, general support, information/awareness, marketing/promotion, Wikipedia-type pages, blank, or other).

Results: Of the 953 FB pages sampled, 673 (70.6%) were relevant to the health condition searched. The greatest number of relevant pages were for breast cancer, diabetes, cancer, thyroid, and arthritis. The lowest number of relevant pages were stroke, HIV, spine, HPV, and diarrhea. Most pages were marketing and promotion (n = 168 or 32.2%) followed by information/awareness (n =108, 20.7%), and Wikipedia-type pages (n = 81, 15.5%). Surprisingly, support pages made up only a small percentage of pages (n = 68, 13.0%). 'Likes' were examined as a measure of user engagement. We found that information/awareness and general support pages received disproportionately large numbers of 'likes' compared to the number of pages. Only 4% of pages were categorized as general support, but represented 36% of 'Likes'. Marketing/promotion represented 32% of pages but comprised 47% of 'likes'. Finally, we compared the relative engagement in a health condition, measured by the relative number of searches on Google Insight to the total 'likes' in FB. Nine conditions (HIV, arthritis, anemia, asthma, lupus, spine, breast cancer, AIDS, and stroke) have relatively more engagement on FB pages compared to searches on Google. For nine conditions (HPV, diabetes, pneumonia, flu symptoms, diarrhea, herpes, stomach, back pain, and blood pressure) the engagement of FB users is relatively lower than searches on Google.

Conclusion: The large percentage of irrelevant pages may pose a problem for people with limited literacy skills who look on FB for health information and to connect with others, whether they may be other disease-sufferers or caregivers. FB users tend to engage more with marketing/promotion and general support pages. Future research is needed to understand why some health conditions are underrepresented on FB pages and what drives user engagement around health conditions.

Poster Number 149

Jethwani, Kamal MD,MPH
Instructor, Dermatology Service
kjethwani@partners.org

Tablet Computer For Personalized Health Information In The Waiting Room: Exploring Patient And Physician Attitudes Towards The Use Of Tablet Computers For Clinic Based Personalized Healthcare Information Exchange

Investigators: Kamal Jethwani, MD, MPH; Vishal Patel, MS4; Timothy M. Hale, PhD; Joseph Kvedar, MD

Introduction: Annual national healthcare expenditure in the United States is expected to surpass $3 trillion by 2013. The majority of this cost will be related to the management of preventable chronic diseases. To reduce the economic burden of chronic disease and deliver efficient, higher quality care, new approaches are needed to actively engage patients, encourage lifestyle changes, and promote effective self-care. To achieve these goals, better use could be made of existing information and communication technologies. One method would be to leverage the power of low-cost, easy to use handheld tablet computers while patients are in the waiting room. The proposed tablet computer for clinic-based personalized health information exchange (TABHIT) system would enable patients to access personalized health information, educational messages and audiovisual materials, and collect patient information prior to the appointment. This study examines patient and healthcare provider (HCP) interest and attitudes towards using TABHIT to guide future design, development, and implementation of healthcare information technology systems.

Methods: This study uses patient surveys and semi-structured phone interviews with Partners HealthCare affiliated HCPs. Surveys were administered to 86 patients in a primary care waiting room in a Boston area community health center. The survey instrument included a diagram and description of the proposed TABHIT system in which the patient, upon sign in at the clinic, receives a tablet loaded with personalized information tailored to their specific conditions and preferences. Perceived efficacy versus traditional patient-provider interactions, usability, and privacy concerns were assessed. Survey data was analyzed using Excel and Stata. Telephone interviews with five HCPs were conducted, assessing both the potential utility and difficulties implementing the proposed system. HCP interviews were transcribed and summarized to identify common responses to questions.

Results: The mean age of patient participants was 43.5 years, with 38% male and 62% female, 93.5% had a GED or higher, and 72% were self-categorized as Caucasian, with the largest single minority being Hispanic at 13%. When asked about interest in the proposed TABHIT application, 85% of patients expressed some interest with 65% being very/extremely interested. The TABHIT model of clinical interaction was considered more motivating, informative, and engaging than traditional printed materials, websites, and e-mails. However, when compared to face-to-face interaction, patients did not find the proposed TABHIT model to be more motivating, engaging, or informative. Forty-four percent of patients thought that it would improve their relationship with their doctor and 60% of patients thought it would improve their knowledge about their health. Only 33% were concerned about privacy. Approximately 96% of patients were already "somewhat" confident in their ability using a basic tablet computer. Four of the five HCPs had positive reactions to the proposed TABHIT model and thought that it would improve clinical workflow regarding patient check-in and patient education. Primary concerns expressed by HCPs involved the physical logistics with keeping tablets in the clinic.

Conclusion: Both patients and HCPs were highly amenable to integrating digital tablets into the clinical experience. Further research is needed to develop, implement, and evaluate the effectiveness of TABHIT type systems

Kleimola, Lauren MPH
Statistician, Mass General Hospital *for* Children
lkleimola@partners.org

Poster Number 150

The Global Impact of Cooking with Solid Fuels on Neonatal Mortality

Investigators: Lauren B. Kleimola, MPH; Jitesh A. Borkar, MSc; Archana B. Patel, MD, DNB, PhD, MSc; Patricia L. Hibberd, MD, PhD

Household air pollution (HAP) from cooking with solid fuels in low to middle income countries is associated with negative health outcomes, particularly in pregnant women, young mothers and young children. Incomplete combustion of solid fuels releases damaging pollutants that can reduce oxygen in the mother's blood and oxygen delivery to the placenta, resulting in adverse perinatal outcomes such as still births and low birth weight. HAP is also associated with childhood pneumonia. However, little is known about the effect of HAP on the health of neonates. We hypothesized that exposure to higher polluting fuels would increase the risk of neonatal mortality.

Demographic and Health Surveys are nationally representative surveys conducted every five years in many low to middle income countries. Data from the most recent DHS of 28 countries was classified into 4 regions: Africa (15), Americas (4), Asia (7) and Europe (2). The study population was all children aged 0-30 days born in the 59 months prior to the survey to mothers residing at the house where the survey was conducted. The primary outcome was neonatal mortality defined as a binary variable, 1 if dead or 0 if alive on day 30 of life. The exposure of interest was type of fuel the household 'mainly use[s] for cooking'. Fuel was dichotomized into low polluting fuels: electricity, LPG, natural gas and biogas; or, medium to high polluting fuels: kerosene, coal, charcoal and biomass such as wood, crop waste and dung. We used forward stepwise Poisson regression models adjusted for clustering effects and individual and household characteristics to compare neonatal mortality in households using medium or high polluting fuels to households using low polluting fuels. All analyses were done using STATA software version 12SE.

The total number of children included in the study was 261,028, out of which there were 7,658 (3%) neonatal deaths. The adjusted risk ranged from 0.34 (95% CI: 0.12, 0.95) in Guyana to 6.98 (95% CI: 1.84, 26.45) in Nepal. India, Indonesia and Nepal had significant increases in risk of neonatal mortality among children in medium to high polluting fuel households compared to children in low polluting fuel households. We found non-significant increases in risk of neonatal mortality among children living in households using medium to high polluting fuels in 3 of the 4 regions studied. The summary effect measures, while not attaining statistical significance, show variability in the impact of cooking with solid fuels on neonatal mortality. There is an important need to obtain actual household measurements of HAP and to collect prospective data on neonatal mortality to more precisely define the risk of exposure of neonates to HAP.

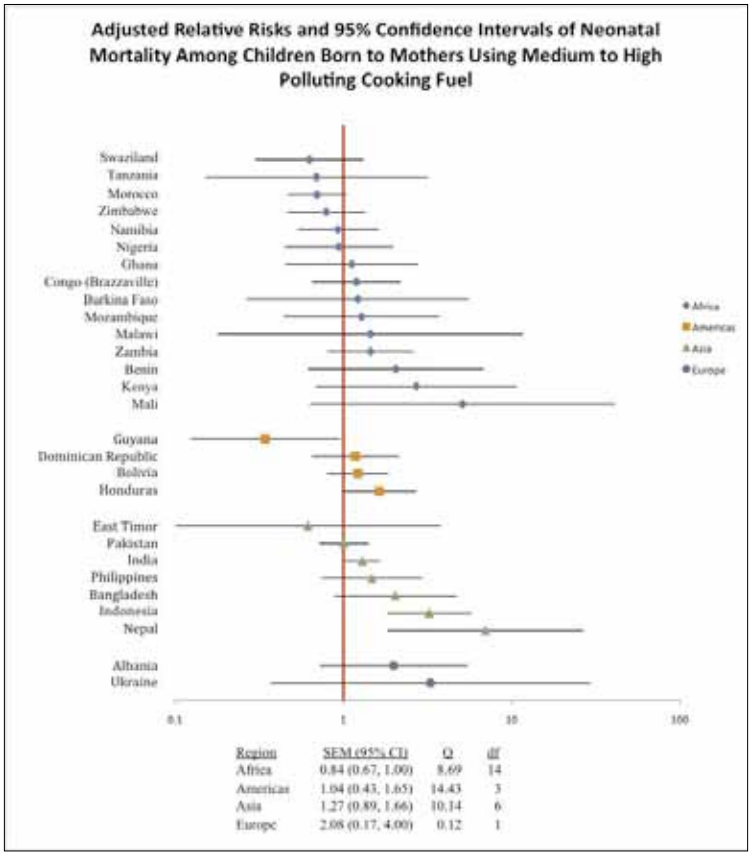

Poster Number 151

Lawson, Elizabeth A. MD
Assistant Professor, Medicine
ealawson@partners.org

Increased hypothalamic-pituitary-adrenal drive is associated with decreased appetite and hypoactivation o f food motivation neurocircuitry in anorexia nervosa

Investigators: Elizabeth A. Lawson, MD; Laura M. Holsen, PhD; Rebecca DeSanti; McKale Santin; Erinne Meenaghan, NP; David B. Herzog, MD; Jill M. Goldstein, PhD; Anne Klibanski, MD

Corticotropin releasing hormone (CRH)-mediated hypercortisolemia has been demonstrated in anorexia nervosa, a disorder characterized by restricted food intake despite low body weight. Although CRH may decrease appetite, the downstream stress hormone cortisol stimulates hunger. We have previously shown hypoactivation of brain regions involved in food motivation in women with anorexia nervosa, even after weight recovery using a novel fMRI paradigm. We hypothesized that CRH-mediated hypercortisolemia may contribute to dysregulation of food motivation circuitry in this disorder. We studied 36 women [13 anorexia nervosa (AN), 10 weight-recovered AN (ANWR), 13 healthy controls (HC)] of comparable age to characterize the relationship between HPA measures, appetite and food motivation neurocircuitry in anorexia nervosa. BMI was lower in AN (17.7±0.3 kg/m2) than ANWR (21.9±0.7 kg/m2) and HC (22.5±0.4 kg/m2) ($p<0.0001$). Peripheral cortisol and ACTH levels were measured fasting and 30, 60, and 120 min after a standardized meal. The Visual Analogue Scale was used to assess appetite. fMRI was performed during visual processing of food and non-food stimuli to measure brain activation pre- and post-meal. Mean fasting, 120 min post-meal, and nadir cortisol levels were high in AN vs. HC ($p<0.02$). Mean ACTH levels were higher in AN and in ANWR vs. HC after the meal ($p<0.03$). Cortisol secretion was associated with lower homeostatic ($R=-0.55$, $p=0.0006$) and hedonic ($R=-0.49$, $p=0.003$) appetite in the fasting state, independent of BMI and depressive symptoms. Cortisol secretion was also associated with between-group variance in activation in food-motivation brain regions, including the hypothalamus (control center for appetitive signals) (pre-meal HC>AN 26%, HC>ANWR 14%), amygdala (important for learning satiety cues, assessing reward value) (pre-meal HC>AN 45%, HC>ANWR 42%; post-meal HC>AN 16%), hippocampus (implicated in processing food-related memories) (pre-meal HC>AN 24%), OFC (integrates emotion, reward expectation) (pre-meal HC>AN 46%) and insula (houses the primary taste cortex, integrates visceral signals, modulates motivational behavior) (premeal HC>AN 12%, HC>ANWR 12%). We conclude that HPA activation may contribute to the maintenance of anorexia nervosa by suppression of appetitive drive.

Poster Number 152

Lei, Lan MD
Research Fellow, Cancer Center
llei2@partners.org

Early Results of Therapeutic and Prophylactic Nipple-sparing Mastectomy with Immediate Reconstruction in BRCA Mutation Carriers

Investigators: Lan Lei, MD; Kari J. Kansal, MD; Rong Tang, MD; Amy S. Colwell, MD; Suzanne B. Coopey, MD; Michelle C. Specht, MD; Michele A. Gadd, MD; William G. Austen, Jr., MD; Barbara L. Smith, MD, PhD

Background: BRCA gene mutations confer a 60-80% lifetime risk of breast cancer, and carriers often consider prophylactic mastectomies to reduce risk. Nipple sparing mastectomy (NSM) provides a superior cosmetic outcome, making risk-reducing surgery more acceptable, but concerns have been raised about the oncologic safety of nipple sparing in BRCA mutation carriers. We examined the safety and early outcomes of NSM in BRCA mutation carriers.

Methods: Retrospective review of NSM in our institution from 6/2006-9/2012 was performed and patients with BRCA mutations identified. Nipple sparing techniques included excision and histological analysis of ductal tissue from within the nipple. Patient and tumor characteristics, complications and early recurrence data were collected.

Results: 70 BRCA mutation carriers (41 BRCA1, 29 BRCA2) underwent bilateral NSM removing 140 breasts in total. 27 NSM were for known cancers (19%) and 113 were prophylactic (81%). Median patient age was 41 (range 23-64). Reconstructions included 72 single stage implants, 60 tissue expanders and 8 other types. 2 of 113 prophylactic NSM (2%) had unexpected malignancy: 1 invasive ductal cancer and 1 DCIS; neither had tumor in excised nipple duct tissue. Mean tumor size in therapeutic NSM was 1.6 cm (range 0.2-2.9 cm) and mean tumor to nipple-areola complex (NAC) distance on imaging was 4.4 cm (range 3-10 cm, 5 unknown). 1 of 27 therapeutic mastectomies (4%) showed DCIS in the excised nipple duct tissue and the NAC was removed. At 11 months median follow-up (range 0-40 months) no therapeutic or prophylactic BRCA mutation carrier had a NAC recurrence. 2 of 27 cancer patients had a local recurrence outside the nipple: 1 chest wall/axilla and 1 axilla alone. Postoperative complications were infrequent: 2/140 (1%) nipple necrosis, 2/140 (1%) skin necrosis, 5/140 (4%) loss of implant due to infection, and 4/140 (3%) hematoma.

Conclusions: Nipple duct involvement by tumor is uncommon in BRCA mutation carriers undergoing prophylactic and therapeutic nipple sparing mastectomies. Nipple sparing mastectomy is an option for BRCA carriers.

Poster Number 153

Matheny, Natalie BA
Research Assistant, Psychiatry
nmatheny@partners.org

Changes in quality of life following treatment with cognitive therapy for obsessive compulsive disorder

Investigators: Natalie Matheny, BA; Jessica Rasmussen, PhD; Irina Kasarskis, MPH; Sabine Wilhelm, PhD; Gail Steketee, PhD

Obsessive-compulsive disorder (OCD) is an anxiety disorder characterized by repeated obsessive thoughts as well as potentially debilitating compulsions. Studies have shown that patients with OCD experience a significant decrease in symptoms following treatment with cognitive-therapy (CT) or cognitive behavioral therapy (CBT; Olatunji et al., 2012; Wilhelm et al., 2009). In addition to a decrease in symptoms, cognitive-behavioral treatment outcome research has found that some patients also experienced significant gains in quality of life from pre to post-treatment (Norberg et al., 2008). Despite prior research on changes in quality of life following CBT, there is limited research focusing on changes in quality of life following CT.

The study sample consisted of 28 participants who met DSM-IV diagnostic criteria for OCD, and completed one of two treatment outcome studies of CT for OCD (Wilhelm et al., 2009). The sample was approximately half male (57.1%), primarily Caucasian (92.9%) and the mean age of participants was 32.9 (SD = 10.9). Participants completed a battery of questionnaires including the Yale-Brown Obsessive Compulsive Scale (Y-BOCS) and the Longitudinal Interval Follow-Up Evaluation (LIFE). Participants were determined to be responders or non-responders based on the percentage change in Y-BOCS total score from baseline to post-treatment. Participants who had a Y-BOCS total score that dropped greater than or equal to 30% were classified as responders. Scoring for the LIFE was conducted using scoring procedures for the Longitudinal Interval Follow-Up Evaluation- Range of Impaired Functioning Tool (LIFE-RIFT).

The mean LIFE-RIFT total score at post-treatment among responders was 8.5 (SD = 2.7) compared to the mean total score of 11.4 (SD = 3.0) for non-responders, resulting in a mean score 2.9 points higher among non-responders and indicating a lower quality of life for non-responders. An independent t-test showed that a significant difference in post-treatment LIFE-RIFT scores exists between responders and non-responders to therapy ($t = 2.19$, $df = 26$, $p = .04$).

In accordance with research demonstrating an increase in quality of life following treatment with CBT, our results suggest that similar improvements may exist for individuals with OCD following treatment with CT. These findings imply that assessment of symptom reduction alone may not fully capture improvement for individuals with OCD following CT. Further analyses will examine whether non-responders to treatment still experienced an increase in quality of life despite a nonsignificant decrease in symptoms. In addition, analyses will explore whether or not age, gender or Y-BOCS severity at baseline moderated any differences in LIFE score changes from baseline to post-treatment. Assessing quality of life changes from pre to post-treatment may give researchers a fresh perspective on the potential benefits of therapy.

Mavros, Michael MD
Research Fellow, Surgery
mmavros@partners.org

Poster Number 154

Additional imaging in alert trauma patients with cervical spine tenderness and a negative CT scan: is it useful?

Investigators: Michael N. Mavros, MD; Haytham M. Kaafarani, MD, MPH; Ali Y. Mejaddam, MD; David R. King, MD; Peter J. Fagenholz, MD; D. Dante Yeh, MD; Marc A. de Moya, MD; George C. Velmahos, MD, PhD

Background: There is controversy regarding the need for additional imaging before cervical spine (C-spine) clearance in alert trauma patients with a negative C-spine CT scan.

Methods: A retrospective review of medical records of adult trauma patients treated at the MGH Emergency Department who underwent a C-spine CT scan between September 2011 and June 2012 was performed. We examined the incidence of acute C-spine injury in patients with C-spine pain or tenderness, a Glasgow Coma Scale of 15, and a negative C-spine CT scan (i.e. without any acute findings), as well as the predictors of performance of additional imaging studies (MRI, Flexion-Extension X-rays) in this population.

Results: A total of 2,015 C-spine CT scans were performed, and 396 (19.7%) patients were eligible (Figure 1). The median age was 43 years (interquartile range: 30 – 53), with about half (n= 180, 45.5%) being female. Only 36 patients (9.1%) underwent further MRI (n=14, 3.5%) or Flexion-Extension imaging (n=20, 5.1%), and 345 patients were later re-examined with resolution of the C-spine pain or tenderness, and were clinically cleared during the same admission. All MRI and Flexion-Extension images had no evidence of ligamentous or spinal injuries, and all 36 patients had their C-spine cleared immediately following the additional imaging without complications; none required treatment besides non-steroid anti-inflammatory medications. Age, gender, timing of patient presentation, mechanism of injury, and non-acute CT findings did not predict performance of additional C-spine imaging.

Conclusion: All alert patients with a negative C-spine CT and initial C-spine pain or tenderness had their C-spine cleared and their collar removed within the same admission, either as a result of resolution of their symptoms or due to the absence of radiologic findings on MRI and/or Flexion-Extension x-rays. Our current findings suggest the safety of C-spine clearance in alert patients with a negative CT, even in the presence of initial C-spine pain or tenderness. The usefulness of additional imaging such as MRI or Flexion-Extension x-rays in this patient population is questionable, although further studies are needed to confirm our findings.

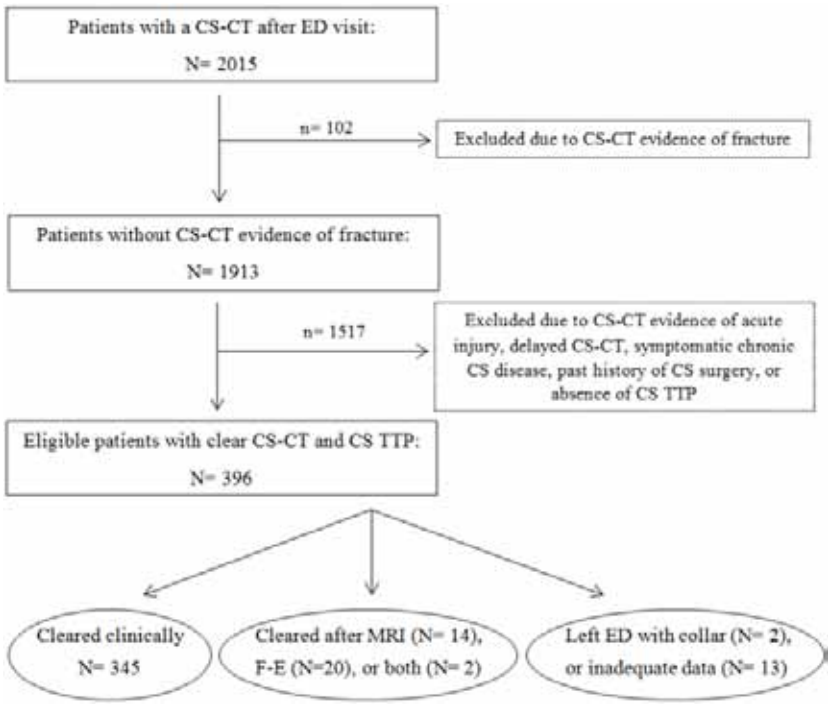

Poster Number 155

Morgan, Jordan BS
Clinical Research Coordinator, Orthopaedics
jhmorgan@partners.org

Short versus Long Cephalomedullary Nails for the Treatment of Intertrochanteric Hip Fractures in Patients over 65 Years

Investigators: Jordan Morgan, BS; Conor Kleweno, MD; James Redshaw, BS; Mitchel Harris, MD; Edward Rodriguez, MD, PhD; David Zurakowski, PhD; Mark Vrahas, MD; Paul Appleton MD

Background: The purpose of this study was to compare failure rates between short and long cephalomedullary nails used for the treatment of intertrochanteric hip fractures in patients over 65 years of age.

Methods: A retrospective review was conducted of patients 65 years or older who underwent treatment of an intertrochanteric hip fracture with a cephalomedullary nail at three Level-1 trauma centers between January 2004 and December 2010 and who had a minimum of one year of follow-up. Data were collected from patient medical records, operative reports, and radiographs. The primary outcome measure was failure of the treatment, defined as either periprosthetic fracture of the femur around or distal to the stem of the nail, or re-operation requiring nail removal, or revision of nail including conversion to arthroplasty.

Results: Incidence of treatment failure was 30 of 559 (5.4%) for the entire cohort; 13 of 219 (5.9%) occurred after placement of a short nail compared with 17 of 340 (5.0%) after placement of a long nail (P = 0.70). There were 11 of 559 (2.0%) patients who sustained a periprosthetic fracture after nailing: 6 of 219 (2.7%) after short nails and 5 of 340 (1.5%) after long nails (P=0.35). The remaining 19 treatment failures were major re-operations requiring removal of nail: 7 of 219 (3.2%) after short nails and 12 of 340 (3.5%) after long nails (P=0.81). The reasons for these 19 revision procedures were: screw/helical blade cutout (16); progressive arthritis with conversion to arthroplasty (1); avascular necrosis of femoral head with conversion to arthroplasty (1); and symptomatic leg length discrepancy with conversion arthroplasty (1). Median follow up period for patients living at least one year post-operatively was 30 months (range: 12-85 months). Overall, 175 of 698 (25%) patients died within one year after index surgery.

Conclusions: We found no difference in the failure rates when using contemporary cephalomedullary implants. We conclude that both short and long cephalomedullary nails offer safe, predictable outcomes for the fixation of intertrochanteric hip fractures in patients 65 years and older.

Musch, Guido MD
Associate Professor, Anesthesia, Critical Care and Pain Medicine
gmusch@partners.org

Poster Number 156

Improving patient information transfer and retention between anesthesia providers at intraoperative hand-off of care

Investigators: Guido Musch, MD; Aalok Agarwala, MD; Meredith Albrecht, MD; Paul Firth, MD; Lisa Warren, MD

Background: Because of increased complexity and hence duration of surgical procedures, limitations on house officers' shift hours and increased representation of anesthesia providers with strict shift times among the workforce, it is becoming increasingly common that intraoperative care is transferred from one anesthesia provider to another. This transfer of care represents both an opportunity to reassess the management of a case from a different perspective but also a challenge insofar as all pertinent information must be relayed from the outgoing to the incoming anesthetist. In fact, transfer of care issues are among the most important issues in anesthesia patient safety because an association between poor-quality handoff and adverse events has been demonstrated

Rationale: We reasoned that poor-quality handoffs may stem from lack of a rational framework that can be consistently used to structure the intraoperative handoff process across anesthesia providers. Consequently, we investigated if a "handoff checklist" could improve the transfer and retention of critical patient information at handoff by providing a standardized minimalist structure for organized, productive conversation between providers.

Methods: We assessed the transfer of critical patient information during intraoperative handoffs by having an observer record, on a preset template, the information that was passed from the outgoing to the incoming anesthetist. We assessed information retention by asking the incoming anesthetist a set of predefined questions on information that was the subject of the handoff conversation, approximately 5 minutes after the outgoing anesthetist had left. These measurements were performed for 2 weeks before and 2 weeks after the "handoff checklist" was introduced in clinical practice.

Results: After introduction of the checklist we observed a substantial rise in the number of handoffs in which information on allergies, airway management, analgesics and vasopressors was discussed. General aspects of case management such as postoperative plan and potential areas of concern were also more frequently discussed after checklist implementation (Table 1). Furthermore, the checklist increased information retention in the incoming anesthetist, as shown by a substantial decrease in the number of anesthetists that did not know the response to specific questions regarding the amount of intravenous fluid, antibiotics and muscle relaxant previously administered by the outgoing anesthetist. (Table 2).

Conclusions: In this study we show that a "handoff checklist" can improve the transfer and retention of critical patient information at handoff between anesthesia providers. This is expected to result in increased patient safety and reduced occurrence of intraoperative adverse events.

Table 1: Information Transfer

	Pre-Checklist (n=26)	Post-Checklist (n=22)
Allergies	69%	91%
Preoperative Meds	50%	68%
Laryngoscopy	56%	100%
Analgesics	64%	90%
Vasopressors	40%	70%
Urine Output	50%	75%
Areas of Concern	58%	91%
Postoperative Plan	42%	91%
Introduction of incoming anesthetist	4%	59%

Table 2 : Information Retention

Does NOT Know	Pre-Checklist (n=26)	Post-Checklist (n=22)
Administered Fluid Amount	27%	5%
Muscle Relaxant	23%	6%
Antibiotic	28%	5%
Next Antibiotic Due	64%	14%

Poster Number 157

Powis, Kathleen MD, MPH
Instructor, Mass General Hospital *for* Children
kpowis@partners.org

Vitamin D inadequacy in HIV-infected women on HAART is not associated with morbidity, mortality or growth impairment of uninfected infants in Botswana

Investigators: Kathleen Powis, MD, MPH; Wafaie Fawzi, MB, BS, MPH, MS, DrPH; Laura Smeaton, MS; Michael Hughes, PhD; Shahin Lockman, MD, MSc; Anthony Ogwu, MB, BS; Sikhulile Moyo, Joseph Makhema, MB, ChB, MRCP; Max Essex, DVM, PhD; Roger L. Shapiro, MD, MPH

Background: Low maternal 25(OH)D (vitamin D) levels have been associated with higher mortality and impaired growth among HIV-exposed uninfected (HEU) infants born to HIV-infected women lacking access to highly active antiretroviral therapy (HAART). Similar endpoints have not been studied for HEU infants born to women on HAART

Methods: The Mma Bana trial provided HIV-infected pregnant women in Botswana with either PI-based, triple NRTI-based, or NNRTI-based HAART regardless of CD4 count. The analysis included HEU infants who were hospitalized or died during 24 months of follow-up (unhealthy) along with a random sample of infants who remained healthy. Stored maternal delivery serum samples were assayed for vitamin D levels, and were compared by infant outcome and season of birth using a Wilcoxon Rank-Sum test. A cutoff of < 32 ng/mL was used to define maternal vitamin D inadequacy, a level above which optimal calcium homeostasis is achieved. Wasting (weight-for-length z score < -2 standard deviation [SD]), stunting (length-for-age z score < -2 SD) and underweight (weight-for-age z score < -2 SD) were compared using the 2006 World Health Organization's Child Growth Standards.

Results: Maternal delivery vitamin D levels were available from 119 (87%) of 137 unhealthy infants and 233 (98%) of 238 randomly selected healthy control infants. Mothers of unhealthy infants were older (median age 29.6 vs 27.0, p=0.009) but were similar in all other characteristics, including median viral load and CD4 cell count at enrollment. Vitamin D inadequacy occurred most frequently among women delivering in winter (Table 1). Median maternal Vitamin D level did not differ significantly between mothers of unhealthy infants and those with healthy infants (36.7 ng/mL; IQR 29.1- 44.7 vs. 37.1 ng/mL; IQR 30.0 - 47.2; p = .32). Proportions of infants stunted, wasted or underweight at 1 year of life did not differ significantly by maternal vitamin D group (Table 2).

Conclusions: Vitamin D inadequacy at delivery was common among mothers taking HAART during pregnancy in Botswana, but was not associated with morbidity, mortality or growth impairment in their HIV-uninfected infants.

Table 1:Proportions of Low Maternal Vitamin D Levels by Season

	Low Level (< 32 ng/mL) (n=112)	Adequate Level (≥ 32 ng/mL) (n=240)	p-value
Season			0.004[1]
Jan-Feb-Mar (Summer)	16 (18.39%)	71 (81.6%)	
Apr-May-Jun (Fall)	34 (34.0%)	66 (66.0%)	
Jul-Aug- Sep (Winter)	34 (44.2%)	43 (55.8%)	
Oct-Nov-Dec (Spring)	28 (31.8%)	60 (68.2%)	

[1]Fisher's exact test

Table 2: Proportions of Infant Stunting, Wasting and Underweight at One Year of Life Based Upon Maternal 25(OH) D Levels

World Health Organization Growth Measure[1]	Low Maternal Vitamin D Level at Delivery (<32 ng/mL)	Adequate Maternal Vitamin D Level at Delivery (≥32 ng/mL)	p-value[2]
Stunting (Length-for-age z score < - 2 SD)	4/94 (4.3%)	11/198 (5.6%)	0.78
Wasting (Weight-for-length z score < - 2 SD)	2/94 (2.1%)	11/198 (5.6%)	0.24
Underweight (Weight-for-age z score < -2 SD)	4/94 (4.3%)	13/200 (6.5%)	0.59

[1]2006 World Health Organization's (WHO) Child Growth Standards
[2]Fisher's exact test

Poster Number 158

Reuman, Lillian BA
Clinical Research Coordinator, Psychiatry
lreuman@partners.org

"Woefully OCD": Clinically significant anhedonia in OCD

Investigators: Lillian Reuman, BA; Amitai Abramovitch, PhD; Sabine Wilhelm, PhD

Obsessive-compulsive disorder (OCD) is an anxiety disorder marked by unwanted, repetitive thoughts and accompanying compulsions. Anhedonia, the inability to experience pleasure from typically enjoyable activities, is a construct associated with impaired reward responsiveness. Extensive research in depressive disorders, schizophrenia, and substance abuse suggests that anhedonia may be more heritable than OCD or depression. Despite recent evidence of associated negative affect and reduced ventral striatum reactivity to positive reward in OCD, anhedonia has never been investigated in the context of OCD.

One-hundred and thirteen participants with OCD completed a battery of questionnaires to assess OCD symptom severity and anhedonia, including the Snaith-Hamilton Pleasure Scale (SHPS), the Depression Anxiety Stress Scale (DASS), the Yale-Brown Obsessive Compulsive Scale (Y-BOCS), and the Obsessive Compulsive Inventory—Revised (OCI-R).

Results reveal that 38% of participants experience clinically significant anhedonia. OCD participants in the anhedonic group exhibited significantly higher OCD symptom severity (as measured by the Y-BOCS) in comparison to the non-anhedonic group ($p < .0001$, Cohen's d effect size =.96). This finding remained significant after controlling for severity of depression ($p=.003$, $d=.59$). Anhedonia severity was significantly correlated with Y-BOCS scores (r ranging from .39 to .44) and all DASS subscales (r ranging from .34 to .54). After controlling for severity of depression, correlations with the Y-BOCS scores and the OCI-R remained significant (r ranging from .26 to .29). When controlling for depressive severity, discriminant function analysis of the OCI-R subscales revealed that the 'obsessing' dimension holds the highest discriminatory power for detecting the presence of clinical anhedonia in OCD.

In accordance with recent research demonstrating deficient reward reactivity in OCD, our results suggest that anhedonia may play an important role in the psychopathology of OCD. This is especially important considering that current assessment procedures and treatment protocols do not target anhedonia. Future research should focus on the nature of anhedonia's association with OC symptomology beyond depressive severity and implications for treatment.

Poster Number 159

Rusu, Corina BS
Research Technician, Medicine
crusu@partners.org

Projecting 10-yr, 20- yr and Lifetime Risks of Cardiovascular Disease in HIV-Infected Individuals in the US: Competing Risks and Premature Aging

Investigators: Losina, E, PhD; Linas, BP, MD, MPH; Hyle EP, MD, MPH; Rusu C, BA, BS; Noubary F, PhD; Berkowitz BK, BA; Sax PE, MD; Weinstein MC, PhD; Walensky RP, MD, MPH; Freedberg KA, MD, MSc

Background: Cardiovascular disease (CVD) is an important cause of morbidity and mortality in HIV+ persons. We estimated the 10-yr, 20-yr and lifetime risk of CVD in HIV+ persons compared to both the US general population and those at high risk for HIV disease.

Methods: We extended a validated computer simulation of HIV disease, the Cost-Effectiveness of Preventing AIDS Complications (CEPAC), to incorporate age- and sex-specific CVD incidence, prevalence and attributable mortality. We simulated 3 male and 3 female cohorts: 1) the general US population; 2) HIV-, but at high risk for HIV; and 3) newly HIV+. Each cohort was followed from mean age of HIV infection in the US (34 yrs) until death. We projected 10-yr, 20-yr, and lifetime cumulative CVD risk for each cohort, accounting for competing mortality. The general population CVD prevalence was from the 2010 National Health Interview Survey; CVD-attributable mortality was from the CDC. To approximate the increased CVD risk in those at high risk for HIV, we used data on smoking prevalence in HIV+ persons (60% vs. 20% in the general population) and the increased CVD risk from smoking from the Framingham Heart Study (HR =1.7/1.9 F/M). We used standardized mortality ratios to adjust for higher all-cause mortality in those at high risk for HIV. In the base case, CVD prevalence, incidence and attributable mortality were shifted up by 10 years for HIV+ persons as a surrogate for "premature aging" (Guaraldi, CID 2010). HIV+ persons were assumed treated per 2012 US ART guidelines. We performed sensitivity analyses on the magnitude of the premature aging "shift" (1-15 years), the increased CVD risk from smoking, and other parameters.

Results: In the base case, the 10-yr CVD risk in the HIV+ cohort increased ~50% compared to the general population (9.4 to 15.3%M, 6.8 to 10.3%F), and was ~35% higher for males and ~25% higher for females compared to HIV- persons at high risk (Table 1). These trends decreased at 20 years. Lifetime CVD risk was lower in the HIV+ (50% M/33% F) compared to the general population (65%M/55%F) due to competing mortality from HIV. In sensitivity analyses, the premature aging shift had the greatest impact. If the shift was <2.5 yrs, then the 10-yr CVD risk among the HIV+ was lower than in the general population.

Conclusions: HIV disease increases 10-yr and 20-yr risk of CVD compared to those not infected, despite competing mortality. CVD prevention should be integral to HIV disease management.

Table 1: 10-yr, 20-yr and lifetime risks of CVD in HIV-infected and uninfected individuals from age 34

	10-yr CVD risk (%)	20-yr CVD risk (%)	Lifetime CVD risk (%)
Males			
General US population	9.4	19.5	65.3
HIV-uninfected/high risk for HIV	11.8	23.7	70.5
HIV-infected	15.3	28.3	49.8
Females			
General US population	6.8	14.4	55.3
HIV-uninfected/high risk for HIV	8.1	15.8	44.8
HIV-infected	10.3	18.7	33.1

Poster Number 160

Searl, Meghan PhD, ABPP-CN
Instructor, Dermatology Service
msearl@partners.org

Predictors of Health Behaviors in a Group of Community-Dwelling Adults

Investigators: Meghan M. Searl, PhD, ABPP-CN; Timothy M. Hale, PhD; Julie Kvedar; Shiyi Zan, BS; Kamal Jethwani, MD, MPH

Introduction: One of the greatest challenges in clinical medicine is getting patients to comply with preventative health recommendations and treatments. Despite knowing the risks of unhealthy lifestyles, most Americans eat poorly, do not exercise, and are non-compliant with treatment regimens. The objective of this study was to explore why some patients engage in healthy behaviors and others do not. Study findings may help align interventions for healthy lifestyles with motivating forces and barriers to change.

Methods: Health Care Providers (HCPs) and community-dwelling patients were recruited from a Boston area community health center. Eight HCPs participated in semi-structured interviews about what motivates and impedes health behavior change in their patients. Following the interviews, HCPs were asked to identify patients from their clinical practices who engaged in unhealthy behaviors and had been resistant to making recommended healthy lifestyle changes ("inactive") and others who had successfully made lifestyle changes and were engaged in healthy behaviors on a regular basis ("active"). In total, sixteen patients participated in two semi-structured focus groups (n = 7 "inactive", n = 9 "active") and completed a brief questionnaire. Focus group transcripts were coded for emergent themes. Survey responses were analyzed for descriptive statistics and differences between the two patient groups.

Results: HCPs cited several barriers for patients attempting to make lifestyle changes, including: time constraints due to work and family obligations; inaccurate perceptions of healthy body weight; longstanding habits of physical inactivity and high caloric intake; and depression and low energy. HCPs noted that patients who had successfully made lifestyle changes tended to take a step-by-step, problem-solving approach to reach key goals. Objective, data-driven feedback had been critical in helping patients understand the connections between their behaviors and health outcomes. Active patients tended to be slightly older than inactive patients (67.3 versus 58.7 years) but did not differ significantly in other socio-demographic characteristics. Active patients had lower BMIs than inactive ones (29, "overweight" versus 37, "severely obese"). Reasons inactive patients gave for not engaging in healthy behaviors included: work and family obligations that took precedence over their personal health, depressive symptoms, lack of energy; exercise-induced pain; and physical limitations. Potential motivators included: preventing future illness, feeling and looking better, having more energy, and being a good role model. Active patients described coming to a turning point where they understood they could either prioritize their health or continue to be ill. Motivators included: pain relief, reduced symptoms, and increased vitality.

Conclusion: For many people, work and family obligations can make it difficult to initiate or maintain new behaviors. Increased activity involves seeing one's personal health as a priority and connecting behavior changes to better health, including fewer symptoms. Active individuals use exercise to reduce pain levels. Inactive individuals report more exercise-induced pain, as well as greater depression and low energy levels overall. Future interventions designed to facilitate lifestyle changes should assess and treat depression, address distress tolerance, and incorporate objective, data-driven feedback on progress towards patient identified goals (i.e., pain reduction, energy level).

Poster Number 161

Sharma, Umesh MD
Research Fellow, Radiology
ucsharma@partners.org

Cardiac MRI identifies the Possible Cause of Sudden Cardiac Arrest in more than 50% of Resuscitated Patients

Investigators: Umesh Sharma, MD, PhD; Brian Ghoshhajra, MD; Asley M. Lee, BS; Stefan Punchner, MD; Udo Hoffmann, MD; Suhny Abbara, MD

Background: Sudden cardiac arrest (SCA) results from malignant ventricular arrhythmias that may be due to myocardial infarct, ischemia, edema, fibrosis or infiltration. The underlying cause is often unknown. Cardiovascular magnetic resonance (CMR) may provide structural and functional data and identify myocardial ischemia, inflammation and fibrofatty infiltration.

This study determines the diagnostic ability of CMR in SCA of unknown cause.

Methods and Results: Seventy-six patients with SCA of unknown cause underwent CMR. The results were adjudicated into either non-diagnostic (no convincing cause identified) or diagnostic CMR. Of the 76 CMR studies 40 (52%) demonstrated potentially causative or related otherwise unknown pathology: 11 (14%) recent ischemia or major LV wall motion defects, 7 (9%) myocarditis, 6 (7%) arrhythmogenic right ventricular dysplasia (ARVD), 5 (6%) LV intramyocardial fibrosis, 7 (9%) LVEF of <40%, and 5 (6%) RV fat. No potential cause for SCA was identified in 35 (46%) patients.

Conclusions: CMR can identify otherwise undetected possible etiologies of SCA in more than half of resuscitated patients.

Tang, Rong MD
Research Fellow, Cancer Center
rtang1@partners.org

Poster Number 162

Impact of Prior Radiation Therapy on Post-operative Complications in Nipple Sparing Mastectomy and Immediate Reconstruction: A Case-Matched, Risk-Adjusted Cohort Study

Investigators: Rong Tang, MD; Kari J. Kansal, MD; Lan Lei, MD; Suzanne B. Coopey, MD; Amy S. Colwell, MD; Michele A. Gadd, MD; Michelle C. Specht, MD; Alphonse Taghian, MD, PhD; William G. Austen, Jr. MD; Barbara L. Smith, MD, PhD

Introduction: Prior radiation therapy is considered a relative contraindication to nipple sparing mastectomy and immediate reconstruction (NSM) due to concerns about increased risk of post operative complications. We examined the attributable risk of prior radiation on post operative complications in patients undergoing NSM in a case-matched series.

Methods: We retrospectively reviewed NSM from 6/06-7/12 at our institution and matched (1:1 or 1:2) previously irradiated to unirradiated breasts. Breasts were matched for risk factors for post-operative complications including: age, smoking status, incision (periareolar vs. non-periareolar), breast volume and type of reconstruction. No patient had insulin dependent diabetes. Patient demographics, operative details and clinical outcomes were collected.

Results: From 511 consecutive NSM, we matched 38 irradiated breasts with 72 unirradiated breasts. Median follow-up was 8.5 months. Among 38 irradiated breasts, 8 breasts (21%) had some complication: 6 (16%) had skin/nipple necrosis requiring additional surgical revision and 1 (3%) had an infection requiring implant removal. Overall, 3 nipples (8%) and 1 implant (3%) were lost to complications in the irradiated cohort. Among 72 matched unirradiated breasts, 9 (13%) had some complication: 3 (4%) had skin/nipple necrosis and 3 (4%) had an infection requiring implant/expander removal. Overall, 2 nipples (3%) and 3 implants (4%) were lost to complications in the unirradiated cohort. Prior radiation was associated with increased skin/nipple necrosis even when adjusted for other risk factors (Odds ratio 4.3, 95% CI 1.1-16.7; p = 0.04). There were no statistically significant differences in infection, implant loss or hematomas between radiated and unirradiated cohorts (Table 1).

Conclusion: Although rates of skin necrosis requiring surgical revision are higher in previously irradiated breasts, implant loss is rare and nipple loss and infection are infrequent. Previous breast irradiation is not a contraindication to nipple sparing mastectomy and immediate reconstruction.

Table 1. Patient characteristics and complications after NSM and reconstruction (per breast)

		Irradiated N=38	Unirradiated N=72	p-value
Patient characteristics				
Mean age (years)		50	49	0.5
Mean breast volume (cc)*		420	423	0.96
Mean BMI		23	24	0.5
Alloderm use		28 (74%)	51 (71%)	0.82
Therapeutic (cancer as indication for mastectomy)		22 (58%)	39 (54%)	0.84
Reconstruction	Tissue Expander	8 (21%)	16 (22%)	1.0
	Single Stage Implant	28 (74%)	53 (74%)	1.0
	TRAM	2 (5%)	3 (4%)	1.0
Complications				
Skin/nipple necrosis requiring surgical management		6 (16%)	3 (4%)	0.04
Nipple loss due to necrosis		3 (8%)	2 (3%)	0.22
Infection		1 (3%)	3 (4%)	0.57
Implant loss**		1 (3%)	3 (4%)	0.57
Capsular contracture requiring implant exchange		0 (0%)	2 (3%)	0.43
Hematoma		1 (3%)	3 (4%)	0.57

*Breast volume was calculated with a half ellipsoid volume (cc) calculator using the three dimensions from the pathology gross measurement.
**All implant/tissue expander loss was due to infection

Poster Number 163

Zaitchik, Deborah PhD
Assistant Professor, Psychiatry
dzaitchiksamet@partners.org

The role of executive function on biological reasoning in healthy elderly: An individual differences study

Investigators: Nathan Tardiff, M.A.; Kaitlin Sandor, BS; Deborah Zaitchik, PhD

An intuitive understanding of biology is universally established in children between the ages of 6 and 10. This initial biological theory (known as 'Vitalist biology') encompasses the understanding that the body is a system whose various parts work together to acquire vital energy from air, food, and water and to move it around the body with the goal of sustaining life. On this view, to be alive is to have vital energy and to die is to lose it. Prior to this development, preschool children—who have little knowledge of the body and the lifecycle—attribute life to entities that appear to be active or moving. This tendency leads to incorrect 'animist' attributions of life to inanimate entities such as the sun and the wind; moreover, it denies life to plants. These animist attributions may be a result of an innate or early learned concept of agency, a concept embedded in a theory of behavior and mental states, not biology. Surprisingly, previous research has shown that some healthy elders (as well as most patients with Alzheimer's disease) make the same sorts of animist judgments as do preschool children. A forthcoming study of 5-7 year olds suggests that one factor affecting children's biological reasoning is their executive function. In this individual differences study, children's performance on executive function tasks predicted their biological reasoning performance, controlling for age and verbal IQ. The current study extends this line of research to healthy elderly, asking the following: Do executive function scores in healthy elderly (who are known to have diminished executive function compared to healthy young adults) predict their biological reasoning scores? In this individual differences study, two batteries were administered to a sample of 29 healthy elderly volunteers from the MGH GRU. The biology battery consisted of the Piagetian animism task, which probes what it means to be alive, an interview about death, and an interview assessing knowledge of body parts and their functions. The executive function battery consisted of the Trail-Making test, the Stroop test, category fluency, and digit span forwards and backwards. The National Adult Reading Test was also administered as a measure of verbal IQ. Preliminary results show that executive function predicts biological reasoning in healthy elderly, controlling for age and verbal IQ. The role of executive function in biological reasoning suggests that immature concepts of agency still exert powerful interference, interference that makes strong demands on executive resources. Decreasing executive resources due to age then allow these immature concepts to resurface.

Poster Number 164

Zarins, Bertram MD
Professor, Orthopaedics
bzarins@partners.org

Release of adductor longus tendon for recalcitrant pain

Investigators: Thomas J. Gill IV, MD; Kaitlin Carroll, BS; Bertram Zarins, MD

Chronic strain and/or tendinopathy of the adductor longus tendon can be a cause of long-standing groin pain in athletes and results in significant time lost from competition. Non-operative treatments can be unsuccessful, and little has been written about the operative treatment of chronic pain in the adductor longus.

Isolated release of the adductor longus tendon for the treatment recalcitrant pain in athletes localized to the adductor longus allows for reliable pain relief and predictable, timely return to sport. The purpose of this study is to present the indications, surgical technique, rehabilitation protocol and 5-year minimum follow-up results of isolated release of the adductor longus tendon for the treatment of recalcitrant adductor pain.

A retrospective review was performed of all patients who underwent isolated release of the adductor longus tendon for chronic groin pain by a single surgeon from April 1999 to February 2003. Every patient was a competitive athlete who reported pain localized to the groin, below the inguinal ligament, lasting greater than 10 weeks, limiting their ability to compete, and pre-operatively, all patients attempted and failed non-operative management., Excluded from this study were patients with osteitis pubis, history of an inguinal, femoral or “sports” hernia, prior abdominal or pelvic surgery, radiographic evidence of degenerative joint disease of the hip, clinical evidence of greater trochanteric bursitis, prostatic or urinary tract disease, or nerve entrapment of the ilioinguinal, genitofemoral, or lateral femoral cutaneous nerves..

Fifteen patients with an average follow-up of 7.2 ± 1.2 years (range, 5.1–8.8 years) underwent the procedure with no complications. Fourteen patients (93.3%) had significant improvement in their symptoms, and 12 patients (80%) were asymptomatic at final follow-up. Fourteen patients (93.3%) returned to their respective sport and 13 patients (86.7%) returned to their previous level of competition and ability. The average length of time to return to sport was 14.3 ± 1.6 weeks, and 26.2 ± 4.6 weeks to be symptom free during competition. Eleven athletes (73.3%) reported that they would undergo surgery again.

In this study of competitive athletes, isolated release of the adductor longus tendon provided overall good and excellent results. Athletes were able to return to a previous level of athletic competition and ability with consistent relief of groin pain emanating from below the inguinal ligament.

Poster Number 165

Arakaki, Ryan BS
Medical Student, Dermatology Service
ryan_arakaki@hms.harvard.edu

The Impact of Dermatology Consultations on Antibiotic Usage for Suspected Cases of Cellulitis Presenting to Outpatient Internal Medicine Offices

Investigators: Ryan Arakaki, BS; Elaine Woo, MD; Daniela Kroshinsky, MD, MPH

Introduction: Cellulitis is an acute infection of the dermis and subcutaneous tissue, often complicating skin trauma. It is a common and costly problem, with an annual estimated prevalence of 14.5 million cases and cost of $3.7 billion dollars. Despite the frequency and associated expense, there are no existing gold standard diagnostic techniques or reliable evidence-based diagnostic criteria.

There are many conditions that clinically mimic cellulitis, but very little research has been performed assessing the magnitude of misdiagnosis or addressing ways to correct the problem. This issue has become more pertinent as rates of antibiotic resistant organisms are on the rise, possibly due to unnecessary administration of antibiotics, such as with pseudocellulitis. Dermatologist expertise in infectious and inflammatory skin diseases facilitates confirmation of diagnoses or identification and proper treatment of a clinical mimicker. Internist utilization of dermatologist consultation may help identify and treat pseudocellulitides.

Our study sought to determine if obtaining dermatology consultations in the setting of primary care offices could assist in diagnosis of mimickers of cellulitis and therefore reduce the rate of antibiotic usage and improve diagnostic accuracy. The primary objective was to measure the rate of antibiotic usage in patients with suspected cellulitis who received a dermatology consultation versus those who received standard of care for cellulitis from their primary care physician.

Methods: This was a randomized controlled study performed in the outpatient internal medicine offices at Massachusetts General Hospital, including the Internal Medicine Associates, Bulfinch Medical Group, and Medical Walk-in offices. The patient population of interest included all adult patients over the age of 18 presenting to primary care with possible cellulitis as determined by their primary care physician, with the exclusion of postoperative site infections, abscesses, human/animal bites, osteomyelitis, hardware/line infections, and pregnant women. The intervention used was an on-site dermatology consultation occurring in the primary care physician's office. Outcomes that were measured included if the patient required hospitalization and if antibiotics were prescribed. Statistical analysis of study results included comparison of antibiotic usage rates between the treatment group (patients who received a dermatology consultation) versus the control group (patients who received usual care through their primary care physician).

Results: This study enrolled 25 total patients with 16 patients randomized to a dermatology consultation (the treatment arm) and 9 patients randomized to receive the standard of care for cellulitis (the control arm). Of the 16 patients randomized to a dermatology consult, 3 patients received antibiotics and 13 did not. None of the patients randomized to a consultation were hospitalized. Of the 9 patients randomized to the standard of care, all 9 received antibiotics and one patient required hospitalization. The original enrollment goal of this study was 248 patients, however, this study was terminated prior to reaching the original enrollment target because interim analysis showed statistical significance. A Fisher's exact test demonstrated a P-value of 0.0001. No adverse events occurred in this study.

Conclusion: This study was notable for demonstrating that the rate of antibiotic usage in patients with suspected cellulitis can be reduced by involving a dermatology consultation during a patient's visit to primary care offices. We believe that the difference in antibiotic usage rates highlights the prevalence of conditions that mimic cellulitis and the potential benefit of early involvement of dermatology in the care of patients presenting with suspected cellulitis. As a result of this study, we have initiated a similar project to assess the impact of dermatologic consultation on the hospital course of patients who have been admitted for cellulitis.

Poster Number 166

Salcedo, Stephanie BA
Clinical Research Coordinator, Psychiatry
ssalcedo@partners.org

The Effects of Different Psychosocial Interventions on Disrupted Sleep Patterns in Patients with Bipolar Disorder: Results from a Randomized Clinical Trial (STEP-BD)

Investigators: Stephanie Salcedo, BA; Louisa Sylvia, PhD; Amy Peters, BA; Andrew Nierenberg, MD; Thilo Deckersbach, PhD

Introduction: Sleep disturbance is a common symptom of bipolar disorder. During manic episodes, bipolar patients report a reduced need for sleep, whereas during depressive episodes, they suffer from insomnia or hypersomnia. Furthermore, sleep disturbance often persists in remission and is associated with a more severe course of illness. Various psychosocial treatments for bipolar disorder intervene on social rhythm patterns, such as sleep wake cycles, but no prior studies have determined whether these treatment modalities differentially improve upon sleep disturbance. The present study examined the relative effect of different psychotherapy interventions for bipolar disorder on sleep patterns in a cohort of participants from the National Institute of Mental Health Systematic Treatment Enhancement Program for Bipolar Disorder (STEP-BD).

Methods: STEP-BD was a national, multi-site study that examined the effectiveness of different treatment combinations for symptoms of bipolar disorder. Embedded within STEP-BD was a randomized control trial of adjunctive psychotherapy for bipolar patients in a depressive episode. Of the 269 participants enrolled in the trial 243 had data available on sleep at baseline and follow up. 107 received a brief control intervention (CC), and 136 received one of three intensive psychotherapies (cognitive behavioral therapy (CBT), n = 63; family-focused therapy (FFT), n = 24; interpersonal and social rhythm therapy (IPSRT), n = 49). Sleep was operationally defined as total sleep time (average sleep time in a week) and sleep variability (difference between the maximum and the minimum hours of sleep per night in a week).

Results: Mixed model analyses of variance (ANOVA's) indicated participants in both the collaborative care and intensive psychotherapy (IP) groups experienced a reduction in total sleep time from baseline (CC: M = 8.46, SD = 2.61; IP: M = 7.97, SD = 2.81) to post treatment (CC: M = 7.71, SD = 2.14; IP: M = 7.39, SD = 1.77) and sleep variability from baseline (CC: M = 3.84, SD = 3.80; IP: M = 3.76, SD = 3.20) to post treatment (CC: M = 2.97, SD = 2.52; IP: M = 2.87, SD = 3.00), $F(1) = 14.33$, $p < .01$ (sleep time), and $F(1) = 10.85$, $p < .01$ (sleep variability). Sleep time and variability did not change differentially between the control versus the treatment groups over the study period, $F(1) = .24$, $p = .62$ (sleep time), and $F(1) = .00$, $p = .96$ (sleep variability). Within the intensive psychotherapy groups, participants in each of the interventions (CBT, FFT, IPSRT) experienced a reduction in overall sleep time and variability from baseline to post treatment, $F(1) = 4.69$, $p < .05$ (sleep time), and $F(1) = 7.28$, $p < .01$ (sleep variability). However, sleep time and sleep variability did not differ according to type of intensive psychotherapy, $F(2) = .38$, $p = .68$ (sleep time), and $F(2) = .69$, $p = .50$ (sleep variability).

Conclusions: Psychosocial interventions, including brief interventions like collaborative care, help improve disrupted sleep patterns by reducing sleep variability in patients with bipolar disorder. Future research should investigate how psychosocial interventions play a role in reducing total sleep time and how changes in sleep patterns are associated with changes in bipolar mood symptoms to better understand the role of sleep in the course of illness.

Poster Number 167

Shenoy, Erica S. MD, PhD
Clinical Research Fellow, Medicine
eseiguershenoy@partners.org

Concordance of PCR and culture from nasal swabs for MRSA in setting of concurrent anti-staphylococcal antibiotics

Investigators: Erica S. Shenoy, MD, PhD; JiYeon Kim, MD, MPH; Eric S. Rosenberg, MD; Jessica A. Cotter, MPH; Farzad Noubary, PhD; Hang Lee, PhD; Rochelle P. Walensky, MD, MPH; David C. Hooper, MD

Background: The effect of concurrent administration of antibiotics with activity against methicillin-resistant Staphylococcus aureus (MRSA) on detection of this organism from nasal surveillance swabs remains unresolved. Given widespread inpatient antibiotic use, whether antibiotics affect the ability to recover MRSA has important implications for clinical practice and Infection Control strategies.

Methods: We performed an analysis of subjects enrolled in a randomized-controlled trial comparing alternative strategies for documentation of MRSA clearance. We examined 259 subjects in the active screening arm who were simultaneously tested using CHROMagar (CA, BD Diagnostics) and molecular methods ("PCR", GeneXpert MRSA, Cepheid). We evaluated the concordance between CA and PCR of paired nasal swabs in the presence and absence of antibiotics with known activity against MRSA. The data were analyzed using exact McNemar's tests for marginal homogeneity.

Results: Among the 259 subjects, 127 paired samples were obtained in the absence of antibiotics, where there was a concordance of 93.7% ((40+79)/127; Table 1A). The exact McNemar's test revealed no significant difference in the proportion of positive test results (P=0.29). Of the 132 paired samples obtained in the presence of antibiotics there was a concordance rate (positive and negative) of 90.9% ((44+76)/132; Table 1B) and a statistically significant increase in the proportion of positive tests using PCR (P <0.01).

Conclusion: In the absence of antibiotic administration, there was no significant difference in the proportion of positive test results between CA and PCR among discordant pairs. With concurrent antibiotic administration, PCR recovered MRSA significantly more frequently. This suggests increased sensitivity of PCR compared to CA for screening and a potential advantage to PCR for detection of MRSA in populations with widespread antibiotic use.

Table 1. Concordance of PCR and Culture

A. Test Results : No Concurrent anti-MRSA Antibiotics (N = 127)			
	CA+	CA –	Total
PCR +	40	6	46
PCR–	2	79	81
Total	42	85	127
B. Test Results: Concurrent anti-MRSA Antibiotics (N= 132)			
	CA+	CA –	Total
PCR +	44	11	55
PCR–	1	76	77
Total	45	87	132

CA= chromogenic agar; PCR= polymerase chain reaction; antibiotics defined by Study Protocol. Blue-shaded cells represent concordant paired results and total subjects.

Poster Number 168

April, Michael BS, DPhil, MD, MS
Resident, Emergency Medicine
Michael.D.April@post.harvard.edu

The Survival Benefits of Antiretroviral Therapy in South Africa

Investigators: Michael D. April, MD, DPhil,[1,2] Robin Wood, FCP, MMed, DTM&H,[3,4] Bethany K. Berkowitz, BA,[5-7] A. David Paltiel, PhD,[8] Xavier Anglaret, MD,[9,10] Elena Losina, PhD,[11-13] Kenneth A. Freedberg, MD, MSc,[5-7,11,12,15] Rochelle P. Walensky, MD, MPH,[5-7,11,14]
Affiliations: [1]Department of Emergency Medicine, San Antonio Uniformed Services Health Education Consortium, San Antonio, TX; [2]Harvard Medical School, Boston, MA; [3]Desmond Tutu HIV Centre, Institute of Infectious Disease and Molecular Medicine, and [4]Department of Medicine, University of Cape Town, South Africa; [5]Division of General Medicine, [6]The Medical Practice Evaluation Center, and [7]Division of Infectious Diseases, Department of Medicine, Massachusetts General Hospital, Boston, MA; [8]Yale School of Public Health, New Haven, CT; [9]INSERM Unité 897, Centre de Recherche "Epidémiologie et Biostatistique" and Université Victor Segalen Bordeaux, France; [10]Programme PAC-CI, Abidjan, Côte d'Ivoire; [11]Center for AIDS Research (CFAR), Harvard University, Boston, MA; [12]Departments of Biostatistics and Epidemiology, Boston University, Boston, MA; [13]Department of Orthopedic Surgery, and [14]Division of Infectious Diseases, Brigham and Women's Hospital, Boston, MA; [15]Department of Health Policy and Management, Harvard School of Public Health, Boston, MA

Objective: To quantify survival gains attributable to antiretroviral therapy (ART) in South Africa.

Methods: We used a state-transition computer model to project survival for seven cohorts, each representing HIV-infected persons who started ART in South Africa in a given year during 2004-2010. Model inputs included cohort-specific mean CD4 at ART initiation (112-178/μL), 24-week ART efficacy for viral suppression (78%), availability of 2nd-line ART (up to 2.4% of all ART patients), and cohort-specific 36-month retention rate (54-69%). For each cohort, survival among patients who started ART was compared to survival of an identical cohort that did not initiate ART. Population life years gained (LYG) were calculated as the sum of the product of per capita survival gain and number of persons initiating ART (based on United Nations data and estimated retention rates) for each cohort. We projected LYG censored as of July 2011 (realized gains), and uncensored LYG (lifetime gains) for those patients who initiated ART during 2004-2010. We conducted sensitivity analyses by repeating our analyses using ranges of inputs reflecting uncertainty in base-case values for CD4 at ART initiation (38-232/μL), ART efficacy for viral suppression (54-97%), availability of 2nd-line ART (0-4.8%), and 36-month retention rate (32-76%).

Results: Realized per capita survival gains in South Africa ranged from 3.3 LYG for persons who started ART in 2004 to 0.1 LYGs for persons who started in 2010. Lifetime per capita survival gains ranged from 8.8 LYG for persons who started ART in 2004 to 8.9 LYG for persons who started ART in 2010 (Table). Accounting for increasing numbers of patients initiating ART, retention, transfers out, and death, the total population lifetime survival benefit for all patients who started ART during 2004-2010 is 14.8 million LYG; 1.7 million (11.5%) of those have been realized by July 2011. Sensitivity analyses revealed the impact on uncensored lifetime survival gains of adjustments to model inputs defining CD4 count at ART initiation (14.4-14.9 million), ART efficacy (9.6-23.9 million), availability of 2nd-line ART (14.7-15.0 million), and retention (14.0-15.7 million).

Conclusions: Even a conservative assessment finds dramatic survival gains, justifying sustained international support of current treatment programs. Extending this analysis to capture the benefits of ART roll-out and reduced HIV transmission might justify further expansion of treatment services.

Poster Number 169

Bassett, Ingrid MD, MPH
Assistant Professor, Medicine
ibassett@partners.org

Risk factors for late-stage HIV disease presentation at initial HIV diagnosis in Durban, South Africa

Investigators: Paul K. Drain, MD, MPH; Elena Losina, PhD; Senica Chetty, MSc; Janet Giddy, MBChB, MFamMed; Douglas Ross, MBChB, MBA; Jeffrey N. Katz, MD; Sharon Coleman, MS, MPH; Laura M. Bogart, PhD; Kenneth A. Freedberg, MD, MSc; Rochelle P. Walensky, MD, MPH; Ingrid V. Bassett, MD, MPH

Background: Despite expanded access to HIV testing, most newly-diagnosed South Africans present with severe immunosuppression. We sought to determine the risk factors for presentation with late-stage HIV disease and the perceived barriers to presenting earlier for care.

Methods: We enrolled and surveyed adults prior to HIV testing at four outpatient clinics in urban and peri-urban areas of Durban from August 2010 to November 2011. Late-stage HIV disease was defined as a CD4 count <100 cells/mm3. We used multivariate logistic regression models to determine the effects of sex, emotional health, social support, distance from the clinic, employment, perceived barriers to receiving healthcare, and foregoing healthcare to use money for food, clothing, or housing ("competing needs to healthcare") on presentation for care with late-stage HIV disease.

Results: Among 3,669 adults screened, 830 (22.6%) were enrolled, newly-diagnosed HIV-infected, and obtained a CD4 result. Among those, 279 (33.6%) presented with late-stage HIV disease. In multivariate analyses, participants who lived ≥5 kilometers away (OR 2.8, 95% CI 1.7-4.7), had reported competing needs to healthcare (OR 1.7, 95% CI 1.2-2.4), were male (OR 1.7, 95% CI 1.2-2.3), worked outside the home (OR 1.5, 95% CI 1.1-2.1), perceived health service delivery barriers (OR 1.5, 95% CI 1.1-2.1), and had poor emotional health (OR 1.4, 95% CI 1.0-1.9) had higher odds of late-stage HIV disease presentation.

Conclusions: In Durban, South Africa, the strongest independent risk factors for presentation with late-stage HIV disease were living further from the clinic, being male, and having competing needs to healthcare. Self-reported barriers related to personal illness, costs of care, and poor perceived service delivery were also significantly associated with late-stage disease presentation. Future studies should examine whether use of mobile units and financial assistance may reduce presentation with late-stage HIV disease in resource-poor settings.

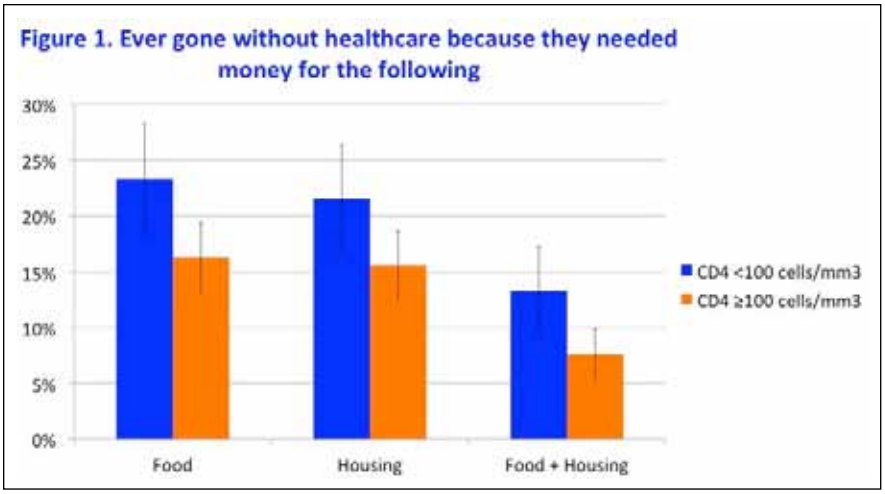

Poster Number 170

DiLorenzo, Madeline BA
Research Technician, Medicine
madilorenzo@partners.org

Routine HIV Screening in Portugal: Clinical Impact and Cost-effectiveness

Investigators: Yazdan Yazdanpanah, MD, PhD; Julian Perelman, PhD; Joana Alves, MA; Henrique Barros, MD; Céu Mateus, PhD; João Periera, PhD; Kamal Mansinho, MD; Madeline A. DiLorenzo, AB; Ji-Eun Park, BS; Eric L. Ross, BA; Elena Losina, PhD; Rochelle P. Walensky, MD, MPH; Farzad Noubary, PhD; Kenneth A. Freedberg, MD, MSc; A. David Paltiel, PhD

Background: Portugal struggles to provide universal HIV testing, counseling and referral in the face of severe epidemiological, clinical, and fiscal challenges. We sought to forecast the clinical impact and cost-effectiveness of alternative approaches to expanded HIV screening in Portugal.

Methods: We used a computer simulation model of HIV detection and treatment, coupled with Portuguese national clinical and economic data, to estimate the cost, life expectancy (LE) and the incremental cost-effectiveness ratios (ICERs) of alternative HIV screening strategies. Costs were reported in 2010 Euros (€), LE was reported in either life years (LYs) or quality-adjusted life years (QALYs), and ICERs were reported in €/QALY. Strategies were considered to be cost-effective by World Health Organization (WHO) standards if the ICER was less than 48,900 €/QALY. We compared current HIV detection practices in Portugal to routine HIV screening in adults aged 18-69. We considered a variety of target populations with differing levels of HIV risk and several testing strategies including the current strategy, one-time screening, screening every three years, and annual screening. Baseline input values included: undiagnosed HIV prevalence (0.16%), annual incidence (0.02%), mean population age (42.6 years), mean CD4 count at care initiation (292 cells/μL), test acceptance (63%), linkage to care (78%), HIV test cost (5.40€), and an annual discount rate (5%). We conducted extensive sensitivity analyses on these base case values.

Results: One-time testing increased discounted HIV-infected LE from 14.55 to 14.75 LYs and undiscounted HIV-infected LE from 36.12 to 36.59 LYs when compared to current detection practice and was associated with a cost-effectiveness ratio of 36,000 €/QALY. One-time testing yielded greater increases in discounted HIV-infected LE and was associated with a more favorable cost-effectiveness ratio in regions with greater HIV prevalence and incidence (Lisbon Region, 33,000€/QALY), compared to regions with lower HIV prevalence (Guarda Region, 45,000€/QALY). Screening more frequently was associated with favorable cost-effectiveness ratios in high-risk populations (annual screening in men who have sex with men, 48,000€/QALY; in injecting drug users, 36,000€/QALY).

Conclusions: One-time, routine, voluntary HIV screening in the Portuguese general population meets accepted international standards of cost-effectiveness. Given the economic crisis as well as the higher disease burden in certain regions, we recommend initiating routine screening both in high prevalence regions and risk groups first.

Poster Number 171

Drain, Paul K. MD, MPH
Research Fellow, Medicine
pdrain@partners.org

A prospective, clinic-based study of a urine lipoarabinomannan (LAM) test for pulmonary or extrapulmonary TB among HIV-infected adults in South Africa

Investigators: Paul K. Drain, MD, MPH; Elena Losina, PhD; Sharon M. Coleman, MS, MPH; Janet Giddy, MBChB, MFamMed; Douglas Ross, MBChB, MBA; Gary Parker; Jeffrey N. Katz, MD; Rochelle P. Walensky, MD, MPH; Kenneth A. Freedberg, MD, MSc; Ingrid V. Bassett, MD, MPH

Background: Despite introducing GeneXpert at centralized labs in South Africa, there is need for a simple, rapid, clinic-based test to diagnose tuberculosis (TB) in HIV+ adults. We sought to determine the test characteristics of a point-of-care urine lipoarabinomannan (LAM) test to diagnose active TB in HIV+ adults, when used in an outpatient setting.

Methods: We prospectively enrolled newly-diagnosed HIV+ adults (≥18 years) at 4 outpatient clinics in Durban from Oct 2011-May 2012, excluding those on TB therapy. All participants were evaluated by a clinician, offered CD4 testing, and provided sputum samples for smear microscopy and mycobacterial culture. Trained study nurses conducted 2 urine LAM (Determine TB LAM, Alere) tests on one urine sample from each participant, and interpreted results after 25 minutes. Participants were considered urine LAM+ if either test was positive. We defined the 'gold standard' of active pulmonary TB as lab-confirmed by positive sputum smear or culture. We calculated LAM diagnostic test characteristics, overall and stratified by CD4 count, for diagnosing lab-confirmed pulmonary TB. We repeated analyses after expanding the definition of active TB to include HIV+ adults with extrapulmonary TB or who were initiated on anti-TB therapy based on clinical suspicion.

Results: Of the 351 HIV+ enrollees, 195 (56%) were male, mean age was 35.3 (SD 9.7) years, and median CD4 was 180 (IQR 73-311)/mm3. Prevalence of lab-confirmed pulmonary TB was 18% (64/346), and 28% (99/351) when including extrapulmonary or clinically-suspected TB. In total, 47 (13%) participants were urine LAM+. Urine LAM test sensitivity and specificity for diagnosing lab-confirmed pulmonary TB were 25% (16/64) and 89% (251/282). Sensitivity and specificity were 23% (23/99) and 90% (228/252) when including extrapulmonary or clinically-suspected TB cases. Results were not significantly different among CD4 strata. The effects of urine LAM testing on post-test probability for lab-confirmed pulmonary TB, and when including extrapulmonary or clinically-suspected TB, are shown in the Figure.

Conclusions: In this first clinic-based study, urine LAM testing had low sensitivity, or a high false negative rate, for detecting active TB in HIV-infected adults in a TB-endemic area. Although urine LAM testing has the advantage of being a rapid, clinic-based test, the role for urine LAM testing among HIV-infected adults in TB-endemic areas is limited by poor sensitivity.

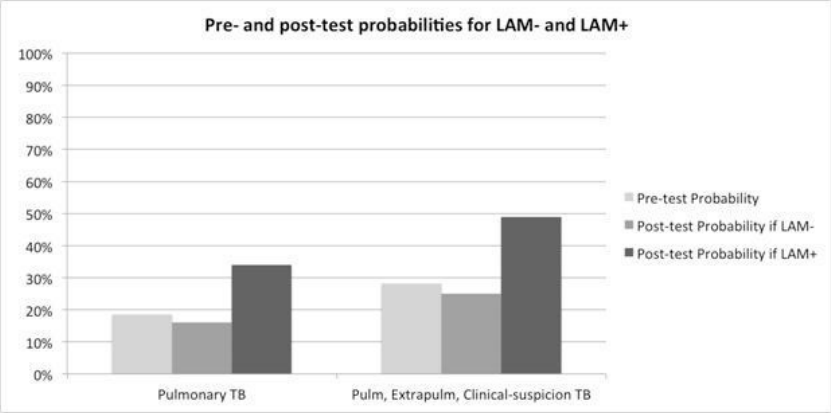

Maguire, Lillias H. MD
Resident, Surgery
lhmaguire@partners.org

Poster Number 172

Higher serum vitamin D is associated with reduced risk of diverticulitis

Investigators: Lillias H. Maguire, MD; Mingyang Song, MD, MSc; Edward Giovannucci, MD, ScD; Andrew T. Chan, MD, MPH

Background: Diverticulitis results in more than 200,000 hospital admissions per year, with incidence rising more than 40% in the last decade. Recent studies have shown geographic and seasonal variation in hospital admissions for diverticulitis, which has been previously observed in the incidence of colorectal cancer (CRC) and inflammatory bowel disease (IBD). Because this geographic and seasonal variation parallels variation in ultraviolet light exposure, the most important contributor to vitamin D status, vitamin D has been hypothesized to contribute to the etiopathogenesis of both CRC and IBD. Subsequent studies have shown that vitamin D deficiency is directly associated with risk of both CRC and IBD. Thus, we examined the association of vitamin D level with the development of diverticulitis.

Methods: We conducted a prospective study within the Partners HealthCare system, an integrated academic health system which provides care for more than 1.8 million patients. Utilizing the Partners Healthcare Research Patient Data Repository (RPDR), we identified 10,038 patients between 1993-2012 that had a measurement of serum 25 hydroxyvitamin D (25-[OH]D) level and were also diagnosed with diverticulosis and/or subsequently developed diverticulitis. We used t-tests to compare serum 25(OH)D levels among patients with uncomplicated diverticulosis to patients with specific subtypes of diverticulitis. We used multivariate logistic regression, adjusting for age, race, gender, and other comorbidities, to estimate odds ratios (OR) and 95% confidence intervals for diverticulitis compared with uncomplicated diverticulosis.

Results: Among the 9,116 patients with uncomplicated diverticulosis, the mean serum 25(OH)D level was 33.0 ng/mL compared with 27.7 ng/mL among the 922 patients with diverticulitis (p<.0001 for the difference), with serum 25(OH)D levels measured a mean of 2.3 years before onset of diverticulitis. Compared to patients with uncomplicated diverticulosis, mean serum 25(OH)D was significantly lower for each specific subtype of diverticulitis: 28.1 ng/mL (p<.0001) for those with acute diverticulitis (n=594), 28.8 ng/mL (p<.002) for those with diverticulitis with abscess/microperforation (n=124), 23.9 ng/mL (p<.0001) for those who required emergent laparatomy (n=65), and 26.5 ng/mL (p<.0001) for those with recurrent diverticulitis (n=139). Compared to patients in the lowest quintile of serum 25(OH)D, the multivariate-adjusted OR for diverticulitis was 0.26 (95% CI, 0.21-0.33) among patients in the highest quintile. Conclusion: Higher serum 25(OH)D level is significantly associated with a lower risk of diverticulitis. These data suggest that vitamin D deficiency may play a role in the pathogenesis of diverticulitis.

Poster Number 173

Merker, Vanessa L. BS
Graduate Student, Neurology Service
vmerker@partners.org

Natural history of hearing loss in newly diagnosed neurofibromatosis type 2 patients

Investigators: Vanessa L. Merker, BS; Fred G. Barker, II, MD; Alona Muzikansky, MA; William Slattery, III, MD; Scott R. Plotkin, MD, PhD

Neurofibromatosis type 2 (NF2) is a neurogenetic disorder in which patients develop bilateral vestibular schwannomas (VS). Patients typically lose hearing because of growth of the vestibular schwannomas, and may acquire other neurological deficits from cranial nerve and brainstem compression. Researchers are beginning to test medical treatments for VS in NF2 patients, and accurate knowledge of expected tumor growth and hearing loss in the untreated state is a necessary part of designing clinical trials for such drugs.

Currently, natural history data has been limited, and does not reflect recently proposed criteria for defining progression in NF2-related VS trials. For this reason, we performed time-to-event analyses on data acquired by the NF2 Natural History Consortium (an international, prospective observational study). This cohort included 118 NF2 patients with 183 VS, who were followed for a mean length of 31.7 months.

Median time to tumor growth (defined as an increase of tumor volume by >20%) was 13.4 months. 17.9% of vestibular schwannomas experienced spontaneous tumor shrinkage during follow-up; however this rate was only 13.0% in tumors ≥1cc. Median time to hearing loss (defined as a decrease in word recognition score below the 95% critical threshold) was 60.7 months. When stratified by size, the median time to hearing loss was 32 months for tumors ≥1cc and was not reached for <1cc tumors (log-rank test, $p<0.0001$). In Cox proportional hazards regressions, larger baseline tumor size was a significant risk factor for future hearing loss (Hazard Ratio 1.7, $p<0.0001$.)

Our results suggest that patients with tumors >1cc could represent a high risk group that can be targeted in hearing loss prevention clinical trials in the future. In addition, evidence that tumor shrinkage is rare in tumors greater than 1cc can be used to minimize the chance of type 1 error in future VS treatment trials.

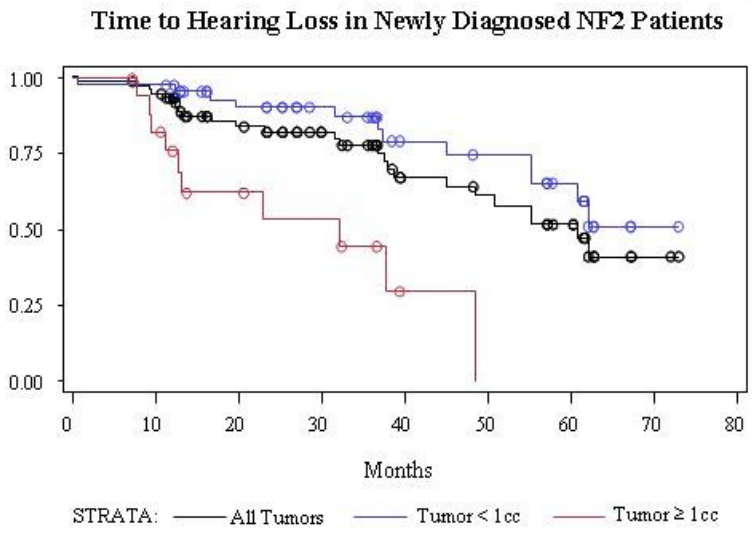

Moschovis, Peter P. MD, MPH
Clinical Research Fellow, Mass General Hospital *for* Children
pmoschovis@partners.org

Poster Number 174

Household air pollution and risk of childhood pneumonia death in low and middle-income countries

Investigators: Peter P. Moschovis, MD, MPH; Lauren B. Kleimola, MPH; Nicolas M. Oreskovic, MD, MPH; Richard T. Campbell, PhD; David C. Christiani, MD, MPH; Patricia L. Hibberd, MD, PhD

Rationale: Pneumonia is the leading cause of mortality in children under five years of age, responsible for about 2 million early childhood deaths annually. The burden of illness is disproportionately borne by developing nations; more than 99% of pneumonia deaths are in developing countries. While household air pollution (HAP) has been associated with increased incidence of childhood pneumonia, the consequences of HAP exposure on deaths due to childhood pneumonia is less clear. We evaluated the effect of HAP on risk of pneumonia death in early childhood across 38 low and middle income countries.

Methods: We used data from the World Health Survey (WHS), a multinational, multistage probability sample, conducted by the World Health Organization in 2002-2003. We restricted our analysis to 79,358 children born in the 10 years prior to the survey. Exposure to HAP was based on reported household cooking fuel and was categorized as clean fuels (liquefied petroleum gas and electricity) vs. polluting fuels (kerosene, coal, charcoal, wood, agricultural crop, animal dung, shrubs/grass and other). We compared exposure to HAP in children who died of pneumonia, defined as cough and chest indrawing on verbal autopsy (per World Health Organization criteria for severe pneumonia) with exposure to HAP in children who were alive or who died of other causes. Data were analyzed using survey procedures in SAS 9.3.

Results: A total of 393 children under age 5 died of pneumonia. Household use of polluting fuels was strongly associated with risk of childhood pneumonia death (OR = 4.33 [95% CI 2.40, 7.80]). After adjusting for sex, birth order, maternal education, maternal smoking, urban setting, and World Bank income level, household use of polluting fuels remained strongly associated with increased risk of death due to childhood pneumonia (OR = 2.41 [95% CI 1.33, 4.39], see Table).

Conclusions: We found that across 38 low and middle income nations, household use of polluting fuels increased the risk of death due to pneumonia in young children. Introduction of improved cookstoves and clean cooking fuels is urgently needed to reduce deaths due to childhood pneumonia.

Table: Multivariate Model of Predictors of Pneumonia Death

Variable	*OR*	*95% CI*	*P value*
Household Air Pollution			
Polluting Fuels	2.41	(1.33, 4.39)	0.0039
Clean Fuels	1.00	(Reference)	
Child's Sex			
Female	1.40	(0.95, 2.07)	0.0902
Male	1.00	(Reference)	
Birth Order			
First Born	1.75	(1.12, 2.75)	0.0149
Second or Later	1.00	(Reference)	
Mother's Education			
None	1.73	(0.55, 5.44)	0.2870
Primary	1.49	(0.46, 4.82)	0.7258
More than Primary	1.00	(Reference)	
Mother's Smoking Status			
Current Smoker	0.96	(0.52, 1.76)	0.8898
Not Current Smoker	1.00	(Reference)	
World Bank Income Category			
Low	1.29	(0.58, 2.87)	0.5726
Lower-Middle	1.39	(0.51, 3.76)	0.6991
Higher-Middle	1.00	(Reference)	

Poster Number 175

Robine, Marion BS
Research Assistant, Medicine
mrobine@partners.org

Finding HIV in Hard to Reach Populations: Mobile HIV Testing and Geospatial Mapping in Umlazi Township, Durban, South Africa

Investigators: Ingrid V. Bassett, MD, MPH; Susan Regan, PhD; Hlengiwe Mbonambi, MTRP; Marion Robine, BS; Jeffrey Blossom, MA; Stacy Bogan, MS; Rochelle P. Walensky, MD, MPH; Bright Mhlongo, MBChB; Hilary Thulare, MSc, MPH; Kenneth A. Freedberg, MD, MSc; Elena Losina, PhD

Background: Mobile HIV testing in community venues may help reach the goal of universal HIV testing in South Africa. Our objective was to identify the yield and characterize the population tested by mobile HIV testing units deployed by the Ithembalabantu People's Hope Clinic (IPHC) in Umlazi Township, Durban, South Africa.

Methods: We prospectively enrolled adults (≥15 years) presenting for HIV testing at a mobile HIV testing unit (mobile testers) and at the IPHC HIV clinic (clinic testers). The clinic operates mobile HIV testing units that visit venues such as taxi stands and malls. We restricted our analysis to testers with home addresses within Umlazi. Patients' addresses were manually geocoded; GPS coordinates were obtained at 26 mobile units testing sites, IPHC, and 11 other Umlazi clinics offering HIV testing and care. ArcGIS and a municipal road shapefile were used to calculate distances by road between patients' home and the site where they tested, as well as their nearest clinics. Each testing site was characterized by average distance traveled by clients, gender and age distributions, number of subjects tested, and number of new HIV cases identified.

Results: From July-November 2011, 4,759 subjects who lived within Umlazi were HIV tested; 56% of them were female. The HIV prevalence was 35% among clinic testers and 11% among mobile testers ($p<0.001$). More than 75% of all subjects tested were mobile testers, which yielded 407 new HIV cases. Mobile sites varied by average age (21-33 years), % males (25% to 77%), and number of clients tested (56-259). HIV prevalence from mobile sites varied from 1.5% (green) at a university campus to 28.0% (red) at a commercial venue (Figure). Sites with higher HIV prevalence were characterized by greater proportion of males and older age. Although the mean distance from subjects' home to a clinic offering HIV services was 1.5km, testers traveled an average of 3.3km from home to a testing site. Half of mobile testers (51%) lived closer to the clinic than to the mobile site where they tested.

Conclusion: Mobile, community-based HIV testing can identify areas of high HIV prevalence and improve access to testing. Individuals commonly access mobile testing sites that are farther from home than their nearest clinic. Geospatial techniques can be useful for optimizing deployment of mobile units in communities to maximize yield and access hard-to-reach populations.

Figure. Geospatial distribution of mobile testing sites with HIV prevalence by site

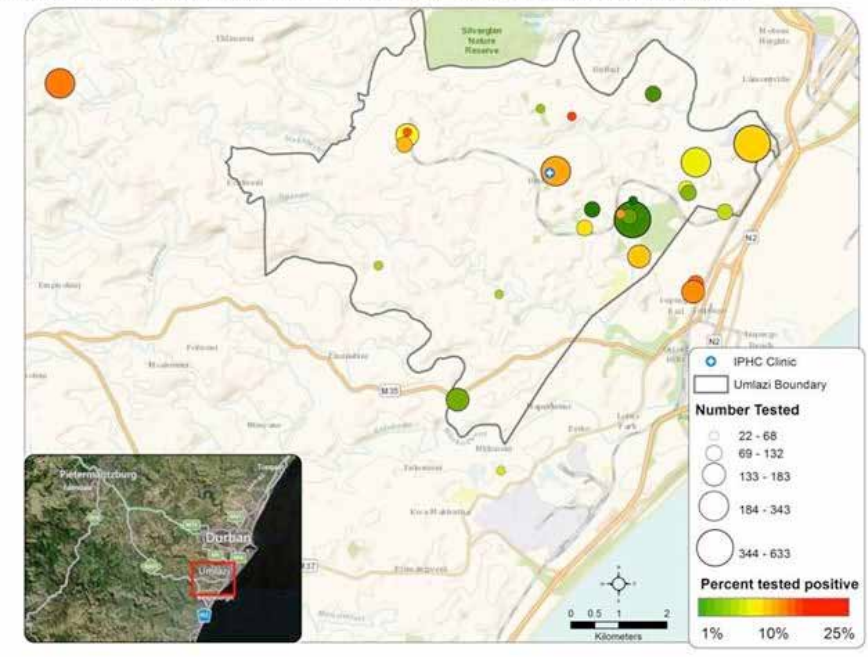

Singer, Daniel E. MD
Professor, Medicine
dsinger@partners.org

Poster Number 176

A New Risk Scheme to Predict Ischemic Stroke and Other Thromboembolic Events in Atrial Fibrillation: The ATRIA Study Risk Score

Investigators: Daniel E. Singer, MD; Yuchiao Chang, PhD; Leila H. Borowsky, MPH; Margaret C. Fang, MD, MPH; Niela K. Pomernacki, RD; Natalia Udaltsova, PhD; Kristi Reynolds, PhD, MPH; Alan S. Go, MD

Background and Objective: Atrial fibrillation (AF) is the most common significant arrhythmia. It raises the risk of ischemic stroke 5-fold. Warfarin anticoagulation markedly reduces stroke risk in AF but raises the risk of major bleeding. Guidelines recommend risk-based use of anticoagulants for AF. However, current standard stroke risk scores, i.e., the CHADS2 and CHA2DS2-VASc scores, have only moderate ability to predict stroke. We developed and internally validated a new stroke prediction model in our original ATRIA AF cohort. We then externally validated the new risk score in a contemporary incident AF cohort.

Methods: The ATRIA risk model was derived and internally validated using the Anticoagulation and Risk Factors in Atrial Fibrillation (ATRIA) AF cohort, n=13,559, assembled in 1996-97 from Kaiser Permanente Northern California and followed through 2003. We externally validated the model in the ATRIA-CVRN incident AF cohort, n=33,247, from Kaiser Permanente Northern and Southern California assembled 2006-2009 with follow-up complete through 2009. Kaiser databases provided patient features, warfarin use, and occurrence of outcome events. Ischemic stroke and other thromboembolic events (both=TE) were confirmed by chart review and a Rankin severity score was assigned. We assessed score performance in patient-time off warfarin with the c-index and net reclassification improvement metric (NRI).

Results: Cox regression models using split-sample and 1000 bootstrap sample approaches identified eight variables, plus an age*prior stroke interaction term for the final model. Point scores were assigned proportional to model coefficients (Figure 1). We observed 685 TE events within the ATRIA cohort (643 ischemic strokes) for a rate of 2.1%/yr. For the full range of point scores, the c-statistic was 0.73 (95% CI 0.71-0.75) for the ATRIA score, 0.69 (95% CI 0.67-0.71) for the CHADS2 score, and 0.70 (95% CI 0.68-0.72) for the CHA2DS2-VASc score. With point scores collapsed to low, moderate, and high scores, ATRIA classified far more patients as either high or low risk (Figure 2). The c-indexes were again higher for ATRIA and its low/moderate/high classification was more accurate (NRI=26% versus CHADS2 and 27% vs the CHA2DS2-VASc score (both p<0.0001)). 399 events were severe (Rankin score ≥3 at discharge or death by 30 days). For the full point range applied to this subset of severe events, the c-indexes increased to 0.76 (95%CI: 0.74-0.79) for the ATRIA score, 0.72 (95%CI: 0.70-0.75) for CHADS2 and 0.73 (95%CI: 0.71-0.75) for CHA2DS2-VASc.

In the ATRIA-CVRN external validation cohort 496 TEs were observed in 26,263 person-years off warfarin, rate=1.9%/yr. C-indices for the full point score for severe events (n=282) were: ATRIA: 0.75 (95% CI 0.72-0.78); CHADS2: 0.69 (95% CI 0.66-0.72); and CHA2DS2-VASc: 0.71 (95% CI 0.68-0.74). Similar, significantly improved NRI due to the ATRIA score was seen in ATRIA-CVRN, as well.

Conclusions: The rigorously developed ATRIA score improved stroke prediction in both the derivation and independent validation cohorts compared to current standard scores. The model performs particularly well in predicting disabling/fatal events which are the greatest concern for patients and physicians. The ATRIA stroke risk score should improve the anticoagulation decision for patients with AF.

ATRIA Stroke Risk Model		
Risk Factor	Points without prior stroke	Points with prior stroke
Age ≥85	6	9
Age 75-84	5	7
Age 65-74	3	7
Age <65	0	8
Add 1 point each for: Female, Diabetes, CHF, Hypertension, Proteinuria and eGFR<45 or ESRD		

Figure 1. ATRIA Stroke Risk Model point scoring system

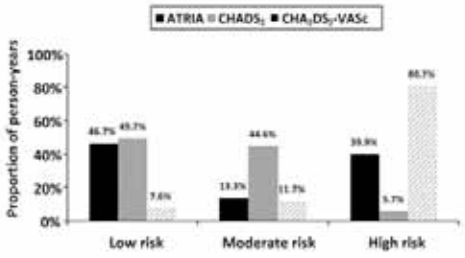

Figure 2. Distribution of person-years by risk category applying the ATRIA, $CHADS_2$ and CHA_2DS_2-VASc stroke risk scores to the full ATRIA off-warfarin cohort using the original published score cut-offs for low, moderate, and high risk categories. Annual stroke rates for low, moderate and high risk groups respectively were 0.63%, 1.91% and 3.89% using the ATRIA score, 0.88%, 2.96% and 5.97% with $CHADS_2$, and 0.04%, 0.55%, and 2.52% with CHA_2DS_2-VASc.

Poster Number 177

Sulemanji, Demet S. MD
Instructor, Anesthesia, Critical Care and Pain Medicine
dsulemanji@partners.org

Mechanical ventilation demographics between 1999 and 2009 at MGH

Investigators: Demet S. Sulemanji, MD; Edward Burns, RRT; Robert Kacmarek, PhD, RRT

Efforts at many levels are being directed at decreasing the economic burden of mechanical ventilation (MV), its related complications and their consequences. Our aim was to determine length of mechanical ventilation, reintubation rates and use of noninvasive ventilation (NIV), over a ten-year-period.

Data were retrospectively collected using the Respiratory Care Services' Database. Number of invasive and noninvasive MV services, their sequence if both were used for a given patient, the duration of the services, and reintubation episodes for years 1999 to 2009 were extracted. Five intensive care units (ICU) were included; Surgical, Medical, Neuro, Coronary and Burn ICUs. If a patient was reintubated within 48 hours (hr) of extubation, the case was regarded as a single episode of MV and duration was calculated accordingly. For NIV, if restarted within 48 hr, it was counted as a single episode as well.

A total of 23,894 IV and 3660 NIV episodes were identified during this period. Number of MV episodes increased from 2011 in 1999 to 2493 in 2009 with an increasing NIV/IV ratio (from 0.06 to 0.21). In the medical and surgical ICUs, median IV days decreased from 4 to 3 and 3 to 2 days respectively. Overall, 76% of IV episodes lasted < 7 days, 14% between 8 and 14 and 10% >15 days. Number of < 7 day- IV episodes increased by 7% and >15 day-episodes decreased by 7% from 1999 to 2009. Overall reintubation rate was 13.5%. Less-than-48-hr reintubation dropped from 14.4% in 1999 to 6.6 in 2009 while more than 48-hr reintubation remained the similar (5.2% in 1999 and 5.6% in 2009). NIV use significantly increased over this time -almost quadrupled (from 117 in 1999 to 466 in 2009). The most prominent increase was noted in the Surgical and Burn ICUs where, in 1999, NIV use was minimal (Burn: 0, SICU: 6 and 16 and 131 in 2009). Medical and Neuro ICUs doubled, CICU tripled their use. 47.7 % of NIV applications were associated with IV within 48 hr of NIV therapy. The sequence of IV-NIV revealed similar patterns through the years, overall, 59.3% of NIV application followed extubation, 25% preceded intubation and 16.7 % was in between.

We found that duration of MV decreased, reintubations within 48 hr decreased and the use of NIV increased over this 10 year period. The analysis of outcomes from our data has yet to be completed, but it would not be premature to speculate these results are related to the incorporation of SBT protocols and awaking trials, lesser use of neuromuscular blocking agents as well as extensive application of lung protective ventilation strategies.

Ciaranello, Andrea L. MD, MPH
Assistant Professor, Medicine
aciaranello@partners.org

Poster Number 178

Individualizing the WHO public health approach to infant feeding guidelines: Optimal breastfeeding duration to maximize infant HIV-free survival

Investigators: Andrea L. Ciaranello, MD, MPH; Valeriane Leroy, MD, PhD; Asinath Rusibamayila, BA; Kenneth A. Freedberg, MD; Roger Shapiro, MD, MPH; Barbara Engelsmann, MD, MSc; Shahin Lockman, MD; Francois Dabis, MD, PhD; Rochelle Walensky, MD, MPH

Introduction: To maximize HIV-free survival (HFS) among HIV-uninfected infants born to HIV-infected women, infant feeding (IF) recommendations must balance the risks of HIV acquisition through breastfeeding (BF) with the setting-specific risks of diarrhea, pneumonia, malnutrition, and death associated with replacement feeding (RF). Current IF guidelines recommend 12 months (m) of BF with antiretroviral (ARV) prophylaxis for mothers or children, but prophylaxis is not uniformly available.

Methods: Using a validated mathematical model of HIV-exposed, uninfected infants from 0-24m of age, we sought to examine BF durations (range, 0-24m) that maximized HFS. We examined combinations of scenarios stratified by: 1) maternal CD4 (< or ≥350/μL); 2) ARV prophylaxis available (none, maternal 3-drug ART, or extended infant nevirapine (NVP, for maternal CD4>350/μL); and 3) relative risk of mortality among RF compared with BF infants ("RR-RF"), ranging from 1.0-6.0 to reflect reported values in African settings. HIV infection risks through BF were from published PMTCT studies in Africa, stratified by ARV regimen and maternal CD4, and infant mortality rates were from pooled UNAIDS data, stratified by infant HIV infection status.

Results: HFS ranges from 67.2-93.6% with BF duration of 0m, and from 71.7-89.6% with BF duration of 24m. The BF duration that optimizes HFS depends on RR-RF, maternal CD4, and ARV availability (Figure). At the most commonly reported value of 2.0 for RR-RF, HFS is maximized by BF durations of: 3m for mothers with CD4 <350/μL when no ARVs are available; 6m for mothers with CD4≤350/μL receiving ART or with CD4 >350/μL when ARVs are not available (however, projected HFS with 6m and 12m of BF differ by <1.0%); and 12m for mothers with CD4>350/μL when infant NVP or maternal ART are available. Where local conditions allow for safe RF (RR-RF=1.0), avoiding BF completely maximizes HFS, regardless of maternal CD4 or ARV availability. As RR-RF increases, the duration of BF that maximizes HFS also increases; where RR-RF=6.0 (e.g., diarrheal outbreaks), optimal durations of BF range from 8m (CD4 ≤350/μL without ARV prophylaxis) to 24m (CD4>350/μL with maternal ART or infant NVP).

Conclusions: Contextualizing infant feeding recommendations remains a public health challenge. When feasible, tailoring BF duration to maternal CD4 count, availability of ARV prophylaxis, and local conditions affecting the safety of RF can optimize infant HIV-free survival.

	Maximized 24-month HIV-free survival (%) at the optimal duration of breastfeeding, indicated by shading:					
	0m	3m	6m	8-12m	18m	24m
Maternal CD4 , drug availability	RR-RF =1.0	RR-RF =2.0	RR-RF =3.0	RR-RF =4.0	RR-RF =5.0	RR-RF =6.0
≤350/μL, no ARVs	93.6	88.0	84.7	82.2	79.9	77.9
>350/μL, no ARVs	93.6	89.8	88.2	87.2	86.6	86.3
≤350/μL, maternal ART (WHO A&B)	93.6	89.2	88.0	87.3	86.9	86.6
>350/μL, infant NVP (WHO A)	93.6	90.2	89.3	88.9	88.6	88.5
>350/μL, maternal ART (WHO B)	93.6	90.6	89.9	88.9	89.4	89.4

RR-RF: relative risk of infant mortality among replacement-fed compared with breastfed infants; **ARVs:** antiretroviral drugs; **ART**: 3-drug combination antiretroviral therapy; **NVP**: nevirapine; **WHO A**: World Health Organization guidelines "Option A;" **WHO B**: World Health Organization guidelines "Option B." Breastfeeding that occurs during the first 6 months of life is assumed to be exclusive breastfeeding (no solids or liquids other than breastmilk).

Poster Number 179

Freedberg, Kenneth, MD, MS
Associate Professor, Medicine
kfreedberg@partners.org

Economic savings versus health losses: The cost-effectiveness of generic antiretroviral therapy in the United States

Investigators: Rochelle P. Walensky, MD, MPH; Paul E. Sax, MD; Yoriko M. Nakamura, BA; Milton C. Weinstein, PhD; Pamela P. Pei, PhD; Kenneth A. Freedberg, MD, MSc; A. David Paltiel, PhD; Bruce R. Schackman, PhD

Background: US guidelines recommend once-daily, one-pill efavirenz/emtricitabine/tenofovir as a preferred first-line ART regimen. With the anticipated availability of generic efavirenz in the US, the cost of a once-daily, three-pill alternative (generic efavirenz, generic lamivudine, tenofovir) will decrease, but adherence and virologic suppression may be lower. We project the clinical impact, cost, and cost-effectiveness of the generic-based vs. brand-name options.

Methods: Using an HIV simulation model (CEPAC-US), we examine 3 strategies: 1) No ART (for comparison); 2) three-pill generic-based ART; and 3) one-pill brand-name ART. Inputs are from peer-reviewed data: ART efficacies (24-week suppression: 78% generic-based vs. 85% brand-name); drug costs are 25% of average wholesale price (AWP) for generics and 77% of AWP for others ($9,200/year vs. $15,300/year for the regimen); the cohort is 84% male, mean CD4 317/μl. From the US health system perspective (2009 USD), we report incremental cost-effectiveness ratios (ICERs, $/QALY) compared against a $100,000/QALY threshold. We also project the potential annual savings for those initiating ART (incident diagnoses, ~2,500) and those eligible to switch to the generic-based regimen (prevalent cases, ~147,000)

Results: Compared to No ART, generic-based ART has an ICER of $21,100/QALY. Compared to generic-based ART, brand-name ART increases lifetime costs by $42,500, and per-person survival gains by 0.37 quality-adjusted life years (due to increased efficacy and reduced resistance from emtricitabine compared to lamivudine), for an ICER of $114,800/QALY (Table). ICERs are sensitive to decreases in generic-based ART efficacy and to generic drug costs; most plausible combinations lead to ICERs >$100,000/QALY (Figure). Estimated annual savings if all eligible US incident/prevalent patients switched to the generic-based regimen are $920 million.

Conclusions: Compared to a slightly-less effective generic-based regimen, the cost-effectiveness of the guideline-recommended brand-name regimen exceeds the $100,000/QALY threshold. Switching to generic-based regimens would yield substantial savings for programs that fund HIV treatment.

Table: Clinical outcomes, cost, and cost-effectiveness of generic-based and brand-name first-line ART regimens

	Per person life expectancy (QALYs)*	Per person lifetime cost* (USD 2009)	ICER ($/QALY)
No ART	4.05	131,300	--
Three-pill generic-based ART	12.08	300,300	21,100
One-pill brand-name ART	12.45	342,800	114,800

QALY: quality-adjusted life year; ICER: Incremental cost-effectiveness ratio
*QALYs and costs discounted at 3% annually; undiscounted life expectancy for one-pill brand-name = 19.32 QALYs

Figure: Incremental cost-effectiveness of brand-name compared to generic-based first-line ART regimen

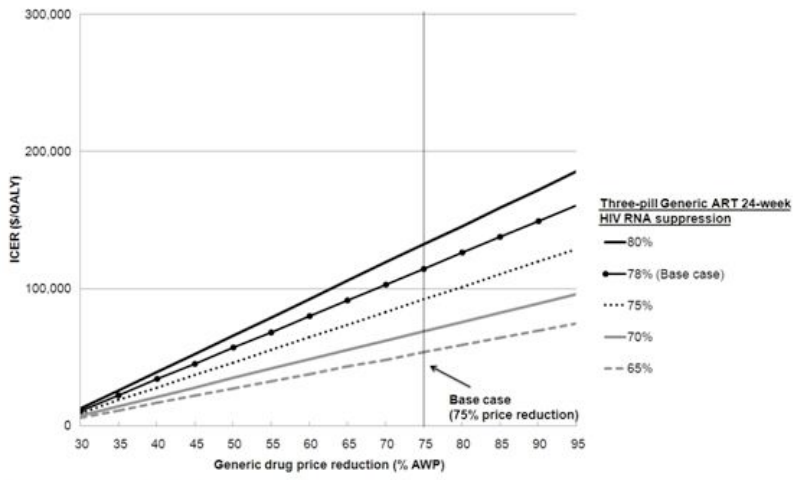

AWP: Average wholesale price

Hawkins, Alexander T. MD
Resident, Surgery
ahawkins@partners.org

Poster Number 180

When to Call it a Day: Incremental Risk of Amputation after Revascularization

Investigators: Alexander T. Hawkins, MD; Maria J. Schaumeier, MD; Ann D. Smith, MD; Nathanael D. Hevelone, MPH; Louis L. Nguyen, MD, MBA, MPH

Introduction and Objectives: Patients with Peripheral Vascular Disease often undergo revascularization procedures prior to amputation. The exact relationship between increased procedures and increased risk of amputation is unclear. We sought to determine the incremental increased risk of amputation for each additional revascularization procedure.

Methods: We searched the Statewide Inpatient Databases for California (2007-2009), identifying patients who underwent one or more lower extremity angioplasty ± stent (PTA) or peripheral bypass graft (PBG) within a one-year period. We analyzed crude risk of 1-year amputation or death with a test of deviation from linearity and multivariable-adjusted outcomes of in-hospital mortality and major amputation.

Results: Out of 5,147,981 patients we identified 14,793 (0.2%) who underwent one or more PTA and/or PBG within a 1-year period. The mean age was 68.44. In a 1-year period, 555 (3.8%) underwent amputation and 1375 (9.3%) died. The crude risk of amputation (1 PTA: 5.3%, 2 PTA: 8.5%, 3+ PTA 11.4%; P-value: < 0.001) increased with multiple PTA. The risk increases appear to be linear (P=0.842). The risk of amputation (1 PBG : 8%, 2+ PBG: 13.1%; P-value: < 0.001) increases with multiple PBG. In a multivariate analysis, the odds of amputation significantly increased with multiple PTA (1 vs 2 PTA- OR: 1.50 (1.21-1.87) P<0.001; 1 vs 3+ PTA - OR: 1.82 (1.29-2.56) P<0.001) and multiple PBG (1 vs 2 PBG- OR: 1.62 (1.24-2.25); P=0.001).

Conclusions: The crude risk of amputation increases in a linear fashion with increasing PTA and PBG procedures. Risk adjusted odds for amputation increase with increasing PTA and PBG procedures.

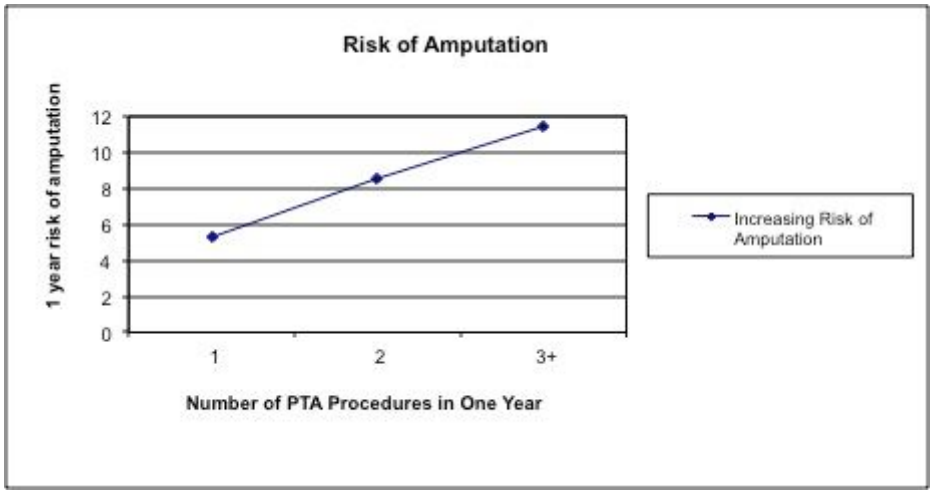

Poster Number 181

Hyle, Emily MD
Instructor, Medicine
ehyle@partners.org

The Clinical and Economic Impact of Point of Care CD4 Testing in Resource-Limited Settings

Investigators: EP. Hyle, MD; I. Jani, MD, PhD; J. Lehe, BA; R. Wood, MBChB, DPhil, AE, Su, BA; J. Quevedo, BA; E. Losina, PhD; IV Bassett, MD, MPH; AD, Paltiel, PhD; KA. Freedberg, MD, MSc; TF. Peter, PhD; RP. Walensky, MD, MPH

Background: Point of care (POC) CD4 at the time of HIV diagnosis can improve linkage to care compared to current standard of care (SOC) in South Africa, laboratory CD4. Our objective was to evaluate use of these two strategies (POC vs SOC) in settings with a range of access to HIV diagnosis and care.

Methods: We used a validated mathematical model (CEPAC-International) to compare two strategies: POC vs SOC CD4 testing. Model outcomes included life expectancy (LE), mortality, and lifetime medical costs, from which we calculated the incremental cost-effectiveness ratio (ICER) of the POC strategy compared to SOC. Model data were from a South African outpatient cohort of newly diagnosed HIV+ persons: mean age 30 (SD 10) yrs, mean CD4 300/μl (SD 102), and 35% were male. POC/SOC test characteristics included: sensitivity (90/100), linkage to HIV care (57%/32%), and cost (US$24/US$14). In both strategies, patients could otherwise link to care by repeat HIV testing or when diagnosed with an OI. After linkage, patients were treated per South African guidelines. We performed sensitivity analyses varying test and cohort characteristics. We also varied the frequency of HIV testing (1/5y, 1/10y, twice, once) and the likelihood of linkage to care with an OI (100%, 75%, 50%, 25%) to represent access to HIV diagnosis and care. Results were discounted at 3%. We considered ICER < US$8,100 (2011 South African per capita GDP) to be very cost-effective.

Results: The estimated LE was 99.3 months for the POC strategy and 92.0 months for SOC. Estimated lifetime costs were 14,440 US$ for POC and 13,380 US$ for SOC, resulting in an ICER of 1,730 US$/YLS. In the base case, the POC strategy projected a 6.9% reduction in deaths compared to SOC over a 5y horizon. Compared to SOC, POC led to the greatest benefits in settings with infrequent HIV testing and poorer rates of linkage with an acute OI (Figure 1). With use of POC at currently reported performance (solid line) compared to SOC (dashed line), 6-13% of deaths could be averted at 5y. Benefits of POC remained robust at linkage rates within a 95% confidence interval of published values (% linkage, 48-66%). POC remained very cost effective for inputs within reasonable ranges.

Conclusions: If POC improves linkage from SOC, then POC averts deaths and is very cost-effective across wide-ranging parameters in South Africa. POC CD4 could have the greatest impact on mortality in areas where health care resources and systems are most limited.

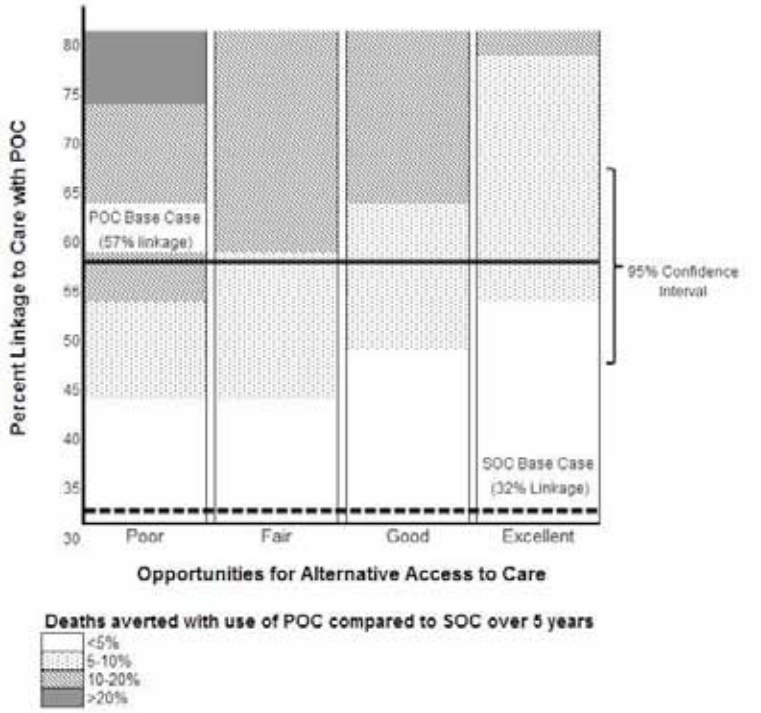

Figure 1 Multi-way sensitivity analysis: Projected reduction in deaths over 5 years with use of POC compared to SOC in 4 settings with different access to care (improving access to care from left to right). More deaths could be averted in settings with fewer opportunities for access to care and with improving POC linkage rates.

Kelly, Kathleen BA
Clinical Research Assistant, Medicine
kkelly24@partners.org

Poster Number 182

The Cost-effectiveness of Point-of-Care CD4 Testing in Antenatal Care in South Africa

Investigators: Andrea L. Ciaranello, MD, MPH; Landon Myer, PhD; Sarah Christensen; Kathleen Kelly, BA; Kristen Daskilewicz, BA; Katie Doherty, BA; Linda-Gail Bekker, MBChB, DTMH, DCH, FCP(SA), PhD; Taige Hou, BS; Ken Freedberg, MD; Rochelle Walensky, MD, MPH

Background: A one-time POC CD4 assay for HIV+ women may facilitate ART initiation in ANC and prevent mother-to-child HIV transmission (MTCT). The value of replacing laboratory flow cytometry with POC CD4 may depend on access to laboratory services.

Methods: Using the validated Cost-effectiveness of Preventing AIDS Complications (CEPAC) model with published clinical and economic data, we simulated a cohort of pregnant, HIV+ women and their infants in South Africa (mean maternal age 27.9y; mean gestational age 28w; mean CD4 451/μL; 6m breastfeeding). We examined 2 strategies for CD4 testing after HIV diagnosis: 1) POC ($23.40), with testing and result-return rates from a study of antenatal POC CD4 testing in Cape Town, and 2) laboratory ($14.00), with "low access" and "high access" scenarios to reflect testing and result-return in a range of settings (Table). We modeled current South Africa PMTCT guidelines (WHO "Option A"). Model outcomes included MTCT risk, maternal and pediatric life expectancy (LE), and maternal and pediatric lifetime healthcare costs (2011 USD). The base case assumed no earlier ART initiation with POC (CD4 ≤350/μL); this was varied in sensitivity analyses (from 0-3 weeks), as well as the proportion of HIV+ women CD4-tested, the proportion receiving CD4 result and initiating ART, and assay costs.

Results: Maternal outcomes following POC and laboratory were similar (not shown). In the base case, POC led to projected 6-month MTCT risk of 5.4%, pediatric LE of 23.40y, and total costs of $770/infant (Table). Depending on access level, laboratory led to 6-month MTCT risks of 5.7-8.7%, pediatric LE of 22.83-23.35y, and total costs of $785-1,030; at both access levels, laboratory led to lower LE and higher costs than POC. Compared to "low access" laboratory, POC remained cost-saving unless the POC assay cost ≥$305/test or the proportion of women tested and receiving POC assay results was ≤14%. Compared to "high-access" laboratory, POC remained cost-saving unless the POC assay cost ≥$45/test or the proportion of women tested and receiving POC assay results was ≤84%. When POC improved not only testing and result-return, but also time to ART initiation (CD4 ≤350/μL), clinical benefits compared to laboratory increased and cost-savings persisted.

Conclusions: In South Africa, any improvement in testing rates, result-return rates, or time to ART initiation will more than offset the cost of POC CD4 assays, due to cost-savings from prevention of MTCT.

Table: Projected outcomes for point-of-care (POC) and laboratory-based CD4 testing in antenatal care

CD4 testing strategy [a]	Model inputs		Model results: Clinical [b]		Model results: Costs (USD) [b]			Summary
	CD4 testing (%) [c]	CD4 result return (%) [c]	MTCT (6m)	Pediatric LE	ANC	Pediatric	Total cost	
"Low" access to laboratory-based CD4 testing and results (UNAIDS data, low/middle-income countries)								
POC	95	95	5.4%	23.40	310	460	770	More effective, less expensive
Laboratory	30	50	8.7%	22.83	280	750	1,030	
"High" access to laboratory-based CD4 testing and results (data from Cape Town antenatal clinic with ART initiation on-site)								
POC	95	95	5.4%	23.40	310	460	770	More effective, less expensive
Laboratory	96	87	5.7%	23.35	300	485	785	

USD: 2011 US dollars; **MTCT**: mother-to-child HIV transmission; **LE**: life expectancy (years after delivery).
a. Per South African and WHO "Option A" PMTCT guidelines, women received zidovudine (ZDV) from HIV diagnosis until receipt of CD4 results; CD4>350/μL led to continued antenatal ZDV, with infant nevirapine through breastfeeding, and CD4 ≤350/μL led to discontinuation of ZDV and initiation of lifelong maternal 3-drug ART (WHO "Option A").
b. All model results except MTCT risks are discounted at 3%/year.
c. CD4 testing: proportion of women with positive HIV test who undergo CD4 testing. CD4 result return: proportion of CD4-tested women who receive CD4 result, and, if CD4 ≤350/μL, change from zidovudine to ART

Poster Number 183

Konijeti, Gauree Gupta MD, MPH
Clinical Research Fellow, Digestive Healthcare Center
gkonijeti@partners.org

Cost Effectiveness Analysis of Chromoendoscopy for Colorectal Cancer Surveillance in Patients with Ulcerative Colitis

Investigators: Gauree Gupta Konijeti, MD, MPH; Mark G. Shrime, MD, MPH; Ashwin Ananthakrishnan, MBBS, MPH; Andrew T. Chan, MD, MPH

Background & Aims: Although ulcerative colitis (UC) is associated with a higher lifetime incidence of colorectal cancer (CRC), recent studies suggest that magnitude of this increased risk is lower than previously estimated. Annual white light endoscopy (WLE) with random biopsies is recommended for early detection of dysplasia to reduce the risk of CRC in patients with long-standing UC. Although several studies have shown improved detection of dysplasia with chromoendoscopy (CE) over WLE, CE is still not widely utilized. We analyzed the cost effectiveness of CE relative to WLE or no endoscopy for dysplasia surveillance in patients with ulcerative colitis.

Methods: We constructed a decision-analytic state-transition (Markov) model with Monte Carlo simulation using a reference case of UC patients from a population-based age distribution. We compared three strategies: annual CE with targeted biopsies, annual WLE with random biopsies, and no endoscopy. The study population was followed annually until age 90 or lifetime. The robustness of the model was assessed using probabilistic sensitivity analysis. One-way sensitivity analyses were performed to evaluate individual variables, and 3-D analysis was used to examine the effects of varying screening intervals.

Results: Annual CE dominated annual WLE, with an incremental cost-effectiveness ratio of $30,355 for CE relative to no surveillance. CE remained the preferred strategy at sensitivity greater than 0.38 for dysplasia detection, cost less than $1880, and all levels of compliance with surveillance. CE yielded the greatest net health benefits across all screening intervals; however, an optimal screening interval could not be determined. The proportion of the population developing CRC over a lifetime ranged from 8% (annual CE) to 22% (CE every 10 years).

Conclusions: From a societal perspective, colorectal cancer surveillance with annual CE dominates annual WLE for patients with UC even after accounting for lower estimates of CRC incidence among patients with long-standing disease.

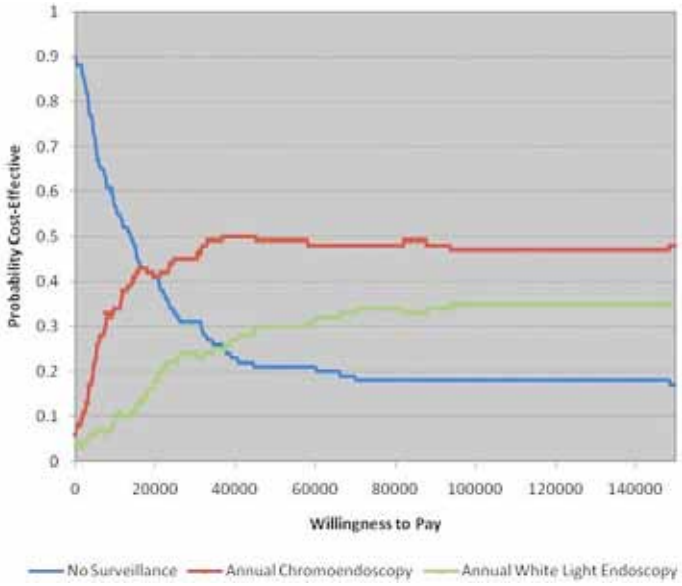

Ross, Eric Lloyd BA
Research Assistant, Medicine
eross9@partners.org

Poster Number 184

Clinical impact and cost-effectiveness of making third-line antiretroviral therapy available in sub-Saharan Africa: a model-based analysis in Cote d'Ivoire

Investigators: Eric Ouattara, MD, MPH; Eric Lloyd Ross, BA; Yazdan Yazdanpanah, MD, PhD; Angela Y. Wong, BS; Marion Robine, BS; Elena Losina, PhD; Raoul Moh, MD; Rochelle P. Walensky, MD, MPH; Christine Danel, MD; A. David Paltiel, PhD; Serge P. Eholié, MD; Kenneth A Freedberg, MD, MSc; Xavier Anglaret, MD, PhD

Background: In sub-Saharan Africa, HIV-infected adults who fail 2nd-line ART (ART2) often do not have 3rd-line ART (ART3) available. We examined the clinical impact and cost-effectiveness of making ART3 available in Côte d'Ivoire.

Methods: We used the CEPAC microsimulation model to compare 4 strategies following observed ART2 failure: (1) Continue ART2 [C-ART2]; (2) Continue ART2 with an adherence reinforcement (AR) intervention [AR-ART2]; (3) Immediate switch to ART3 [IS-ART3]; and (4) Continue ART2 with adherence reinforcement, switching to ART3 in patients with persistent failure [AR-ART3]. ART2 consisted of a LPV/r-based ART in patients who had previously received a NNRTI-based 1st-line regimen, and ART3 of 2 recycled NRTIs+RAL+DRV/r, according to Côte d'Ivoire guidelines. Patients were monitored with biannual CD4 counts, and HIV-1 viral load (VL) was available only to confirm virologic failure in those with immunologic failure. Immunologic failure was defined according to WHO criteria, and virologic failure as a VL>1000 copies/mL. AR involved 6 monthly adherence training sessions and weekly SMS reminders. Patients failing to achieve a 2 log decrease in VL following AR were switched to ART3. Annual cost of drugs was $528 (ART2) and $1969 (ART3). Six-month virologic suppression was 80% for ART3 and 30% for AR (50% success rate among the 60% of patients without resistance to LPV/r). Main outcomes were 10-year survival, and lifetime incremental cost effectiveness ratios [ICERs] in $/year of life saved [YLS]. In sensitivity analysis, we varied inputs widely. We employed WHO standards to define ICERs below 3x Côte d'Ivoire per capita GDP (3 * $1195=$3,585) as 'cost-effective', and below 1x GDP ($1195) as 'very cost-effective'.

Results: In the absence of ART3, AR-ART2 was very cost effective ($1100/YLS) compared to C-ART2. Introducing ART3 alternatives provided substantially greater survival benefits. AR-ART3 was cost-effective ($3500/YLS) compared to AR-ART2, and became very cost-effective if the annual cost of ART3 decreased by 60%. Routine availability of VL monitoring did not alter these results materially.

Conclusion: Use of 3rd line ART in Côte d'Ivoire improves survival; the addition of an adherence reinforcement before switching to 3rd line provides the greatest long-term survival benefits and is cost-effective. Further 60% reductions in the price of 3rd-line agents would make the AR-ART3 strategy very cost-effective.

Table. Outcomes of different strategies after observed 2nd-line ART failure

	Survival		Cost -effectiveness		
	% alive at 2 years	% alive at 10 years	Life expectancy (months)	Lifetime cost (2011 USD)	ICER (USD/YLS)
C-ART2	72.3	5.4	47.1	4,580	-
AR-ART2	78.3	18.1	64.3	6,130	1,100
AR-ART3	83.2	36.2	88.9	13,420	3,500
IS-ART3	85.2	34.3	86.7	13,390	Dominated*

* Costs more and yields lower life expectancy than AR-ART3

Poster Number 185

Walensky, Rochelle, MD, MPH
Professor, Medicine
rwalensky@partners.org

The Cost-effectiveness of Treatment as Prevention: Analysis of the HPTN 052 Trial

Investigators: Rochelle P. Walensky, MD, MPH; Eric L. Ross, BA; Nagalingeswaran Kumarasamy, MBBS, PhD; Robin Wood, FCP (SA), DSc (Med); Farzad Noubary, PhD; A. David Paltiel, PhD, MBA; Yoriko M. Nakamura, BA; Sheela V. Godbole, MD; Ravindre Panchia, BSc, MBBCH; Ian Sanne, MBBCh, FCP, DTM&H; Milton C. Weinstein, PhD; Elena Losina, PhD; Kenneth H. Mayer, MD; Ying Q. Chen, PhD; Lei Wang, PhD; Marybeth McCauley, MPH; Theresa Gamble, PhD; George R. Seage III, DSc, MPH; Myron S. Cohen, MD; Kenneth A. Freedberg, MD, MSc; For the HPTN 052 Investigators

Background: HPTN 052, a multi-country randomized trial, showed that early ART initiation produced a 96% reduction in HIV transmission among serodiscordant couples. Using an HIV microsimulation model (CEPAC-International), we project the clinical impact, costs, and cost-effectiveness of early ART.

Methods: Per the 052 protocol, we compare two ART initiation strategies: early (at presentation-to-care) vs. delayed (CD4<250/μl). Each strategy is modeled in South Africa (RSA) and India using trial-derived data: mean age 33.8y, mean CD4 449/μl (±120/μL), 42% (RSA) and 67% (India) male, 0.103/1.483 transmissions/100PY while virologically suppressed/unsuppressed. ART strategies are applied consistently to transmitted and index cases. Outcomes include: first-order HIV transmissions, survival, costs, and cost-effectiveness. We designate early ART very cost-effective or cost-effective if its cost-effectiveness ratio is <1x or <3x per capita GDP (GDPs: $8,000 [RSA]; $1,400 [India]).

Table

	Initially-infected cohort				*New transmissions*		
	Survival (%)	Life expectancy (months)	Costs (2011 USD)	Transmissions /index case (Δ%)	LMs lost due to transmissions	Cost increase due to transmissions	Overall ICER ($/YLS)
South Africa							
5-year Horizon							
Delayed ART	84	52*	4,400	0.05 (--)	0.10	80	--
Early ART	93	55*	4,600	0.02 (-59%)	0.03	30	700
Lifetime Horizon							
Delayed ART	--	162	16,100	0.14 (--)	7.19	1,180	--
Early ART	--	184	18,400	0.15 (+6%)	4.84	1,190	1,200
India							
5-year Horizon							
Delayed ART	87	52*	1,700	0.04 (--)	0.07	30	--
Early ART	94	55*	2,300	0.02 (-57%)	0.02	10	2,900
Lifetime Horizon							
Delayed ART	--	177	9,400	0.14 (--)	5.41	680	--
Early ART	--	193	11,300	0.15 (+3%)	3.65	730	1,300

Cost, clinical impact, and cost-effectiveness of early and delayed ART initiation strategies. All cost and life expectancy results are presented *per initially-infected patient*; these values are discounted at a rate of 3% annually.
*Life expectancy at a 5-year horizon indicates the average length of survival through 5 years.
LMs, life months; ICER, incremental cost-effectiveness ratio; YLS, years of life saved.

Figure

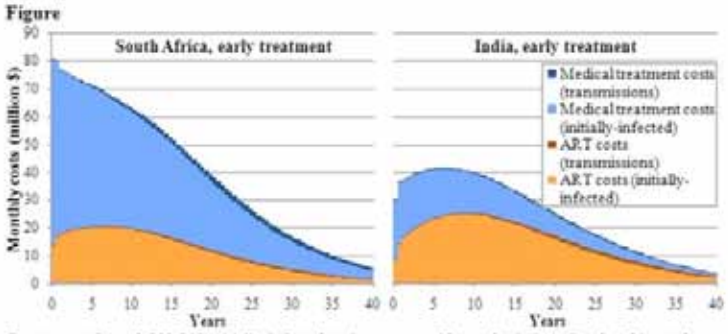

Costs accrued per 1,000,000 initially-infected patients over a 40-year horizon in South Africa and India under the early ART initiation strategy. ART costs comprise the direct cost of antiretroviral medication. Medical treatment costs comprise all other costs, including routine care, treatment of opportunistic infections (OIs), OI prophylaxis, mortality-related costs, and lab monitoring.

Results: In RSA, early ART increases survival, prevents costly OIs (partially offsetting ART costs), averts early transmissions, and is very cost-effective over both 5-year ($700/YLS, Table) and lifetime horizons ($1,200/YLS, Table). In India over a 5-year horizon, early ART increases survival and averts transmissions. Because ART is expensive relative to other medical treatment in India (Figure), OI prevention offsets fewer ART costs. Early ART, however, is cost-effective ($2,900/YLS, Table); over a lifetime horizon, it becomes very cost-effective ($1,300/YLS, Table). In sensitivity analyses in both countries, early ART remains very cost-effective over a lifetime horizon under a wide range of assumptions regarding the clinical and preventive efficacy of ART. Consideration of second-order transmissions increases the clinical and cost benefits of early ART.

Conclusions: Early ART averts HIV transmissions over shorter horizons, but increased survival attenuates this affect over time. Over 5 years, early ART is cost-effective in India and very cost-effective in RSA; in both countries, early ART is very cost-effective over a lifetime horizon.

Poster Number 186

Ahn, Bummo PhD
Research Fellow, Imaging
bahn2@partners.org

Ocular and Craniofacial Trauma Simulator: Augmented Reality Surgical Microscope, CT-Derived Physical Anatomy, Sensor and Actuator Systems

Investigators: Bummo Ahn, PhD; John Cho Moore, BFA; Simone Zivieri, BEng; Gianluca De Novi, PhD; Ryan S. Bardsley, BFA; Mark P. Ottensmeyer, PhD

Craniofacial trauma and ocular injury were elements of over 25% of all battlefield injuries suffered in Operations Iraqi Freedom and Enduring Freedom between 2001 and 2008. Body armor improvements reduced trunk and extremity injuries, however the face and eyes remain less protected. Physician training in eye trauma is increasingly concentrated in referral centers, resulting in fewer ophthalmologists with extensive trauma expertise. Medic training emphasizes saving limb first, although loss of sight through delayed intervention can also result in permanent disability. Facial and neck trauma can be complex, and techniques such as application of tourniquet may be inappropriate; control of hemorrhage may conflict with maintenance of airway, as when packing the oral cavity to control bleeding. A multi-purpose simulation, teaching and performance measurement system to provide exposure of realistic, dynamic scenarios of ocular and craniofacial trauma to physicians and medics is needed.

At SAC 2012, we presented the prototype simulator platform, which included a silicone head and neck with replaceable eye lid laceration modules, magnetic position tracking for a suite of ophthalmic surgical instruments and initial concepts for sensing interventions on, and animation of, the eye globe.

In this poster we present new simulator elements including: an augmented reality binocular surgical microscope for globe surgery scenarios; production of a new head-form and trauma modules based on 3D computer-aided-design (CAD) models converted from segmented CT data; improvements to the eye globe anatomy and motion/sensing components; creation of a cricothyroidotomy module with incision sensing; and design of a neck with anatomical range and active motion.

The AR microscope provides 3D graphical overlays combined with stereoscopic views of the surgical field. It provides guidance and feedback to the trainee derived from our Event Driven Surgical Gesture Recognition algorithms (described in companion poster), without requiring that the trainee look up from the microscope. Sensors measure zoom level and position relative to the trauma module so that augmented and real imagery are properly registered.

Our original life-cast head/neck model has been replaced using anatomy segmented from CT data, imported into CAD. This allows for modification of the anatomy to create different trauma/injury modules, and their exact replication through "3D printing" techniques for mold-making. The models can be directly imported into the AR systems (projected and microscopic) as they are derived from the same data set.

We present a globe-trauma system which includes replaceable globe modules mounted to a pitch-yaw/proptosis motion platform. It includes a sensor to measure whether excess force is applied to the globe during treatment and whether canthotomy/cantholysis has relieved retrobulbar hemorrhage.

The neck is based on segmented cervical vertebrae allowing normal anatomical range of motion. Using pneumatic "muscles," it simulates a struggling patient resisting intubation or cricothyroidotomy, a feature not found on other medical simulators. The cric module prototype can detect the length and orientation of incisions through the skin and cricothyroid membrane, to provide feedback on performance quality and success.

This system is expected to undergo a second round of user testing at the Uniformed Services University 2013 Ocular Trauma course.

Poster Number 187

De Novi, Gianluca PhD
Research Fellow, Imaging
DeNovi.Gianluca@mgh.harvard.edu

Ocular and Craniofacial Trauma Simulator: Event Driven Surgical Gesture Recognition, Contextual Feedback Interface and User Trial Results

Investigators: Gianluca De Novi, PhD; Ryan S. Bardsley, BFA; Rajesh J. Shah, MS; Bummo Ahn, PhD; John Cho Moore, BFA; Mark P. Ottensmeyer, PhD

Craniofacial trauma and ocular injury were elements of over 25% of all battlefield injuries suffered in Operations Iraqi Freedom and Enduring Freedom between 2001 and 2008. Body armor improvements reduced trunk and extremity injuries, however the face and eyes remain less protected. Physician training in eye trauma is increasingly concentrated in referral centers, resulting in fewer ophthalmologists with extensive trauma expertise. Medic training emphasizes saving limb first, although loss of sight through delayed intervention can also result in permanent disability. Facial and neck trauma can be complex, and techniques such as application of tourniquet may be inappropriate; control of hemorrhage may conflict with maintenance of airway, as when packing the oral cavity to control bleeding. A multi-purpose simulation, teaching and performance measurement system to provide exposure of realistic, dynamic scenarios of ocular and craniofacial trauma to physicians and medics is needed.

At SAC 2012, we presented a simulator platform which combines: a synthetic head and neck with replaceable eye trauma "modules"; sensors to track position, orientation and function of a suite of ophthalmic surgical instruments; and a concept for segmentation of surgical gestures into a series of quantifiable "events" that can be used to evaluate performance and provide contextually relevant feedback.

This poster presents progress in development of the Event Driven Surgical Gesture Recognition (EDSGR) algorithms; the user interface which provides instructional material and feedback to the trainee; and preliminary results showing event detection accuracy.

EDSGR is based on a hierarchical task analysis of surgical tasks, in this case, repair of a full-thickness eye lid laceration. Major steps, such as examination of the injury, approximation of lid margin, suturing of the tarsal plate, etc. are broken down into tissue manipulation steps, needle throws, knot tying, suture trimming, etc., which are in turn broken down into distinct instrument motion events. The lowest level events correspond with instrument tip entry into or exit from geometric regions of interest around important structures, avoiding the need for computationally expensive continuous motion analysis. EDSGR is designed to recognize correct completion of task elements, even when differences in performance style diverge from a "standard" sequence.

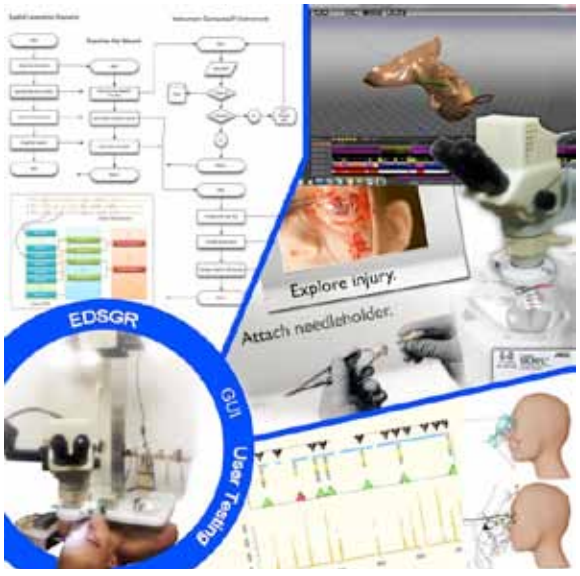

The user interface, using screen-based displays, video projection onto the surgical field and a novel augmented reality surgical microscope (reported in companion poster), is driven by the user's performance of surgical tasks. Recommendations on, for example, suture material selection, suture placement and feedback on performance are presented to the trainee in the context of the particular phase of the training scenario. The early, simplified EDSGR detected suture placement completion based on scissor usage has been enhanced to detect features such as instrument tip proximity and grasping of needle vs. tissue, and provide scoring metrics.

We are continuing to develop EDSGR using video and position tracking information collected in a user trial exercise at the annual Ocular Trauma Course conducted at the Uniformed Services University, in which 12 senior ophthalmic surgeons and 8 residents performed lid laceration repair on the system. Results showing the accuracy of the event detection will be presented.

Goetter, Elizabeth M. PhD
Clinical Research Fellow, Psychiatry
egoetter@partners.org

Poster Number 188

Videoconference-Mediated Exposure and Ritual Prevention for Obsessive Compulsive Disorder

Investigators: Elizabeth M. Goetter, PhD; James D. Herbert, PhD; Evan M. Forman, PhD

Background: Exposure and ritual prevention (ERP) is the gold-standard behavioral treatment for obsessive compulsive disorder (OCD). However, given the maldistribution of specialist providers and therapist underutilization of exposure therapy, many individuals do not have access to this highly effective treatment. Internet-mediated interventions (e.g., videoconferencing) show promise in reducing barriers to evidence-based mental health care. To further examine the feasibility and effectiveness of these methods, we pilot tested an intensive, twice weekly ERP therapy for adults with OCD via videoconference.

Method: Fifteen adults with OCD consented and 13 participants began treatment. Participants were assessed by an independent evaluator at pre-, mid-, and post-treatment using well-established diagnostic interviews (i.e., Yale-Brown Obsessive Compulsive Scale, YBOCS; Structured Clinical Interview for DSM-IV Axis I Disorders, SCID-IV) and validated self-report measures of OCD (i.e., Obsessive Compulsive Inventory-Revised, OCI-R), quality of life (i.e., Sheehan Disability Scale, SDS), and treatment satisfaction.

Results: Ten participants completed treatment and there was a high rate of treatment satisfaction. Drop out rates were equivalent to what is seen in in-person treatment modalities. Intent-to-treat analyses suggested that ERP was associated with improvements in clinician-rated (YBOCS: $t = 6.51$, $p < .001$) and self-reported (OCI-R: $t = 4.46$, $p < .001$) OCD symptoms and quality of life (SDS: $t = 4.04$, $p < .05$). Thirty-three percent no longer met criteria for OCD at post-treatment. Importantly, pre- to post- treatment effect sizes were comparable to those seen in in-person trials of ERP (Cohen's $d = 2.31$).

Conclusion: Remote interventions are effective and viable alternatives to face-to-face treatment methods for OCD. Importantly, these methods increase the availability of empirically supported treatments to individuals who might not otherwise have access to specialized mental health care.

Im, Hyungsoon PhD
Research Fellow, Center for Systems Biology
im.hyungsoon@mgh.harvard.edu

Poster Number 189

Profiling of human cells with a portable holographic imaging system

Investigators: Hyungsoon Im, PhD; Jun Song, BS; Monty Liong, PhD; Lioubov Fexon, MS; Misha Pivovarov, MS; Ralph Weissleder, MD, PhD; Hakho Lee, PhD

Identification of specific prokaryotic and eukaryotic cells is critical in rapid diagnostics, in screening, and in resource limited settings. Here we describe the development of a chip-based, portable holographic imaging system initially developed for the detection and profiling of cancer cells. The system consists of a cost efficient CMOS chip onto which was built a microfluidic system. A new algorithm for rapid holographic image reconstruction and analysis was developed. Compared to conventional microscopes, the holographic system can image much larger areas (> 20 mm2) and obtain cellular images including phase information of cells in real-time (10 frames/sec). We furthermore show that molecular specificity can be obtained by using antibody-microbead conjugates to label cells. The developed system was able to accurately count thousands of cells per image frame. Importantly, the assay works well without the need for any washing steps, minimizing cell loss and simplifying the assay procedure. This cost-effective, portable, flow-based holographic imaging system is applicable to detecting rare cancer cells in a large volume of blood samples for point-of-care applications. We anticipate that similar algorithm can be adapted for use on low cost portable systems (i.e. iPhone).

Poster Number 190

Tricomi, Brad BS
Research Fellow, Oral and Maxillofacial Surgery
btricomi@partners.org

Automated Continuous Distraction Osteogenesis May Allow Faster Distraction Rates

Investigators: Brad Tricomi, BS; Matthew E. Lawler, DMD; Brian Murphy, PhD; John Magill, PhD; Leonard B. Kaban, DMD, MD; Maria Troulis, DDS, MSc; Zachary S. Peacock, DMD, MD

Purpose: To evaluate bone formation after automated, continuous, curvilinear distraction osteogenesis (DO) in a minipig model.

Materials and Methods: 10 Yucatan minipigs in the mixed-dentition stage underwent automated, continuous, curvilinear DO of the right mandible. Animals were distracted 12mm at rates of 1.5 (n=5) and 3.0mm/day (n=5) followed by 24 days of consolidation. Bilateral mandibles were harvested, formalin-fixed and coronal sections were cut. They were paraffin-embedded and stained with hematoxylin-eosin (H&E). Superior (tooth-bud area), middle (inferior alveolar nerve) and inferior (below nerve) regions of the regenerate were evaluated. Percent surface area (PSA) of the distraction wound occupied by bone, cartilage, fibrous tissue and hematoma were determined by computerized histomorphometric analysis and compared to a control group of discontinuous DO at 1mm/d. A P-value $\leq$0.05 was considered statistically significant.

Results: All 10 minipigs survived the operation, distraction and consolidation periods. Histomorphometric analysis revealed no significant differences between mean PSA occupied by bone at 1.5 (PSA=64.36±5.87) and 3.0mm/d (PSA=63.83±3.37), P=0.939 and fibrous tissue at 1.5 (PSA=34.05±4.88) and 3.0mm/d (PSA=34.80±3.06), P=0.898. There was no significant difference in total bone PSA at continuous rates of 1.5 and 3.0mm/d versus discontinuous DO at 1.0mm/d (P=0.993; P=0.770 respectively). Average bone PSA values were highest in the superior region (1.5mm/d PSA=69.55±2.28, 3.0mm/d PSA=64.99±5.80) and lowest in the inferior region (1.5mm/d PSA=55.25±11.21, 3.0mm/d PSA=62.60±2.99). There were no significant differences in regional bone formation between 1.5 and 3.0mm/d continuous DO (superior, P=0.497; middle, P=0.584; or inferior, P=0.556). Hematoma and cartilage occupied less than 1.1% of the total surface area in both continuous distraction groups.

Conclusion: Results of this study indicate that bone fill of the continuous distraction wound at rates of 1.5 and 3mm/d was similar to that of discontinuous DO at 1mm/d. In this minipig model, continuous DO allows for bone fill at a faster distraction rate than possible with discontinuous distraction.

Ahmed, Omar J. PhD
Research Fellow, Neurology Service
ojahmed@partners.org

Poster Number 191

Human inhibitory single neurons switch off before dramatic increases in seizure intensity

Investigators: Omar J. Ahmed, PhD; Wilson Truccolo, PhD; Jacob A. Donoghue, BSc; Emad N. Eskandar, MD; Joseph R. Madsen, MD; W. Stan Anderson, MD; G. Rees Cosgrove, MD; N. Stevenson Potter, MD, PhD; Andy S. Blum, MD, PhD; Leigh R. Hochberg, MD; Sydney S. Cash S, MD, PhD

Rationale: Epilepsy is thought to be the result of an imbalance between excitatory and inhibitory neuronal activity. Due to the tremendous technical challenges of recording from individual human neurons, the activity of inhibitory interneurons during seizures in human epilepsy patients has never been examined. There are several theories, based on slice and animal experiments, proposing that a decrease in inhibition is a necessary prerequisite of epileptic activity. However, there are competing theories that suggest a dramatic increase in inhibition is necessary to synchronize the activity of excitatory cells into epileptiform discharges. It is also unclear what happens to the firing of inhibitory neurons as a seizure progresses. Here, we present the first ever description of what human inhibitory neurons do during different phases of focal seizures with secondary generalization.

Methods: Four patients were implanted with intracranial grid electrodes as part of the clinical process of identifying the precise site of origin of their drug-resistant epilepsy. A 4x4 mm Neuroport microarray was also placed in a region of the neocortex that was expected to be in the resection site. We used these arrays to simultaneously record the activity of dozens of individual neurons during ictal activity from layer 3 of the neocortex. We then identified putative inhibitory neurons using well-established criteria, including action potential shape. These neurons most likely correspond to the class of fast-spiking, parvalbumin-expressing inhibitory interneurons. The activity of these inhibitory neurons was then analyzed during different phases of human seizures.

Results: We show that interneuron activity initially parallels that of excitatory cells as the seizure first spreads to the neocortex, a finding consistent with what is known about feedforward drive of both inhibition and excitation. Unexpectedly, however, we find that inhibitory neurons switch off well before the end of a seizure. This cessation of inhibitory firing is accompanied by a dramatic increase in the amplitude of local spike-and-wave seizure events. We present evidence based on a novel set of analyses that suggests that these inhibitory interneurons stop firing because they enter depolarization block, where most sodium channels are inactivated and incapable of sustaining another action potential. This pattern of human interneuron activity was observed during all spike-and-wave seizures, independent of etiology (cortical dysplasia vs mesial temporal sclerosis) or site of origin (hippocampus vs neocortex) of the seizure. Thus we believe we have identified a remarkably consistent pattern of inhibitory neuronal activity during human focal seizures with secondary generalization.

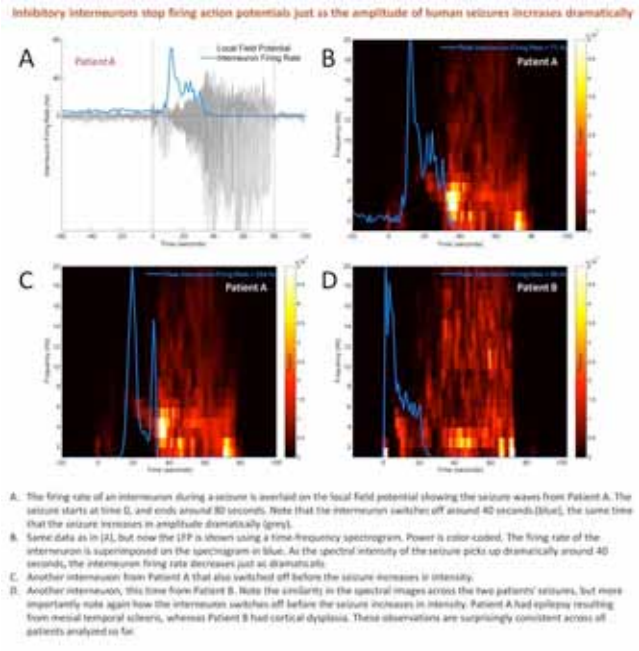

Conclusions: Our results show that there is a complete lack of inhibition towards the end of a human seizure—when seizure symptoms are often at their worst. This cessation results from inhibitory interneurons entering depolarization block well before the termination of the seizure. Strikingly, this absence of inhibitory activity is accompanied by large increases in the amplitude of seizures. These findings suggest that it may be possible to alter or prevent seizures by using pharmacological manipulations that prevent inhibitory interneurons from entering depolarization block. This represents a potentially novel and powerful therapeutic avenue in the treatment of human epilepsy.

Poster Number 192

Carter, Jocelyn MD
Instructor, Medicine
jcarter0@partners.org

Improving the reliability of care coordination and reducing hospital readmissions in an academic medical center

Investigators: Chris Annese, RN; Elizabeth Bishop, RN; Andrea Bonanno, PT; Laura Carr, PharmD; Jocelyn Carter, MD; Jacqui Collins, RN, ACNS-BC; Gwen Crevensten, MD; Jenna Delgado, RN; Joanne Doyle Petrongolo, PharmD; Patricia Durning, RN, Case Mngt; Kathryn Hall, RN, Nurse Dir, W13; Diane Hubbard, RN, Case Mngt; Yanie Jackson, MS; Joanne Kauffman, RN Mgr, Case Mngt; Sarah Keegan, RN; Deborah Kiely, PHS Home Care; Catherine Mullin, RN; Jane Murray, MBA; Stefanie Pylypink, RN; Jessica Smith, RN, CNS; Lee Ann Tata, RN, DNP, ANP-BC; Ashley Truong, PharmD Sponsors: Theresa Gallivan, RN; Associate Chief Nurse; Andrew Karson, MD, MPH; Elizabeth Mort, MD, MPH; MGH Cross Continuum Team

With over $12 billion in health care costs related to avoidable 30-day hospital readmissions, interest in care transitions has blossomed. Initial measurement of 30-day hospital readmission rates on Ellison 16, a 36 bed general medicine unit at the Massachusetts General Hospital demonstrated opportunities for improvement (18.3%). As part of the Institute for Healthcare Improvement (IHI) STate Action on Avoidable Rehospitalizations (STAAR) initiative, patient-centered interventions to reduce hospital readmissions were implemented on Ellison 16 in 2009 at MGH as a part of a four year initiative.

The two interventions included the introduction of the discharge nurse role and increasing collaboration with the Pharmacy Department through pharmacist pre-discharge visits to patients and making post-discharge phone calls.

The discharge nurse manages high-risk patients defined by specific criteria from admission through discharge. The discharge nurse provides education to the patients and families throughout the hospital stay, and prepares the patient discharge folder that includes follow-up instructions, labs/test appointments and provider contact information. Aside from providing patient education, the discharge nurse is essential in coordinating care with all providers. Acting as the point person for the care team, the discharge nurse facilitates multidisciplinary rounds and aligns the care team as they prepare for the patient's transition to the next level of care.

The pharmacist and discharge nurse work closely together to provide medication reconciliation and identify patients that would benefit from a pharmacist consultation (pre-discharge visit). The pharmacist provides counseling and coordinates dispensing of medication if necessary. The pharmacist also conducts post-discharge calls to patients discharged home or home with services.

Here we show that readmission rates on the Ellison 16 unit with a discharge nurse decreased from 21.0% to 15.9%. Pharmacy calls to patients after hospital discharge demonstrate that 52% of patients deviate from medication instructions after leaving the hospital. Readmission rates were 12.9% among patients that received post-discharge pharmacy calls as compared to 17.2% among those that did not receive calls.

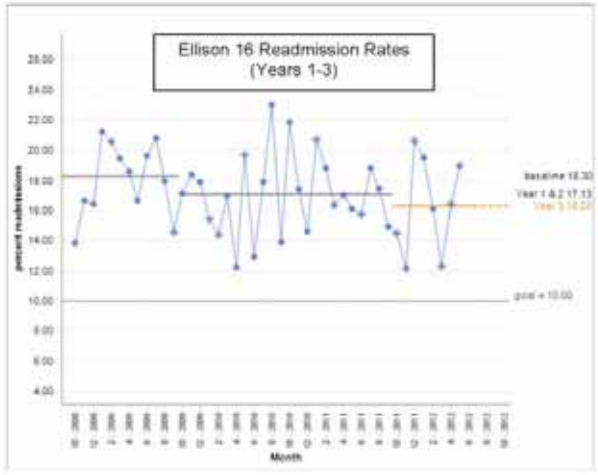

Poster Number 193

Chan, Yee-Ming MD, PhD
Clinical Research Fellow, Medicine
ymchan@partners.org

The kisspeptin-stimulation test as a potential tool for the evaluation of delayed puberty

Investigators: Yee-Ming Chan, MD, PhD; Valerie F. Sidhoum, BA; Margaret F. Lippincott, MD; Stephanie B. Seminara, MD

Patients with idiopathic hypogonadotropic hypogonadism (IHH) fail to undergo normal puberty and are infertile due to defective secretion or action of the master reproductive hormone GnRH (gonadotropin-releasing hormone) by neurons of the hypothalamus. Currently, a definitive diagnosis of IHH can only be made in patients 18 years or older, to differentiate IHH from constitutional delay of puberty (CDP), a benign, self-limited delay in pubertal timing. This leads to considerable diagnostic uncertainty in all adolescents with delayed puberty, whether due to IHH or CDP, and a prospective diagnostic method is critically needed.

The recently discovered reproductive hormone kisspeptin presents an opportunity to address this unmet medical need. Our group and others have shown that kisspeptin potently stimulates GnRH secretion, and we have now used kisspeptin as a probe of GnRH neuronal function in humans. We hypothesized that IHH patients would have diminished responses to kisspeptin compared to healthy adults. We further hypothesized that patients with complete absence of GnRH secretion would have no responses to kisspeptin, whereas those with some GnRH secretion (but not enough to sustain normal reproductive function) would have detectable but subnormal responses to kisspeptin.

To test these hypotheses, nine men and one woman with IHH underwent 12-14h of q10 min blood sampling before and after IV administration of kisspeptin as well as GnRH. Because the pituitary glands of patients with IHH may respond only feebly to GnRH due to disuse, subjects were studied a second time after "priming" with exogenous GnRH for 6 days to restore pituitary responsiveness.

None of the ten subjects responded to kisspeptin (ΔLH 0-0.3 mIU/mL), either before or after priming with exogenous GnRH. In contrast, the responses to GnRH were variable. Seven subjects had small pre-priming responses to exogenous GnRH (ΔLH 0.5-2.6 mIU/mL), indicating that their pituitary glands were "unprimed" from lack of exposure to GnRH and demonstrating that these subjects lacked endogenous GnRH secretion. Consistent with this interpretation, priming enhanced their responses to exogenous GnRH (ΔLH 4.2-18.8 mIU/mL). The other three subjects had pre-priming responses to GnRH (ΔLH 4.6-6.8 mIU/mL) that were already in the range of post-priming responses, suggesting endogenous GnRH stimulation of the pituitary gland. One of these endogenously primed patients returned for a second visit in which multiple boluses of kisspeptin were given, and still no responses to kisspeptin were seen.

Consistent with our first hypothesis, patients with IHH failed to respond to kisspeptin at a dose previously shown to robustly stimulate GnRH-induced LH secretion in healthy men. Thus, the kisspeptin-stimulation test holds promise for the diagnosis of IHH in adolescents with delayed puberty. However, counter to our second hypothesis, even patients with evidence of some endogenous GnRH secretion failed to respond to kisspeptin. In other words, these patients appeared to have GnRH neurons that do not respond to kisspeptin. Administration of multiple boluses of kisspeptin still did not induce responses to kisspeptin in one patient, and future work will examine other potential factors that may regulate GnRH neuronal responsiveness to kisspeptin in these patients.

Poster Number 194

Chhatwal, Jasmeer MD, PhD
Clinical Research Fellow, Neurology Service
jchhatwal@partners.org

Impaired default network functional connectivity in autosomal dominant Alzheimer's disease: Findings from the DIAN study

Investigators: Jasmeer Preet Chhatwal, MD, PhD; Aaron P. Schultz, PhD; Keith A. Johnson, MD; Tammie L. Benzinger, MD, PhD; Clifford R. Jack, MD; Stephen Salloway, MD, MS; John M. Ringman, MD; Robert A. Koeppe, PhD; Daniel S. Marcus, PhD; Paul M. Thompson, PhD; Andrew J. Saykin, PsyD; Stephen Correia, PhD; Peter R. Schofield, PhD; Christopher C. Rowe, MD, PhD; Nick C. Fox, MD; Adam M. Brickman, PhD; Richard Mayeux, MD, MSc; Eric M. McDade, DO; Randall J. Bateman, MD; Anne M. Fagan, PhD; Allison Goate, PhD; Chengjie Xiong, PhD; Virginia Buckles, PhD; John C. Morris, MD; Reisa A. Sperling, MD, MsC

Background: Functional connectivity MRI (fcMRI) has shown great promise as a tool to non-invasively assess the organization and synaptic integrity of anatomically distributed cortical networks, including neural networks whose coordinated activity appears to be critical for successful memory formation. Recent studies using fcMRI have revealed that functional connectivity within the Default Mode Network (DMN) is closely tied to memory performance. Profound decreases in DMN functional connectivity have been observed in older subjects with sporadic, late-onset Alzheimer's Disease (AD), in older subjects with Mild Cognitive Impairment (MCI) and in amyloid-positive clinically normal older subjects, suggesting that degradation of the DMN may be an early marker of AD-related synaptic failure. The Dominantly Inherited Alzheimer Network (DIAN) cohort offers a unique opportunity to probe AD related network dysfunction in young subjects with genetically driven Alzheimer's disease due to highly-penetrant mutations in presenilin-1 (PS-1), presenilin-2 (PS-2), and amyloid precursor protein (APP). As the age of symptom onset is conserved within families, we also model DMN connectivity based on how close each individual is to the expected age of symptom onset in their family (eAO), allowing us to examine the network level changes throughout the spectrum of disease.

Methods: Eighty-three mutation carriers, ranging from asymptomatic to mild dementia, and thirty-seven asymptomatic non-carriers from the same families underwent functional MRI during resting state. Using group- independent component analysis, functional connectivity (fcMRI) was analyzed and compared using mutation status and clinical dementia rating (CDR) to stratify groups, and then related to the estimated age of AD symptom onset (eAO) in each participant's family.

Findings: We observed significantly decreased DMN fcMRI in mutation carriers with increasing CDR, with the strongest effect in the Precuneus/Posterior Cingulate (PPC;$p<0.001$). Comparison of asymptomatic mutation carriers to non-carriers demonstrated significantly decreased fcMRI in the PPC and parietal cortices. We observed a significant interaction between mutation carrier status and eAO ($p=0.017$), with decreases in DMN fcMRI observed as mutation carriers approached and surpassed their eAO, an effect that was absent in non-carriers.

Interpretation: Functional disruption of the DMN occurs early in the course of dominantly-inherited AD. This degradation of the DMN is present even prior to clinically evident symptoms (similar to reports in late onset, sporadic AD) and appears to worsen with progression to more advanced states of impairment. The apparently linear decline in DMN connectivity as carriers approached and surpassed their estimated age of disease onset suggests that fc-MRI may prove to be a useful biomarker across a wide spectrum of disease, and provides support for the inclusion of fcMRI as an outcome measure in upcoming AD prevention trials.

Cipriani, Nicole A. MD
Graduate Assistant and Clinical Fellow in Surgical Pathology, Department of Pathology
ncipriani@partners.org

Poster Number 195

BRAF Mutation in "Sarcomas": A Possible Method to Detect Melanomas

Investigators: Nicole A. Cipriani, MD; Patrick J. McLaughlin; Darrell R. Borger, PhD; G. Petur Nielsen, MD

Background: BRAF is commonly mutated in melanomas (over 60%), as well as some thyroid and colon carcinomas. BRAF mutation has been anecdotally reported in up to 2% of sarcomas. Immunohistochemically, some poorly-differentiated melanomas lose melanocytic markers and some sarcomas demonstrate no lineage of differentiation. Making a definitive diagnosis of melanoma versus sarcoma in this setting can be challenging. This study addresses the rate of BRAF mutation in patients with sarcomas and in patients with both melanoma and sarcoma.

Design: A clinico-pathologic database was queried for patients with sarcoma, with or without melanoma. SNaPshot mutational analysis was performed on formalin-fixed paraffin-embedded tumor tissue from: 1) 50 patients with sarcoma-only, without melanoma; 2) 13 patients with both sarcoma and melanoma (melanoma tissue was not available for 3 of these patients).

Results: In the sarcoma-only group (n=50), BRAF mutation was not identified. Nine sarcoma-only patients had other molecular aberrations. In the sarcoma-melanoma group (n=13), two sarcomas showed BRAF mutation, both undifferentiated sarcomas. Tissue from the two corresponding melanomas was not available for comparison. Three melanomas showed BRAF mutation but the corresponding sarcomas did not. Three sarcomas and one melanoma showed other molecular aberrations.

Conclusion: Rate of BRAF mutation in sarcoma is low. In patients with sarcoma WITHOUT melanoma, the rate in this study is 0%. Interestingly, BRAF mutation was only identified in sarcomas from patients who also had melanomas. Both sarcomas were high grade, poorly differentiated, did not stain for melanocytic markers, and occurred chronologically after the melanomas. In one case, the melanoma was in the left buttock with left groin metastases; the sarcoma was in the left pelvis. In the other case, the melanoma was in the left breast; the sarcoma was in the left lung. The presence of BRAF mutation in these tumors raises the possibility that poorly differentiated sarcomatoid malignancies with BRAF mutation may represent melanomas. Further investigation into this topic is warranted. BRAF mutational analysis should be considered in patients with poorly differentiated malignancies (especially those with histories of melanoma), as a positive result may indicate melanocytic differentiation.

Poster Number 196

Kahle, Kristopher T. MD, PhD
Resident, Neurosurgery
kkahle@partners.org

A novel mechanism and therapeutic target for intraventricular hemorrhage-associated communicating hydrocephalus

Investigators: Kristopher T. Kahle, MD, PhD; Philippe F. Simard; Volodymyr Gerzanich, PhD; J. Marc Simard, MD, PhD; David E. Clapham, MD, PhD

Communicating hydrocephalus (CH) is a source of morbidity and mortality for thousands of patients annually, and is commonly associated with intraventricular hemorrhage (IVH) due to germinal matrix hemorrhage in premature infants, traumatic brain injury in young adults, aneurysmal subarachnoid hemorrhage in middle-aged patients, and hypertensive strokes in the elderly. Extension of hemorrhage into the ventricle in any of these conditions is a poor prognostic indicator, and can lead to death. IVH survivors often suffer marked cognitive, psychological, and functional impairment. The current treatment for refractory CH is a ventriculoperitoneal shunt, with the associated risks of surgery, malfunction, and infection.

The pathophysiology underlying IVH-induced hydrocephalus is poorly understood; classically, it has been attributed to decreased CSF reabsorption at the arachnoid granulations, resulting in an excess accumulation of CSF. However, there is little evidence to support this theory in the literature. An improved understanding of the molecular basis of this disease would likely lead to more specific treatments and improved outcomes.

NKCC1 is an intrinsic membrane protein that transports Cl-, together with Na+ and K+, across the basolateral membrane of epithelial cells in multiple tissues. In the choroid plexus (CP) epithelium, NKCC1 is expressed on the apical membrane and is essential for CSF secretion. At low concentrations (2–10 μM), bumetanide is a potent and specific inhibitor of NKCC1. It was recently shown that IVH induces inflammation of CP cells which secrete CSF, but the significance of this finding is unknown. Because inflammation is a known activator of NKCC1, we hypothesized IVH-induced inflammation might contribute to hydrocephalus by increasing NKCC1-mediated CSF secretion.

Using a rat model of IVH, 160 μl of autologous blood or saline was infused into the lateral ventricle, resulting in hydrocephalus within 48h. Via ventriculosotomy, rats were administered vehicle, bumetanide, or glibenclamide (an inhibitor of SUR1, an inflammation-induced regulator of ion transport). At 48h, rats were assessed for ventricular size and tissues were studied with biochemistry and quantitative immunohistochemistry.

IVH triggered inflammation of CSF barrier cells, as documented by up-regulation of NF-κB and SUR1, and abnormal uptake of serum-derived IgG. IVH also increased the functional expression of NKCC1 via WNK1/SPAK-kinase mediated catalytic phosphorylation at threonines 212 and 217, sites required for NKCC1 activation. Inhibition of NKCC1-mediated CSF secretion by administration of intraventricular bumetanide or glibenclamide completely corrected IVH-induced hydrocephalus. Glibenclamide reversed the inflammation-induced activation of NKCC1 by inhibiting T212/T217 phosphorylation.

These data provide in vivo evidence in that IVH-induced inflammation of the CP is associated with an increase in the phosphorylation and functional expression of NKCC1 in a SUR1-dependent manner, and that pharmacologic inhibition of either NKCC1 or SUR1 can correct IVH-induced hydrocephalus when administered via ventriculostomy within 48h of hemorrhage. These results suggest that increased CSF secretion via inflammation-induced NKCC1 activation, not dysfunctional CSF reabsorption, is a primary driver of IVH-associated hydrocephalus. Intraventricular administration of either bumetanide or glibenclamide (both FDA approved drugs) might be useful adjuncts in patients already being treated unsuccessfully with ventriculostomy or shunt for CH hydrocephalus due to IVH or even other causes.

Poster Number 197

Kochevar, Irene E. PhD
Professor, Wellman Center for Photomedicine
kochevar@helix.mgh.harvard.edu

Rapid Collagen Photo-crosslinking Method for Treatment of Keratoconus

Investigators: Irene E. Kochevar, PhD; Daniel Cherfan, MS; Thomas E. Gisel, MS; Erol E. Verter, MS; Robert W. Redmond, PhD; Samir Melki, MD

Background: Keratoconus is characterized by progressive protrusion of the corneal surface due to thinning and weakening of the corneal stroma. Severe astigmatism and poor visual acuity result and may require a corneal transplant. Keratoconus typically begins in puberty and progresses over two decades or longer.

Purpose: To develop a method to photo-crosslink corneal collagen, thus stiffening the cornea, that can be used to inhibit progression of corneal bulging in keratoconus eyes.

Methods: Rose Bengal dye (RB) was applied to the de-epithelialized cornea surface of ex vivo rabbit eyes, and the cornea was then exposed to green light for 1 to 5 min. Results of mechanical testing using a tensiometer were used to calculate Young's modulus, a measure of corneal stiffness. Depth of penetration of RB into the corneal stroma was determined by fluorescence confocal microscopy and viability of corneal keratocytes was measured 24 hr after treatments.

Results: The stiffness of RB-treated corneas increased in a light dose-dependent manner. A 3-fold increase was obtained after exposure to 5 min of green light (n=6-8/group; $p<0.05$). RB penetration into the cornea stroma was limited to only ~100 microns from the anterior surface. Thus RB + green light-initiated crosslinks are produced close to the anterior surface. RB + green light did not decrease keratocyte viability.

Conclusions: RB + green light rapidly and effectively crosslinked corneal collagen, thus producing a stiffer cornea that can resist deformation by the intraocular pressure. This technology may be developed into a treatment to block the progression of keratoconus.

Poster Number 198

Lippincott, Margaret F. MD
Clinical Research Fellow, Medicine
mlippincott@partners.org

Continuously administered kisspeptin as a pseudo-antagonist of the kisspeptin receptor

Investigators: Margaret F. Lippincott, MD; Yee-Ming Chan, MD, PhD; Valerie F. Sidhoum, BA; Stephanie B. Seminara, MD

Introduction: Kisspeptin sits atop the reproductive axis and potently stimulates secretion of gonadotropin- releasing hormone (GnRH) from the hypothalamus. In numerous animal species, including the human, single boluses of kisspeptin have been shown to stimulate GnRH-induced secretion of luteinizing hormone (LH) and follicle-stimulating hormone (FSH) from the pituitary gland.

Though the power of single boluses of kisspeptin to stimulate GnRH-induced LH release is consistent across species, disparate effects have been observed when kisspeptin has been administered as a continuous infusion. In the rhesus macaque, a continuous infusion of kisspeptin initially causes LH to increase, but eventually causes LH levels to drop due to desensitization at the level of the kisspeptin receptor. When similar infusion studies have been performed in the human male, albeit at a 10-fold lower dose of 4 µg/kg/h, LH levels also initially rose, but stayed elevated throughout the infusion.

We hypothesized that in the human a 24-hour infusion of kisspeptin at a sufficient dose will result in desensitization of the kisspeptin receptor, causing LH levels to decrease.

Methods: Three healthy male volunteers underwent blood sampling q10-60 min x36 hours to evaluate their LH responses to continuous kisspeptin administration, with 6 hours of baseline sampling before the kisspeptin infusion, continued sampling during a 24-hour infusion of kisspeptin at 12.5 µg/kg/h, and a final 6 hours of sampling after the infusion was stopped.

Three 3-hour windows were selected for comparison:
1) PRE INFUS: the three hours just before the kisspeptin infusion started
2) PEAK INFUS: the 3-hour time interval with the highest mean LH level during the kisspeptin infusion
3) END INFUS: the final three hours of the kisspeptin infusion

To determine whether LH levels fell during the kisspeptin infusion, as would be expected with desensitization, LH levels during PEAK INFUS and END INFUS were compared within individuals using unpaired t-tests. To determine whether LH levels fell below baseline LH, which would suggest full suppression of LH secretion, PRE INFUS and END INFUS were similarly compared.

Results: Over the 24 hours of the kisspeptin infusion LH initially increased, plateaued, and then started to fall before the infusion stopped. Each subject experienced a statistically significant LH decline from PEAK INFUS to END INFUS ($p<0.005$). Across individuals, mean LH levels (averaged across all three subjects) were not significantly lower at END 16.7 ± 3.5 mIU/mL compared to PEAK 22.4 ± 4 mIU/mL ($p>0.05$). LH pulsatility was seen during the continuous kisspeptin infusion.

Conclusion: In contrast to previously reported studies in the human, continuous kisspeptin administered at a rate of 12.5 µg/kg/h for 24 hrs results in declining LH levels during the infusion. This finding suggests that continuous kisspeptin can desensitize the kisspeptin receptor in the human. With these encouraging preliminary results, future studies will examine other populations (healthy cycling women, postmenopausal women) and will determine the kisspeptin dosage required to achieve full desensitization. Surprisingly, contrary to the hypothesis that kisspeptin pulsatility drives GnRH pulsatility, discrete pulses of GnRH/LH can be detected in the setting of continuous kisspeptin.

McMullin, Ryan PhD
Research Fellow, Department of Pathology
rpmcmullin@partners.org

Poster Number 199

A BRCA1 Deficient-Like Signature is Enriched in Breast Cancer Brain Metastases and Predicts DNA Damage-Induced PARP Inhibitor Sensitivity

Investigators: Ryan McMullin, PhD; Chunwei Yang, PhD; Ben Wittner, PhD; Raj Singavarapu; Sharon Moulis, PhD; Kenneth Aldape, MD; Patricia Steeg, PhD; Sridhar Ramaswamy, MD; Dennis Sgroi, MD

Identification of biomarkers and treatment options for breast cancer-derived brain metastases represent an area of crucial clinical need. This need is evident in HER2+ breast cancer, where the inability of Herceptin to transverse the blood-brain barrier limits its overall efficacy. In order to identify gene signatures and biological pathways associated with brain metastases, gene expression analysis was conducted on HER2+ brain metastasis specimen and HER2+, Estrogen Receptor (ER)-matched nonmetastatic primary breast tumors. A gene signature of BRCA1 deficiency showed highly significant correlation with the brain metastases in our cohort. This signature, when calculated into a BRCA1 Deficient-Like Metagene (BD-L), demonstrated enriched value in brain metastases from an independent cohort. BD-L values are increased in primary tumors from BRCA1 mutation carriers and HER2-/ER- sporadic cancers, but high values are found in a subset of ER+ and HER2+ sporadic breast cancer. The BD-L metagene is associated with increased risk of overall relapse, brain relapse, and decreased survival in an independent cohort. To assess biological relevance, BD-L values were derived from existing breast cancer cell line datasets to examine the correlation of the BD-L metagene with pharmacologic response to the PARP Inhibitor Olaparib and DNA alkylating agent Temozolomide. A highly significant association between BD-L value and pharmacologic response was found in two independent datasets, and the metagene also outperformed 4 extant signatures of BRCA1 deficiency in prediction of treatment sensitivity. These results suggest the BD-L metagene may identify a subset of the breast cancer population that unexpectedly share an increased risk of brain metastasis and increased sensitivity to a combination of DNA damage and PARP inhibition with BRCA1-deficient cancers.

Poster Number 200

Mirzakhani, Hooman MD
Clinical Research Fellow, Anesthesia, Critical Care and Pain Medicine
hmirzakhani@partners.org

Burden of hypertension associated alleles in genomic risk prediction of preeclampsia

Investigators: Hooman Mirzakhani[1,2]; Brian Bateman[1,2]; Ananth Karumanchi[3]; Melissa L. Wilson[4]; Brendan Keating[5]; Richa Saxena[1,2]

[1]Department of Anesthesia, Critical Care and Pain Medicine and Center for Human Genetic Research, Massachusetts General Hospital, Harvard Medical School, Boston, MA [2]Program in Medical and Population Genetics, Broad Institute, Cambridge, MA [3]Beth Israel Deaconess Medical Center, Boston, MA [4]University of Southern California, Los Angeles, CA [5]Children's Hospital of Philadelphia, University of Pennsylvania, Philadelphia, PA

Introduction: Preeclampsia (PE) affects 3-8% of pregnancies and is a leading cause of maternal and fetal morbidity and mortality. It is associated with increased long-term maternal risk of cardiovascular diseases. Hypertension, a major and heritable risk factor for cardiovascular disease, is one of the cardinal diagnostic features of PE. Several common genetic variants (single nucleotide polymorphisms [SNPs]) associated with blood pressure levels have been identified and hypertension has been known as a risk factor for PE, however, no genes are yet known to be robustly associated with risk of PE and its major symptoms and no aggregate effects of HTN risk alleles on PE have been studied. The purpose of this study is to investigate the association of identified blood pressure-related SNPs with preeclampsia and investigate burden of hypertension risk alleles in preeclampsia.

Methods: We conducted a multi-center case–control study in 785 subjects of European ancestry (315 preeclamptic cases and 470 normal term control women from the same geographical area). Preeclampsia was defined by development of proteinuria and hypertension according to ACOG guidelines.1 Preeclamptic cases with chronic hypertension were excluded. DNA samples were genotyped using the Cardiovascular Bead Chip Array comprising ~53,000 SNPs from ~2000 cardiovascular candidate genes. 29 independent SNPs previously associated with blood pressure (systolic and diastolic) levels at P<1x10E-7 were selected from the NHGRI genome wide association study catalog and 25 with direct genotypes or proxies with r2>0.8 in HapMap CEU were evaluated for association with preeclampsia using logistic regression analysis adjusted for 10 principal components to correct for population structure. We also created a genetic risk score (GRS) to assess association of the hypertension risk variants in aggregate with preeclampsia. The risk score was weighted using SBP and DBP effects for the 29 SNPs.

Results: We identified study-wide significant association between preeclampsia and a blood-pressure associated variant near the gene "Natriuretic peptide receptor C/guanylate cyclase C" known as NPR3 (rs1173766; P=0.00078, Padj=0.002). The hypertension risk allele at this locus was associated with an increased risk of preeclampsia (OR: 1.45, 95% CI [1.16-1.76]). The burden of risk alleles for hypertension, as measured by GRS (weighted and unweighted), was not associated with risk of preeclampsia (p >0.4).

SNP	Nearby Gene (s)	CHR	Major	Minor	MAF	Coded allele	Coded allele frequency	Risk effect	OR	P value
rs1173766	*NPR3*	5	T	C	0.45	C	0.62	Increased	1.45 (1.16-1.76)	0.000779
rs1421811	*NPR3*	5	C	G	0.433	G	0.39	Decreased	0.823 (0.667-1.015)	0.06799
rs661348	*LSP1/TNNT3*	11	T	C	0.4	T	0.57	Decreased	1.206 (0.979-1.485)	0.07789
rs3819526	*CACNA1C*	12	T	C	0.45	T	0.61	Increased	0.808 (0.655-0.997)	0.04636
rs4846049	*MTHFR-NPPB*	1	G	T	0.358	T	0.31	Decreased	1.163 (0.93-1.45)	0.1769
rs13333226	*UMOD*	16	A	G	0.192	G	0.187	Decreased	0.9257 (0.702-1.22)	0.5843
rs1801253	*ADRB1*	10	C	G	0.283	G	0.273	Decreased	0.933 (0.785-1.26)	0.9545
rs2074311	*NUCB2/KCNJ11/ABCC8*	11	G	A	0.467	G	0.58	Decreased	1.0.92 (0.884-1.349)	0.4124
rs13306560	*MTHFR*	1	C	A	0.05	A	0.0527	Decreased	1.062 (0.65-1.72)	0.806
rs2004776	*AGT*	1	C	T	0.242	T	0.24	Increased	1.24 (0.80-1.3)	0.85
rs17367504	*MTHFR-NPPB*	1	A	G	0.183	G	0.14	Decreased	1.04 (0.773-1.4)	0.6626
rs7129220	*ADM*	11	G	A	0.117	G	0.89	Decreased	0.992 (0.719-1.369)	0.9615
rs1378942	*CYP1A1-CSK*	15	A	C	0.3	C	0.35	Decreased	0.902 (0.72-1.12)	0.3415
rs2014408	*SOX6*	11	C	T	0.25	T	0.21	Increased	1.053 (0.827-1.34)	0.675
rs5068	*NPPA/NPPB*	1	A	G	0.075	A	0.06	Increased	1.059 (0.65-1.72)	0.8157
rs11105354	*ATP2B1*	12	A	G	0.1	G	0.16	Decreased	0.999 (0.755-1.32)	0.9934
rs2398162	*NR2F2-AS1*	15	A	G	0.167	A	0.26	Increased	1.087 (0.836-1.414)	0.5324
rs17030613	*ST7L-CAPZA1/CAPZA1*	1	A	C	0.175	C	0.49	Increased	0.851 (0.65-1.11)	0.2377
rs2071410	*FURIN-FES/FES*	15	C	G	0.367	G	0.371	Increased	0.9336 (0.746-.168)	0.5475
rs12946454	*PLCD3*	17	A	T	0.242	T	0.28	Increased	1.047 (0.825-1.328)	0.7076

Conclusions: Our genetic association results require additional replication and offer insights into the etiology of high blood pressure in preeclampsia. The genetic risk score needs to be tested in studies of higher sample size.

References: 1. ACOG (2002)

Poster Number 201

Mormino, Elizabeth C. PhD
Research Fellow, Neurology Service
bmormino@nmr.mgh.harvard.edu

Beta-amyloid influences the relationship between hippocampus volume and episodic memory in aging

Investigators: Elizabeth C. Mormino, PhD; Trey Hedden, PhD; Dorene M. Rentz, PsyD; J. Alex Becker, PhD; Andrew M. Ward, BA; Aaron P. Schultz, PhD; Gad A. Marshall, MD; Brendon Boot, MD; Randy L. Buckner, PhD; Keith A. Johnson, MD; Reisa A. Sperling, MD

Advanced aging is associated with increases in beta-amyloid plaque deposition, a pathology central to Alzheimer's disease (AD), as well as reductions in hippocampus volume and episodic memory performance. Although these changes are consistently observed in studies of aging, the degree to which beta-amyloid, hippocampus volume and episodic memory are directly related and influence each other within cognitively normal aging cohorts remains unclear. One hundred eighteen cognitively normal older individuals from the Harvard Aging Brain study were scanned with PIB-PET amyloid imaging and volumetric MRI. The association between age and hippocampus volume was 2-3 times greater than the association between beta-amyloid and hippocampus volume. A relationship between hippocampus volume and episodic memory was absent among beta-amyloid negative individuals, but emerged when subjects with slightly elevated PIB values were introduced into the sample. Thus, although age and beta-amyloid are related to hippocampus volume, hippocampus volume was only associated with episodic memory amongst beta-amyloid+ individuals. These results suggest that the earliest stages of AD-related volumetric changes may be present in cognitively normal samples at a level of amyloid burden that is lower than the level traditionally considered biologically relevant. Furthermore, the observation that the link with episodic memory in cognitively normal samples may be predominantly associated with beta-amyloid burden despite large age-related changes in hippocampal volume suggest that AD-independent mechanisms of hippocampal volume loss minimally influence episodic memory in aging.

Poster Number 202

Moscovitch-Lopatin, Miriam PhD, PMP
Instructor, Neurology Service
mmoscovitchlopatin@partners.org

Marker Validation of Huntingtinin PHAROS PBMCs Reveals Prodromal Elevation

Investigators: Miriam Moscovitch-Lopatin, PhD, PMP; Rachel E. Goodman, BSc; Shirley Eberly, MSc; James J. Ritch, BSc; H. Diana Rosas, MD, MSc; Samantha A. Matson, BSc; Wayne Matson, DSc; David Oakes, PhD; Anne Buckingham Young, MD, PhD; Ira Shoulson, MD; Steven M. Hersch, MD, PhD on behalf of the Huntington Study Group PHAROS Investigators

To help develop therapies targeting huntingtin (Htt), it is essential to be able to reliably measure Htt in preclinical and clinical studies. However, its multiplicity of forms has made assay development challenging and results difficult to interpret. A semi-quantitative cell-based assay has been developed to simultaneously measure soluble mutant (mtHtt) and total (tHtt) huntingtin, using Homogeneous time-resolved Forster Resonance Energy Transfer (HTRF) for use in biological and clinical tissues. We previously optimized and technically validated the HTRF assay according to Good Laboratory Practice (GLP) standards and wrote a Standard Operating Procedure (SOP) for analyzing mtHtt and tHtt in clinical buffy coat samples. We report using this SOP in a blinded evaluation of the relative blood levels of mtHtt and tHtt in the blood sample set from the Prospective Huntington At-Risk Observational Study (PHAROS), an NIH sponsored multicenter observational study of about 1000 individuals at 50% risk for developing HD but not yet symptomatic at study entry. At the time of blood sampling, the PHAROS cohort included controls, presymptomatic carriers, and carriers that had been diagnosed clinically (phenoconversion) during the course of the study. Deploying the HTRF assay in a cross-sectional study of PHAROS participants provided an opportunity to assess its performance in a multicenter study with dozens of sites preparing blood samples according to a prescribed protocol and to examine the HTRF signals for mutant and total huntingtin protein in subjects far from clinical onset, near to clinical onset, and recently diagnosed.

Motiwala, Shweta R. MD
Clinical Research Fellow, Heart Center
smotiwala@partners.org

Poster Number 203

Serial Measurement of Galectin-3 Predicts Chronic Heart Failure Outcomes and Ventricular Remodeling: Results from the ProBNP Outpatient Tailored Chronic Heart Failure Therapy (PROTECT) Study

Investigators: Shweta R. Motiwala, MD; Jackie Szymonifka, MA; Arianna Belcher, BS; Rory B. Weiner, MD; Aaron L. Baggish, MD; Patrick Sluss, PhD; Hanna K. Gaggin, MD, MPH; Anju Bhardwaj, MD; James L. Januzzi, Jr, MD

Background: Galectin-3 is a prognostic heart failure biomarker that may mediate cardiac fibrosis and ventricular remodeling.

Methods: 151 subjects with left ventricular systolic dysfunction were followed through 908 visits over 10 ± 3 months. Amount of time spent with galectin-3 level ≤20.0 ng/mL (study median) was considered across study visits, and used to assess risk for adverse cardiovascular events and associations with echocardiographic parameters of LV remodeling. Medication effects on galectin-3 were examined.

Results: Median galectin-3 values at baseline, 3 months, and 6 months were higher in patients with cardiovascular events (21.7 vs. 18.4 ng/mL, p = 0.03; 21.7 vs. 16.5 ng/mL, p = 0.03; 23.2 vs. 16.0 ng/mL, p = 0.007). Galectin-3 concentration changed in 35.2% of subjects during study procedures. Duration of time spent with galectin-3 level ≤20.0 ng/mL was significantly associated with a lower rate of cardiovascular events (Figure), independently predicted cardiovascular events even when adjusted for relevant variables including NT-proBNP and renal function (OR = 0.90; 95% confidence interval [CI] = 0.82-0.99, p = 0.04), and was predictive of increase in left ventricular ejection fraction (OR = 1.20; 95% CI = 1.01-1.42, p = 0.04). Serial galectin-3 measurement at 6 months added prognostic value beyond baseline level (p = 0.02), and increases in loop diuretics were associated with galectin-3 increase (p = 0.01).

Conclusion: In chronic heart failure due to left ventricular systolic dysfunction, serial galectin-3 measurement adds incremental prognostic information and predicts left ventricular remodeling. In this study, most heart failure therapies did not significantly change galectin-3 levels.

Figure:

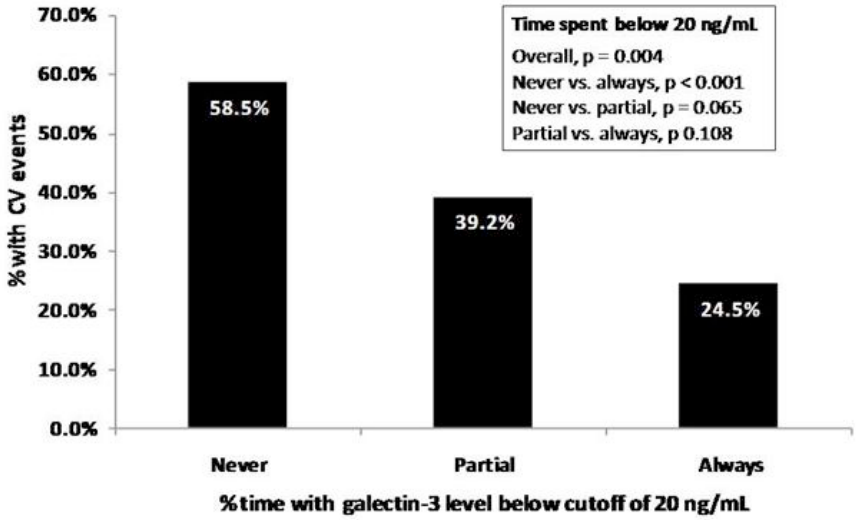

Poster Number 204

Papp, Kathryn V. PhD
Clinical Research Fellow, Psychiatry
kpapp@partners.org

Are Problems Retrieving Proper Names a Harbinger of Neurodegenerative Disease in Older Adults?

Investigators: Kathryn V. Papp, PhD; Sarah E. Wigman, BA; Rose Bamfo J.; Alex Becker; Keith A. Johnson, MD; Reisa A. Sperling, MD; Dorene M. Rentz, PsyD

Background: Retrieval of proper names is a common complaint of older patients and neurologists often question whether this symptom is an aspect of "normal aging" or a harbinger of incipient neurodegenerative disease.

Objective: This study explored retrieval for names and occupations of both novel and famous faces in cognitively normal (CN) and Mild Cognitive Impairment (MCI) subjects. We sought to determine if decrements in associative retrieval and semantic knowledge could differentiate normal aging from MCI. We also sought to explore whether these early deficits were related to A-beta deposition as assessed with PiB-PET amyloid imaging.

Methods: We studied 27 older subjects:17 CN (mean age 74.8 +/- 6.4 years, MMSE = 29.4 +/- 0.7) and 10 amnestic MCI (71.9 +/- 8.8 years, MMSE = 27.7 +/- 2.7) using a modified Face Name Associative Memory Exam (FNAME), which tested retrieval for 12 novel face-name-occupation pairs, and 12 famous face-name-occupation pairs. A subgroup (n=18) also underwent PiB-PET imaging. Using multiple linear regression analysis, we related FNAME to PiB retention (DVR, cerebellar reference) as a continuous variable in the precuneus, co-varying for age.

Results: MCI subjects performed significantly worse on the retrieval of newly learned face-name pairs ($p<0.006$) but not face-occupation pairs ($p=0.155$) whereas MCI performed similarly to CN on the retrieval of famous face-name pairs ($p= 0.33$) and famous face-occupation pairs ($p= 0.12$). Within the PiB-PET subgroup, famous face-name retrieval demonstrated a negative relationship with increasing A-beta deposition in both CN ($R2= 0.067$) and MCI ($R2= 0.237$). Famous face-occupation performance showed a negative relationship with A-beta in MCI ($R2 = 0.53$) but not CN ($R2 = 0.005$).

Conclusions: These findings suggest that with increasing A-beta burden, retrieval of proper names is difficult across all individuals but further A-beta-related decrements in semantic knowledge, a clinically more worrisome symptom, tends to dissociate MCI from CN.

Poster Number 205

Pinto, Alvaro P. MD, PhD
Research Fellow, Department of Pathology
apinto6@partners.org

Correlative study of SMARCB1/INI1 mutation status and INI1 immunohistochemical expression in hereditary and sporadic clinical subtypes of non-vestibular schwannomas

Investigators: Alvaro P. Pinto, MD, PhD; James Kim Stephen Yip MD, PhD; Scott R. Plotkin MD, PhD; Anat O. Stemmer-Rachamimov, MD

Background: Schwannomas are the hallmark of two hereditary syndromes, neurofibromatosis type 2 (NF2) and schwannomatosis. Mutation of the tumor suppressor gene SMARCB1/INI1 and mosaic expression of its protein has been found in schwannomas associated with familial and sporadic forms of schwannomatosis. However, review of the literature shows a discrepancy between reports of high rates of altered expression (by immunohistochemistry) and low rates of mutations (by mutation analysis) in schwannomas associated with schwannomatosis.

Objectives: 1) to correlate SMARCB1/INI1 genetic alterations with protein expression in a cohort of tumors associated with familial and sporadic schwannomatosis; 2) to define the SMARCB1/INI1 mutation rate in neurofibromatosis type 2 and correlate to protein expression.

Material & Methods: SMARCB1 mutation analysis and immunohistochemical expression were performed in 59 non-vestibular schwannomas from four clinical subgroups: sporadic schwannomatosis (18 tumors), familial schwannomatosis (10 tumors), neurofibromatosis type 2 (12 tumors) and solitary sporadic schwannomas (18 tumors). The 9 coding exons including 3'UTR of SMARCB1/INI1 were amplified by PCR and submitted to direct automated sequencing for mutation detection. INI1 immunostaining was performed using the BAF47 antibody and established protocols.

Results: SMARCB1 mutations were most common in familial schwannomatosis (60%). Mosaic pattern was seen in all cases in which mutations of SMARCB1 gene were present. However, in many cases in which mosaic expression was seen, there was no SMARCB1 mutation detected. NF2 showed >75% of the cases with mosaic pattern and none had mutations of the SMARCB1 gene.

Conclusions: There is a discrepancy between a mosaic pattern of expression of INI1 protein and detected SMARCB1 mutations in schwannomatosis and NF2 associated tumors. This may suggest epigenetic events or a loss of another protein that interacts with INI1. In cases in which clinical distinction between NF2 and schwannomatosis is difficult; the presence of SMARCB1 mutation in a tumor is supportive of underlying schwannomatosis.

Poster Number 206

Psychogios, Nikolaos PhD
Research Fellow, Heart Center
npsychogios@partners.org

2-aminoadipic acid is a novel biomarker of diabetes risk and modulates glucose homeostasis

Investigators: Robert E. Gerszten. MD; Nikolaos Psychogios, PhD; Martin G. Larson, PhD; Ramachandran S. Vasan; Anahita Ghorbani; Susan Cheng, MD; Eugene P. Rhee, MD; Andre Dejam, MD, PhD; Elizabeth McCabe; Caroline S. Fox, MD; Christopher J. O'Donnell, MD; Jennifer E. Ho, MD; Jose C. Florez, MD, PhD; Amanda Souza, Olle Melander, Clary B. Clish, PhD; Thomas J. Wang, MD

Introduction: Improvements in metabolite profiling techniques are providing increased breadth of coverage of the human metabolome. We recently developed a liquid chromatography-tandem mass spectrometry method capable of profiling ~70 small molecules preferentially ionized using negative mode electrospray ionization, including intermediary organic acids, purines, pyrimidines and other compounds.

Methods: We performed a nested case-control study with 2,422 normoglycemic individuals from the Framingham Heart Study who were followed for 12 years. "Intermediate" metabolites were profiled in the plasma of 188 individuals who developed diabetes during follow-up and 188 propensity-matched controls. Analyses were conducted using multivariable conditional logistic regression adjusting for standard diabetes risk factors. Replication analyses were performed in the Malmö Diet and Cancer Study (n=324). To test the hypothesis that 2-aminoadipic acid plays a role in glucose homeostasis, we also performed intervention studies in mice.

Results: The metabolite most strongly associated with the risk of developing diabetes was 2-aminoadipic acid ($p=0.0009$). Individuals with 2-aminoadipic acid concentrations in the top quartile had >4-fold risk of developing diabetes (adjusted odds ratio, 4.5, 95% confidence interval, 1.9 to 10.9. These findings were replicated in the Malmö Diet and Cancer Study ($p=0.004$; pooled result, $p<0.0001$). Levels of 2-aminoadipic acid were poorly correlated with other metabolite biomarkers of diabetes, such as branched chain amino acids ($r=0.04$ to 0.24) and aromatic amino acids ($r=0.01$ to 0.13). In functional studies in vivo, administration of 2-aminoadipic acid to mice lowered fasting plasma glucose levels; the mechanism behind this observation is under investigation.

Conclusion: These data highlight a pathway not previously associated with diabetes that is activated up to 12 years before the onset of overt disease. Our findings suggest that 2-aminoadipic acid is a novel marker of diabetes risk and potential modulator of glucose homeostasis.

Seminara, Stephanie MD
Associate Professor, Medicine
sseminara@partners.org

Poster Number 207

Combinatorial Mutations in Two Genes Link Disordered Ubiquitination with a Syndrome of Ataxia, Dementia, and Hypogonadotropic Hypogonadism

Investigators: David H. Margolin, MD, PhD; Maria Kousi, PhD; Yee-Ming Chan, MD, PhD; Elaine T. Lim, MS; Jeremy D. Schmahmann, MD; Marios Hadjivassiliou, MD; Janet E. Hall, MD; Ibrahim Adam, MD; Andrew Dwyer, NP; Lacey Plummer, BS; Stephanie V. Aldrin, BA; Julia O'Rourke, PhD; Andrew Kirby, BS; Kasper Lage, PhD; Aubrey Milunsky, MBBCh, DSc; Jeff M. Milunsky, MD; Jennifer Chan, MD; E. Tessa Hedley-Whyte, MD; Mark J. Daly, PhD; Nicholas Katsanis, PhD; Stephanie B. Seminara, MD

Hereditary ataxias are genetic disorders characterized by slowly progressive incoordination of gait. Poor coordination of the limbs and of speech is often present, and atrophy of the cerebellum frequently occurs. Ataxia can also be a feature of syndromic disorders that affect multiple systems. For example, cerebellar ataxia was found to be associated with hypogonadism (Gordon Holmes syndrome) over 100 years ago. Despite the rapid evolution in genetic technologies over the last several years, there remains little understanding of the pathophysiologic mechanisms that bind together the disparate phenotypes of ataxia and hypogonadism. An international, multi-center, and interdisciplinary collaboration led by MGH researchers was organized to characterize the phenotype, pathophysiology, and genetic etiology of Gordon Holmes syndrome, beginning with three affected siblings within a seven-generation consanguineous family.
Exomic sequencing was performed on DNA from one affected sibling from the index kindred, followed by targeted sequencing on other patients. Brain tissue from one patient underwent histopathological analysis and electron microscopy. Neuroendocrine phenotyping was performed on several subjects through q10 min measurement of luteinizing hormone at baseline and in response to exogenous gonadotropin-releasing hormone (GnRH). A zebrafish model recapitulating clinical findings of the patients was generated and the biological effects of likely causal gene variants and epistatic interactions were assessed quantitatively.

Homozygous mutations in RNF216 and OTUD4, which encode an E3 ubiquitin ligase and a deubiquitinase, respectively, were identified in all three affected siblings of the index kindred. Additional screening identified compound heterozygous truncating mutations in RNF216 in an unrelated patient with ataxia and hypogonadotropism, and heterozygous mutations in RNF216 were found in four other patients. All patients with RNF216 mutations had dementia as a prominent feature of their disorder, with cerebellar atrophy and white-matter changes in the cerebral hemispheres on neuroimaging. Selective neuronal loss was observed in cerebellar pathways and the hippocampus, with surviving hippocampal neurons containing ubiquitin-immunoreactive intranuclear inclusions. Furthermore, all patients presented with reproductive dysfunction before developing ataxia; administration of exogenous GnRH to four patients demonstrated defects at both hypothalamic and pituitary levels of the reproductive endocrine axis. Finally, knockdown of rnf216 and otud4 in zebrafish embryos resulted in mild reduction in size of the optic tectum and microphthalmia, while combinatorial suppression of the two genes resulted in a significant exacerbation of the above phenotypes, as well as disorganization of the cerebellum. Each of these defects could be rescued by co-injection of wild-type but not mutant human mRNA for either RNF216 or OTUD4.

We have identified a new syndrome of ataxia, dementia, and hypogonadotropic hypogonadism and determined that it can be caused by inactivating mutations in RNF216 or by the combination of missense mutations in RNF216 and OTUD4. These findings link disordered ubiquitination to neurodegenerative disease and reproductive endocrine dysfunction and highlight the power of whole-exome sequencing in combination with functional studies to unveil complex genetic interactions that inform causality.

Poster Number 208

Wang, Yangyang MD
Research Fellow, Surgery
ywang54@partners.org

CSPG4 and SHH pathway as targets of a combinatorial therapy for Triple Negative Breast Cancer (TNBC)

Investigators: Yangyang Wang, MD[1]; Francesco Sabbatino, MD[1]; Xinhui Wang, MD, PhD[1]; Richard A. Morgan, PhD[2]; Soldano Ferrone, MD, PhD[1]
[1]Department of Surgery, Massachusetts General Hospital, Boston, MA, 02114 [2]Surgery Branch, National Cancer Institute, national Institutes of Health, Bethesda, MD, 20892

Introduction: TNBC represents about 15% of all breast cancer. The prognosis for patients with TNBC is generally poor. Recent evidence suggests that TNBC cell lines and tumors might be enriched with cancer initiating cells (CICs) and express high level of Sonic Hedgehog Homolog (SHH) pathway components. The suggested high frequency of CICs in TNBC is consistent with the failure of conventional therapies to control disease progression, because according to the cancer stem cell theory, CICs are chemo-and radio-resistant. These findings and the lack of curative therapy for TNBC patients with metastatic disease emphasize the urgent need to develop effective novel therapies for this type of breast cancer to reduce its high mortality. Therefore, we have developed a combinatorial therapeutic strategy which targets chondroitin sulfate proteoglycan (CSPG)4, a tumor antigen highly expressed on TNBC cells and tumor associated pericytes, and the SHH pathway. T cells engineered to express a chimeric antigen receptor (CAR+ CTL) constructed with our CSPG4-specific human mAb and mAb which recognize distinct epitopes of CSPG4 are used as effectors, since they use different effector mechanisms. CSPG4-specific mAb inhibit signaling pathways associated with TNBC cell growth and survival, while CAR+ CTL effect their lysis. LDE225, an inhibitor of the SHH pathway, is used to enhance the effect of immunotherapy on TNBC CICs.

Methods: The human TNBC cell lines SUM149 and MDA-MB-231 were cultured in RPMI 1640 medium with 10% FCS. Cells were treated with mAb 225.28 (0.25mg/ml) and/orLDE225 (10μM) in RPMI 1640 medium with 1% FCS. The percentage of CICs, identified as aldehyde-dehydrogenase1A1 bright (ALDHbright) cells, was determined after a 72 hour treatment by flow cytometry using ALDEFLUOR kit. The human TNBC cell line MDA-MB-231 was also co-incubated with CSPG4-specific CAR+ CTL; culture supernatants were harvested 18-24 hrs after the initiation of co-culture and assayed for IFN-γ by ELISA.

Results: Treatment of SUM149 cells with mAb 225.28 or LDE225 reduced the percentage of ALDHbright cells from the basal value of 1.9% to 1.3 % and 0.5%, respectively. The reduction in CICs was more marked when mAb 225.28 was combined with LDE225 (0.2%). Treatment of MDA-MB-231 cells with mAb 225.28 or LDE225 reduced the percentage of ALDHbright cells from the basal value of 4.9% to 3.7% and 1.5%, respectively. The reduction in CICs was more marked when mAb 225.28 was combined with LDE225 (1.0%). Moreover, IFN-γ release level is significantly higher in the culture supernatant from co-culture of MDA-MB-231 cells and CSPG4-specific CAR+ CTL than in that from co-culture of MDA-MB-231 cells and irrelevant CTL.

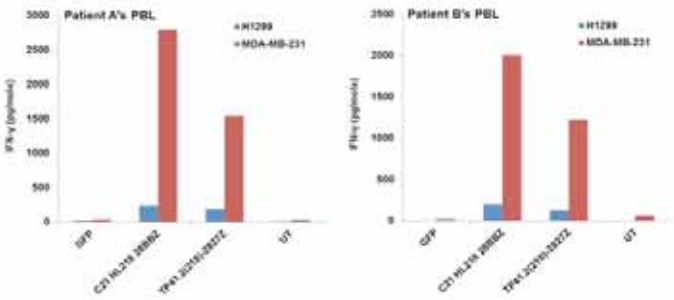

Figure 1. Recognition of TNBC cells by T lymphocytes transduced by CSPG4 specific-CAR . Briefly, frozen PBMC were thawed and cultured in AIM-V media (Invitrogen) supplemented with 5% human AB serum, plus antibiotics, 300 IU/mL IL-2, and 50 ng/mL OKT-3. Two days later, cells were transduced at 0.25 x 10^6/mL with retroviral supernatant spun onto RetroNectin (Takara Bio, Otsu, Japan) coated non-tissue culture treated 6-well plates as described by the manufacturer. Transduced cells were allowed to expand in AIM-V media as above, without OKT-3. CAR engineered PBLs were tested for antigen specific reactivity in cytokine release assays using the indicated tumor cells. In these assays effector T cells (1 x 10^5) were cocultured with equal number of target cells in AIM-V medium in a final volume of 0.2 mL in duplicate wells of a 96-well U-bottom microplate. Culture supernatants were harvested 18-24 hrs after the initiation of co-culture and assayed for IFN-γ by ELISA (Thermo Scientific, Rockford, IL).

Conclusions: Our experiments demonstrate that targeting TNBC cells with CSPG4-specific mAb in combination with LDE225, a SHH pathway inhibitor, could effectively eliminate TNBC CICs. We also show that CSPG4 could effective mediate the recognition and destruction of MDA-MB-231 cells by CAR+ CTL constructed with our CSPG4-specific human mAb. Therefore our combinatorial therapeutic strategy appears to eliminate both differentiated TNBC cells and TNBC CICs. If corroborated by preclinical model results, they provide a strong rationale for the use of the described combinatorial strategy for TNBC treatment.

Poster Number 209

Welt, Corrine K. MD
Associate Professor, Medicine
cwelt@partners.org

Mutations in eIF4ENIF1 Cause Autosomal Dominant Primary Ovarian Insufficiency

Investigators: Thushiga Kasippillai; Daniel G. McArthur, PhD; Andrew Kirby; Brett Thomas; Mark J. Daly, PhD; Corrine K. Welt, MD

Background: Primary ovarian insufficiency results from a premature absence of follicles and oocytes, with a consequent elevation of FSH levels before age 40 years. The majority of women do not have an etiology for their ovarian dysfunction. The disorder is familial in 10-15% of cases, suggesting that family genetic studies could identify new genes for the disorder.

Methods: We identified a family in which nine women in 3 consecutive generations developed primary ovarian insufficiency and menopause at approximately age 30 years. Family based whole exome sequencing was performed in 6 affected women and the father of the proband to identify a hypothesized autosomal dominant genetic mutation.

Results: Family based whole exome sequencing and Sanger sequencing in 7 affected women and an obligate carrier identified a heterozygous stop codon (Ser429X) in the eukaryotic translation initiation factor 4E nuclear import factor 1 (eIF4ENIF1). The stop codon was not identified in five unaffected women or the father of two unaffected daughters. The stop codon was not present in the mRNA transcript isolated from blood. There were no mutations in eIF4ENIF1 or eIF4E in 38 unrelated women with POI, although additional studies are ongoing.

Conclusions: A nonsense mutation in EIF4ENIF1 results in autosomal dominant primary ovarian insufficiency and early menopause. EIF4ENIF1 appears to be a critical protein in ovarian follicle development.

Poster Number 210

Zheng, Zongli PhD
Research Fellow, Department of Pathology
zzheng1@partners.org

Anchored multiplex PCR for detection of gene rearrangements and mutations using next-generation sequencing

Investigators: Zongli Zheng, PhD; Boryana Zhelyazkova; Divya Panditi; Hayley Robinson; Jeffrey A. Engelman, MD, PhD; John A. Iafrate, MD, PhD; Long Le, MD, PhD

We describe a rapid targeted RNA-seq library construction method for the detection of gene fusions in cancer using next generation sequencing. The method involves ligation of half-functional sequencing adaptors to double strand cDNA, followed by two successive PCR reactions using hemi-nested gene-specific 3′ primers with the 5′ adaptor primer, and generates libraries ready for bi-directional sequencing. RNA extracted from formalin-fixed paraffin-embedded biopsies can be used directly without the need to deplete ribosomal RNA, non-target mRNA or genomic DNA. Importantly, the assay can be performed without the need to know the 5′ partner in a gene fusion event. The method can also be applied to genomic DNA for detection of gene mutations, insertions, deletions and copy number changes. The method is very flexible and can allow multiplexing of over 500 targets. We have designed a lung cancer translocation panel which includes 18 amplicons for detections of gene rearrangements involving ALK, ROS1 and RET. For targeted genomic DNA-seq, we have designed a small 96-amplicon panel including tumor hotspots and entire coding sequences of key tumor suppressor genes TP53 and PTEN, and a 623-amplicon panel for 370 exons of 18 tumor suppressor genes. Unlike conventional PCR-based method, this method generates libraries with random sequencing start sites and allows for direct sequencing without having to spiking in controls (e.g. PhiX) on those platforms where high starting site complexity is required, such as the Illumina Miseq sequencer. The assays generally achieve high on-target specificity (>90%), and are very cost-effective. The targeted RNA-seq assay has detected various gene rearrangements in known FISH-positive cases with previously unknown 5′ partners using our archived samples. The small 96-amplicon genomic DNA assay showed 100% of targeted bases having >100-fold coverage and 99.9% having >500-fold coverage with minimal optimization. In our first attempt of targeting 370 exons (626 amplicons, target size 52.3 kilobases), this assay achieved 97% of targeted bases having >100-fold coverage and 93% having >500-fold using ¼ of a Miseq sequencing run.

ECOR Administrative Offices
50 Staniford Street, 10th Floor
Boston, MA 02114
ecor@partners.org

Executive Committee on RESEARCH | *Fostering Innovation at MGH*

MGH 1811 RESEARCH Management | *Mainstay of MGH Innovation*